Master Thesis, Department of Geosciences

PETROLEUM GEOCHEMISTRY OF THE SO-CALLED "DRY WELLS" OFF MID-NORWAY

CLUES TO IGNORED AND OVERLOOKED PETROLEUM SYSTEMS

HAJI MUHAMMAD AZHAR

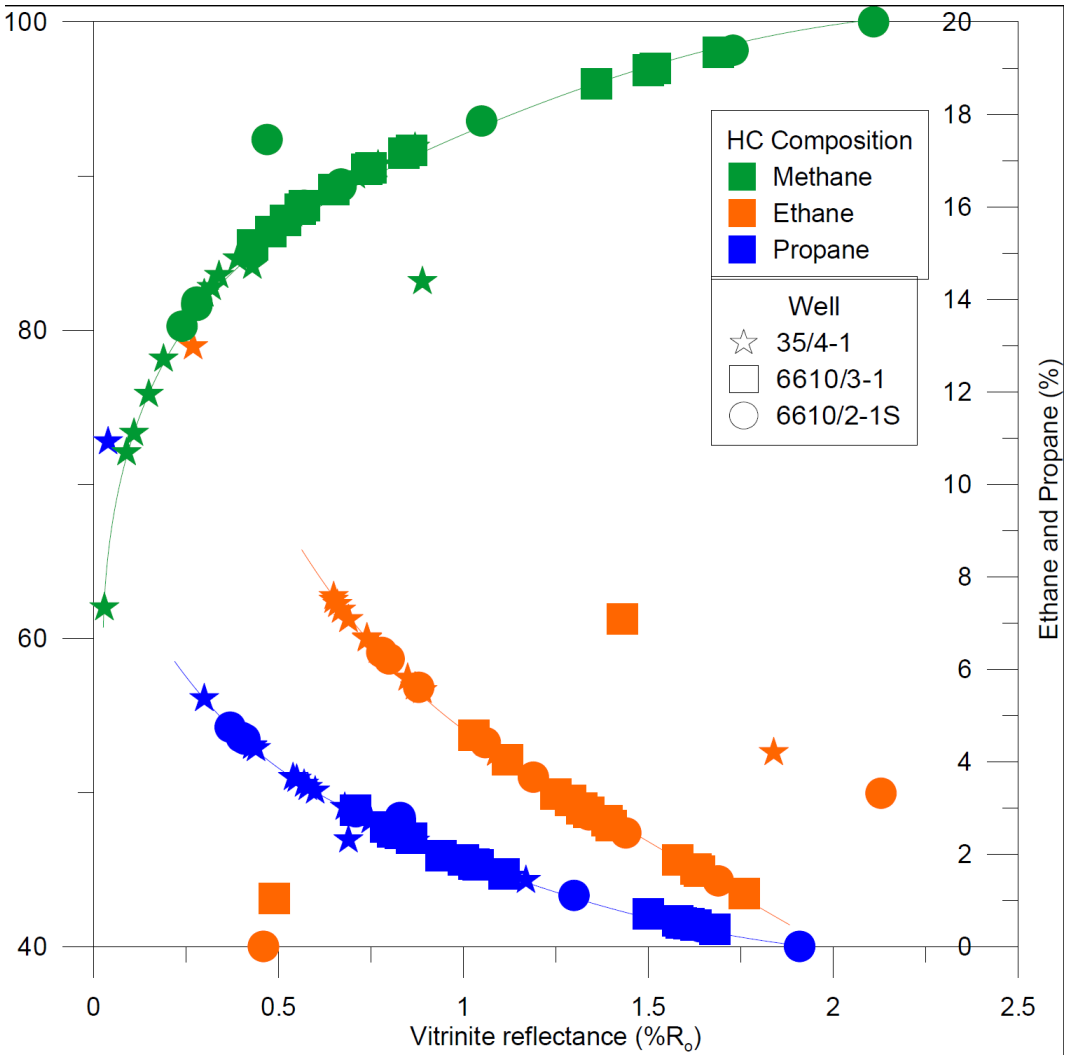

UNIVERSITY OF OSLO

FACULTY OF MATHEMATICS AND NATURAL SCIENCES

PETROLEUM GEOCHEMISTRY OF THE SO-CALLED "DRY WELLS" OFF MID-NORWAY

CLUES TO IGNORED AND OVERLOOKED PETROLEUM SYSTEMS

HAJI MUHAMMAD AZHAR

Master Thesis in Geosciences

Discipline: Petroleum Geology & Petroleum Geophysics

Department of Geosciences

Faculty of Mathematics and Natural Sciences

University of Oslo

February, 2012

Abstract

Forty-eight (48) core samples from well 35/4-1, 6610/3-1 and well 6610/2-1S were obtained from the North Sea and the Norwegian Sea. These wells are classified by NPD as dry. These core samples have been studied geochemically, and also using microscopy to look for petroleum inclusions. All core samples from these wells have been taken from the anticipated reservoir units and are mainly sandstones and cemented sandstones but also partly sandstone/siltstones. The focus of this study is to try to carry out geochemical analysis of the samples to characterize the gas from inclusions and the core extracts, provided in these so called dry wells off Mid-Norway. An important element of these investigations is also to try to document, using UV-microscopy, if any petroleum inclusions are present. If such are found, this will signify that the "dry wells" did earlier contain petroleum. Furthermore, the existence of core extracts representing migrated petroleum signifies that the "dry wells" may indeed have intersected what in the pre-history was a paleo-oil charge.

Destructive analytical methods like gas analysis are used to define the presence of HC gas in inclusions, and GC-FID of core extracts is used to determine if allochthonous bitumen exists in the core material. Chromatograms are produced from destructive analytical methods to determine the presence of light HCs in inclusions in mineral cements, and bitumen in the core samples and on the basis of these chromatograms, different source rock facies and maturity parameters were computed. Using these data, cross plots were generated to evaluate dry/wet gases, maturity and the organic facies of the bitumen. Visual examination of petroleum inclusions in these core samples was also used to define the presence of paleo-gas and oil charges in the samples.

Well 35/4-1 from North Sea is rich in light HCs and n-alkanes but the majority of the samples are biodegraded and well 6610/3-1 is also rich in light HCs but less amount of n-alkane signatures are recorded on chromatograms. Well 6610/2-1S contains HC gas bearing inclusions and also fluorescent inclusions and there are no n-alkanes signatures recorded. This is due to massive core contamination by circulating drilling fluids. The fact that this well contains oil type inclusions proves that oil was present as a mobile phase. Thus, the core samples studied from well 6610/2-1S has under microscope shown oil signature in UV light which has indicated that there would have been detectable n-alkane on chromatograms produced by GC-FID, but

unfortunately was the core extracts heavily contaminated by polyethylene glycols, rendering further analytical work useless.

Although light HCs are present in inclusions in all three wells, bitumen representing truly migrated petroleum could only be extracted from well 35/4-1 and 6610/3-1. The core samples from the well 35/4-1 are richer in HCs than in well 6610/3-1. The core samples from the well 35/4-1 show higher maturity and less biodegradation, while the well 6610/3-1 shows lower maturity and more biodegradation than the well 35/4-1. The source rock facies from the well 35/4-1 is clearly a type II source rock whilst well 6610/3-1 also show a type II source rock facies, albeit with some more terrestrial input. A likely source rock facies of well 35/4-1 is distal Draupne, while a more proximal Spekk Formation is the likely source for the petroleum found in well 6610/3-1. It is concluded that both well 35/4-1 and 6610/3-1 intersects paleo-reservoir units of either a migration an avenue or a reservoir and that thermogenic petroleum at one time migrated in this system. This has implications to further exploration in these regions.

Acknowledgements

I would like to thank my supervisor, Dr. Dag Arild Karlsen for giving me this great opportunity to study and explore the facts about so called dry wells off Mid-Norway by using geochemical analysis and for providing me feedback and support when I needed it the most. I sincerely pay gratitude for his excellent professional attitude, enthusiasm and courage during this tenure. He has always been openhearted and invigorated me to discuss and ask questions for the improvement of my work both practically and theoretically. I would like to pay my special thanks to Norwegian Petroleum Directorate (NPD) as study could not have been performed without samples gathered from NPD.

I would like to pay my gratitude to Kristian Backer-Owe for helping me and providing me the guidance in the lab and informative discussion on my study. I also, would like to thank Tesfamariam Berhane Abay for his comprehensive guidance throughout my study and especially in the last part.

Finally, my deepest gratitude goes to my family, friends and fellow students at the department of Geosciences, we had a lot of amazing time.

February, 2012
University of Oslo
Department of Geosciences
Haji Muhammad Azhar

Contents

Chapter 1

Introduction

The definition of petroleum geochemistry given by Hunt (1996) is "the application of chemical principles to the study of origin, migration, accumulation and alteration of petroleum oil and gas and the use of this knowledge in exploring and recovering petroleum".

The integrated study of petroleum inclusions in terms of their fluorescence colors (indicating API), the relative size of the gas bubble (indicating GOR), coupled with C_1-C_5 hydrocarbon (HC) gas analysis of inclusion gas and geochemical analysis of trace amounts of bitumen in reservoir rock porosity is a comparatively a new technique to understand the petroleum system evolution (Karlsen et al. 1993: 2006), also as applied to "dry wells". Petroleum inclusions are small amounts of reservoir hydrocarbon (oil or gas) or mixture of both that was trapped during the progress of diagenesis. Several types of evidences recommend that inclusions preserve the original composition of hydrocarbons which at one time occupied the porosity in reservoirs. Biomarkers are vital in geochemistry and they are considered as fingerprints of source rocks and there is little or no change in their structure during maturation and migration. A variety of sources propose that fluid inclusions preserve the original composition of the hydrocarbons and that they therefore can represent paleo-petroleum in traps and thus provide precious information about numerous significant aspects of petroleum genesis and migration. Fluid inclusions can provide an answer to whether there has been one or a number of hydrocarbon migration pulses into a trap. The content of the inclusions will provide clues to the source rock facies (type of source rock) and its maturity. Their occurrence and composition, fluorescence colors and the relative size of the gas bubble compared to the oil phase, can also provide evidences for the API and the gas to oil ratio (GOR) of the once entrapped reservoir charge. A major use of petroleum inclusions in diagenetic minerals is to ascertain if there have been one singular, or several source rocks involved in field filling through geologic time. Petroleum inclusions can also provide vital information about the time for the influx of hydrocarbons to the trap system.

Petroleum fluids are extremely complex in nature (Munz, 2001). The main objective of this chapter is to go through some of the essential background data on the

relationship between the physical and chemical nature of petroleum fluids for the interpretation of fluid inclusions. Major constituents of petroleum are hydrocarbon compounds, NSO compounds (i.e. resins and asphaltenes), and inorganic gases such as H_2S, N_2 and CO_2 (Munz, 2001). Structurally, hydrocarbon compounds in petroleum can be subdivided into three types:

- **Paraffins or alkanes:** Consist of normal and branched alkanes (iso-alkanes).
- **Naphthenes or cycloalkanes:** Consist of compounds with a ring structure like cyclohexane.
- **Aromatic HCs:** Compounds which contain cyclic structures with double bonds.

Inclusions can occur if sufficient oil saturation exists in mineralogy which is undergoing diagenesis. This will normally happen in oil and gas reservoirs if at sufficient depth and temperature for diagenesis to occur. Petroleum inclusion formation in reservoirs may occur from the beginning of filling of a trap to present day (Nedkvitne et al., 1993) as in case of drainage caused by a borehole (Munz, 2001). Petroleum inclusions are important delimiting factor for petroleum migration and filling of reservoir and they can serve as started point for modeling of such processes (Karlsen et al., 1993; Nedkvitne et al., 1993; Munz 1999a).

The presence of petroleum inclusions is correlatable with porosity and permeability in clastic reservoirs (Oxtoby et al., 1995; Munz et al., 1999a; Munz, 2001). Majorly, petroleum inclusions are found as secondary inclusions within detrital grains for example quartz and feldspars. Petroleum inclusions distribution and abundance represent the style in which the petroleum occupies the pore spaces in the host rock of different permeability, including migration routes below the present oil water contact (Oxtoby et al., 1995; Munz, 2001). Inclusions in chalk and limestone reservoirs can be found in cemented fractures, recrystallized macrofossils and other types of coarse grained cement (Burruss et al., 1983; Jensenius and Burruss, 1990; Munz, 2001). Therefore, the petroleum inclusions in carbonate reservoirs are more irregular than in clastic reservoirs (Munz, 2001). According to Munz et al. (1999b), the local abundance of petroleum inclusions in fractured cement samples of carbonates can be 2-3 times higher in comparison with the clastic reservoirs (Munz, 2001).

Examination of the textural relationship between the host mineral and the petroleum inclusions can be beneficial to determine the timing of reservoir filling or migration in relation to the diagenetic sequence (Karlsen et al., 1993; Nedkvitne et al., 1993: Munz, 2001). The association of quartz cementation and trapping of petroleum inclusions can be demonstrated from petroleum inclusions within the dust rim of quartz overgrowths (Nedkvitne et al., 1993; Oxtoby et al., 1995; Munz, 2001). Inclusions (primary and pseudosecondary) in fracture cements may give indication for the presence of petroleum during fracturing and the consequent cementation (Munz et al., 1998; Munz, 2001). According to Bodnar (1990), petroleum migration can be deduced from differences in composition between inclusions in consecutive growth zones of fracture cement samples, or from the occurrence of different populations of inclusions in periodic phases of cement generation (Burruss et al., 1983; Munz, 2001).

This study represents the attempt to look for inclusions systematically in selected North Sea and Norwegian Sea wells and so called "dry wells" were selected for this study. These wells are accordingly wells which did not discover accumulated nor migrated oil or gas. Well 35/4-1 from the North Sea and well 6610/3-1 and 6610/2-1S from Norwegian Sea were sampled at NPD for the purpose of this study and were analyzed applying specific analytical methods. These samples will in this project also be compared in terms of their similarities and differences concerning maturity and facies if core extracts (bitumen) or inclusions with gas are found.

The aim of this thesis is to try to answer the following questions:

- Are there any evidences for migrated oil, condensates or gas in these so called "dry wells"? This is to be evaluated by looking to find, if possible, bitumen core extracts, gas from inclusions or fluorescent oil type inclusions.
- To determine if it is possible to extract methane up to pentane (C_1-C_5) from the inclusions in the sandstone samples by using gas analysis. If such gas species are found, the aim is to determine gas wetness parameters to say, if possible, if the gas in the strata was dry or wet (oil associated).
- Is there any detectable n-alkane, pristane/n-C_{17} and phytane/n-C_{18} signatures in any of these core samples, by using GC-FID? While previous techniques used by the industry classifies these wells as dry, the modern methodology developed at Department of Geosciences, UiO allows for

trace amount analyses of bitumen core extracts. If such are found to represent migrated petroleum, a completely different scenario opens up to the understanding of the Petroleum System understanding of the regions represented by these "dry wells". If good signatures are found it will be attempted to classify the bitumen signatures as condensates, oil and attempts to determine tentatively the source rock type and maturity will be made and in this case will comparisons be made to the North Sea Oil Standard from Oseberg.

- Is there any petroleum inclusions observable under microscope among these selected samples? If this is the case, the purpose is to try to make microphotographic documentations of these inclusions and to tentatively evaluate API and GOR (in terms of gas-condensate, condensate or oil). Observable inclusions are singular manifestations of paleo-petroleum in traps. Lack of observable fluorescent inclusions is not proof of absence, instead petroleum inclusions may exist but they may be too small to be observed or too high in GOR to fluoresce. Often is dry gas trapped in water inclusions which quantitatively may grossly out-number true petroleum inclusions?
- Any migrated bitumen should be attempted classified in terms of condensate, light oil or black oil. Its maturity should be evaluated?
- To evaluate if there are any differences in maturity or facies between these three wells from two different regions of the North Sea and the Norwegian Sea and to suggest if the findings could have any bearing on future exploration in these regions.

Chapter 2

Geological History

The objective of this chapter is to provide a brief introduction and description of the geological setting of the study area.

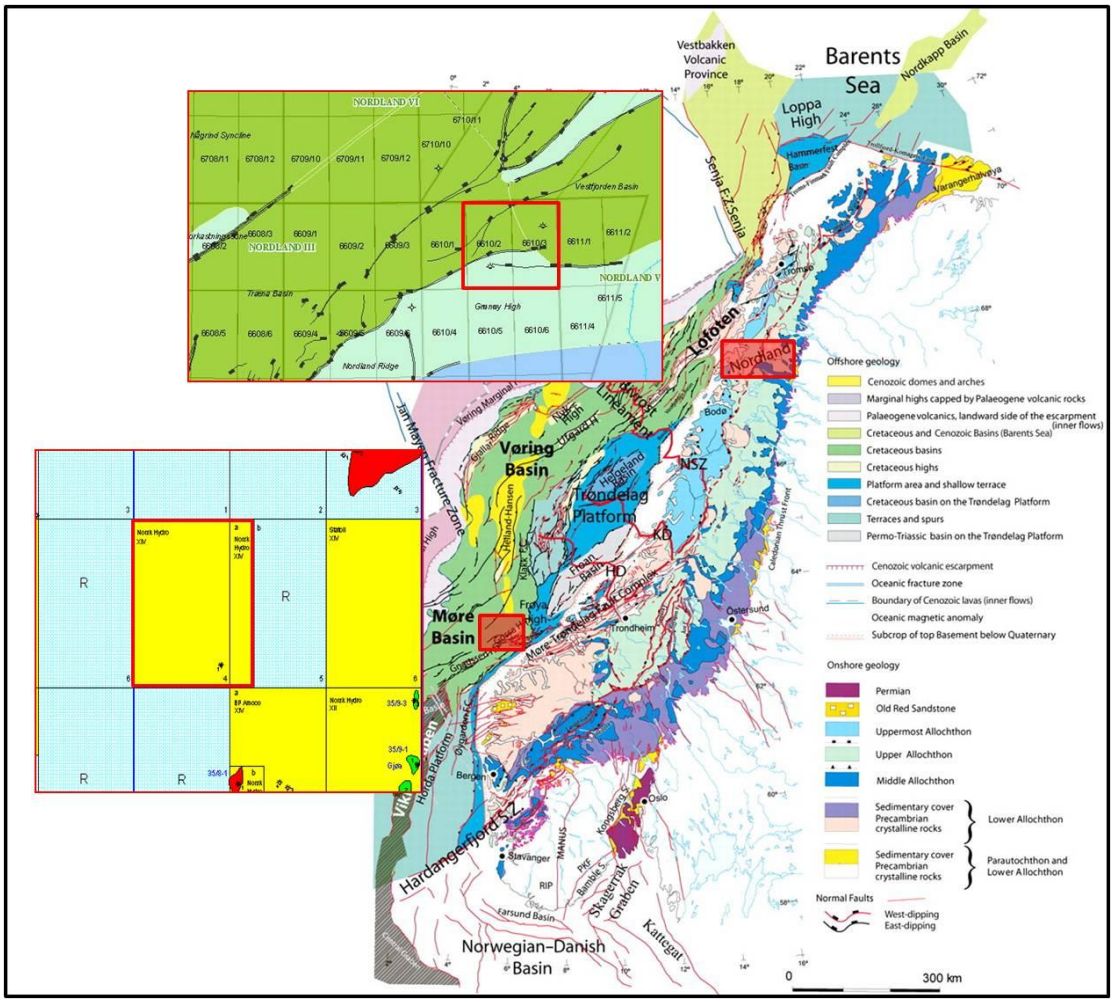

Fig.2.1 Regional geological map of the study area, inserts show location of wells used during the study i.e., top insert shows location of Nordland III (6610/3-1 & 6610/2-1S), bottom insert shows location of Sogn Graben (35/4-1) (modified from www.npd.no). Due to the fact that the wells of this study are classified as dry, there has been no more recent exploration in these regions. If this project suggests these wells have contained oil, condensate or gas, this may have implications to future exploration.

2.1 Geological framework of the Norwegian Continental Shelf

Area of mid Norway is part of a passive continental margin. The current structural style of the passive continental margin of the Norwegian Sea can be dated back to Permo-Carboniferous time (Fig. 2.1) (Bukovics et al., 1984; Brekke 2000).

Palaeozoic time of Norwegian Continental Shelf is characterized by two stages of tectonic development which is followed by creation of Norwegian-Greenland Sea in Cenozoic time. In early Palaeozoic, the Caledonian Orogeny resulted in production of basement underlain by Norwegian Continental Shelf. In late Palaeozoic to Early Triassic times extension affected the area which resulted in Pangea to break up. Second event of rifting and extension occurred in Late Jurassic to Early Cretaceous. In Early Cenozoic, final major rifting event occur which resulted in complete break up of Pangea. This also resulted in sea floor spreading and formation of new oceanic crust with opening of North East Atlantic including Norwegian-Greenland Sea (e.g. Blystad et al., 1995; Skogseid et al., 2000; Brekke 2001; Gradstein et al., 2004).

2.2 Tectonic development of the Norwegian Continental Shelf

There are various processes involved in interaction of various processes like lithospheric scale processes, the composition of Precambrian basement and Caledonian root, climatic changes and tectonic forces. It is also thought that tectonic development of Northeast Atlantic region is the main cause of the post Caledonian growth of the Norwegian Sea continental margin (Smelror et al., 2007).
The main tectonic events are described below:

2.2.1 Palaeozoic

Two major tectonic events occurred in Palaeozoic i.e. creation of Caledonian Orogeny and rifting events from Carboniferous to Permian. After the closure of Iapetus Caledonian mountain chain was formed in time of Ordovician-Early Devonian. Later in Early to middle Devonian time, the Caledonian mountain chain collapsed (Fig.2.2) (Bukovics 1984; Blystad et al., 1995; Gee 1975; Smelror et al., 2007). Today the main building blocks of Norwegian mainland are the result of deeply eroded Caledonian Orogeny (Smelror et al., 2007).

2.2.2 Mesozoic

Later Permian to Early Triassic time is characterized by extensional tectonic phase of Norwegian Sea, which is believed to be a mark of the initial break up of Pangea (Smelror et al., 2007).

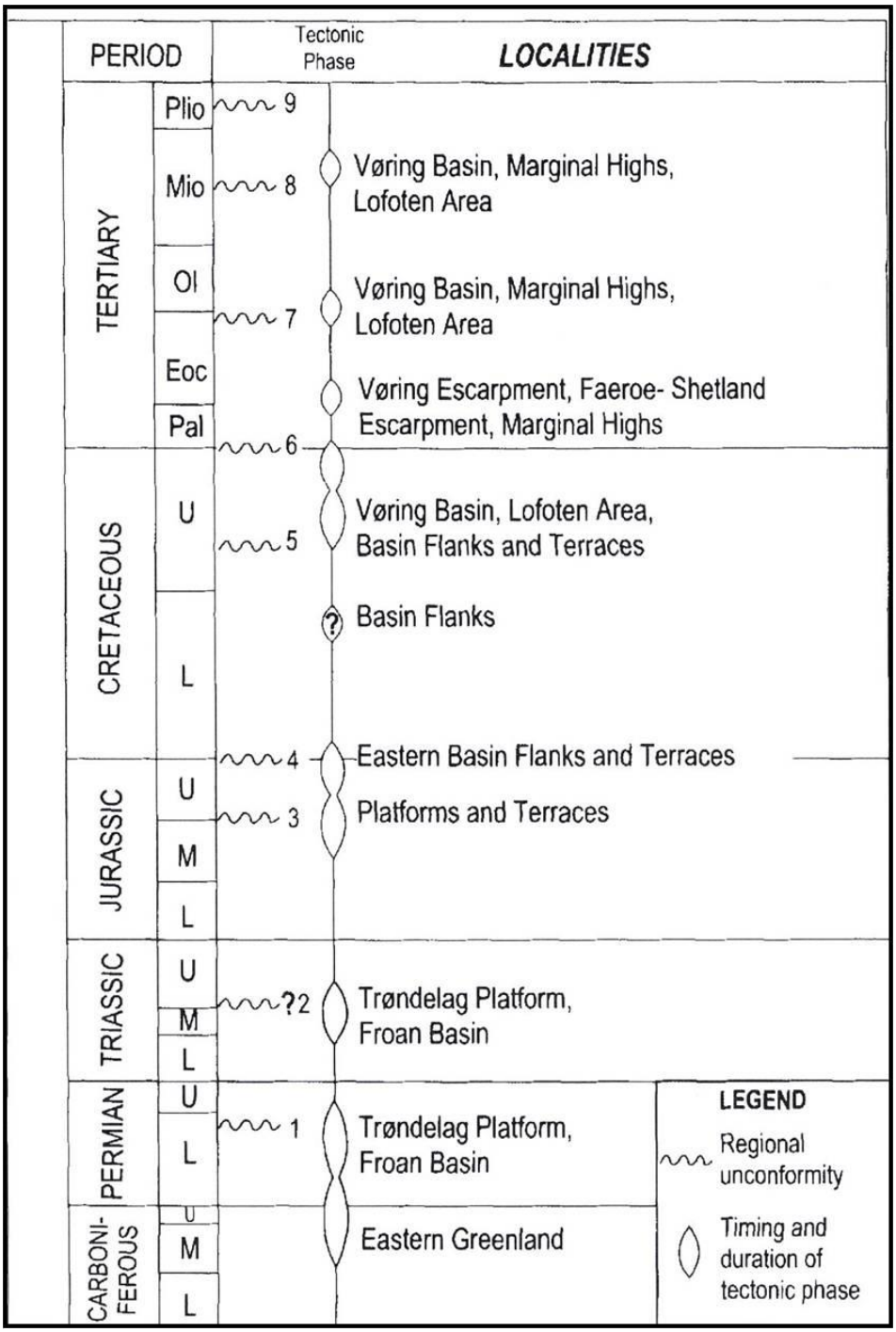

Fig.2.2 Tectonic history of Norwegian Sea Continental Margin (from Brekke, 2000)

During Triassic, alluvial and fluvial depositional environments prevailed over Norwegian Sea which was subjected by marine transgressions from north which resulted in mid-late Triassic halite (Brekke et al., 2001; Muller et al., 2005; Smelror et al., 2007).

Main source of sediments for the basin is thought to be the Scandinavian Caledonides in the west of present Norwegian Continental Shelf (Smelror et al., 2007). Major phase of uplift and erosion occurred in middle Triassic to early Jurassic time. This resulted in deposition of thick sequences of stacked channel continental conglomerates, sandstones, and fine clastics. These all sequences were deposited at the basin margins and boundaries (Brekke et al., 2001; Smelror et al. 2007; Gabrielsen et al., 2010).

Late Jurassic to the latest Ryazanian times are characterized by major regional tectonic extensional phase (Underhill, 1998; Brekke et al., 2001; Gabrielsen et al., 2001; Kyrkjebø et al., 2004; Smelror et al., 2007). This phase of extensional tectonics resulted in a clastic horst and graben province. The Halten Terrace area was exposed in E-W and NW-SE extensional regimes (Koch and Heum 1995; Smelror et al., 2007). The central parts like Møre and Vøring basins sank rapidly because they were already elevated and eroded areas. In Jurassic, Halten Terrace area was subjected to development of tilted fault blocks. Later it was buried at depth of 2.5 and 5 km (Fig. 2.2) (Smelror et al., 2007).

In Triassic to Middle Jurassic time, sea lever rose up and it flooded the major parts of the rift margins. This resulted in the deposition of formations like Melke and Spekk formation over large parts of Norwegian-Greenland Sea (Brekke et al., 2001; Smelror et al., 2001&2007). Regional sea level rise and tectonic movements created sill basin which restricted bottom water circulation. These silled basins became the most ideal area for the organic rich shales deposition together with deposition of Spekk formation (Smelror et al., 2007).

Base Cretaceous Unconformity (BCU) was formed by the erosion of tectonic fault blocks, which were buried during Cretaceous and Cenozoic times. Early Cretaceous is characterized by deposition of condensed carbonates on the structural highs in the area (Dalland et al., 1988; Smelror et al., 2007).

Early Cretaceous was time in which uplifting and tilting converted the bounding platform area to basin areas. Also in late Cretaceous, basin was subjected to uplifting and erosion which eroded the basin platforms and its flanks (Blystad et al., 1995; Brekke et al., 2001; Smelror et al., 2007).

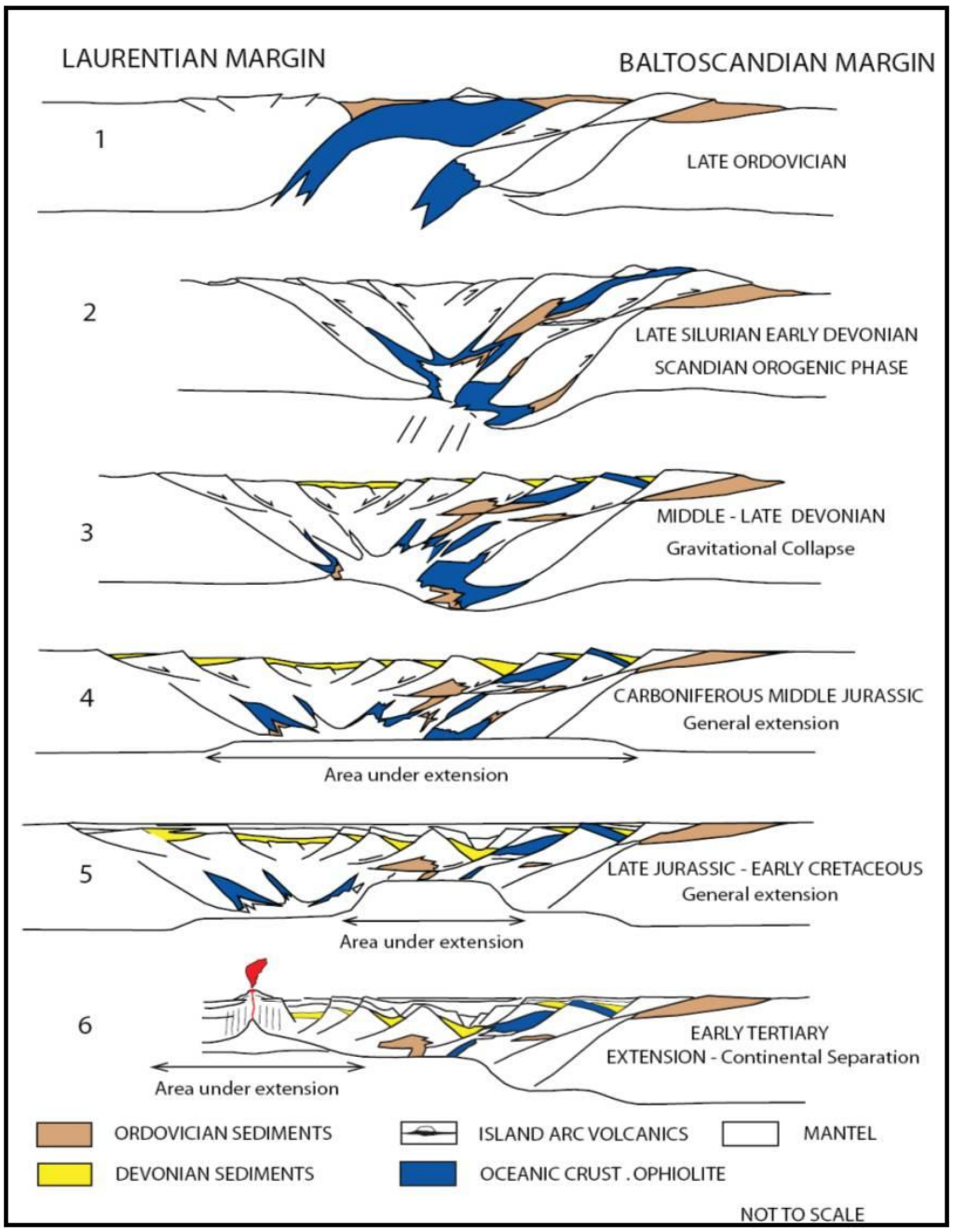

Fig. 2.2 Diagram illustrating the tectonic development of the Norwegian Continental Margin (after Skogseid et al., 1992)

2.2.3 Cenozoic

In latest Cretaceous and Early Paleocene, final rifting phase between Norway and Greenland occurred which resulted in continental separation in Early Eocene time (Fig. 2.2). Due to this rifting phase the western basins and the areas north of the Jan Mayen Lineament may have been affected (Smelor et al., 2007).

2.3 Opening of the Norwegian-Greenland Sea

Final break up of continental crust in between Norway-Greenland was caused in Early Eocene. This was coupled with uplifting of while Norwegian-Greenland Sea. In Late Cretaceous-Paleocene, crustal extension was mostly influential on Møre and Vøring basins. This crustal extension later shifted towards the centre of the basin with time (Doré et al., 1999; Brekke et al., 2001; Lundin and Doré, 1997; Smelror et al., 2007).

Late Cretaceous initial faulted started the tectonism and magmatism which continue for 15-20 My (Million years) till Paleocene-Eocene boundary. In final stages of Norway-Greenland continental separation, this magmatism and tectonism were at its peak. This resulted in pouring great quantity of lava on the main land of Norway (Henriksen et al., 2005).

2.3.1 Basin Inversion (Early Oligocene and Middle Miocene)

In Middle Eocene/Earl Oligocene and Middle Miocene, all basin present in Norwegian Sea margin faced compression (Doré and Lundin, 1996; Lundin and Doré, 2002; Smelror et al., 2007).

In Middle Miocene area was subjected to second phase of compression. This caused the uplifting of outer parts of the basin margins. These margins became the dominant sites of clay sedimentation. Till the end of Miocene, most of the Vøring Basin was filled with clay sediments (Brekke et al., 2001; Smelror et al., 2007).

"On the prominent part of the shelf, a prograding coastal/deltaic sequence of Upper Miocene-Lower Pliocene sand and siltstones(i.e. the Mole formation) developed from the Lofoten Islands in the north down to Haltenbanken (i.e. over a distance from 63-67°N)" Smelror et al., 2000 pp. 399).

2.3.2 Late Pliocene/Pleistocene

Late Neogene period is considered to be very active time for Norwegian mainland. In this time all area was subjected to kilometre scale uplifting, extensive erosion, and progradation which resulted in depositing Naust Formation. During Late Neogene, Møre shelf prograded 30-50 km while shelf edge of mid Norway shifted 100-150 km westwards (Rise et al., 2005; Smelror et al., 2007).

2.4 Tectonic elements of the Norwegian Continental Margin

The tectonic framework of Norwegian passive continental margin is characterized by NE-SW Cretaceous deep basins. Vøring and Møre basins are the part of these basins. These basins are surrounded by Paleo highs, platforms and elevated mainland. Møre and Vøring Marginal Highs are situated in west as platforms (Brekke, 2000).
Eastern side of the central part is covered by Late Jurassic-Early Cretaceous Torøndelag Platform. Main basin area in the north is bordered by NW-SE trending Bivrost Lineament. Deep Vøring basin and uplifted continental margin around the Lofoten are separated by this lineament (Brekke, 2000).
Møre Basin, Vøring Basin, and other lineaments are the main structural elements of the Norwegian Continental Shelf. Lineaments include Jan Mayen Lineaments, Bivrost Lineaments, Torøndelag Platform, Vøring Marginal High, Møre-Torøndelag Fault, Complex Møre marginal High and Storegga Slides. These elements are discussed below.

2.4.1 Jan Mayen Lineaments

The boundary between southern part of Møre Basin and northern part of Vøring basin is marked by Jan Mayen Lineament. Jan Mayen Lineament is defined by synistral shift of basin axis and flank (Brekke, 2000).

2.4.2 Bivrost Lineaments

Bivrost Lineament acts as a boundary between Vøring basin and narrow continental margin around Lofoten in the north. Bivrost Lineament can be characterized as dextral shift in the basin axes and flanks and it marks the northern limit of Torøndelag Platform (Brekke, 2000).

2.4.3 Vøring Basin

The Vøring Basin (64-68°N and 2-10°E) is a large basin which is characterized by graben, structural highs and sub basins (Bukovics and Ziegler, 1985). Vøring Marginal High and Vøring escarpment surrounds the Vøring Basin in the west and in east fault complexes and edges of Torøndelag Platform dounds the Vøring Basin. Various sills from Late Cretaceous-Paleocene age have intruded the Vøring Basin. These sills hide the seismic signature of underlying strata in the east (Blystad et al., 1995; Bukovics et al., 1984; Brekke, 2000).

2.4.4 The Vøring Marginal High

Jan Mayen and Bivrost Lineaments flank the Vøring Marginal High in the west of Vøring Escarpments. Cenozoic sediments overlie on the thick succession of Lower Eocene flood basalts. It is believed that these flood basalts are underlain by continental crust (Brekk, 2000).

2.4.5 Møre Basin

Møre Basin is defined by base Cretaceous unconformity. Møre Basin is bounded by Jan Mayen Lineament in north, Møre+Trøndelag Fault Complex in the southeast and Faeroe-Shetland Escarpment in the west. Mainly the structures lye in NE-SW direction (Brekk, 2000).

2.4.6 The Møre-Trøndelag Fault Complex

Møre-Trøndelag Fault Complex lies in the south-eastern part of the Møre Basin. This complex can be characterized by structural elements of NE-SW to ENE-WSW trending system of fault controlled highs ridges and small basins (Brekk, 2000).

It is believed that Møre-Trøndelag fault complex has been active and passive in geological history. And ENE-WSW trending structures of this complex can be related Caledonian deformation. It seems that this reactivation has an effect on the Precambrian basement and rocks of lower Palaeozoic Devonian and Jurassic ages (Bering 1992; Grønlie et al., 1994; Brekke, 2000).

2.4.7 The Møre Marginal High

Møre Marginal High is situated in the west of Faeroe-Shetland Escarpment. It is surrounded by Jan Mayen Fracture zone in the north and Faeroe Plateau in the south. Cenozoic sediments lye over the top of thick early Eocene flood basalts. Eastern flank of the Møre Basin is marked by the Early Cretaceous rift unconformity (Brekke, 2000).

2.4.8 Trøndelag Platform

Trøndelag Platform is defined by 160 km wide area between Norwegian mainland and Vøring Basin. Main structural elements of Trøndelag Platform are Nordland Ridge, Helgeland Basin Frøya High, Froan Basin, Vingleia fault complex and Ylvingen Fault zone. Trøndelag platform is surrounded by Revfallet Fault Complex in NW and in south it is bounded by Klakk fault complex. Bremstein Fault Complex bounds the

Trøndelag Platform in the west. In eastern flank crystalline basin outcrops from the sea floor along the coast (Bukovics et al., 1984; Blystad et al., 1995; Brekke, 2000).

2.4.9 Storegga Slide

Vøring basin in the North and the North Sea in the South bounds the Storegga Slide on the Norwegian Continental Shelf. Edges of the basin were the prominent location of depocentres in Late Pliocene-Pleistocene time (Hjelstuen et al., 1999 & 2004).

Low sediment supply and repetitive slide events are the major causes of thinner sediments in Storegga Slide of Plio-Pleistocene time supply (Evans et al., 2002; Hjelstuen 2004). Sedimentary successions are divided on the Norwegian Continental Shelf because of glacial erosion (Hjelstuen et al., 2004).

2.5 Stratigraphic Framework

The wells on the Mid Norwegian shelf have penetrated down to the pre Triassic succession. Borehole coverage of the upper Triassic through Tertiary sequence is good; however, less information is available for pre Triassic succession (Dalland et al., 1988). The Seismic reflection data suggests the presence of thick sequence in local fault bounded basins probably consisting of upper Paleozoic strata (Ehrenberg et al., 1992).

Middle Triassic to the Early Jurassic times continental strata were deposited on the Halten Terrace and the Trøndelag Platform. Triassic sedimentary succession comprises of two evaporates formation, red beds overlain by coal bearing delta plain clastic deposits of Åre Formation (Fig. 2.3) (Ehrenberg et al., 1992, Whitley, 1992).

In the Halten Terrace and Trøndelag Platform lower Jurassic succession corresponds to the Båt Group which is characterized by alternating sandstone and shale/siltstone units, while sandstone dominates the lithology, see Fig 2.3. The Båt Group is completely missing from the highest parts of the ridge. During the deposition of this group shallow marine to deltaic environment is dominated. (The Båt Group comprises of Åre Formation, Tilje Formation, Ror Formation and Tofte Formation. (Dalland et al., 1988).

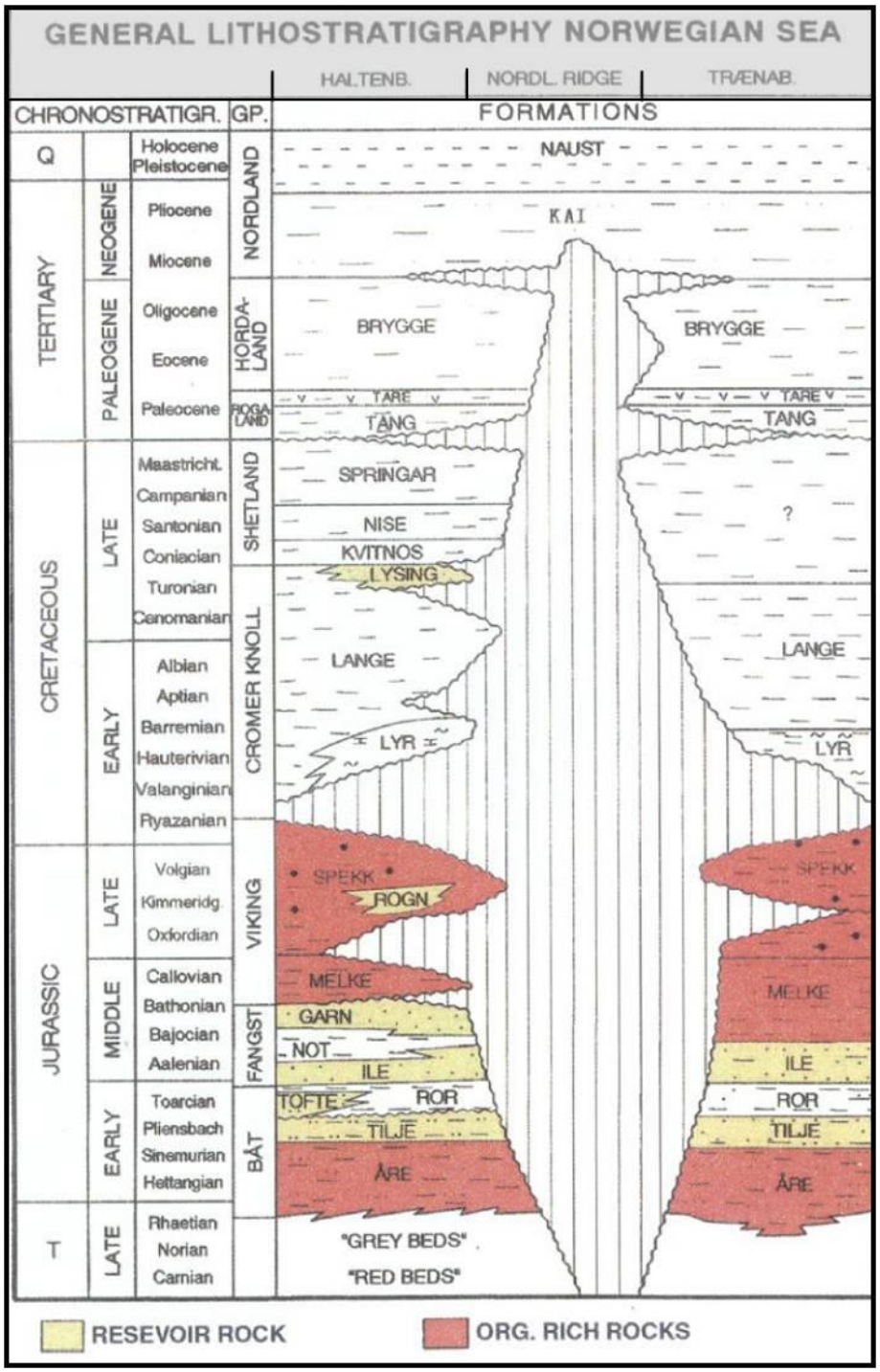

Fig.2.3: Generalize lithostratigraphic section and time from the Halten Terrace and Trænebanken. Colour formations are indicating source rocks and reservoir rocks in the area. (Modified from Karlsen et al., 1995).

The Åre Formation comprises of sandstone and clay interbedded with coal and coaly claystone (Dalland et al., 1988). Coal bearing part of Åre Formation is considered to have enormous hydrocarbon source potential (Heum et al., 1986; Forbes et al., 1991). Tilje Formation underlain by the Åre Formation and comprises of very fine grain to

coarse grain sandstone are interbedded with silt stone and shale (Dalland et al., 1988). However content of sand considerably increases from bottom to top (Heum et al., 1986). The Toft Formation overlies the Tilje Formation has been only documented in the western part of the Halten Terrace where it is consist of coarse grain sandstone. (Dalland et al., 1988) see Fig2.3. The sandstone of Toft formation interfinger with Ror Formation which is underlain by Tilje Formation on the Trøndelag Platform. The Ror Formation consists of grey to dark grey mudstone interbedded with silty and sandy coarsening upward sequence. (Dalland et al., 1988)

The Fangst Group signifies the Middle Jurassic sedimentary succession and generally correlated to the Brent group in the North Sea. The Fangst Group comprises of Ile Formation, Not Formation and Garn Formation and these units were deposited as a result of regression (Ehrenberg et al., 1992). The Ile Formation is characterized by fine to medium grain sandstone are interbedded with thinly laminated siltstone and shales. The formation has been recognized over the entire Haltenbanken area. On the Trøndelag Platform this unit generally thins towards east (Dalland et al., 1988). This unit is believed to have good reservoir rock properties (Provan, 1992). The Not formation consists of claystones and bioturbated fine grained sandstones which are locally mica rich and carbonate cemented. In the North Sea, no similar unit is identified (Dalland et al., 1988). The Garn formation is encountered on the most part of the Haltenbanken area; however the entire unit may be eroded from the structural highs. This unit consists of medium to coarse grained, moderately to well-sorted sandstones. (Dalland et al., 1988) This unit favoured the good to excellent reservoir rock properties (Heum et al., 1986).

During late Jurassic the Viking Group is deposited on the Haltenbanken and Trænebanken. It extends towards the basin margin on the eastern part of the Trøndelag Platform, where it has been encountered just beneath the sea floor at several locations (Bugge et al., 1984; as cited in Dalland et al., 1988). The Group is deposited in marine conditions, mainly below wave base on the Haltenbanken. It comprises of three formations; the Melke, the Spekk and Rogn formations. The Melke formation consists of abundantly grey to dark brown claystone, with siltstone and limestone interbeds. It is deposited in an open marine environment (Dalland et al., 1988). The Melke Formation is moderately organic rich (ca.1-4% TOC) (Ehrenberg et al., 1992), However it is not affirmed as source rock in the Haltenbanken area (Heum

et al., 1986). The overlying Spekk Formation was deposited throughout the Haltenbaken-Trænabanken area, however may be now absent from structurally high positions. It consists of dark brown to dark grey shale, predominantly noncalcareous. The organic content of this unit is very high, mainly Type II kerogen. The Spekk Formation was deposited in anoxic bottom water conditions and correlated with Draupne Formation in the Northern North Sea. (Dalland et al., 1988). This unit is acclaimed as source rock bearing oil generation potential. (Hollander et al., 1984; Heum et al., 1986; Karlson et al., 1984). The Rogn Formation is developed within Spekk Formation and it has coarsening upward sequence from siltstone and shale to sandstone (Dalland et al., 1988). This unit is proclaimed to have good reservoir properties as a result of upward decrease in clay and mica content. It is interpreted as shallow marine bar deposits (Ellenor & Mozetic, 1986; Dalland et al., 1988).

During the Cretaceous, shallow to deep marine environment is prevailed. The Comer Knoll and the Shetland groups were deposited on the Haltenbanken area (Dalland et al., 1988) consist mainly of shale with occasional turbiditic sandstones (Ehrenberg et al., 1992). These units are identified on the Halten Terrace, however the Comer Knoll Group locally absent from the Trøndelag platform. (Dalland et al., 1988). The Tertiary witnessed the clastic sedimentation (mainly claystone) on the Haltenbanken area comprises of the Rogaland and the Hordaland groups. (Dalland et al., 1988). These units consisting of marine shale can be separated from the upper cretaceous shales by regional unconformity (Heum et al., 1986).

On the Haltenbanken area, Kai Formation of Nordland Group makes unconformable contact with the underlying Paleogene sedimentary succession. The overlying Naust Formation were deposited in the late Pliocene and continuing through the Quaternary, consisting of alternating layers of grey shale and poorly sorted sand on the Haltenbanken (Ehrenberg et al., 1992).

Chapter 3

The Sample Set and Analytical Methods

In this chapter, the sample set and analytical methods (destructive analytical methods and non-destructive analytical methods), which are used for the investigation of organic contents in petroleum inclusions and core extracts are discussed. Analytical methods used in geochemical studies and correlations have developed tremendously over the last sixty years. Correlation techniques based on geochemical properties are detailed chemical characteristics (specific properties). The specific properties describe the sample on molecular level using for example gas chromatography-flam ionization detector (GC-FID) to give a chemical characterization of specific sample fractions.

The following section will describe the sample set and analytical methods used in this study and how they are used to calculate different parameters.

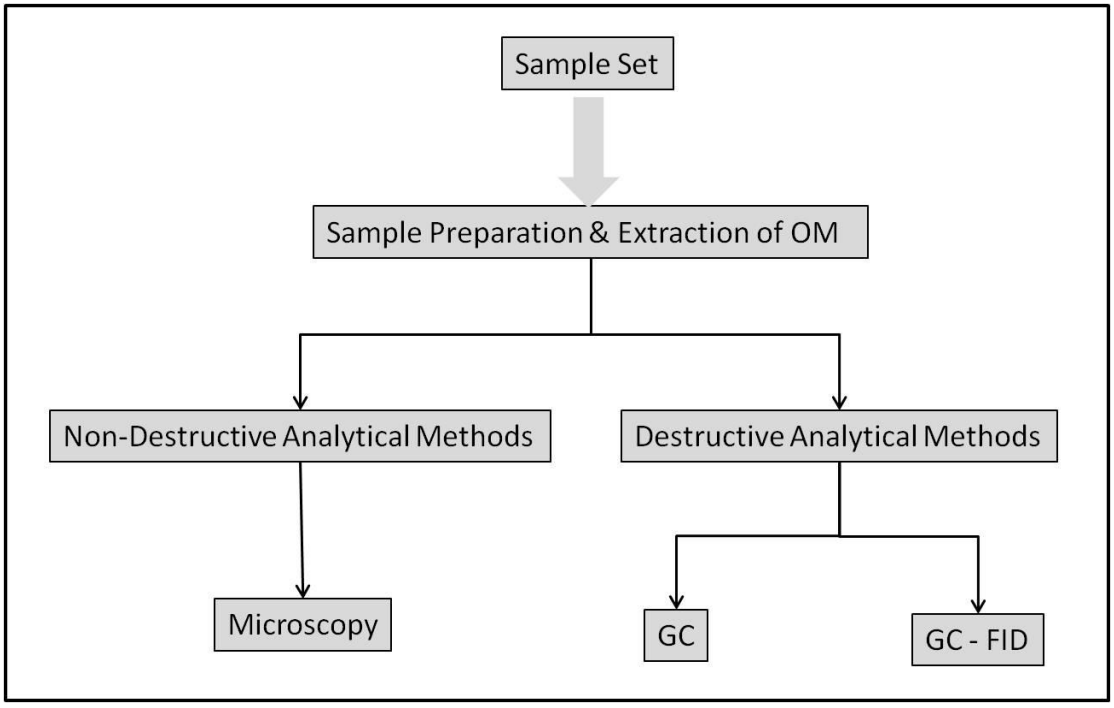

Figure 3.1: Workflow followed during the present study.

3.1 The sample set

18 core samples from the well 35/4-1 from North Sea, 16 core samples from the well 6610/3-1 and 14 core samples from the well 6610/2-1S from Norwegian Sea were obtained from the Norwegian Petroleum Directorate (NPD). All samples are shown in the table 3.1 representing their wells, depth and lithology.

Table 3.1 sample data set used during the study.

NO	Well	Depth (m)	Lithology	Well	Depth (m)	Lithology	well	Depth (m)	Lithology
1	35/4-1	4118.30	Sandstone	6610_3-1	1682.50	Sandstone	6610_2-1S	2091.50	Sandstone
2	35/4-1	4120.10	Sandstone	6610_3-1	1683.50	Sandstone	6610_2-1S	253.00	Sandstone
3	35/4-1	4125.10	Sandstone	6610_3-1	1711.50	Sandstone	6610_2-1S	2054.50	Sandstone
4	35/4-1	4151.55	Sandstone	6610_3-1	1714.50	Sandstone	6610_2-1S	2056.50	Sandstone
5	35/4-1	4152.50	Sandstone	6610_3-1	2294.50	Sandstone	6610_2-1S	2058.00	Sandstone
6	35/4-1	4154.50	Sandstone	6610_3-1	2299.50	Sandstone	6610_2-1S	2059	Sandstone
7	35/4-1	4155.50	Sandstone	6610_3-1	2301.00	Sandstone	6610_2-1S	2060.50	Sandstone
8	35/4-1	4156.50	Sandstone	6610_3-1	2306.00	Sandstone	6610_2-1S	2066.50	Sandstone
9	35/4-1	4157.05	Sandstone	6610_3-1	2311.00	Mudstone	6610_2-1S	2073.50	Sandstone
10	35/4-1	4166.30	Sandstone	6610_3-1	2521.00	Sandstone	6610_2-1S	2074.50	Sandstone
11	35/4-1	4172.60	Sandstone	6610_3-1	2522.80	Sandstone	6610_2-1S	2344.20	Sandstone
12	35/4-1	4184.50	Sandstone	6610_3-1	2664.50	Sandstone	6610_2-1S	2344.50	Coal
13	35/4-1	4205.30	Sandstone	6610_3-1	2670.50	Sandstone	6610_2-1S	2346.50	Coal
14	35/4-1	4216.0	Sandstone	6610_3-1	2677.50	Sandstone	6610_2-1S	2351.50	Coal
15	35/4-1	4219.00	Cemented sandstone	6610_3-1	3316.50	Sandstone	"	"	"
16	35/4-1	4222.00	Cemented sandstone	6610_3-1	3324.80	Sandstone	"	"	"
17	35/4-1	4242.50	Cemented sandstone	"	"	"	"	"	"
18	35/4-1	4248.30	Sandstone	"	"	"	"	"	"

The core sample were collected from the sandstone units in the wells but in well 6610/3-1, mudstone was encountered at the depth of 2311 m as shown in the table, and from well 6610/2-1S one coal seam sample is included from the depth 2344.50 m to 2351.50 m. Most of the sandstone samples are clean and well sorted from coarse to medium grain size.

3.2 Sample preparation and extraction of organic contents

The sandstone core samples were crushed manually to individual grains and were treated with H_2O_2 and washed with water to remove any clay and organic matter from the grains (Karlsen et al., 1993). These individual grains were used for gas analysis. Bitumen extract were produced by crushing sample aliquots powder to extract the solvent extractable organic contents and later these extractions were used for GC-FID. H_2O_2 is used to remove any residual and non-extractable organic matter from the fissures and cracks – prior to gas inclusion analysis. To extract the organic contents from the crushed core samples a conventional Soxtec system HT 1043 is used. Approximately 10 grams of the crushed sample (powder form) was filled into pre-extracted cellulose cartridges and covered with glass wool. Mixture of 93% dichloromethane and 7% of methanol is used as a solvent to extract the sample. For the extraction of organic contents, thimbles are used and each thimble is pre-extracted for about 10 minutes boiling and 20 minutes rinsing before used for sample extraction. Copper is added to the extraction solvent for the removal of elemental sulphur, but before using copper it was activated in concentrated HNO_3 and then washed with water, DCM and methanol. 50 ml solvent is then heated by the underlying stove to 60°C. Up to six samples are extracted at the same time by boiling for one hour and rinsing for two hours. The extract is transferred into 15 ml glass vial and these vials are sealed with Teflon lined plastic corks.

The extracted organic solvent is then concentrated and geochemically analyzed by GC-FID.

3.3 Destructive analytical methods

3.3.1 Gas Chromatography

Gas chromatography is a technique that separates a complex mixture of organic compounds like oil or gas into individual molecular type. Gas chromatography is a popular organic analytical technique as it is relatively easy to use and easily

automated. It separates substances on molecular level from a complex composition according to boiling point and the results are both reproducible and accurate. The principle for boiling point chromatography is that the analyte will partition between the stationary phase (the column) and the mobile phase (the carrier gas plus analyte) itself. Complex organic mixtures will be separated – sometimes into individual molecular types like n-alkanes - according to boiling point and also to some extent according to isomer contrasts.

3.3.1.1 Carrier Gas

The mobile phase in gas chromatography is the carrier gas which moves the analyte through the column during chromatography. The carrier gas must be inert to avoid interaction with the sample that is analyzed. Nitrogen, helium and hydrogen are commonly used gases in this technique. Hydrogen gas is explosive in nature and it needs special precautions. Helium is very expensive and has low viscosity at high temperature meaning that chromatography can be done rapidly. Nitrogen is not as expensive as helium and it is safe to use. It is a heavy gas which results in low peak broadening during chromatography. The type of carrier gas has an effect on the efficiency of the column and the analysis time. Gas is transported from the cylinder into the chromatograph by a given pressure that can be adjusted. Typical pressures of 2-3 bars are normal. The control system makes sure that the required pressure value and flow-speed of the gas into chromatograph is correct.

3.3.1.2 Injector and column

In gas chromatography, the unit where the sample is vaporized and introduced into the column is called the injector. The injector is kept isothermally at 300^{o}C and column. Sample prepared for analysis is injected, vaporized and transported through the column. Some high boiling substances from the sample do not flow through column and the reason is that they are absorbed in the injector. The columns are historically made of metal, glass or as today quartz and two types are common.

Support coated open tubular – in particular for analysis of gases. These have a “thick” wall coating of inorganic or organic adsorbent which helps to retain the analyte and cause separation. Open tubular capillary column usually has small diameter and there is an organic coating on the inner tube wall acts as the stationary phase. Substances flow through the hole in the center of the column.

The temperature has to adjust and it should be high enough for the sample to be vaporized – together with the solvent - straight away.

The analytical program for the column is a time temperature programmed function with one or several gradients adjusted to cause the required separation of the components in the analyte.

3.3.1.3 Detector

As components exit the column, they need to be detected and quantified. Thus, a detector detects the different substances separated in the column. Two types of detectors, like the concentration dependent detectors and the mass flow dependent detectors represent different ways of detecting these substances. The two most commonly used detectors are the Thermal Conductivity Detector (TCD) and Flam Ionization Detector (FID). The change in heat properties of the column effluent is measured by the TCD as the sample passes through and it does not destroy the organic compounds in that process, but its major drawback is that it has less dynamic linear range compared to a FID and also lowers absolute detection. The FID destroys the sample as it burns the organic compounds. However, the FID is at least two orders of magnitude more linear than the TCD. It is also more sensitive and requires less service.

3.3.1.4 GC analysis of core samples

The GC analysis will in this project be used to identify light hydrocarbons including C_1-C_5 which is our objective in this study. To measure the accuracy of the apparatus, a standard gas which is a combination of methane, ethane and propane with the same concentration i-e 500ppm is run and it will produce a GC-FID trace of C_1, C_2 and C_3 as shown in Figure 3.1.

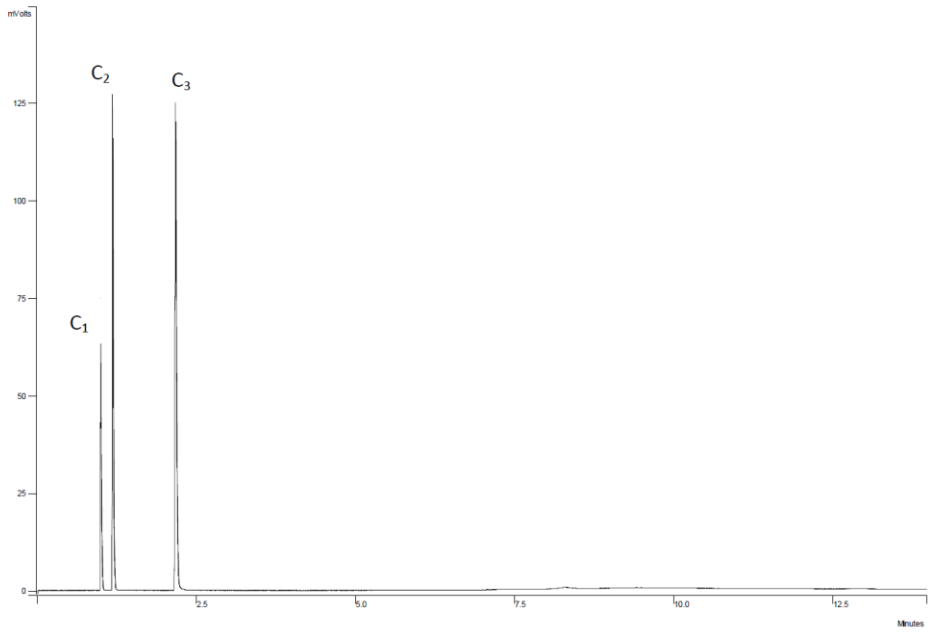

Figure 3.1 the standard gas used to calibrate the response factors. All methane, ethane and propane (C_1-C_3) gas species in this chromatogram are present in 500ppm concentrations, showing C_1, C_2 and C_3 produced from standard gas that is composed of methane, ethane and propane.

A sample from the well 35/4-1 from the depth 4118.3 m is analyzed on gas chromatography and produced a chromatogram showing C_1-C_5 (methane-pentane) which is shown in figure 3.2.

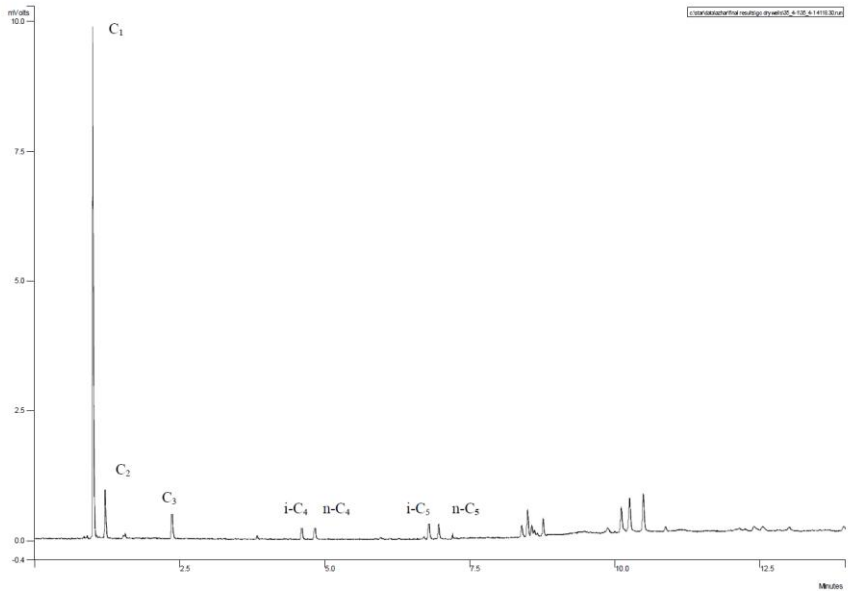

Figure 3.2 GC-FID analysis of gas from inclusions reveals the HCs species in the inclusions. In this sample from 35/4-1, 4118.3m are the C_1- C_5 components clearly discernible and the common gas wetness parameters can be calculated.

3.3.2 Gas Chromatography-Flame Ionization Detector (GC-FID)

This technique is used for quantification of individual hydrocarbon components and is carried out on whole oil, total extracts or saturated or aromatic hydrocarbon fractions of crude oils and bitumen. GC-FID can also provide general basic information on the source rock type and maturity of the analyzed oil or bitumen and is also used to map the regional, vertical, and temporal extent of contamination, to differentiate petroleum contamination from natural background, and to assess the effectiveness of biodegradation (Peters et al., 2005).The GC-FID instrument shown in figure 3.1 is used for geochemical screening of samples to obtain information about n-alkanes and isoprenoid distributions. Information about steranes and terpanes may also be obtained in some cases.

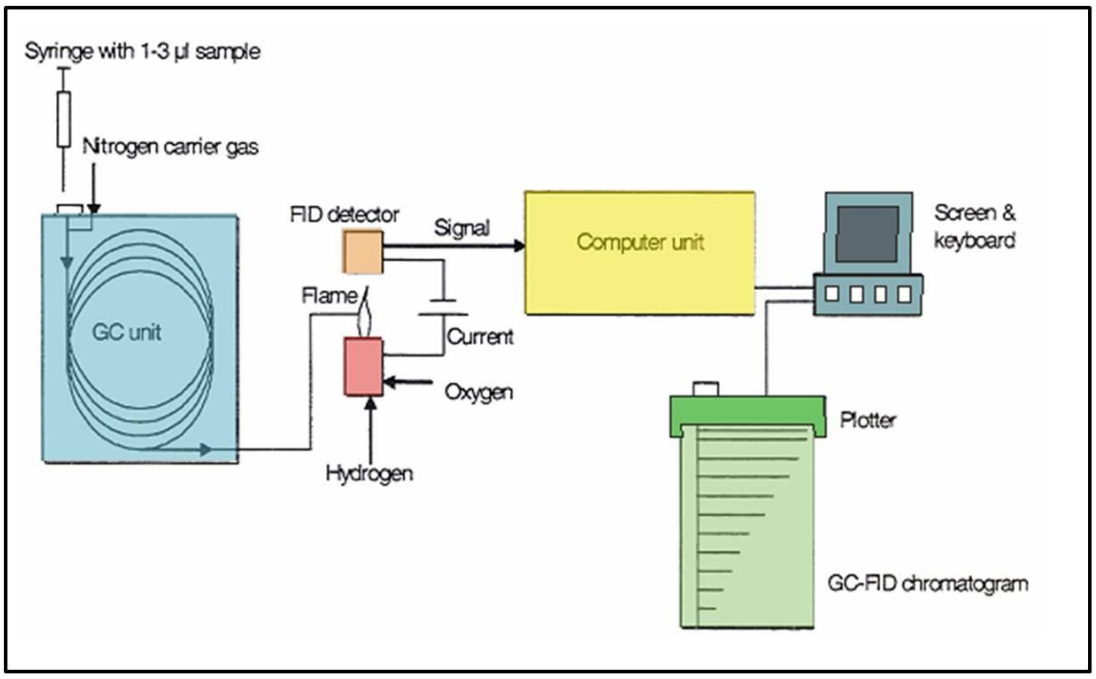

Figure 3.3.The principles of the GC-FID instrument (Modified after Pedersen, 2002)

GC-FID analysis is aimed to obtain specific description of molecular compounds, some of the most common parameters are:

Pristane/Phytane (Pr/Ph)

Pristane/n-C_{17}

Phytane/n-C_{18}

These compounds are common parameters used in organic petroleum geochemistry, and they are mainly used as maturity and facies indicators, but GC-FID chromatograms can also be applied for general fingerprinting of the sample.

Other important elements of the GC-FID analysis is the display of the n-alkane profile, is this front end biased as from algal source rocks, or heavy end-biased as from land plants? Is there an unresolved complex mixture (UCM) present or not? Is there any carbon preference index (CPI)? See Peters et al. (2005) for a review of these parameters.

The GC-FID instrument used in this study is Varian CP- 3380 gas chromatograph with flame ionization detector (FID) and nitrogen as carrier gas. Temperature programming was 80°C for 1 minute then an increase of temperature at a rate of 4.5 °C /min to a final temperature of 320°C held for 20 minutes. Total analytical time of the whole process for one sample was 79 minutes.

3.3.2.1 GC-FID of core samples

The GC-FID of core samples has been used to analyses n-C_{17}, n-C_{18}, pristane and phytane that can give important information about source and depositional facies, maturity.

3.3.2.2 Pristane/Phytane

The common type of isoprenoid isoalkanes are pristane and phytane. According to Tissot and Welte (1978) they are derived from phytol, which is a side chain of chlorophyll, and is the most abundant source of isoprenoid. Tissot and Welte (1984) stated that this relation indicates the red-ox potential of the source rock, i.e. reflecting the amount of oxygen present during deposition. Phytol is altered into pristane or phytane and that is determined by the depositional environment. If oxygen is not present during deposition, phytane is formed by simple reduction of phytol, while in case of abundant oxygen; phytol is oxidized to phytanic acid and decarboxylated to form pristane. Thus pristane/phytane is vital tool that will provide information about the depositional environment with respect to oxic or anoxic deposition environment, and following intervals will help to describe them; If

i. Pr/Ph > 1 indicates oxidizing or hypersaline environment.

ii. Pr/Ph < 1 indicates anoxic, carbonate or lacustrine environment.

iii. Pr/Ph = 1. 3 – 1. 7 indicates marine environment.

iv. Pr/Ph → 2. 5 indicate marine environment with considerable amount of terrestrial contents.

v. Pr/Ph > 3 – 10 indicates that abundant woody material exists in the source rock for oils or that the petroleum is derived from coal.

Since phytane is more unstable with increasing source rock temperature than pristane, the Pr/Ph ratio will increase as maturity increases. A core sample from well 35/4-1 at a depth of 4205.30 m is analyzed on GC-FID and chromatogram is produced showing pristane, phytane, n-C_{17} and n-C_{18}, and the pr/ph ratio in this chromatogram indicating the marine environment which is shown in figure 3.4.

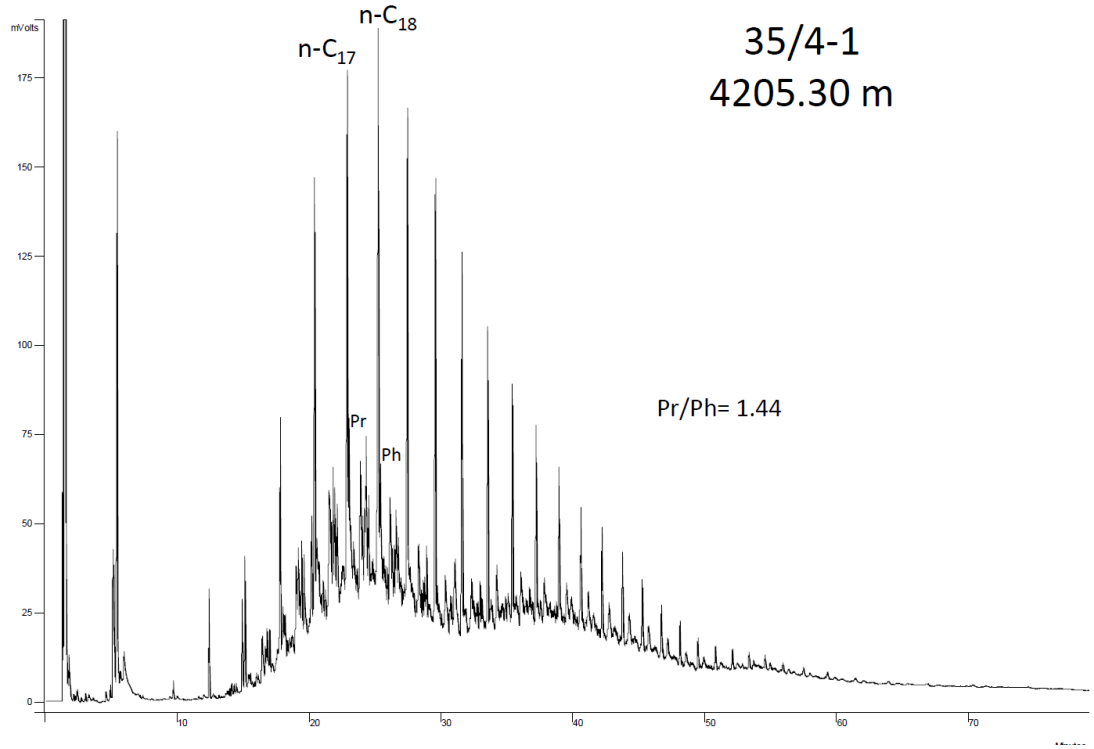

Figure 3.4 GC-FID chromatogram of extracted bitumen from sandstones from well 35/4-1, 4205.30 m showing n-C_{17} and n-C_{18} and the isoprenoid pristane and phytane. Also note the significant unresolved complex mixture (UCM) signifying paleo-biodegradation before arrival of a later oil charge (Karlsen et al., 2006).

3.3.2.3 Pristane/n-C_{17} and Phytane/n-C_{18}

Pr/n-C_{17} and Ph/n-C_{18} are used as a maturity indicator for organic matters of the same source facies as their values decrease with increasing maturity. According to Tissot et al (1971) Isoprenoids are thermally more unstable than n-alkanes. This parameter should be interpreted with caution because the Pr/n-C_{17} and Ph/n-C_{18} ratios are also

affected by biodegradation. Their low ratios indicate more mature samples because the isoprenoid will break down earlier than n-alkanes during maturation as tertiary carbon-carbon bonds have lower stability than primary and secondary carbon bonds. Note that a shift along the axis 90 degrees to the maturity/biodegradation axis in figure 3.4 will reflect facies shifts.

3.4 Non-destructive analytical methods

3.4.1 Microscopy - identification of petroleum inclusions

Microscopy is well established technique for petrographic studies of petroleum inclusions. When thin sections or simple cleansed sand grains are exposed to UV light, petroleum emits fluorescent light in the visible range that makes it possible to separate from aqueous fluids which are non-fluorescent (Karlsen et al, 1993). The fluorescent color of petroleum inclusions reflects the composition. The main fluorescent components in petroleum are aromatic hydrocarbons (Hagemann and Hollerbach, 1986: Khorasani, 1987), and NSO compounds. Sellwood et al. (1993) described the general fluorescence response for different gravity oils and made it possible to indicate the oil type visually.

The most common occurrence of petroleum inclusions in clastic reservoirs is in secondary quartz (Munz, 2000). The precipitation of quartz cement in sandstone is controlled by the rise in temperature during burial (Walderhaug, 1994). The rate of inclusion formation is exponential in temperature and starts effectively from about 100 ^{o}C (Nedkvitene et al., 1993). Observations of inclusions in the microscope allows tentative estimates of the gas to oil ratio (GOR) of the entrapped fluid and similar first order estimates of the API (Nedkvitne et al., 1993; Karlsen et al., 1993). It is possible that during rapid subsidence most of the inclusions will be formed at greater depth and when subduction is slow inclusions will be formed at several levels during burial. The amount of inclusions is determined by observing samples through the microscope. The microscope used in this study is Nikon Microscope (MICROPHOT S-A). All samples viewed in the microscope were cleansed to remove any residuals from the surface of the grain and also any external HCs species attached to the grains.

Chapter 4

Results

Results from the various analytical methods utilized on these samples are presented in this chapter. The methods used in this study are described in more detail in chapter 3, and on the basis of the results the discussion and interpretations will be followed in chapter 5. The purpose of this chapter is to provide a description of the geochemical results and parameters for each well by presenting the results in the form of chromatograms and tables. Results obtained from the different analytical methods are presented as followed.

- Gas Chromatography (GC) analysis of gases (C_1-C_5)
- Gas Chromatography-Flam Ionization Detector (GC-FID) of C_{15}+ core extracts
- Microscopy of fluid inclusions

4.1 Gas Chromatography (GC) analysis of gases (C_1-C_5)

Core samples from three different wells from the North Sea and the Norwegian Sea were analysed for gas in inclusions using GC-FID. The compounds of main interest in this study are in particular methane to pentane C_1-C_5. According to the Norwegian Petroleum Directorate (NPD) oil based mud, water based mud and ANCO 2000 mud was used during drilling in well 35/4-1, 6610/3-1 and 6610/2-1S respectively. Such organic material is cleansed off the grains prior to analysis. The presentation of each well and their percentage values of C_1-C_5 compounds are given in table 4.1, 4.2 and 4.3. All chromatograms from gas analysis are found from figure 4.1-4.13. Some of the chromatograms were not easy to interpret because they were having a low signal to noise ratio particularly in well 6610/3-1, and therefore - in some chromatograms from these samples the peaks of C_2-C_5 has been "zoom-up" from mille-volts to micro-volts to facilitate peak identification which is necessary for parameter calculations.

Well 35/4-1

According to geochemical information on NPD oil based mud is used from 2650m to 4812m that contains considerable hydrocarbon signature and that has caused a huge amount of uncertainty in the geochemical interpretation of core extracts, but gas chromatography of inclusions is one of the most reliable ways to obtain geochemistry

from such contaminated strata. This is due to the fact that inclusions are hermetically sealed testers of reservoir fluid and as such impervious to drilling muds. Still, the full GC-FID results of core extracts are presented below as there are cases in which even extensively contaminated wells will produce "non-contaminated" core extracts. The data obtained from core samples of well 35/4-1 by using GC analysis is presented in this section. The compound of interest in the gas analysis are mainly C_1-C_5 HCs. Table 4.1 gives the gross composition in terms of volume % of light HCs and other calculated parameters. These core samples are taken from the reservoir zone and the major lithology is very fine grained sandstone grading into siltstones and mudstones, but there is small interval of cemented sandstone from 4219 m to 4242.5 m. The values of C_1-C_5 vary as the depth increases but the lowest values of C_1-C_5 content is calculated at 4184.5 m depth and highest values of C_1-C_5 is calculated at 4248.3 m depth. Representative chromatograms of samples from this well are shown in Figure 4.1-4.4 and all chromatograms with their peak identification are found in in Appendix A, and tabulated parameters are found in Table 4.1. Some of the chromatograms are selected to illustrate variations or uniformities are discussed below.

35/4-1, 4118.3 m: The chromatogram from the gas analysis of the core sample from the depth 4118.3 m gives a C_1% 82.36, C_2% 6.41, C_3% 3.51, iC_4% 2.25, nC_4% 2.53, iC_5% 2.95 and nC_5%2.25. The sample contains light $_{HCs}$ in the range of C_1 to C_5. There are no light $_{HCs}$ identified below C5 (See Table 4.1, Figure 4.1 and Appendix A).

35/4-1, 4155.5 m: On the gas analysis of the core sample from the depth 4155.5 m the produced chromatograms contains light $_{HCs}$ from $C_1$to C_5. The calculated values in terms of % are illustrated in Table 4.1 and highest value is C_1% which is 82.77% and lowest value is 1.3% which belongs to i-C_4 (See Table 4.1, Figure 4.2 and Appendix A).

35/4-1, 4184.5 m: The chromatogram produced by the gas analysis from the depth 4184.5 m (See Table 4.1, Figure 4.3 and Appendix A) contains light HCs in the range of C_1-C_5 and no light $_{HCs}$ are observed below C_5. The highest value of C1% is computed in this sample set from this well which is 91.86% of the total light HCs and lowest value of n-C_4 is computed which 0.91% of the total light HCs in this sample set (See Table 4.1, Figure 4.2 and Appendix A).

35/4-1, 4248.3 m: The lowest C_1% value from the sample set from this well is computed on the basis of chromatogram produced by gas analysis. The C_1% 61.98,

C_2% 12.97, C_3% 10.92, i-C_4% 2.57, n-C_4% 8.13, i-C_5% 3.43 and n-C_5% 6.53 is computed. The light $_{HCs}$ ranges from C_1-C_5 is identified and below C_5 no light HCs are observed (See Table 4.1, Figure 4.4 and Appendix A).

Well 6610/3-1

The data on gas from inclusions obtained from well 6610/3-1 is presented in Table 4.2. Peaks are measured from C_1-n-C_5, and computed different parameters which are presented in Table 4.2. Representative chromatograms from this well are shown in Figure 4.5 to 4.9 and all chromatograms with identified peaks are found in Appendix A. Chromatograms from the sample set from this well is selected to illustrate the homogeneities or discrepancies are discussed below.

6610/3-1, 1682.5 m: The chromatogram produced by gas analysis from the depth 1682.5 m contains C_1-C_5 light HCs. The % values of C_1-C_5 are computed on the basis of peaks identified on chromatograms and their values are 98.01, 1.15, 0.46, 0, 0, 0.38 and 0.61 for C_1%, C_2%, C_3%,i-C_4%, n-C_4%, i-C_5% and n-C_5% respectively (See Table 4.2, Figure 4.5 and Appendix A). On the basis of computed values, wetness and/or dryness parameter can be calculated.

6610/3-1, 2301 m: The chromatogram from the depth 2301 m produced and computed C_1% 86.37, C_2% 2.9%, C_3% 1.96, i-C_4% 3.93, n-C_4% 1.51, i-C_5% 3.32 and n-C_5% 1.06. The light $_{HCs}$ ranges from C_1-C_5. The highest peak observed in the chromatogram is C_1 and the lowest peak is n-C_5 (See Table 4.2, Figure 4.6 and Appendix-A)

6610/3-1, 2664.5 m: From the chromatogram produced by gas analysis from the depth 2664.5 m (See Table 4.2, Figure 4.7 and Appendix A) C_1%-C_5% values are computed. The light $_{HCs}$ ranges from C_1-C_5 in this chromatogram. The computed values of C_1%, C_2%, C_3%, i-C_4%, n-C_4%, i-C_5% and n-C_5% are 97, 1.87, 0.37, 0.32, 0.23, 0.21, and 0.18 respectively.

Table 4.1 Results on the amount and composition of gas from inclusions from well 35/4-1 including C_1%-C_5%, i-C_4/n-C_4, i-C_5/n-C_5, C_2+, C_1ppm and C_1ppm/g rock.

No	Well	C1%	% Ro C1	C2%	% Ro C2	C3%	% Ro C3	sum%	∑C2+	C1ppm	C1ppm/g rock	C1/(C2+C3)
1	35/4-1	82.36	0.30	6.41	0.77	3.51	0.57	100.00	17.64	94.75	18.95	8.30
2	35/4-1	84.15	0.43	5.62	0.87	3.36	0.60	100.00	15.85	124.01	24.80	9.37
3	35/4-1	83.54	0.34	7.57	0.65	3.44	0.58	100.00	16.46	116.29	23.26	7.59
4	35/4-1	82.33	0.30	6.68	0.74	4.28	0.44	100.00	17.67	132.72	26.54	7.51
5	35/4-1	83.15	0.89	7.49	0.65	4.34	0.43	100.00	16.85	189.69	37.94	7.03
6	35/4-1	78.12	0.19	7.40	0.66	5.36	0.30	100.00	21.88	219.94	43.99	6.12
7	35/4-1	82.77	0.32	7.27	0.67	4.33	0.43	100.00	17.23	194.60	38.92	7.13
8	35/4-1	84.62	0.39	7.07	0.69	3.62	0.55	100.00	15.38	115.94	23.19	7.92
9	35/4-1	87.54	0.54	5.81	0.85	2.72	0.75	100.00	12.46	113.98	22.80	10.26
10	35/4-1	90.01	0.71	4.51	1.04	1.56	1.11	100.00	9.99	91.83	18.37	14.82
11	35/4-1	90.72	0.77	4.19	1.84	1.43	1.17	100.00	9.28	86.12	17.22	16.13
12	35/4-1	91.86	0.87	3.28	1.27	1.52	1.13	100.00	8.14	68.53	13.71	19.15
13	35/4-1	87.91	0.56	4.19	1.09	2.28	0.87	100.00	12.09	76.72	15.34	13.60
14	35/4-1	75.83	0.15	4.40	1.06	3.01	0.68	100.00	24.17	122.78	24.56	10.23
15	35/4-1	87.85	0.56	5.54	0.89	2.31	0.69	100.00	12.15	100.71	20.14	11.20
16	35/4-1	73.31	0.11	4.18	1.09	1.74	1.05	100.00	26.69	99.70	19.94	12.37
17	35/4-1	72.05	0.09	6.66	0.74	3.65	0.54	100.00	27.95	121.18	24.24	6.99
18	35/4-1	61.98	0.03	12.97	0.27	10.92	0.04	100.00	38.02	561.24	112.25	2.59

6610/3-1, 3316.5 m: The chromatogram resulting from the gas analysis of core sample from the depth 3316.5 m shows C_1% 91.47, C_2% 4.57, C_3% 1.76, i-C_4% 0.59, n-C_4% 0.88, i-C_5% 0.73 and n-C_5% 0.59 (See Table 4.2, Figure 4.8 and Appendix A). The chromatogram ranges light $_{HCs}$ from C_1-C_5. The i-C4/n-C4 and i-C5/n-C5 ratios are calculated and their values are 0.67 and 1.25 respectively.

6610/3-1, 3324.8 m: The chromatogram of the core sample from the depth 3324.8 m (See Table 4.2, Figure 4.9 and Appendix A) gives C_1%, C_2%, C_3%, i-C_4%, n-C_4, i-C_5 and n-C_5% values which are 85.53, 7.09, 2.95, 1.48, 1.48, 1.48 and 0.89 respectively and the sum of these % is 100 which show the accuracy of the results. The chromatogram shows that the light $_{HCs}$ ranges from C_1-C_5 and below C_5 no detectable $_{HCs}$ are identified from the produced chromatogram.

Well 6610/2-1S

Samples from the depth of 2051.5m to 2351.5m are used for geochemical analysis in this well. According to NPD, it is the case that in well 6610/2-1S polyethylene glycol has been used as a drilling mud which has also affected the conventional core extracts from this well. All samples from this well show well define C_1- C_5 peaks, exemplified in Figure 4.10 to 4.13 and Appendix A. These peaks were identified, calculated and presented in Table 4.3 and values from C_1 to n-C_5 vary from the depth of 2051.5 m to 2351.5 m.

Some of the chromatograms produced by gas analysis are illustrated in terms of variations or uniformities which are as follows:

6610/2-1S, 2053 m: The chromatogram produced by gas analysis from the depth 2053 m (See Table 4.3, Figure 4.10 and Appendix A) shows C_1% 81.6, C_2% 6.22, C_3% 4.48, i-C_4% 1.82, n-C_4% 3.64, i-C_5% 2.24 and n-C_5% 2.66. The sum of % from C_1-n-C_5 is 100 which show no error in the computing procedure. Ratio of i-C_4/n-C_4 and i-C_5/n-C_5 gives 0.5 and 0.84 respectively.

6610/2-1S, 2066.5 m: The chromatogram resulting from the gas analysis from the depth 2066.5 m (See Table 4.3, Figure 4.11 and Appendix A) gives i-C_4/n-C_4 ratio 0.57 and i-C_5/n-C_5 ratio 0.8. C_2+, C_1ppm and C_1ppm/g are also computed and values are 11.91, 66.54 and 13.31 respectively. The values of C_1% to n-C_5% is computed which are 88.09, 4.41, 2.91, 1.22, 2.14, 1.22, and 1.53 respectively.

Table 4.2 Gas data on gas from inclusions from the well 6610/3-1 using GC-FID analysis of inclusion.

No	Well	C1%	% Ro C1	C2%	% Ro C2	C3%	% Ro C3	sum%	∑C2+	C1ppm	C1ppm/g rock	C1/(C2+C3)
1	6610_3-1	98.01	1.69	1.15	1.76	0.46	1.63	100.00	1.99	36.75	7.35	60.86
2	6610_3-1	96.84	1.50	1.04	0.49	0.55	1.58	100.00	3.16	41.70	8.34	60.57
3	6610_3-1	96.89	1.50	1.63	1.64	0.49	1.61	100.00	3.11	39.99	8.00	45.85
4	6610_3-1	96.85	1.50	1.67	1.63	0.51	1.59	100.00	3.15	42.36	8.47	44.48
5	6610_3-1	87.86	0.56	4.04	1.12	2.45	0.83	100.00	12.14	44.67	8.93	13.55
6	6610_3-1	88.08	0.57	3.15	1.29	2.34	0.86	100.00	11.92	38.06	7.61	16.05
7	6610_3-1	91.65	0.86	2.72	1.39	1.79	1.03	100.00	8.35	23.69	4.74	20.33
8	6610_3-1	89.12	0.65	2.98	1.32	2.48	0.81	100.00	10.88	125.89	25.18	16.34
9	6610_3-1	86.37	0.48	2.90	1.34	1.96	0.94	100.00	13.63	18.62	3.72	17.75
10	6610_3-1	95.96	1.36	1.62	1.64	0.71	1.50	100.00	4.04	42.00	8.40	41.18
11	6610_3-1	90.44	0.74	2.99	1.32	1.88	1.00	100.00	9.56	49.20	9.84	18.57
12	6610_3-1	97.00	1.52	1.87	1.58	0.37	1.68	100.00	3.00	88.36	17.67	43.23
13	6610_3-1	90.52	0.75	2.62	1.40	1.56	1.11	100.00	9.48	49.37	9.87	21.66
14	6610_3-1	87.11	0.52	3.29	1.25	2.59	0.79	100.00	12.89	57.41	11.48	14.82
15	6610_3-1	91.47	0.84	4.57	1.03	1.76	1.04	100.00	8.53	206.74	41.35	14.45
16	6610_3-1	85.53	0.43	7.09	1.43	2.95	0.71	100.00	14.47	202.84	40.57	8.52

6610/2-1S, 2073.5 m: The Chromatogram produced from the gas analysis of core sample from the depth 2073.5 m (See Table 4.3, Figure 4.12 and Appendix A) shows C_1%, C_2%, C_3%, i-C_4%, n-C_4%, i-C_5% and n-C_5% which are 81.81, 2.85, 2.79, 3.9, 4.19, 4.46 and 3.63 respectively and their sum is 100%. The i-C_4/n-C_4 and i-C_5/n-C_5 ratios are 0.93 and 1.23 correspondingly.

6610/2-1S, 2344.2 m: C_1%, C_2%, C_3%, i-C_4%, n-C_4%, i-C_5% and n-C_5% are computed from the chromatogram produced by gas analysis from the depth 2344.2 m and their respective values are 98.16, 1.42, 0.43, 0, 0, 0 and 0 (See Table 4.3, Figure 4.13 and Appendix A). The chromatogram shows that the light $_{HCs}$ ranges from C_1-C_5 and below C_5 no light HCs peak is identified on the chromatogram. These values are helpful in determining the wetness parameters of light HCs. The C_1 ppm and C_1ppm/g is also calculated and their values are 55.03 and 11.01 respectively and the weight of the core sample which is used in this gas analysis is 5 gram.

Table 4.3 Analytical results and peak ratios on $_{HCs}$ gas species C_1-C_5 for gas in inclusions from well 6610/2-1S.

No	Well	C1%	% Ro C1	C2%	% Ro C2	C3%	% Ro C3	sum%	∑C2+	C1ppm	C1ppm/g rock	C1/(C2+C3)
1	6610_2-1S	81.60	0.28	6.22	0.80	4.48	0.41	100.00	18.40	106.96	21.39	7.63
2	6610_2-1S	81.67	0.28	5.60	0.88	4.53	0.40	100.00	18.33	122.38	24.48	8.06
3	6610_2-1S	89.48	0.67	3.66	1.19	2.44	0.83	100.00	10.52	96.98	19.40	14.67
4	6610_2-1S	89.32	0.67	3.31	2.13	2.45	0.83	100.00	10.68	90.99	18.20	15.49
5	6610_2-1S	80.25	0.24	6.36	0.78	4.74	0.37	100.00	19.75	162.44	32.49	7.23
6	6610_2-1S	88.09	0.57	4.41	1.06	2.91	0.71	100.00	11.91	66.54	13.31	12.03
7	6610_2-1S	81.81	0.28	2.85	1.34	2.79	0.83	100.00	18.19	48.89	9.78	14.52
8	6610_2-1S	92.36	0.47	2.45	1.44	1.10	1.30	100.00	7.64	55.90	11.18	25.96
9	6610_2-1S	98.16	1.73	1.42	1.69	0.43	1.64	100.00	1.84	55.03	11.01	53.23
10	6610_2-1S	0.00	0.00	0.00	0.46	0.00	1.91	100.00	0.00	0.00	0.00	0.00
11	6610_2-1S	100.00	2.11	0.00	0.46	0.00	1.91	100.00	0.00	94.64	18.93	0.00
12	6610_2-1S	93.56	1.05	2.87	1.34	1.44	1.16	100.00	6.44	70.44	14.09	21.68

4.2 Gas Chromatography-Flame Ionization Detector (GC-FID) of C_{15}+ core extracts

While no core extract have earlier been produced form these wells, application of more detailed trace-amount analytical work has in other "dry wells" often revealed core extracts – never before detected. Following the careful extraction of the organic matter from the core samples of the three wells, the extracts were concentrated significantly to get better results prior to analysis on the GC-FID for detecting n-alkanes, pristane and phytane. The GC-FID traces give direct information about the n-alkane and isoprenoid distributions of the samples which will give information about the source rock facies and maturity of the samples (Peters and Moldowan, 1993). The main objective of using GC-FID in this study is to identify and calculate pristane/ phytane, pristane/ n-C_{17} and phytane/n-C_{18} ratios. It is also important to evaluate if the n-alkane envelope represents an asymptotic oil profile or an abbreviated condensates profile. All chromatograms from the GC-FID are presented in figure 4.14-4.24 and selected typical traces are discussed.

The North Sea Standard Oil (NSO-1) has been analysed on GC-FID as a reference to calculate the response factor for n-alkanes and to ensure accuracy of the GC-FID apparatus. The NSO sample is widely used as a standard sample during geochemical analysis in the Norwegian Continental Shelf (NCS).

Well 35/4-1 core extracts

These sandstone samples were taken from a depth ranging from 4118.30 m to 4248.30 m. The organic matter extracted from in these sandstone samples has shown quite markedly different n-alkanes distribution. Most of the samples contain normal alkanes in the range of C_{16} to C_{32}. Normal alkanes lower than C_{16} were not identified. This could be due to loss of these lighter hydrocarbons while handling the core samples. Samples from the depth 4118.30 m and 4120.10 m have shown n-C_{18} as their highest peak and below n-$C_{18,}$ peaks decrease rapidly down to n-C_{22} and the decrease becomes moderate as n-alkanes increase beyond C_{22}. The pristane and phytane peaks are short as compare to n-alkane peaks but pristane peaks are always higher than phytane peaks in these samples. Examples of these traces are shown in figure 4.14 to 4.18.

Still from the depth ranging from 4125.10 to 4157.05 m, n-C_{17} peaks are getting higher than n-$_{18}$ peaks but pristane and phytane peaks are not affected. These peaks (n-C_{17}, n-C_{18} and associated isoprenoid pristane and phytane) are identified and their ratios are calculated (pristane/phytane, pristane/n-C_{17} and phytane/n-C_{18}) and presented in table 4.4. Representative chromatograms of samples from this well are shown in figure 4.14 to 4.18 and all chromatograms are found in Appendix B with identified peaks and calculated parameters. Some of the chromatograms are selected and discussed as follows.

35/4-1, 4118.30 m: The GC-FID chromatogram produced from the analysis of the core extracts from the depth 4118.30 m gives a pr/ph ratio is 1.25, pr/n-C_{17} ratio is 0.54 and ph/n-C_{18} ratio is 0.39. The sample contains n-alkanes in the range of C_{15} to C_{32}. There are no n-alkanes identified below C_{15} in this chromatogram. The peaks representing the isoprenoids (Pr, Ph) are smaller as compare to associated n-alkanes (n-C_{17}, n-C_{18}) respectively. The unresolved complex mixture (UCM) is present in the chromatogram (See Table 4.4, Figure 4.14 and Appendix B).

35/4-1, 4120.10 m: The chromatogram resulting from the GC-FID analysis of the core extracts from the depth 4120.10 m (See Table 4.4, Figure 4.15 and Appendix B), the pr/ph ration is 1.54. The pr/n-C_{17} and ph/n-C_{18} ratios are calculated as 0.56 and 0.36 respectively. The sample contains n-alkanes in the range of C_{15} to C_{32} and there are no detectable n-alkanes below C_{15}.The pristane and phytane peaks are smaller than the associated peaks of n-C_{17} and n-C_{18} in this chromatogram. The UCM in the chromatogram is obvious which shows the biodegradation.

35/4-1, 4154.50 m: The GC-FID chromatogram produced by the analysis of core extracts from the depth of 4154.50 m (See Table 4.4, Figure 4.16 and Appendix B) gives the pr/ph, pr/n-C_{17} and ph/n-C_{18} ratios 1.66, 0.66 and 0.48 respectively. From the chromatogram n-alkanes are in the range of C_{15} to C_{32}. Sudden change in peaks is observed from n-C_{19} to n-C_{23} and below that change is moderate up to n-C_{32}. In this sample significant unresolved complex mixture (UCM) is observed.

35/4-1, 4205.30 m: The pr/ph, pr/n-C_{17} and ph/n-C_{18} ratios are computed 1.44, 0.36 and 0.23 respectively. This chromatogram produced from this well is one of the best as it has moderate unresolved complex mixture (UCM) and n-alkanes starts from n-C_{13} to n-C_{32}. The pr and ph peaks are shorter than associated n-C_{17} and n-C_{18} peaks

(See Table 4.4, Figure 4.17 and Appendix B). The sample is clean and showing no contamination in the chromatogram.

35/4-1, 4248.30 m: The GC-FID chromatogram resulting from the analysis of core extract from the depth 4248.30 m gives pr/ph ratio is 2.1 which is the highest pr/ph ration in the sample set from the well and pr/n-C_{17} and ph/n-C_{18} ratios are 0.27 and 0.16 respectively (See Table 4.4, Figure 4.18 and Appendix B). The chromatogram shows n-alkanes ranges from n-C_{15} to n-C_{32}. The pristane and phytane peaks in this chromatogram are observed relatively shorter and highest peak in this chromatogram is n-C_{16}. The UCM is moderate and base line is smooth.

Table 4.4 sample list showing results from GC-FID analysis.

No	Well	Sample depth (m)	Lithology	Pr/Ph	Pr/n-C_{17}	Ph/n-C_{18}
1	35_4-1	4118.30	Sandstone	1.25	0.54	0.39
2	35_4-1	4120.10	"	1.54	0.56	0.36
3	35_4-1	4125.10	"	1.74	0.60	0.37
4	35_4-1	4151.55	"	1.54	0.53	0.36
5	35_4-1	4152.50	"	1.45	0.66	0.49
6	35_4-1	4154.50	"	1.66	0.66	0.48
7	35_4-1	4155.50	"	1.38	0.61	0.45
8	35_4-1	4156.50	"	1.71	0.58	0.40
9	35_4-1	4157.05	"	1.46	0.50	0.37
10	35_4-1	4166.30	"	1.25	0.56	0.43
11	35_4-1	4172.60	"	1.22	0.62	0.52
12	35_4-1	4184.50	"	1.38	0.43	0.30
13	35_4-1	4205.30	"	1.44	0.36	0.23
14	35_4-1	4216.00	"	1.80	0.39	0.28
15	35_4-1	4219.00	Cemented Sandstone	1.07	0.65	0.53
16	35_4-1	4222.00	"	1.77	0.48	0.32
17	35_4-1	4242.50	"	1.85	0.40	0.27
18	35_4-1	4248.30	Sandstone	2.10	0.27	0.16

Well 6610/3-1 core extracts

These core samples are taken from the depth of 1682.50 m to 3324.80 m and the major lithology is sandstone. These samples all show well defined n-C_{17}, n-C_{18}, pristane and phytane peaks except the two samples at a depth of 2521 m and 2522.80 m that are not having detectable n-alkanes. Representative chromatograms of the bitumen extracts are shown in Figure 4.19 to 4.23. The abrupt decrease in peak height after n-C_{16} is observed in these chromatograms (See Appendix B). In these samples, the peak representing n-C_{17} is always higher than the n-C_{18} peak but after the n-C_{18} peak there are hardly detectable n-alkane peaks. Thus, we have "front-end" biased profiles. Pr/Ph ratios range between 1 and 4, with minimum ratio is observed in sandstones and maximum ratios observed in mudstone lithology, Pr/n-C_{17} ratios range between 0.49 and 0.84, while Ph/n-C_{18} ratios range between 0.36 and 0.93 for these core samples.

Selected chromatograms from the well are discussed to illustrate the uniformities and/or variation as follows.

6610/3-1, 1682.50 m: The GC-FID chromatogram produced from the core extract of sample from the depth 1682.50 m (See Table 4.5, Figure 4.19 and Appendix B) shows pr/ph ratio 1.72 and pr/n-C_{17}, ph/n-C_{18} ratios are 0.58 and 0.79 respectively. The chromatogram shows n-alkanes ranges from n-C_{13} to n-C_{18}. Pristane and phytane are shorter peaks as compare to associated n-C_{17} and n-C_{18} peaks.

6610/3-1, 1683.50 m: From the GC-FID chromatogram of the sample (See Table 4.5, Figure 4.20 and Appendix B), the pr/ph, pr/n-C_{17}, ph/n-C_{18} ratios are 1.0, 0.59 and 0.93 respectively. The chromatogram shows n-alkanes ranging from C_{12} to C_{18}. The pristane and phytane peaks are shorter as compare to the associated peaks of n-C_{17} and n-C_{18}. The highest peak in this chromatogram is n-C_{15}.

6610/3-1, 2311.00 m: The GC-FID chromatogram resulting from the core extracts (See Table 4.5, Figure 4.21 and Appendix B) gives pr/ph ratio of 4.0 which is the highest ratio in the sample set. The pr/n-C_{17} and ph/n-C_{18} ratios are 0.71 and 0.36 respectively. The chromatogram shows that the n-alkanes ranging from n-C_{12} to n-C_{18}. The pristane and phytane are relatively short isoprenoids peaks as compare to the associated n-C_{17} and n-C_{18} peaks. This sample contains a relatively moderate unresolved complex mixture (UCM) as an irregular base line.

6610/3-1, 3316.50 m: From the GC-FID chromatogram of the sample (See Table 4.5, Figure 4.22 and Appendix B) the pr/ph, pr/n-C_{17} and ph/n-C_{18} ratios are 1.68, 0.6 and 0.42 respectively. The chromatogram shows n-alkanes ranging from n-C_{12} to n-C_{32}. This sample unlike other samples of the same well has more n-alkanes but three unlikely peaks observed along n-C_{15}, n-C_{18} and n-C_{21} respectively.

6610/3-1, 3324.80 m: The GC-FID chromatogram produced from the core extracts (See Table 4.5, Figure 4.23 and Appendix B) gives pr/ph ratio 2.13 and pr/n-C_{17}, ph/n-C_{18} ratios are 0.69 and 0.66 respectively. The sample contains n-alkanes from n-C_{15} to n-C_{18}. These peaks representing isoprenoid pristane and phytane and their associated n-alkanes n-C_{17} and n-C_{18}. The pristane and phytane peaks are relatively smaller than n-C_{17} and n-C_{18} peaks in this chromatogram.

Well 6610/2-1S core extracts

According to NPD initial analytical work and analysis proved that an oil-based mud additive was used from depth ranges of 2063 m to 2673 m and the samples used in this study are from that particular zone. For this study core samples from the depth interval of 2051.50 m to 2351.50 m were analysed and no detectable natural hydrocarbon (n-alkane) signatures were identified on the GC-FID. Typical GC-FID traces (See Figure 4.24, Table 4.6 and Appendix B). All chromatograms display 3-4 dominant polyethylene glycol peaks and little more. Although the major lithology is sandstone, there is hardly any significant oil or gas signatures to be found. However, as shown in Figure 4.24 a typical feature observed in these chromatograms I represented by polyethylene glycols which were used to preserve the core samples for wettability studies.

Table 4.5 showing results from GC-FID analysis from core sample of well 6610/3-1

No	Well	Sample depth (m)	Lithology	Pr/Ph	Pr/n-C_{17}	Ph/n-C_{18}
1	6610_3-1	1682.50	Sandstone	1.72	0.58	0.79
2	6610_3-1	1683.50	"	1	0.59	0.93
3	6610_3-1	1711.50	"	1.75	0.66	0.55
4	6610_3-1	1714.50	"	2.1	0.5	0.59
5	6610_3-1	2294.50	"	1.85	0.66	0.55
6	6610_3-1	2299.50	"	3.1	0.75	0.59
7	6610_3-1	2301.00	"	2.66	0.83	0.55
8	6610_3-1	2306.00	"	3.5	0.73	0.5
9	6610_3-1	2311.00	Mudstone	4	0.71	0.36
10	6610_3-1	2521.00	Sandstone	0	0	0
11	6610_3-1	2522.80	"	0	0	0
12	6610_3-1	2664.50	"	2	0.49	0.4
13	6610_3-1	2670.50	"	1.23	0.84	0.75
14	6610_3-1	2677.50	"	2.5	0.57	0.46
15	6610_3-1	3316.50	"	1.68	0.6	0.42
16	6610_3-1	3324.80	"	2.13	0.69	0.66

Table 4.6 list showing no values of pr/ph, pr/n-C_{17} and ph/n-C_{18} as no n-alkane peaks are identified. ND = No Data

No	Well	Sample depth (m)	Lithology	Pr/Ph	Pr/n-C_{17}	Ph/n-C_{18}
1	6610_2-1S	2051.50	Sandstone	ND	ND	ND
2	6610_2-1S	2053.00	"	ND	ND	ND
3	6610_2-1S	2054.50	"	ND	ND	ND
4	6610_2-1S	2056.50	"	ND	ND	ND
5	6610_2-1S	2058.00	"	ND	ND	ND
6	6610_2-1S	2059.00	"	ND	ND	ND
7	6610_2-1S	2060.50	"	ND	ND	ND
8	6610_2-1S	2066.50	"	ND	ND	ND
9	6610_2-1S	2073.50	"	ND	ND	ND
10	6610_2-1S	2074.50	"	ND	ND	ND
11	6610_2-1S	2344.20	"	ND	ND	ND
12	6610_2-1S	2344.50	Coal	ND	ND	ND
13	6610_2-1S	2346.50	"	ND	ND	ND
14	6610_2-1S	2351.50	"	ND	ND	ND

*ND = No Data

4.3 Microscopy

The detailed explanation of identifying the HCs inclusions under the microscope in sandstone samples is found in chapter 3.4.1. Some selected sandstone samples from the well 35/4-1 at a depth 4156.50 m, 6610/3-1 at a depth 2670.50 m and one sample at a depth 2051.50 m from the well 6610/2-1S were examined under the microscope to determine if any fluorescent petroleum type inclusions could be detected. In case such are observed, the relative size of the gas bubble signifies tentatively the GOR of the petroleum phase which at one time existed in the trap. Fluorescence colours (Tab. 4.7) correlate roughly with API and is of great help in assessing the API of any paleo-petroleum in "dry traps".

Commonly, the selected sandstone samples studied under microscope have shown different types of inclusions from different wells (see figure 4.1), for instance the sandstone sample from the well 35/4-1 has possible oil inclusions with tiny water inclusions while the sample from the well 6610/3-1 has shown water inclusions with gas bubbles and the sandstone sample from the well 6610/2-1S at a depth 2051.50 m has shown blue/greenish oil inclusions.

On the basis of subjective observation under microscope and description of the amount of fluorescent inclusions under UV light a scale has been used ranging from 1-50 as 1 will reflect the low amount of inclusions while 50 will represent the high amount of inclusions. The selected sample from the well 35/4-1 have low amount of inclusions and have values ranging from 15-20 on the basis of scale (see Table 4.7). The well 6610/3-1 contains slightly more inclusions that were observed under microscope using UV light and values ranging from 20-25 and finally in well 6610/2-1S highest inclusions were examined among the selected samples and value ranging from 25-40 as blue/greenish oil inclusions were observed when sample is exposed under UV light.

Table 4.7 common fluorescence response when core samples/different gravity oils are exposed under UV light.

FLUORESCENCE WAVELENGTH (nm)	A. P. I	FLUORESCENCE COLOR	OIL TYPE
560	19	FULL YELLOW/RED	LOW MATURITY HEAVY OILS
548	25	GREEN	BLACK OILS
528	33	GREEN/BLUELIGHT OILS	
494	44	BLUE VERY LIGHT OILS	
450	50+	VIOLET	CONDENSATES

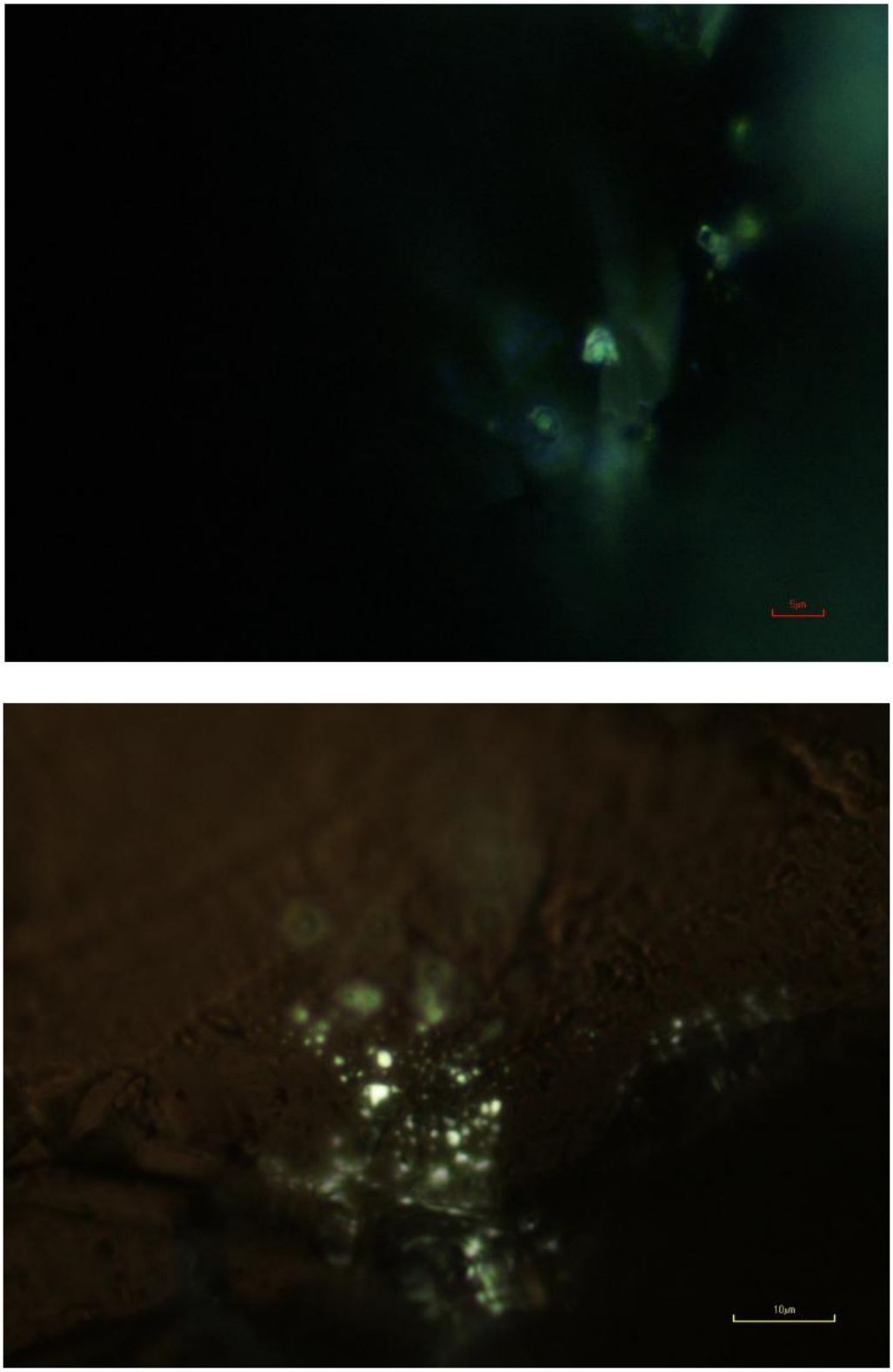

Figure 4.1 fluid inclusions samples from the well 6610/3-1 (upper) and 6610/2-1S (lower image) from Norwegian Sea showing in the upper photomicrograph greenish/bluish oil inclusions with large gas bubbles representing high GOR light oil, and below medium GOR oil, respectively.

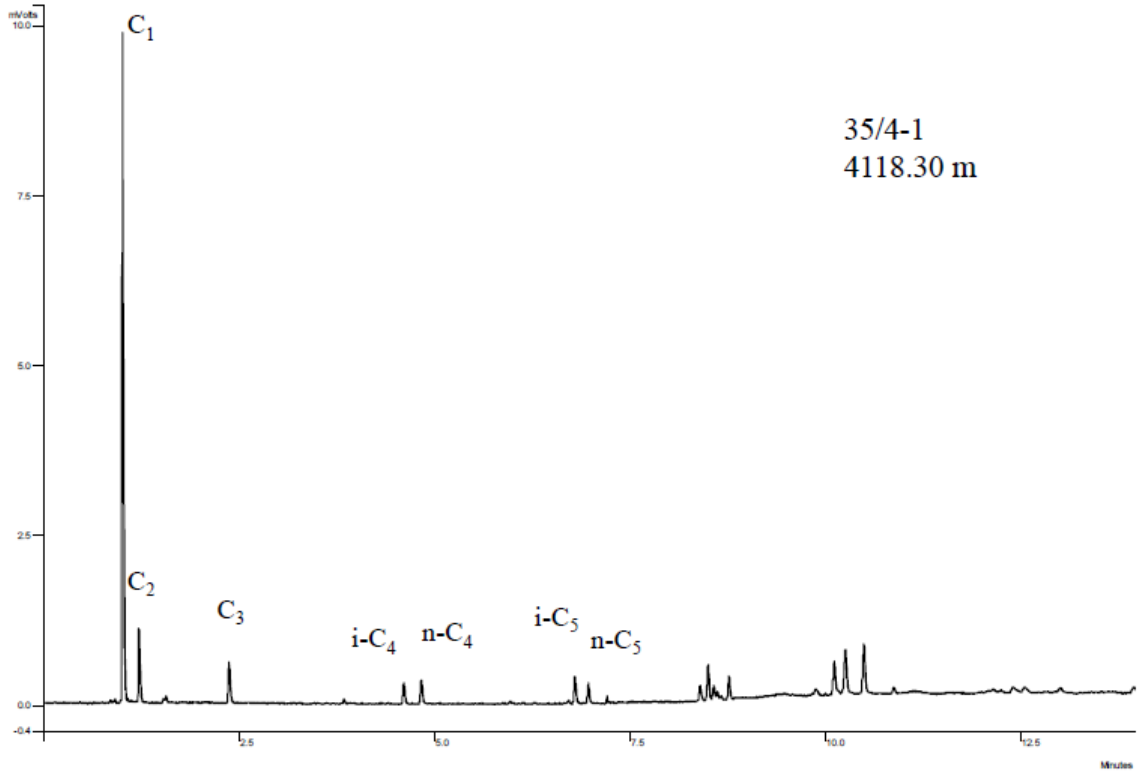

Figure 4.1 Gas analysis result of core sample from the depth 4118.30 m from well 35/4-1.

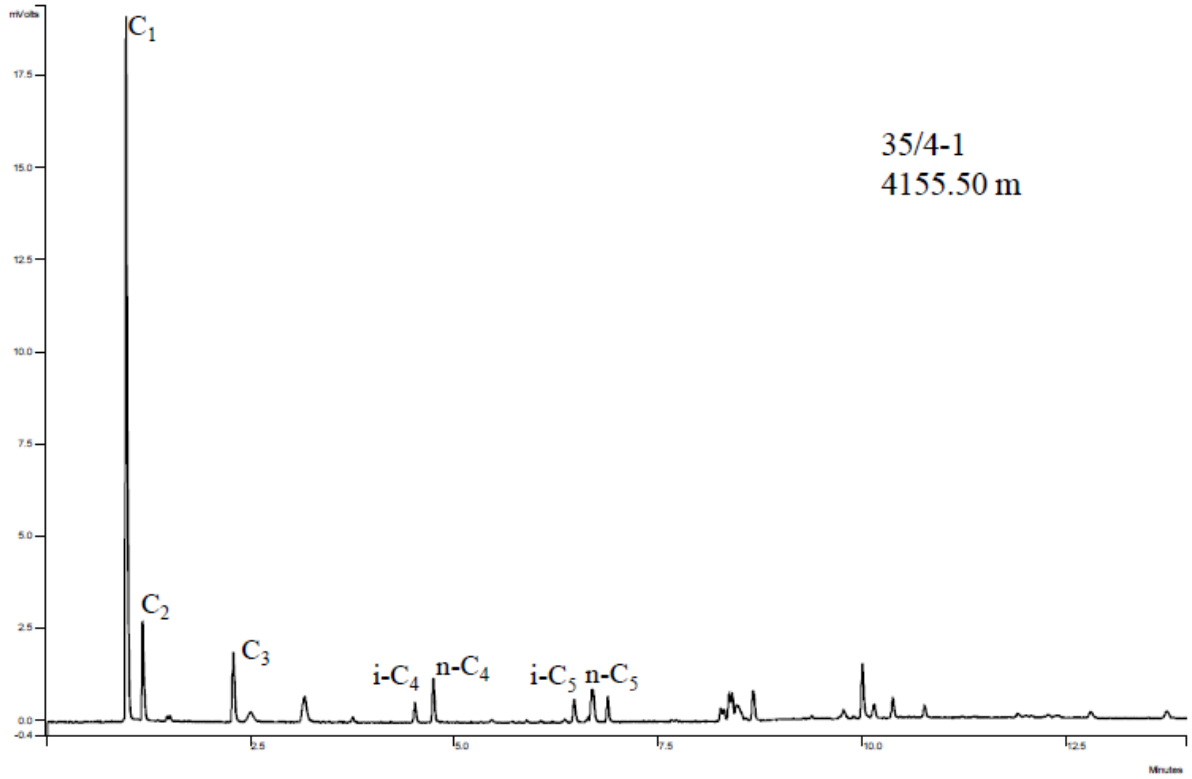

Figure 4.2 Gas analysis result for core sample from 4155.5 m depth from the well 35/4-1.

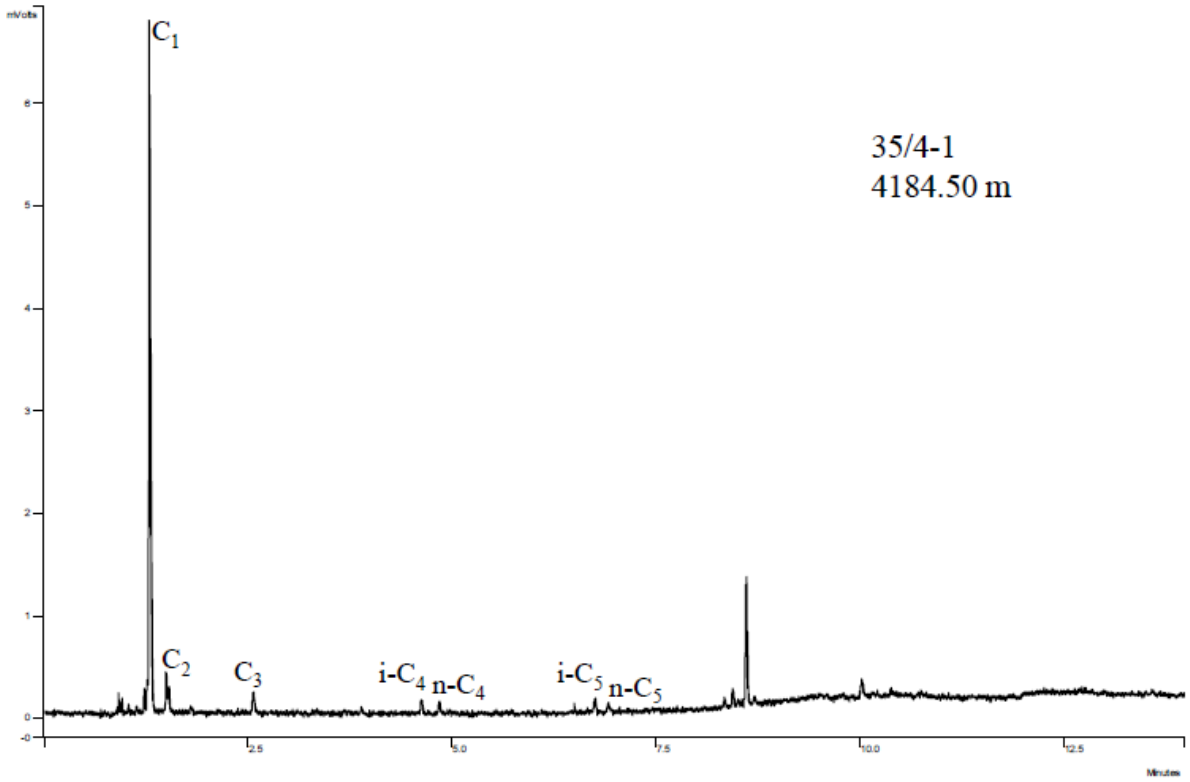

Figure 4.3 Gas analysis result for core sample from 4184.50 m depth from the well 35/4-1.

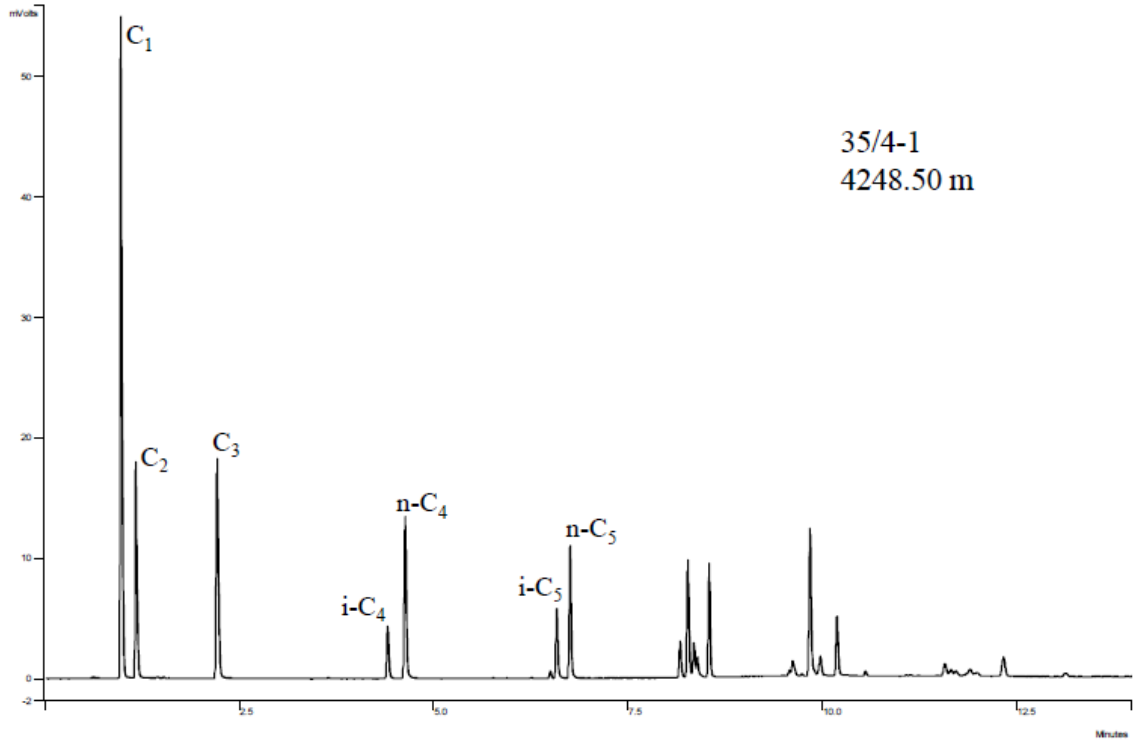

Figure 4.4 Gas analysis result for core sample from the depth 4248.50 m from well 6610/3-1 showing light HCs ranging from C1-C5.

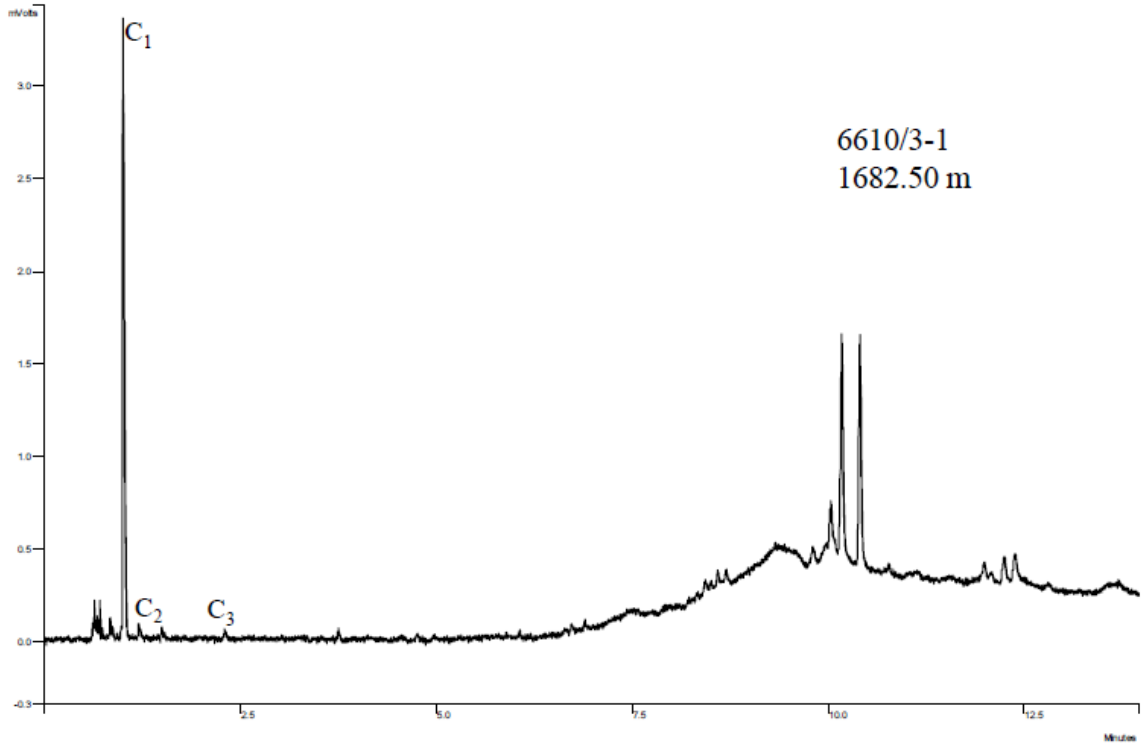

Figure 4.5 Gas analysis result for core samples from the depth 1682.50 m of well 6610/3-1 showing light n-alkanes ranging from C1-C3.

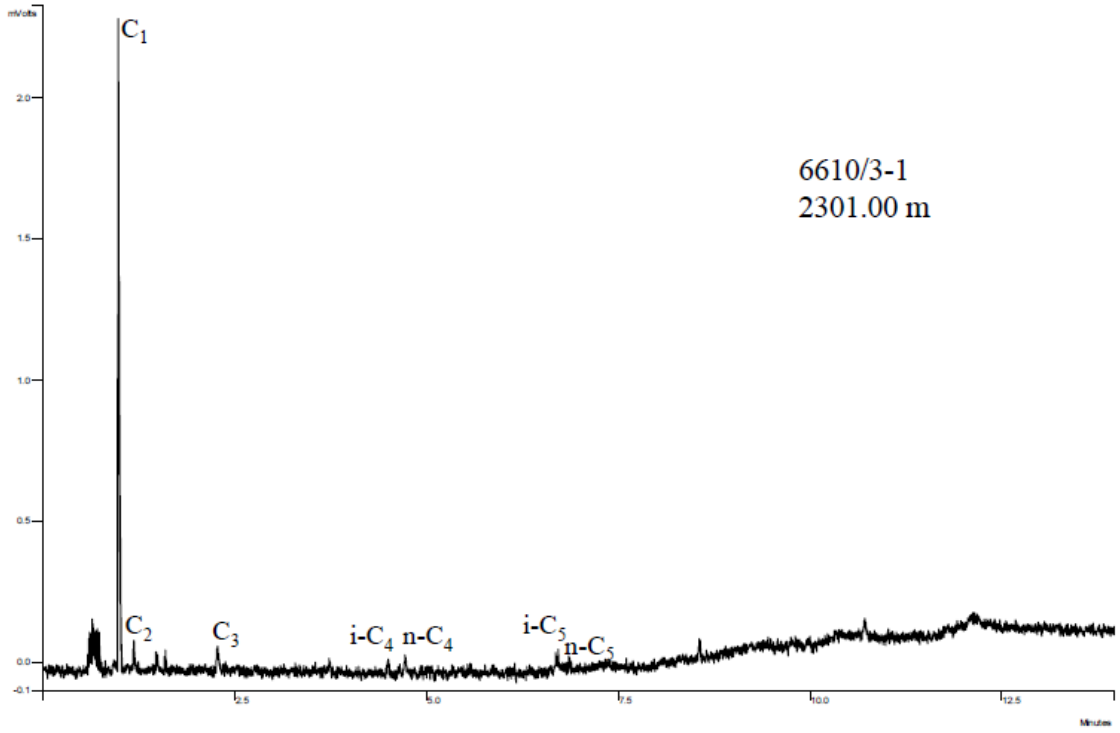

Figure 4.6 Gas analysis result for core sample from the well 6610/3-1 at a depth of 2301 m showing light HCs ranging from C1-C5.

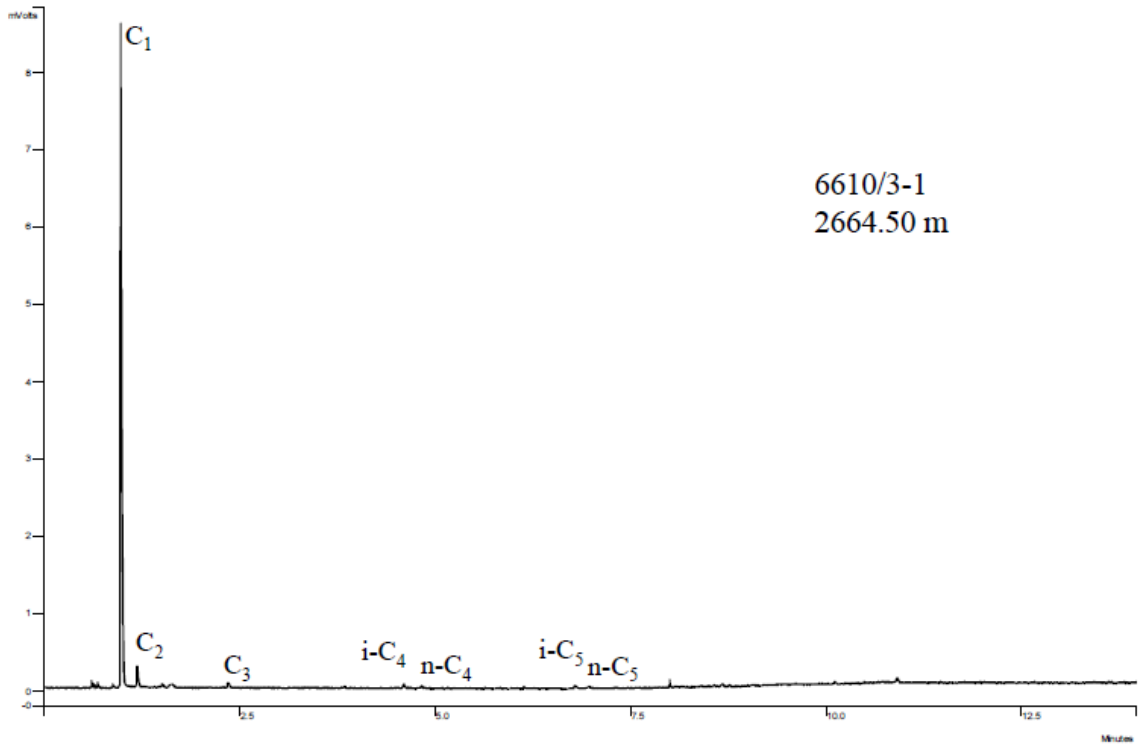

Figure 4.7 Light HCs from the well 6610/3-1 ranging from C1-C5 at a depth of 2664.50 m.

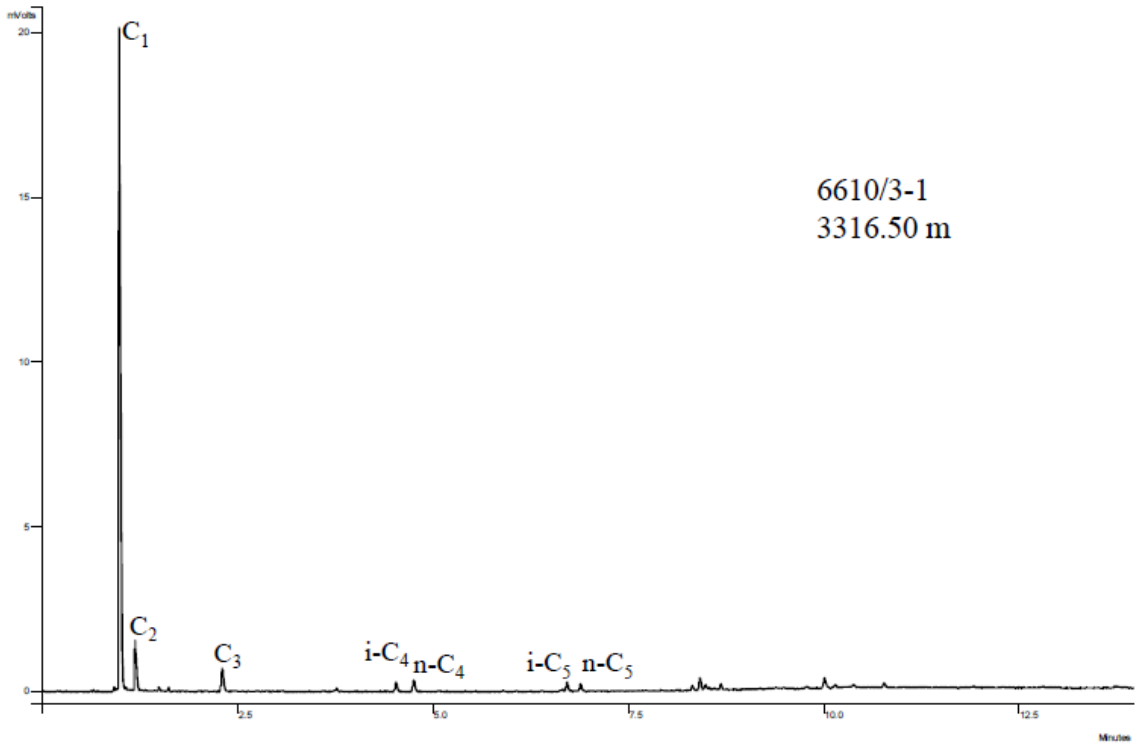

Figure 4.8 Gas analysis result from core sample from the depth 3316.50 m from well 6610/3-1 showing n-alkanes ranging from C1 to C5.

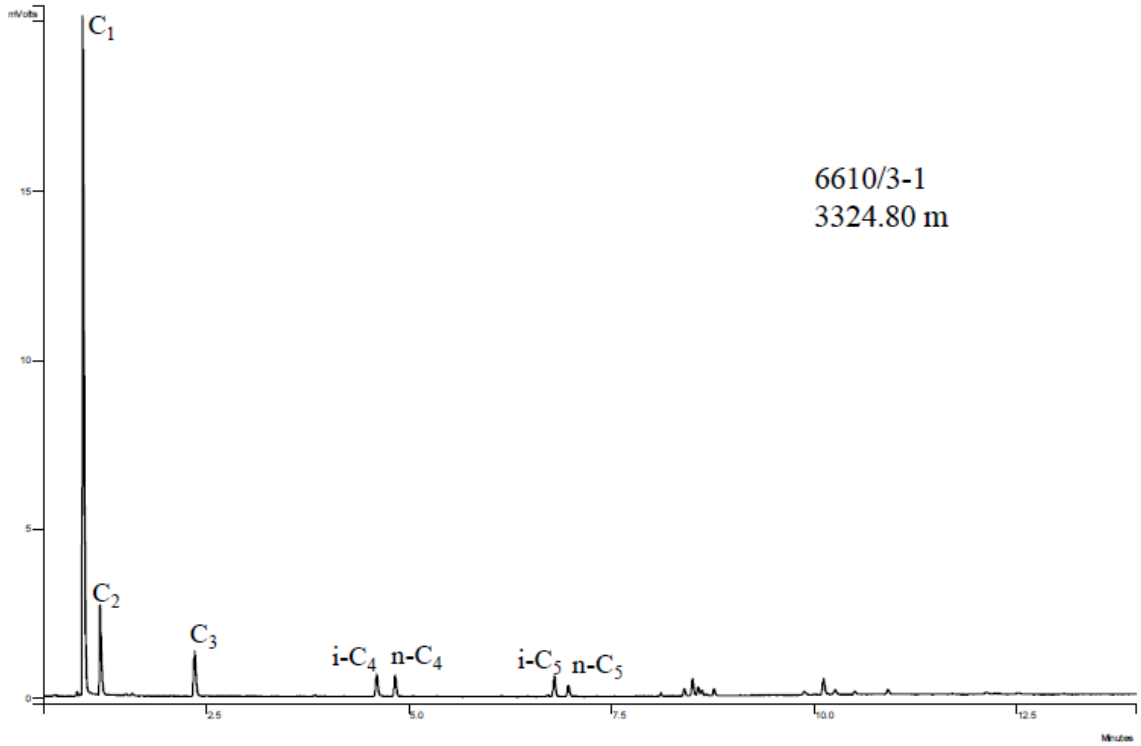

Figure 4.9 chromatogram produced from the depth 3324.80 m by gas analysis from the well 6610/3-1 showing light HCs ranging from C1-C5.

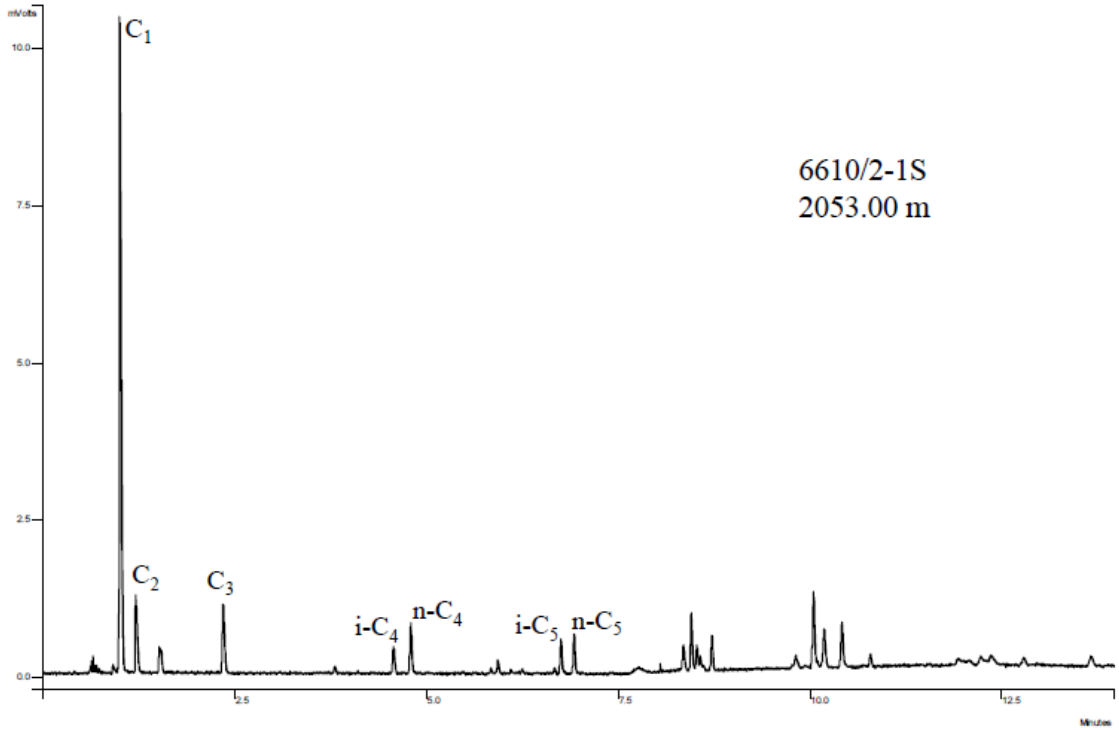

Figure 4.10 Gas analysis result from core sample from the depth 2053.00 m from the well 6610/2-1S showing light HCs ranging from C1 to C5.

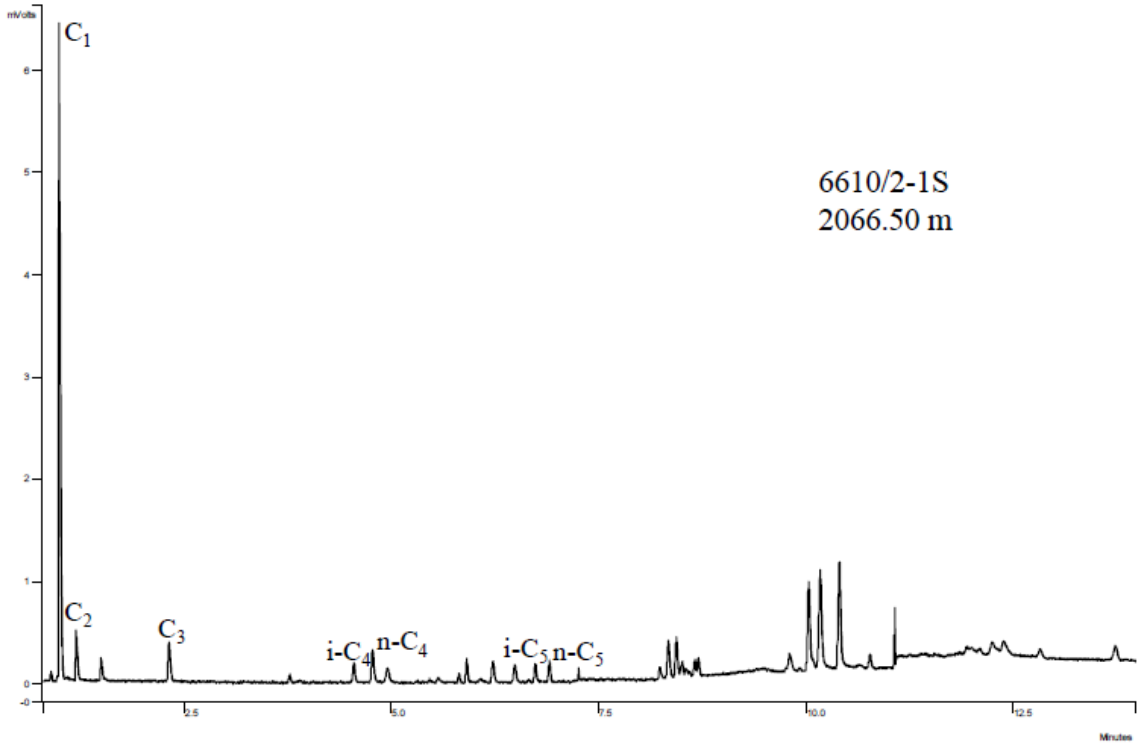

Figure 4.11 Gas analysis result from core sample from the depth 2066.50 m from the well 6610/2-1S is showing C_1 to C_5 n-alkane range.

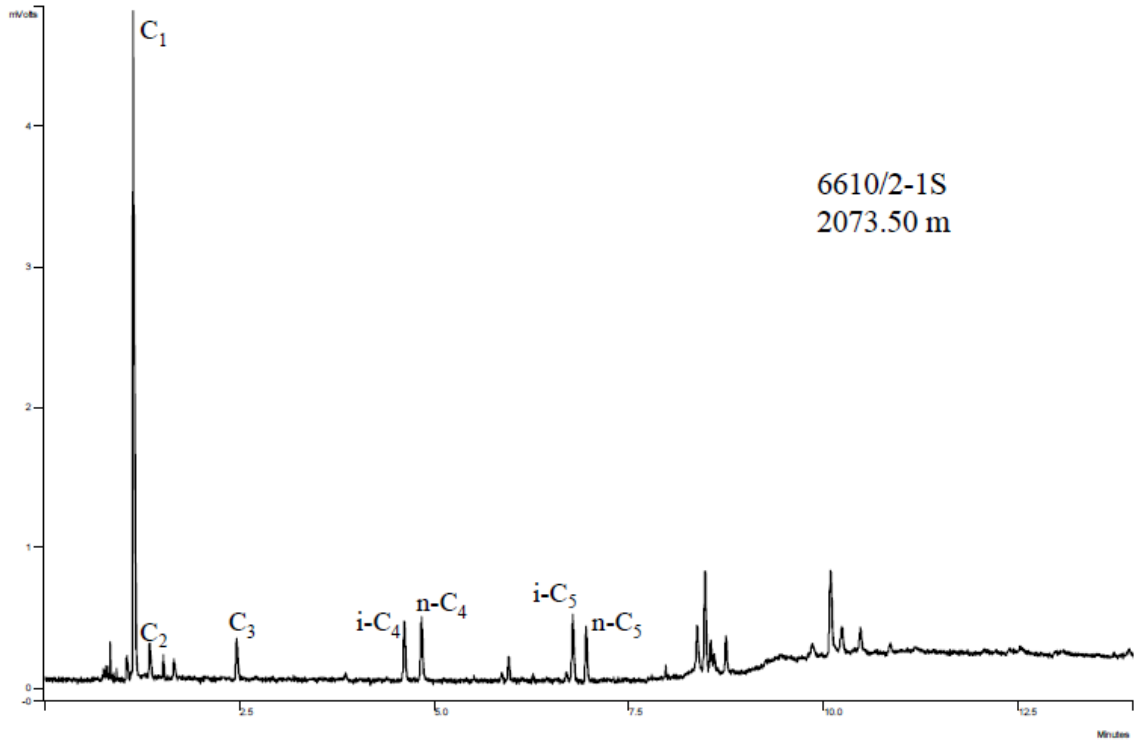

Figure 4.12 Gas analysis result showing light HCs ranging from C_1 to C_5 from the well 6610/2-1S at a depth 2073.50 m.

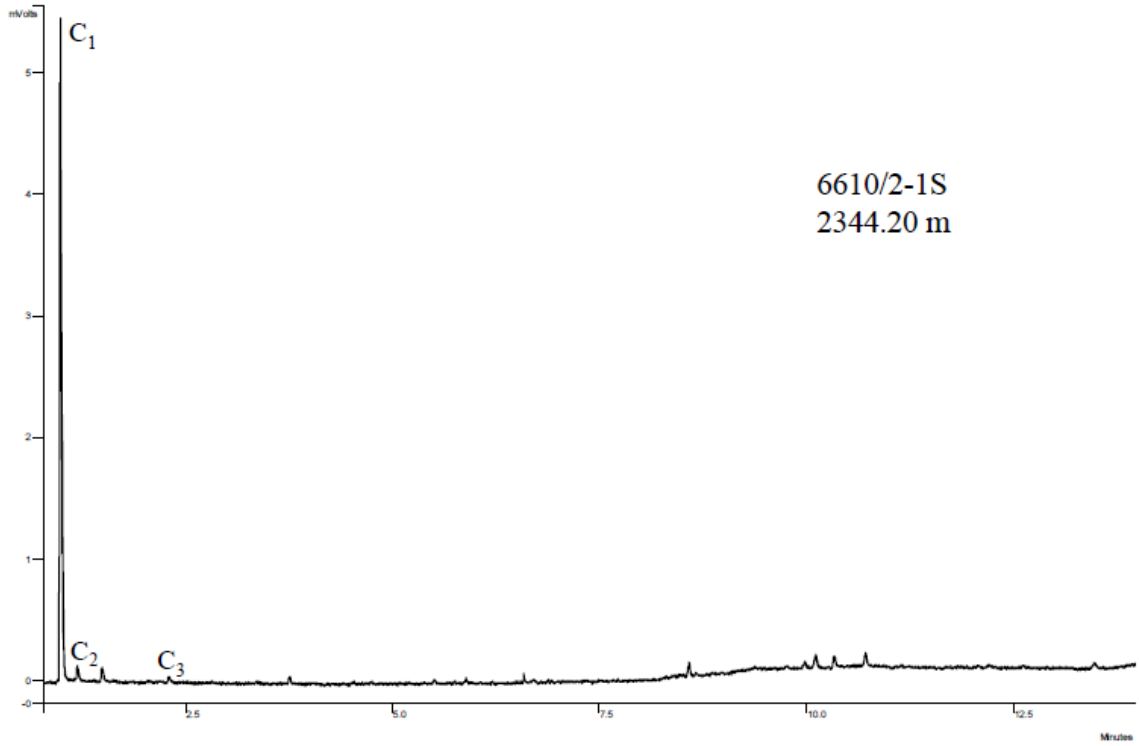

Figure 4.13 Gas analysis result showing light HCs ranging from C_1 to C_3 from the well 6610/2-1S at 2344.20 m depth.

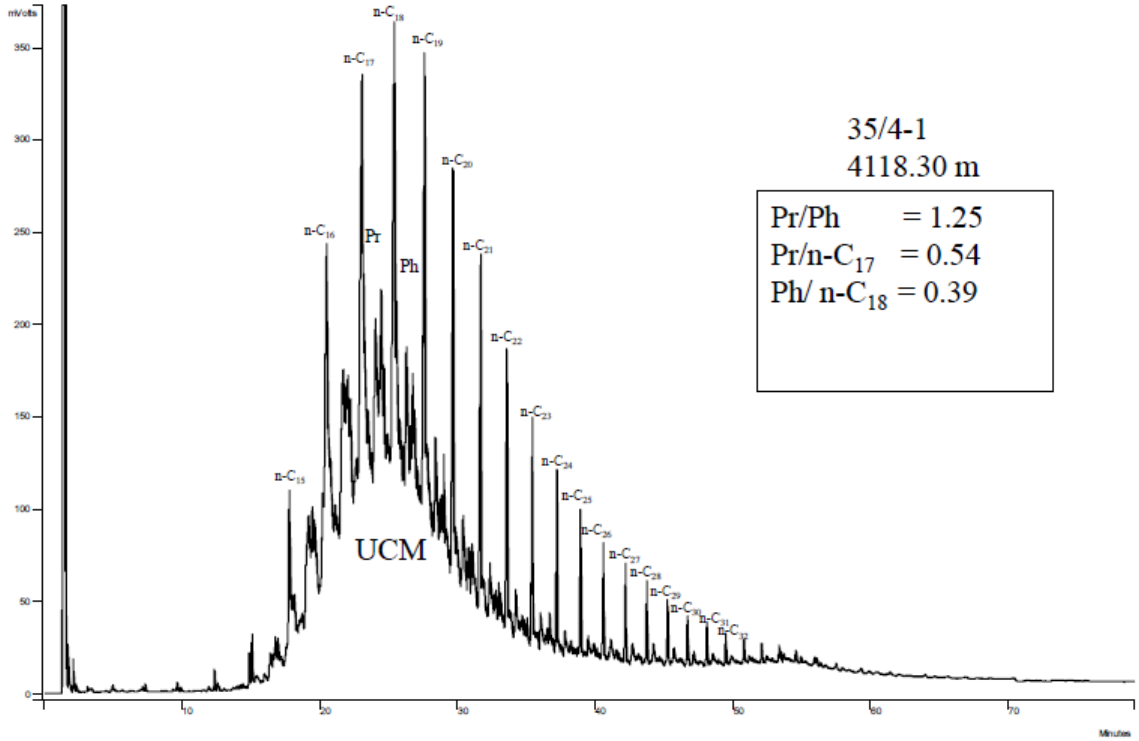

Figure 4.14 GC-FID result showing n-alkanes ranging from n-C_{15} to n-C_{32} from the well 35/4-1 at a depth 4118.30 m.

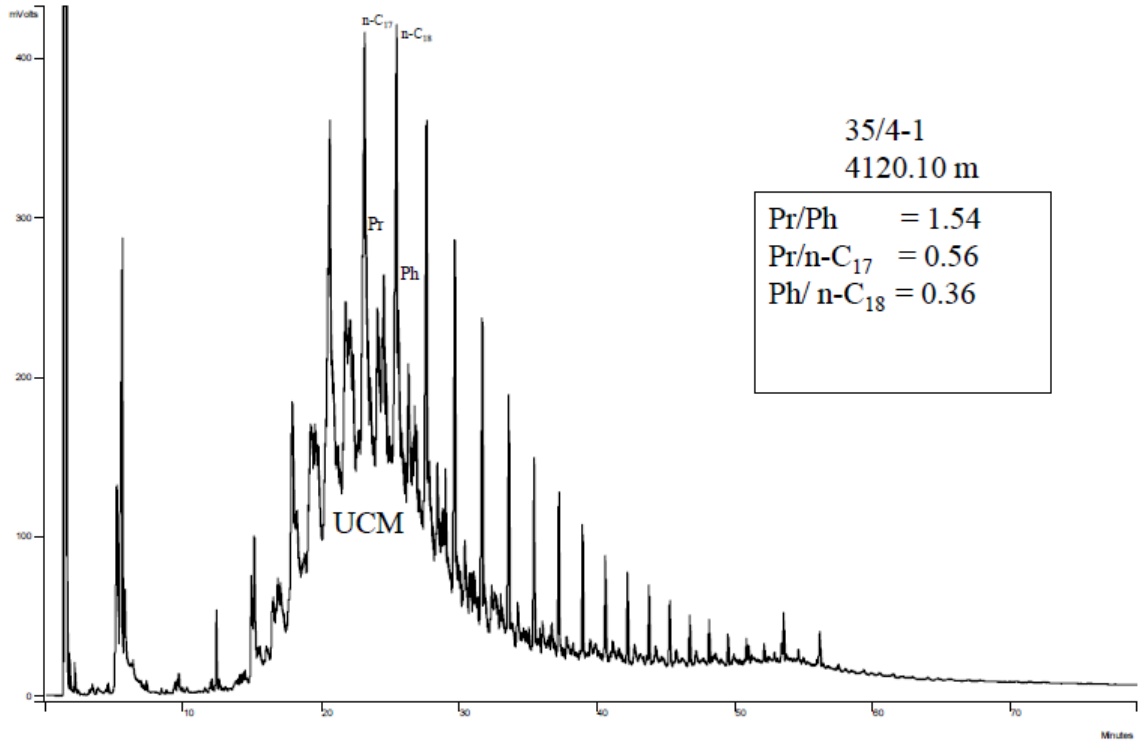

Figure 4.15 GC-FID result showing n-C_{17} and n-C_{18} with associated isoprenoid Pr and Ph and UCM bulge from the well 35/4-1 at 4120.10 m depth.

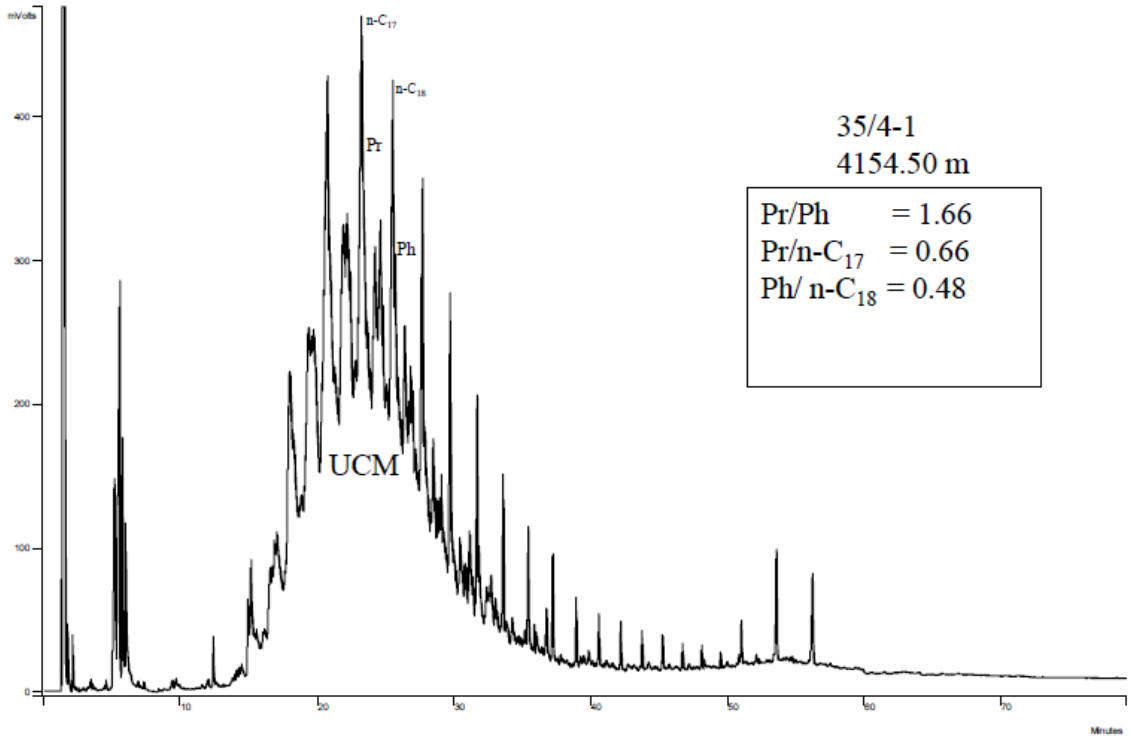

Figure 4.16 GC-FID result showing n-C_{17} and n-C_{18} with associated isoprenoid Pr and Ph from the well 35/4-1 at 4154.50 m depth.

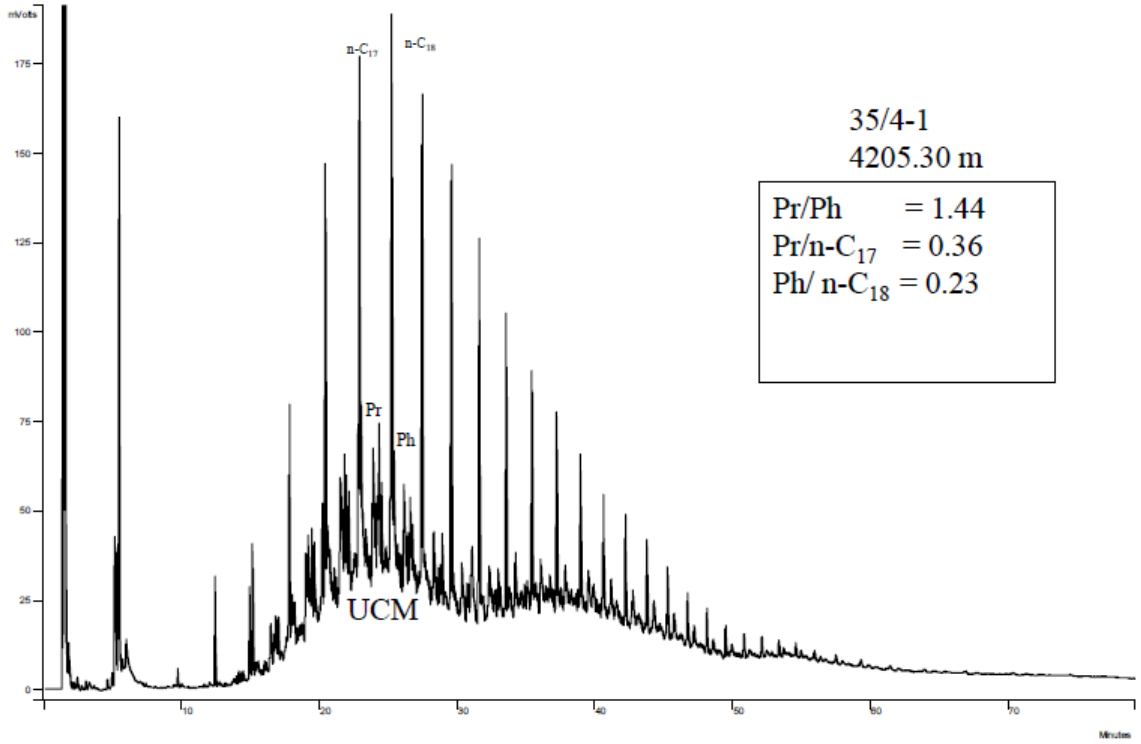

Figure 4.17 GC-FID result showing n-C_{17} and n-C_{18} with associated isoprenoid Pr and Ph from the well 35/4-1 at 4205.30 m depth.

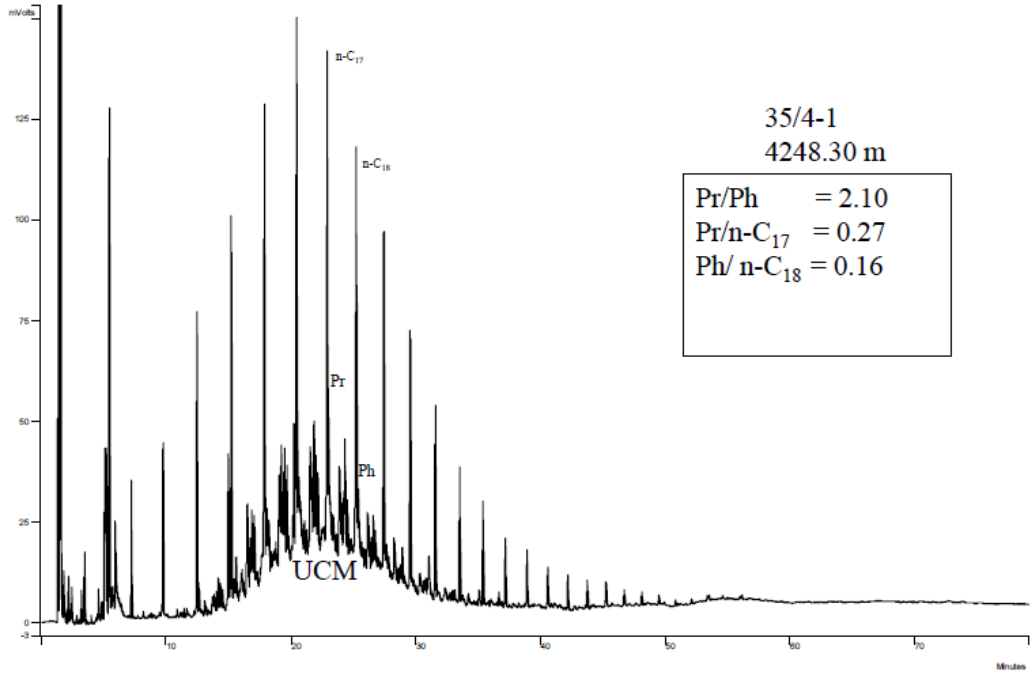

Figure 4.18 GC-FID result showing n-C_{17} and n-C_{18} with associated isoprenoid Pr and Ph from the well 35/4-1 at 4248.30 m depth.

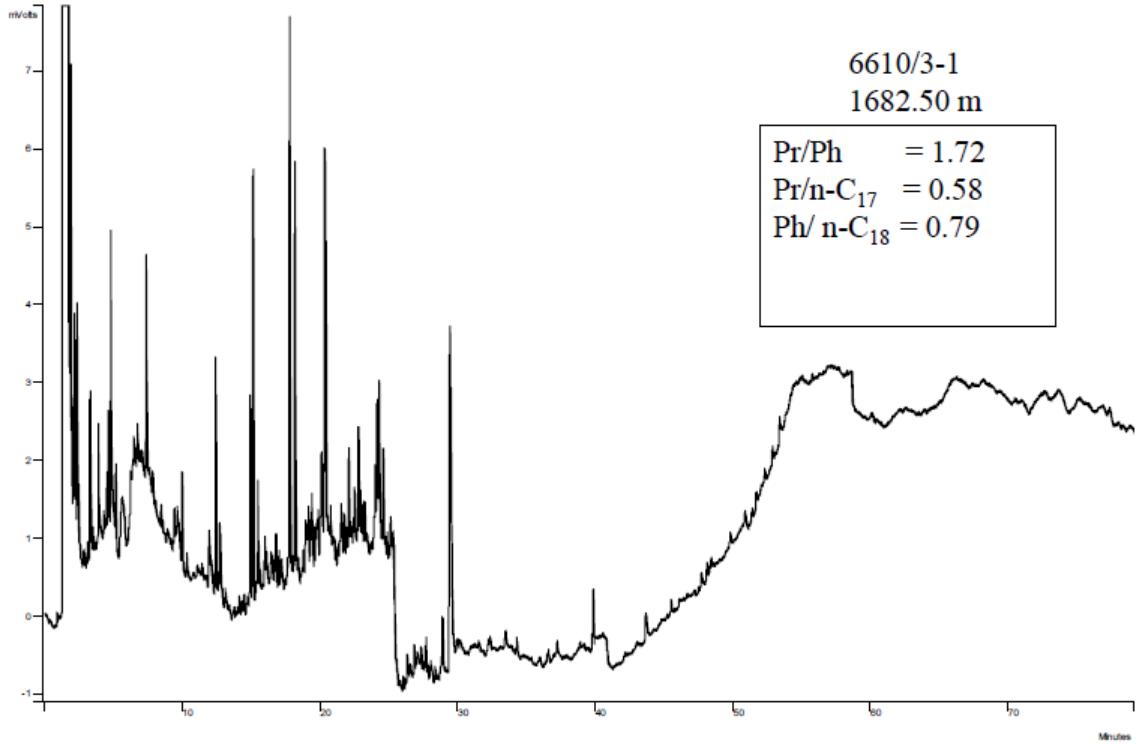

Figure 4.19 GC-FID results produced from the core extract from the well 6610/3-1 at 1682.50 m depth.

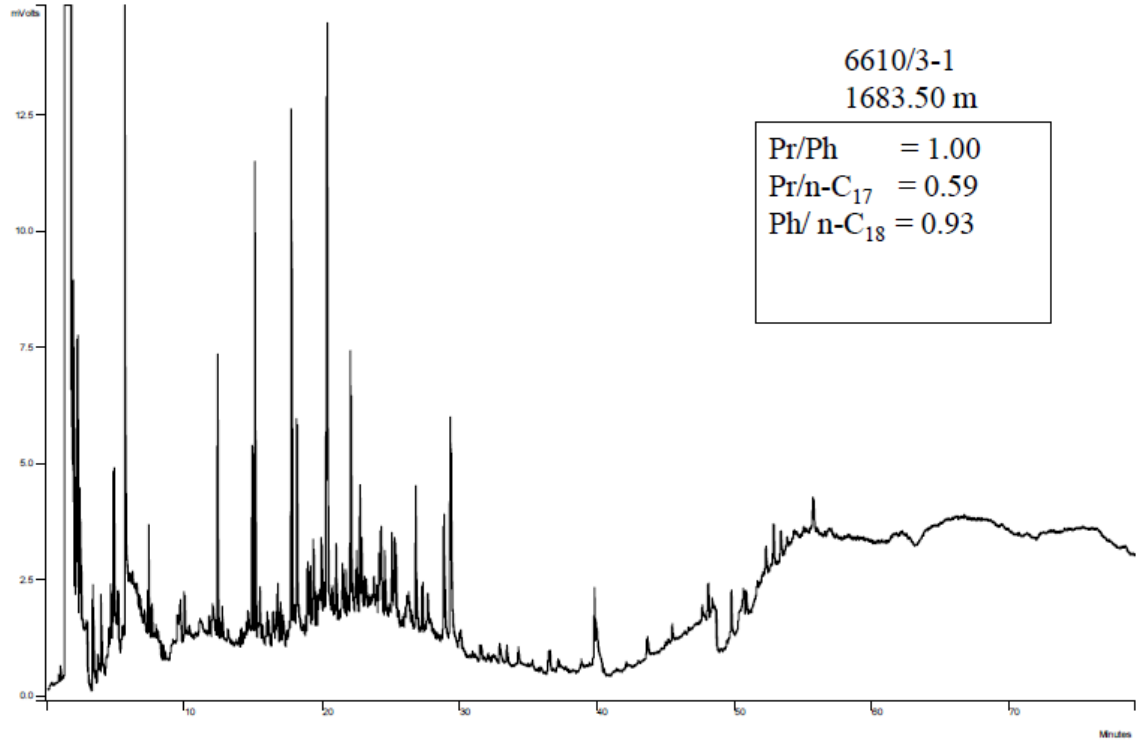

Figure 4.20 GC-FID results produced from the core extract from the well 6610/3-1 at 1683.50 m depth.

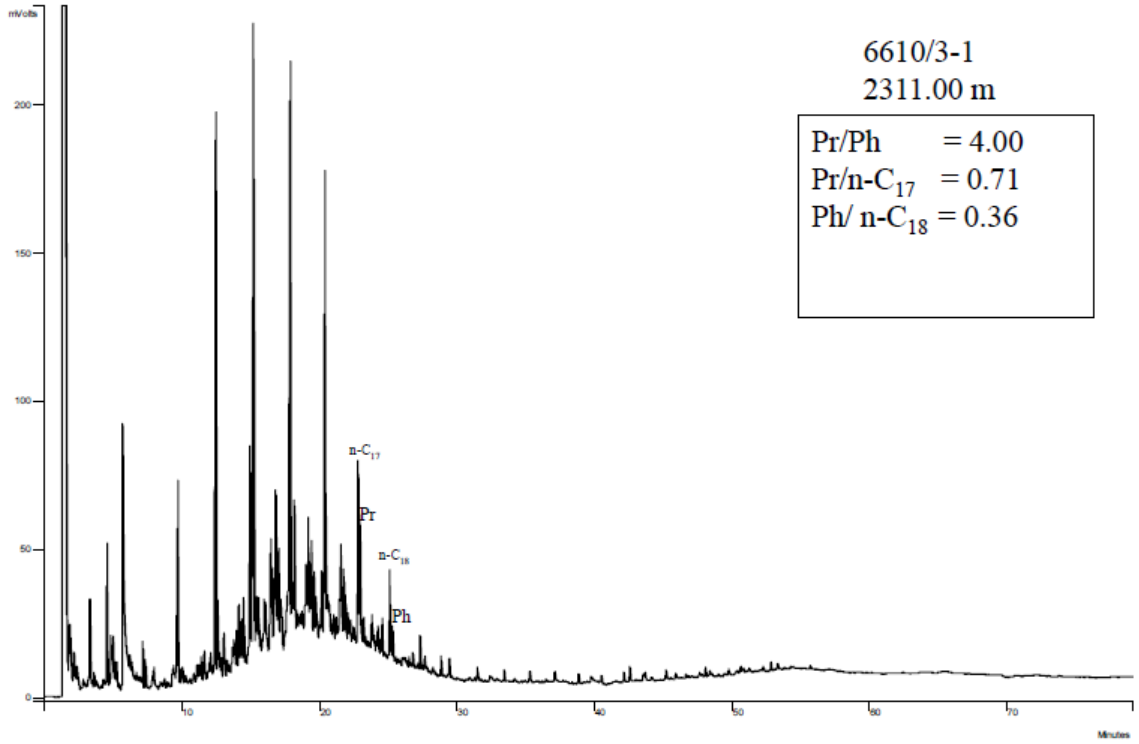

Figure 4.21 GC-FID results produced from the core extract from the well 6610/3-1 showing n-alkanes and associated isoprenoid at 2311.00 m depth.

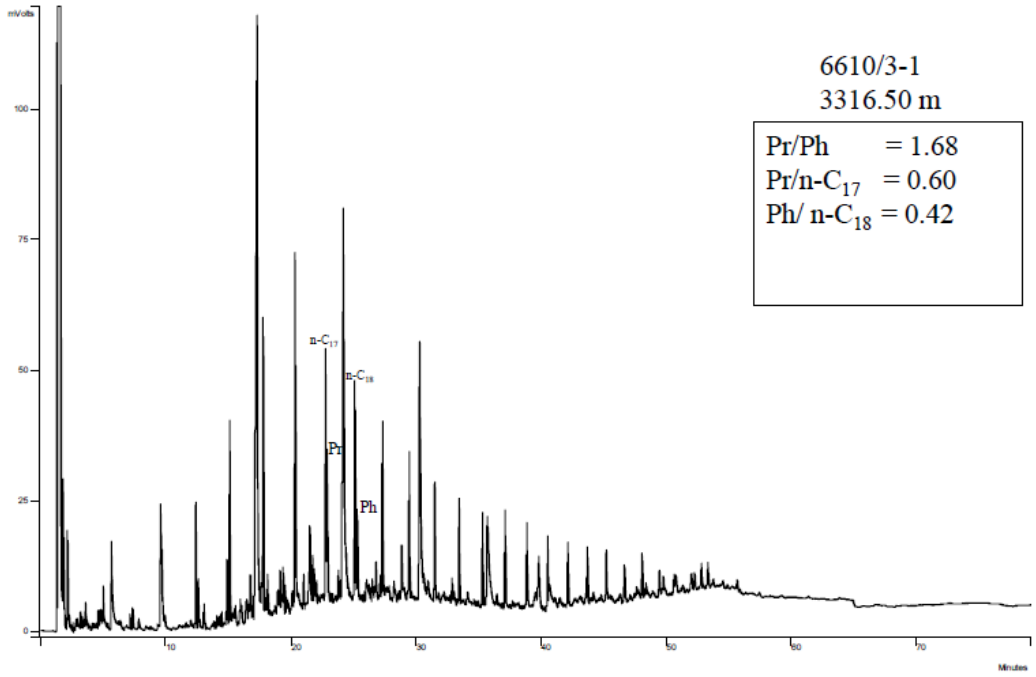

Figure 4.22 The Chromatogram produced by GC-FID from the well 6610/3-1 showing n-C_{17} and n-C_{18} with associated isoprenoid at 3316.50 m depth.

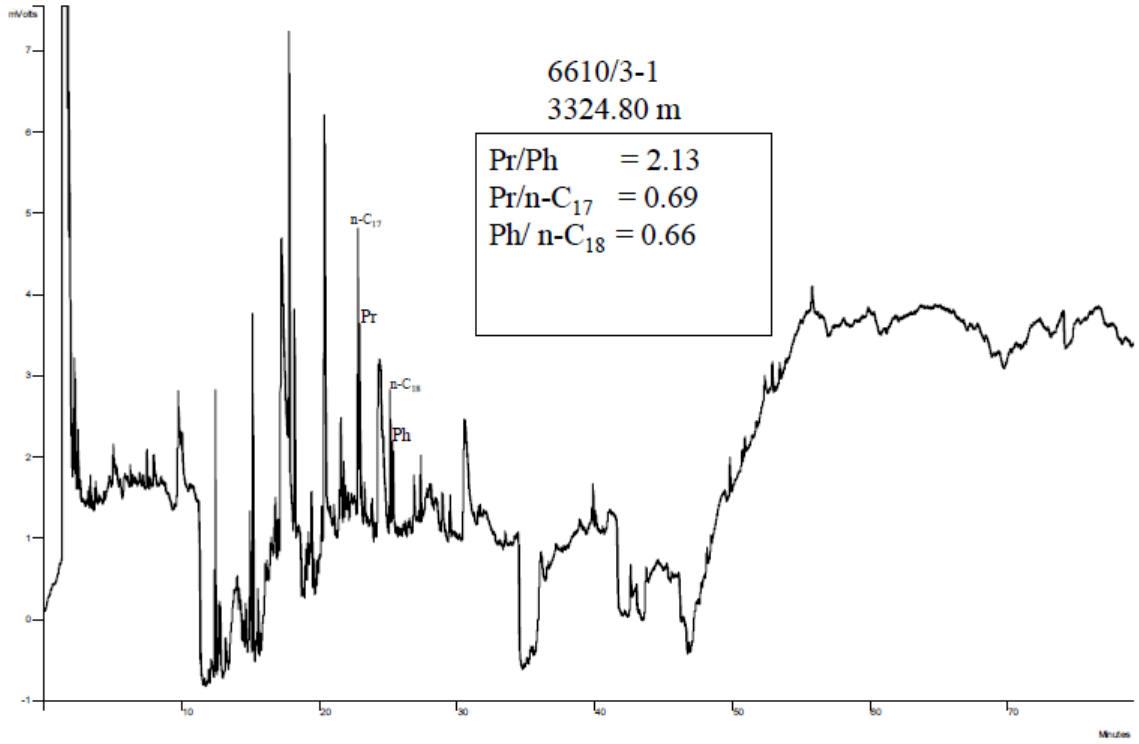

Figure 4.23 GC-FID result showing n-C_{17} and n-C_{18} with associated isoprenoid Pr and Ph from the well 6610/3-1 at 3324.80 m depth.

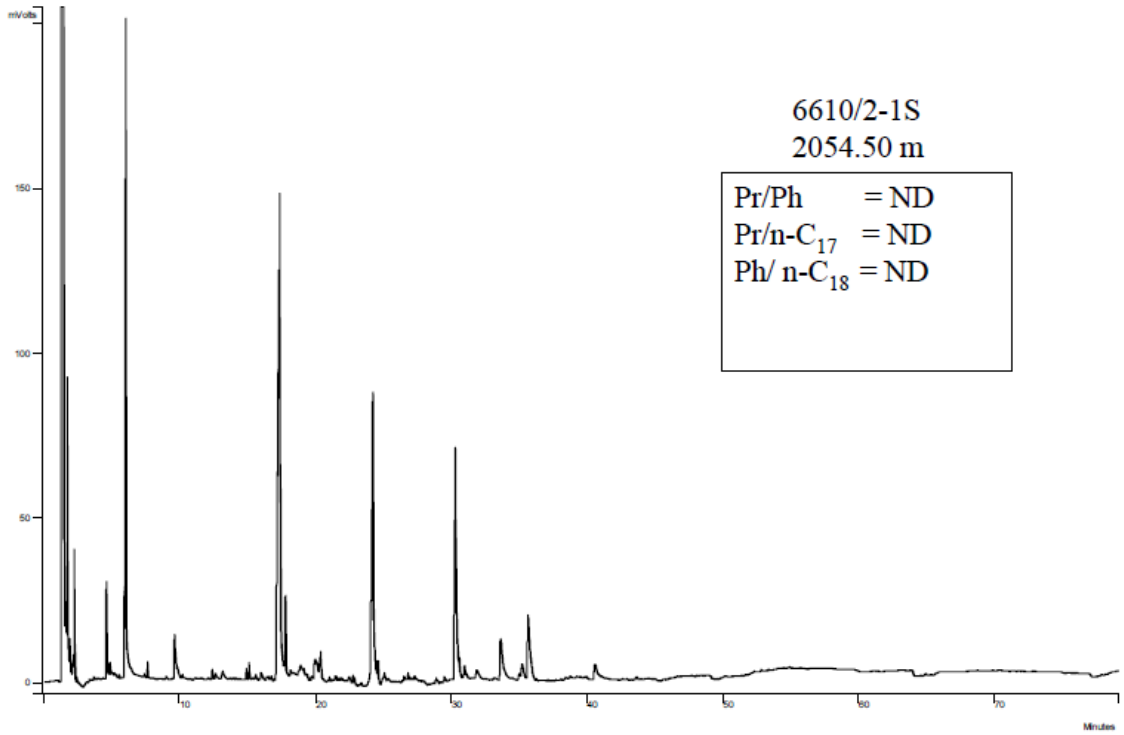

Figure 4.24 GC-FID result from the core extracts of well 6610/2-1S showing typical polyethylene glycol signatures at 2054.50 m depth. This represents drilling mud. No record was made in this well of core extracts with natural petroleum compounds. Still, it contains fluorescent oil inclusions and wet gas.

Chapter 5

Discussion and Conclusion

The results presented in Chapter 4 will be discussed in detail in this chapter. Several plots have been generated on the basis of analytical results obtained from gas GC-FID analysis and GC-FID analysis of extracts in the laboratory to illustrate the compositional heterogeneities, maturity, and organic facies. Major issues which were the main concerns in this study will be concluded at the end of this chapter.

5.1 Presence of light HCs (C_1-C_5) and wetness parameters

On the basis of gas analysis of core samples light HCs ranging from C_1-C_5 was detected and identified on chromatograms and values of vol. % C_1-C_5 were computed. Almost all samples from the different wells (35/4-1, 6610/3-1 & 6610/2-1S) contain light HCs ranging from C_1-C_5. However few samples from 6610/3-1 & 6610/2-1S contain either up to propane or only methane and one samples show no signature of light hydrocarbon. For example a sample from the well 6610/3-1 at a depth of 1682.50 m produced light HCs ranging from C_1-C_3 (see table 4.1 and Appendix A). The well 6610/2-1S, sample at a depth 2344.20 m contains light HCs ranging from C_1-C_3 and sample from the depth 2344.50 m have shown no light HCs signature and another sample which represents a depth interval of 2346.5 m and 2351.50 m have shown only C_1 signature (See Table 4.3 and Appendix A).

The concentration and type of light HCs formed are dependent on several factors and one of the most important is kerogen type i-e sapropelic and humic (Whiticar, 1994). The type I and type II kerogen generate, over appropriate time periods, substantial amounts of thermogenic hydrocarbon gases at temperature over 70^{o}C (Figure 5.1).

The $\sum C_2+$ parameter is usually used to distinguish between biogenic and thermogenic gases. This is because C_2+ gases are normally believed to be formed due thermal cracking of the kerogen or higher hydrocarbons. Biological activities are known to produce pure methane where C_2+ is less than 1% (Whiticar, 1994). Whiticar also stated that these biogenic gases are formed mostly by methanogenic bacteria at near-surface due to fermentation reactions at the final stage of diagenesis, where the temperature is less than 50^{o}C.

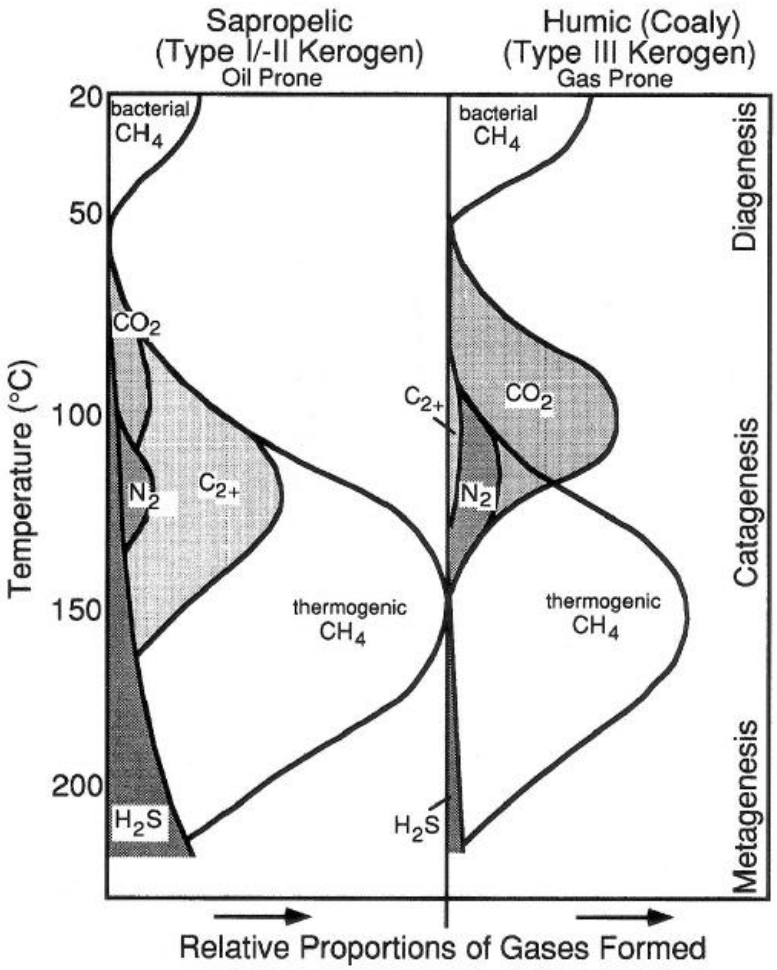

Figure 5.1 showing the relative proportions of natural gases types generated from the different kerogen types such as: sapropelic (type I and type II) and humic (type III) source rocks with as a function of thermal maturity (From hunt, 1979).

The initial gases generated at low thermal maturity (<0.5% Ro) is relatively dry (<5%$\sum C_{2+}$) (Hunt, 1979; Whiticar, 1994), but the percentage of higher hydrocarbon intensifies with additional maturation into and through the oil window and produces more lighter hydrocarbons, where the temperature of peak natural gas generation is 150^{o}C -160^{o}C (Fig. 5.1). As the maturation continues into the late mature (1.3-2.0% Ro), successive kerogen conversion and cracking of hydrocarbons leads to a greater proportion of shorter chained hydrocarbons and essentially a methane-rich gas or dry gas at the base of the catagenic stage, roughly at 200 ^{o}C (Hunt, 1971; Whiticar, 1994) (Figure 5.1).

Based on the gas analysis and computed parameters, equation 1, 2 and 3 are used to characterize natural gases (Table 4.1, 4.2 and 4.3, Figure 5.2).

Gas wetness (vol. %) = $(C_2+C_3+i\text{-}C_4+n\text{-}C_4) / (C_1+C_2+ C_3+i\text{-}C_4+n\text{-}C_4) * 100$ (1)
% $\sum C_2+$ (Vol. % HC) = $(C_2 + C_3 + i\text{-}C_4 + n\text{-}C_4)$ (2)
Bernard parameter (vol. %) = $C_1 / (C_2 + C_3)$ (3)

Essentially, the above ratios all serve the same tenacity, but they accentuate diverse ranges in compositional distinctions. Equation 1 and 2 are applied functions for the presentation of the wetness ratios of natural gas accumulations or lithology with elevated amounts of higher hydrocarbons (Whiticar, 1994). Equation 3 is more supportive to explain the compositional deviations observed in seep gases, near-surface sediments and soil, and drill cuttings and mud gas logs, where extreme dynamics in composition are possible (Whiticar, 1994). Illustrations of depth versus time of hydrocarbon generation profiles can be seen in Figure 5.1 (Hunt, 1979). Hydrocarbon gas generation is neither uniform nor consistent in composition throughout its generation history (Figure 5.1), for instance sapropelic source rocks of thermogenic natural gas initially release a wet gas, one with abundant higher hydrocarbons and $C_1 / (C_2 + C_3)$ □ 5, as the source rocks become more thermally mature, the higher hydrocarbon content drops continually to $C_1 / (C_2 + C_3)$ ratios of > 20 and at over maturity, the $C_1 / (C_2 + C_3)$ ratios can be >50, as the earlier generated higher hydrocarbons are afterward cracked to lesser molecular weight species (mainly methane).

It is also interesting to investigate the maturity level of the samples from the different wells studied based on the available data from the gas analysis. Whiticar, 1994 showed a relationship between volume concentration of three thermogenic gases (methane, ethane and propane) and maturity level of the source rock by calculating the values of % Ro from vol. % methane, vol. % ethane and vol. % propane by using equation 4, 5 and 6.

% methane = 9.1 ln (% Ro) + 93.1 (4)
% ethane = -6.3 ln (% Ro) + 4.8 (5)
% propane = -2.9 ln (% Ro) + 1.9 (6)

The calculated values of maturity for samples of well 35/4-1, 6610/3-1 & 6610/2-1S are presented in table 4.1, 4.2 and 4.3 respectively.

Based on the data computed by gas analysis methane is the dominant hydrocarbon gas at all level of generation and the gas composition becomes even more methane rich as

the thermal maturity increases, this is also indicated by Bernard parameter (C_1 / (C_2 + C_3) and shown in Figure 5.4.

5.1.1 Dry gases

The concentration of dry gases increases with increasing maturity of organic matter of the source rock; however, the hydrogen isotope fractionation is the same for organic matter (Schoell, 1980). Based on the $\sum C_{2+}$ values dry gases can be identified from the data set, $\sum C_{2+}$ <5% values represents the dry gases. Figure 5.2 presents a cross plot of C_{2+} versus methane. Calculated values are indicated in table 4.1, 4.2 & 4.3. The methane percentage of well 35/4-1 ranges from 61.98 to 91.86 (average = 82.23) and the percentage of methane for well 6610/3-1 and 6610/2-1S are 85.53 to 98.01 (average = 91.86) and 80.25 to 100 (average = 88.75) respectively. The C_{2+} percentage values for well 35/4-1, 6610/3-1 and 6610/2-1S ranges from 8.14 to 38.02 (average = 17.77), 1.99 to 14.47 (average = 8.14) and 0 to 19.75 (average = 11.25) respectively. In general well 6610/3-1 has the highest percentage of dry gases compared to the other two wells. On the other hand well 35/4-1 with an average C_{2+} value of 17.77 contains more of the heavier gases. This indicates that this well with indication of concentrated higher C_{2+} molecules may contain oil compared to the other two wells which mainly contain gases as indicated by the Bernard parameter. Lowest values of $\sum C_{2+}$ calculated in the three wells could suggest that the petroleum at the specific depth is at a higher maturity level. This can be exemplified by samples taken from well 6610/3-1 at the depths of 2521 m and 2664.50 and samples representing the interval between 1682.50 m to 1714.50 m and. These later samples are indicated in fig 5.2 as having very high methane concentration. Therefore regarding well 6610/3-1, the studied samples indicate the presence of both dry and wet gas.

This is also illustrated in the Figure 5.3 on the basis of thermal maturity of source rock relative to the volume % of methane, ethane and propane. On the basis of data set, graphical representation shows that small number of core samples especially from the well 6610/3-1 and 6610/2-1S contains dry gases. Bernard parameter also confirms that most of the gases are in the range of >5 and <50 except two samples from the well 6610/3-1 (See Table 4.1, 4.2 and 4.3).

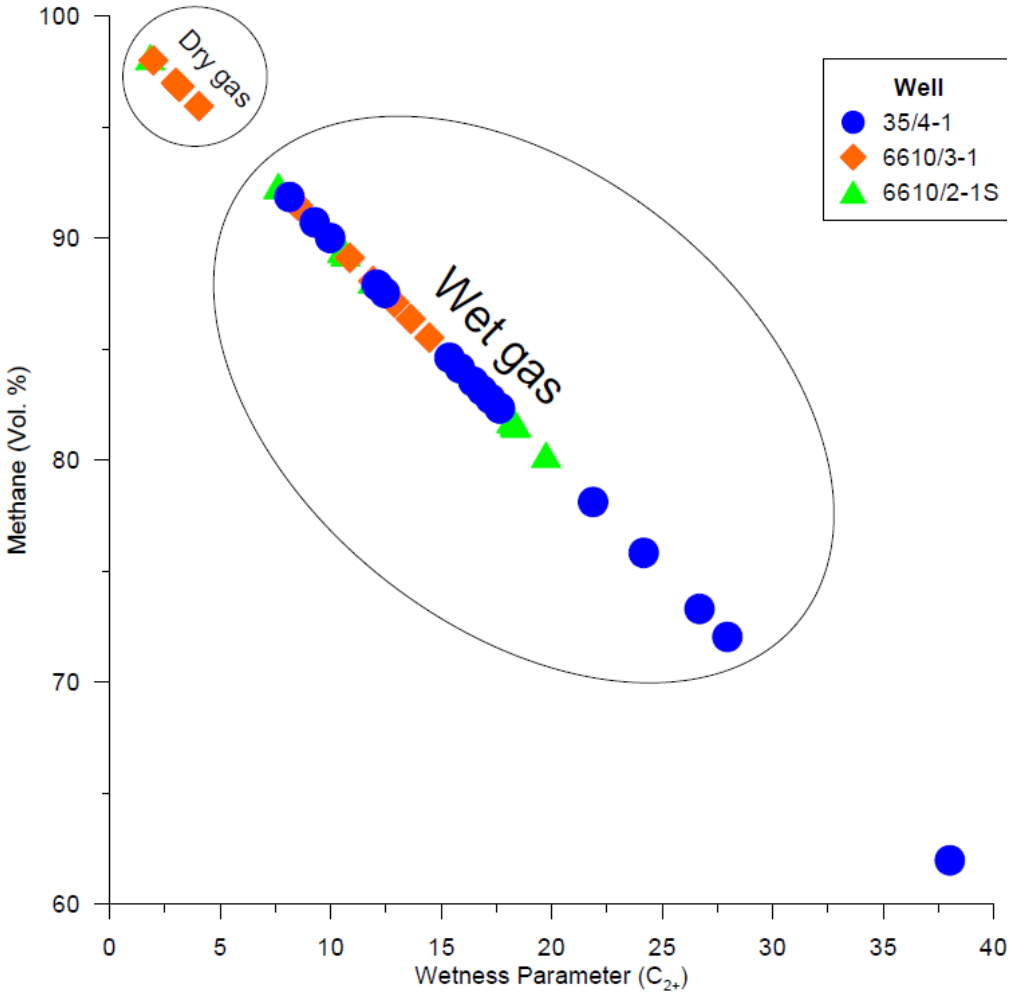

Figure 5.2 cross plot of vol. % C_1 and wetness parameter computed from the sample data set represent the small proportion of dry gases in well 6610/3-1 and 6610/2-1S from the Norwegian Sea. A surprising number of the samples from these "dry wells" are "condensate-wet" and many are "oil-wet".

5.1.2 Wet/Oil associated gases

The wet gases (C_2-C_7) generated from a source generally represent more than 5% of the total HC generation and $\sum C_2+ > 5$ represent wet gas existence (Floodgate and Judd, 1992). Wetness parameters calculated from the sample data set (See Table 4.1, 4.2 and 4.3) show that the samples contain wet gases as the value of $\sum C_2+ > 5\%$ in well 35/4-1, 6610/2-1S. Whereas in well 6610/3-1 there are relatively less wet gases identified. As methane is the major gas produced at all stages and gas composition also become methane rich as thermal maturity increases. Based on the data set relative amount of methane, ethane and propane by volume is compared to the vitrinite reflectance (Ro) of source rock according to equation 4, 5 and 6 and results are presented in Table 4.1, 4.2 and 4.3 and plotted in fig 5.3.

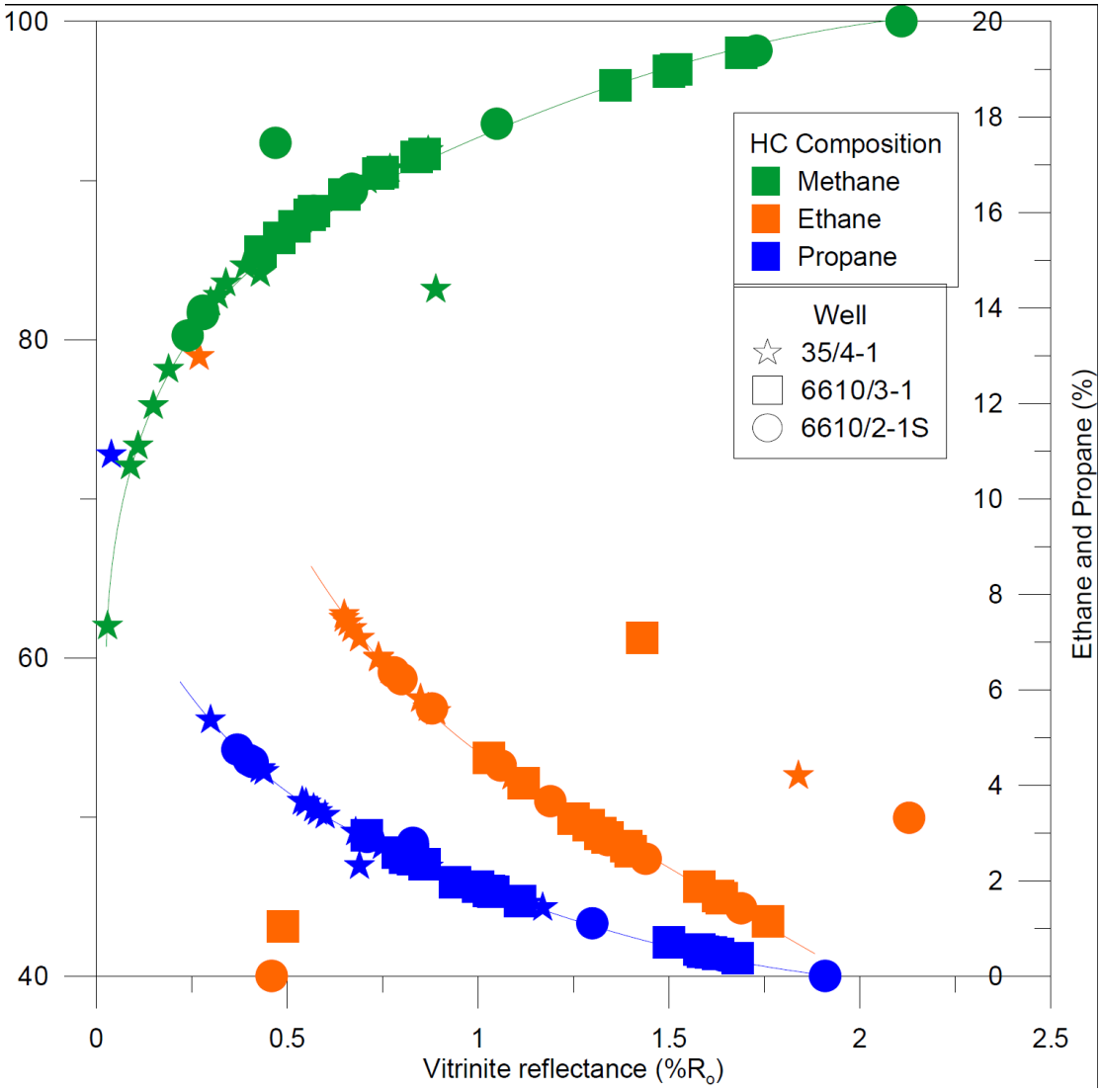

Figure.5.3 thermal maturity of source rock compared to the relative amount of methane, ethane and propane by volume (based on Berner, 1989; Whiticar 1994).
According to Evan and Staplin (1971) oil-associated natural gases can have more than 80% $\sum C_{2+}$ and on the bases of sample data set there are no oil associated gases present in these well. However, based on Schoell (1983) all samples with more than 13-15% C_2+ are clearly oil associated. Samples with 5-15% C_2+ content are condensate associated.

As mentioned above the vitrinite reflectance of the studied samples have been calculated based on the analytical formulas proposed by Whiticar (1994). Following this vitrinite reflectance plotted against the concentrations of methane, ethane and propane. This kind of plot, according to Whiticar, will give assessment on the maturity level of the samples and the hydrocarbon contained in the samples. As it is shown in fig 5.3, the concentrations of methane increase as the vitrinite reflectance increase, while the concentration of C_2+ (ethane and propane) decreases with maturity. This graph is well in agreement as proposed by Whiticar (1994).

Fig 5.4 is a cross plot of Ro versus Bernard parameter showing that wet gases are encountered in these wells. The $C_1/ (C_2+C_3)$ values for the samples representing well 35/4-1 ranges from 2.59 to 19.15 (average = 9.91). Well 6610/3-1 contains relatively higher values of $C_1/ (C_2+C_3)$ ratios with values ranging from 8.52 to 60.86 (average = 28.64). The samples from well 6610/2-1S have $C_1/ (C_2+C_3)$ ratios of values ranging from 7.63 to 21.68. Whiticar 1994 showed that the value of this parameter increase as the maturity increase. The samples representing well 35/4-1 contain relatively lower ratio of this value, suggesting that the petroleum in these samples is relatively lower in maturity compared to the samples from the other wells. On the other hand the $C_1/ (C_2+C_3)$ values of well 6610/3-1 are relatively higher with some values up to 60. According to Whiticar (1994) over mature samples may show values of $C_1/ (C_2+C_3)$ more than 50.

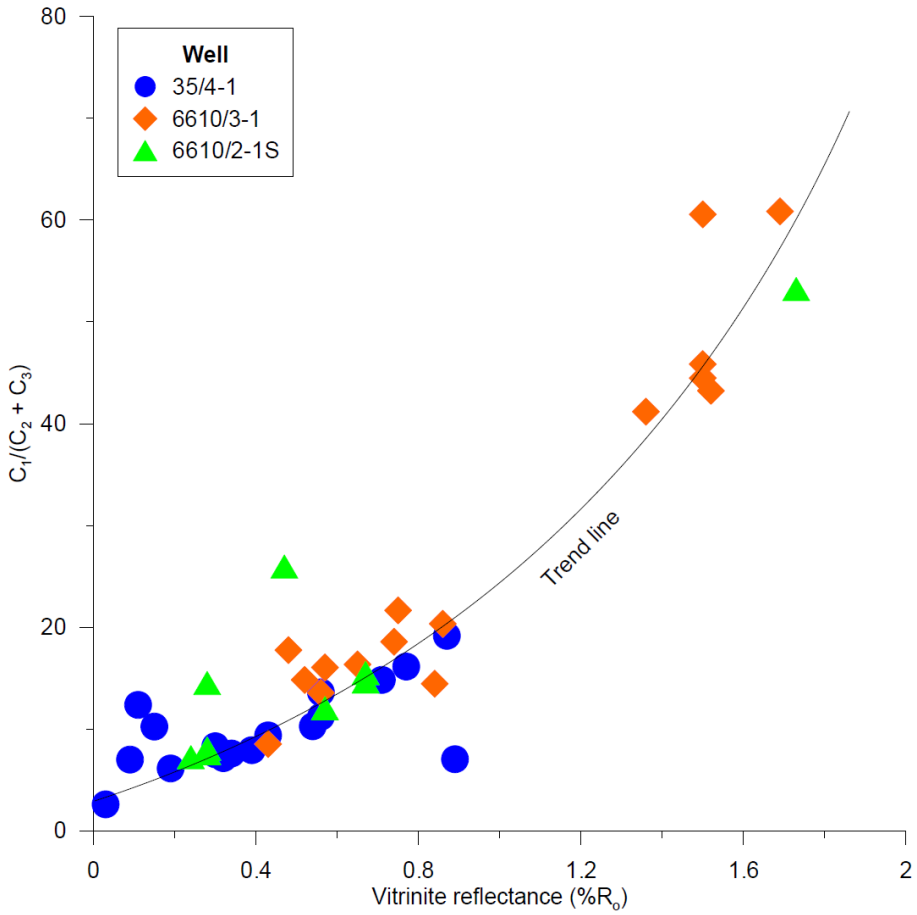

Figure.5.4 cross plot of thermal maturity versus Bernard parameter indicating the small proportion of over mature facies that contain dry gases and major proportion of thermally mature facies which contains wet gases.

5.2 Bitumen

The GC-FID traces from the core extracts were used to compare the pristine/phytane (Pr/Ph), isoprenoid/n-alkane (Pr/n-C_{17}, Ph/n-C_{18}) ratios and n-alkane distribution in well 35/4-1 and 6610/3-1. More n-alkanes are generated from kerogen due to increase in thermal maturity and as a result pr/n-C_{17} and ph/n-C_{18} ratios decrease (Tissot et al., 1971). The highly mature rock extracts represent the least concentration of biomarker as almost all biomarkers destroyed due to high temperature (Peters and Moldowan, 1993). Bitumen or core extracts were analysed from three wells and the sample set shows high signal to noise ratio in well 35/4-1, slightly high variation in pr/ph ratio and low signal to noise ratio is observed in well 6610/3-1except two sandstone samples at a depth 2521 m and 2522.80 m, whereas no n-alkanes were monitored in well 6610/2-1S at all.

5.2.1 Maturity

The isoprenoids/n-alkanes ratios have been widely used by petroleum geochemists as maturity assessments. Based on the pr/n-C_{17} and ph/n-C_{18} ratios (See Figure 5.5) the core extracts from the well 35/4-1 and 6610/3-1 are cross plotted and can be identified in terms of maturation and biodegradation, as maturity and biodegradation are inversely proportional parameter. As can be seen from the figure those samples with low values of pr/n-C_{17} and ph/n-C_{18} ratio represent higher maturity compared to those with higher ratios.

In general the samples represent well 35/4-1 contains hydrocarbon which is more mature than the hydrocarbon available in well 6610/3-1. There is a trend which suggests maturity variation within the samples in well 35/4-1. A sample at depth 4248.30m with the lowest Pr/n-C_{17} and Ph/n-C_{18} ratio represents the most mature sample in the dataset of well 35/4-1. On the other hand core samples taken at the depth interval between 4152.50 m and 4154.50 shows the highest Pr/n-C_{17} and Ph/n-C18 ratios and hence the least mature of the samples in well 35/4-1. The details on the calculated parameters of GC-FID for the well 35/4-1 are presented in Table 4.4. The bitumen samples from the well 6610/3-1 are less mature and more biodegraded than core extracts from the well 35/4-1. The increase in thermal maturity will increase the pr/ph ratios that can be used as a maturity indicator (Alexander et al., 1981).

The highest pr/ph ratio from the well 35/4-1 is at a depth 4248.30 m which is the same depth for the least value of pr/n-C_{17} and ph/n-C_{18} and confirms the Alexander et al

statement (See Figure 5.5 and Table 4.4) whilst core extracts from the well 6610/3-1 show the highest value of pr/ph at a depth 2311.00 m representing the highest maturity in that well.

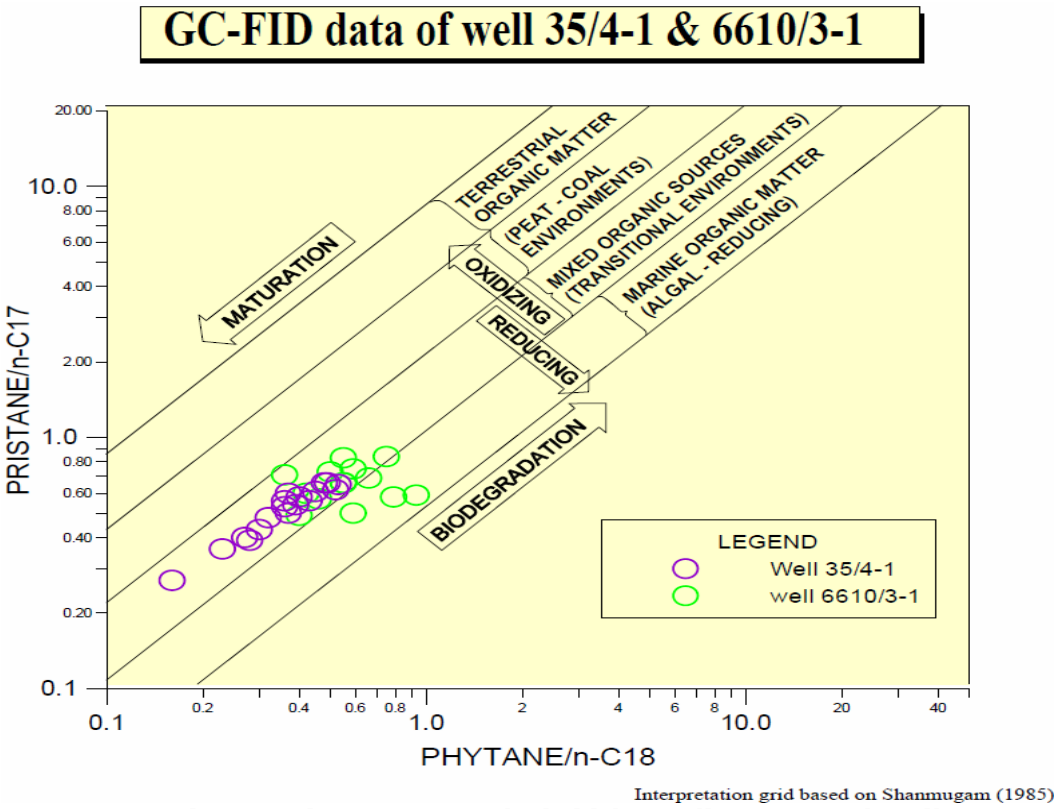

Figure 5.5 petroleum inclusions presently held by well 35/4-1 and well 6610/3-1, showing high maturity in well 35/4-1 core extracts compared to the well 6610/3-1 core extracts. The samples plot in the region typical for the Spekk or Draupne formations, albeit with possibly some more varied kerogenmaceral composition indicated for 6610/3-1, i.e. potentially a more proximal version of the Spekk Formation.

A common tendency with the sample data set from the well 35/4-1 show higher maturity samples comparing to the samples from the well 6610/3-1 and it may indicate that the petroleum in well 35/4-1 is trapped before the petroleum in well 6610/3-1. It also indicated that the source rock of well 35/4-1 was deposited more deeply than the source facies of well 6610/3-1 and showing high maturity level in well 35/4-1, which also supports the outcome from this study. According to Munz et al., 1999 the cementation have a general cause on petroleum and it is most likely that fluid inclusions are trapped during fill of the reservoir than at later stages when huge amount of water has been dislodged.

5.2.2 Organic facies

This section express how GC-FID data is used to investigate the organic facies and sedimentary environment of the core extracts from the well 35/4-1 and 6610/3-1. It is impossible to describe a legitimate conclusion on the oxicity of the depositional environment of source rock from pr/ph ratios single-handedly (Ten Haven et al., 1987). Several other factors like thermal maturity can also change the pr/ph ratios (Peters and Moldowan, 1993). Hunt, 1996 defined organic facies as "mapable subdivisions of stratigraphic units distinguished from the adjacent subdivisions by the character of their organic matter". Different amounts and types of HCs are produced by various types of organic facies. According to Didyk et at., 1978 the pr/ph ratios of oils or bitumen have been used to indicate the redox potential of the source sediments. Typical pr/ph ratio for type II marine shale is ranging between 0.6 to 1.6 (Elvsborg et al., 1985: Cohen and Dunn, 1987). Most of the samples from well 35/4-1 shows pr/ph ratio ranging from 1.07 to 1.85 (See Table 4.4) except one sample having a pr/ph ratio of 2.1 at a depth 4248.30 m which indicate type II marine shale. Whilst the data obtained from well 6610/3-1 showing normally pr/ph ratios greater than 1.6 indicates a more terrestrial input. According to NPD thin claystones encountered in the Top Intra-Nise Sandstone show the best source rock potential in the well 6610/3-1 and these claystones include terrigenous organic matter in a huge amount, with a fair to good potential for generation of light oil, or gas/condensates which correlate our results from the core extracts that indicate the pr/ph ratios are 3.5 and 4.0 at depth 2306 m and 2311 m respectively and confirms the terrestrial facies and correlate our results from the core extracts of well 6610/3-1 (See Figure 5.6). However, according to figure 5.5 some samples from well 6610/3-1 could be categorized as more marine influenced than terrestrial which contradicts the higher values of Pr/Ph ratio. This could be explained by the effect of maturity and biodegradation over organic facies.

In conclusion referring to tables (4.4 & 4.5) and figures (5.5 & 5.6) the depositional environment for the source of the studied samples is Type II/III marine with slightly more terrestrial input to the samples from the more proximal well 6610/3-1, indicating source rock deposited more marine reducing environment than those samples representing well 35/4-1 which is distal Type II/III of the Draupne type. Therefore, on the basis of sample dataset from both wells one can say that the source rocks that has

generated the HCs were mostly of mixed organic facies of the general Spekk or Draupne (Kimmberidge Shale) type.

5.3 Microscopic Investigation of Inclusions

Micro samples of fluid trapped within crystals during mineral formation as imperfections are called fluid inclusions (S.Michael Sterner and Robert Bodnar, 1984). Formation of fluid inclusions is dependent on numerous physical and chemical conditions that might lead for that cause and some are limited to definite minerals or even particular crystal faces in individual minerals (Watanabe 1987; R. J. Bodnar, 2003).

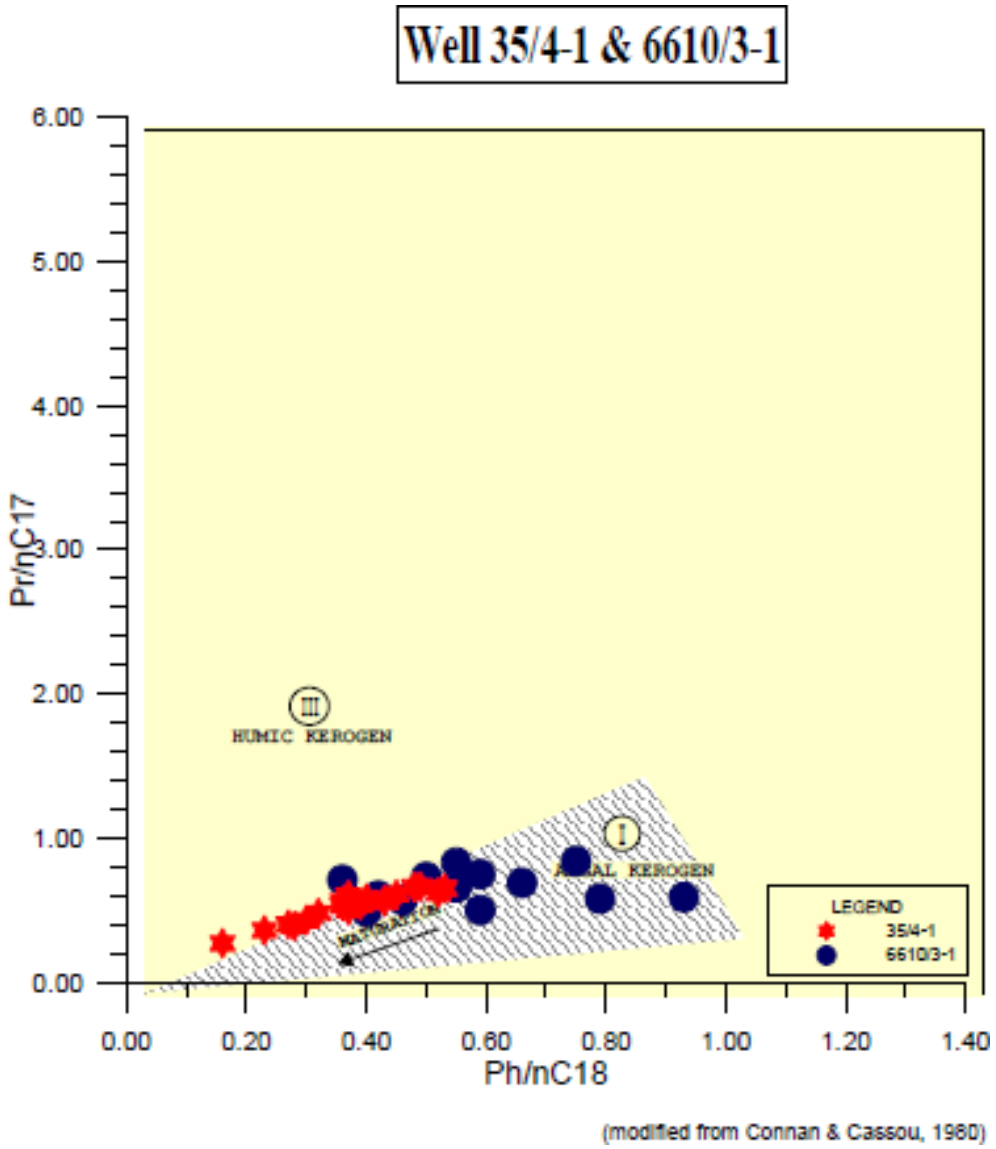

Figure.5.6. Showing the depositional environment for organic facies for selected wells. All samples fall in the span typical for the "Kimmeridge Shale" as known from the North Sea and the Norwegian Sea (Karlsen et al., 1993:2006); the variation along the 45 degree vector is due to variable degree of maturity or biodegradation.

In all disciplines of the geologic sciences the study of fluid inclusions has broad application by executing comparatively simple tests and obtained valuable results for the investigation of trapped HCs. However, the mechanism of trapping of inclusions and subsequent changes during initial fluid entrapment is not fully explicable (Roedder, 1984).

The schematic diagram showing different types of oil population along overgrowth, dust rim and healed fracture (See Figure 5.7). On the basis of the microscopic analysis of samples from 35/4-1, 6610/3-1 and 6610/2-1S wells showing water/condensates inclusions, gas bubbles and oil inclusions respectively (See Figure 4.1). Water inclusions in nature are one of the simplest categories of fluid inclusions that restrain fundamentally pure water (S. M. Sterner and R. J. Bodnar). Microscopic study of the sample at a depth 4156.50 m from the well 35/4-1 showing minute water inclusions and possible oil inclusions and this was the only sample from the well 35/4-1 that has shown some inclusions under microscope. From the well 6610/3-1, abundant amount of water/condensates inclusions and gas bubbles were studied whilst from the well 6610/2-1S oil inclusions were identified when sample was exposed under UV light.

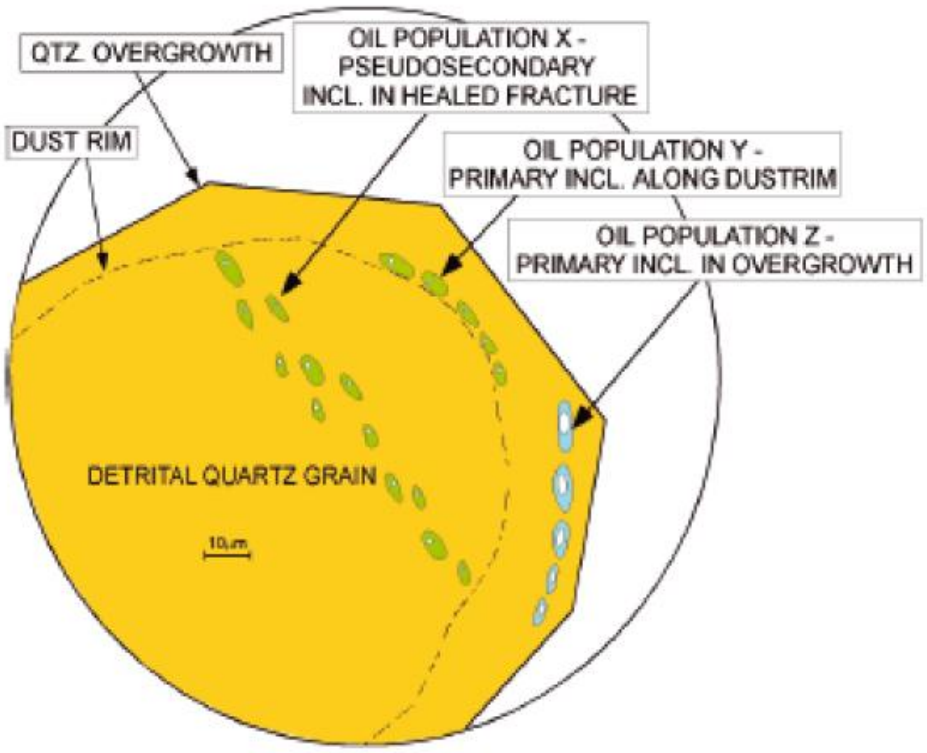

Figure 5.7 Schematic diagram of fluid inclusions showing oil inclusion populations in several zones (modified from Karlsen et al., 2006).

The aqueous and oil fluid inclusions occurring in petroleum reservoir cements generally provide vital information about the physical and chemical conditions of diagenetic processes (Roger K. Mclimans, 1987). In these samples more than one type of oil/gas/condensates inclusion is present that recommend numerous migrations or different sources for oil and this is also confirmed by the gas analysis and GC-FID data that has provided different types of gases (dry gas and wet gas) and oils of different maturities from different facies respectively.

5.3.1 Color and API gravity

The visible color of the fluorescence emission varies with the API gravity of the oil and it varies from 19 to 50+ (See Table 4.7). According to Lumb, 1978, the composition of HCs reveal about the fluorescence color and its intensity. In reservoir oils, increase in maturity shows the trend shifting toward the blue fluorescence color (McLimans, 1987). Those HCs with API gravity ranging from 19-33 and the fluorescence color in the red-yellow region of the visible spectrum are called immature HCs while yellow to green and green to white fluorescence color represent oils with gradually shorter wavelength response and higher maturity. The fluorescence color ranging from blue-violet region represents the condensates (Guilhaumou et al., 1990). Based on the microscopic results from well 35/4-1, minute aqueous inclusions were observed with possible oil inclusions and color of the HCs was not describable under the microscope. In well 6610/3-1 aqueous inclusions with considerable amount of gas bubbles is observed but weak fluorescence color were observed in this well which may symbolize a weak inclusions that could be water or condensates. While in well 6610/2-1S green/blue substantial amount of fluid inclusions is observed which represent oil. Micro photographic images of fluid inclusions are available in chapter 4 and figure 4.1.

5.4 Comparison of maturity and facies of fluid inclusions

In this section a comparison of maturity and facies of the two wells will be discussed based on the available data. On the basis of results from the GC-FID such as pr/n-C_{17} and ph/n-C_{18} ratios from the well 35/4-1 and 6610/3-1 the core extracts from samples can be organized into a succession on the basis of maturity. Comparing the two wells the utmost maturity in the core extracts is found in well 35/4-1 as the ratio of pr/ph is maximum in the dataset and pr/n-C_{17} and ph/n-C_{18} ratios are minimum, while the values of pr/ph, pr/n-C_{17} and ph/n-C_{18} from the core extracts of samples from the well

6610/3-1 are minimum as compare to the well 35/4-1. The least mature sample from the well 35/4-1 is at a depth 4172.60 m whilst the sample at a depth 1683.50 from the well 6610/3-1 is observed to be the least mature. In general the samples from well 35/4-1 were found to represent the more mature hydrocarbon of the data set than the well 6610/3-1. However, this maturity comparison is only on the basis of the available n-alkane and isoprenoid data which are highly affected by other post generation processes such as biodegradation. Hence it is recommended that other maturity parameters such as biomarkers should support this finding for a better understanding of the thermal maturity of the samples.

The increase in thermal maturity also enhance the ratios of pristane to phytane (pr/ph) and that can also be used a maturity indicator (Alexander et al., 1981), but care should be taken when relating pr/ph ratios and reason could be that facies and diagenetic processes might cause this parameter and pr/ph ratios cannot produce a desirable result. So from the data set one can say that well 35/4-1 have higher maturities than the well 6610/3-1 and depth can also play a vital role in terms of maturity as source rock is more deeply buried higher maturity is observed. Samples from the well 35/4-1 are much deeper and hence the source rock is buried deeply than the well 6610/3-1, therefore this could be the possible explanation that well 35/4-1contains more mature HCs.

The high ratio of pristane to phytane (pr/ph) can also indicate the different depositional environments and those high ratios can indicate a different facies as in the well 6610/3-1. The highest value of pristane to phytane ratio (pr/ph) is 4 at a depth 2311 m and the lithology at this depth is mudstone which is not a normal sequence in that well and showed a different ratio for pr/ph as compare to the other samples (www.npd.no).

Previous studies (e.g. Elvsborg et al., 1985: Cohen and Dunn, 1987) have found that type II marine shale have pr/ph ratio ranging from 0.6 to 1.6. The ratios of pristane to phytane (pr/ph) in the sample set from well 35/4-1 ranges from 1.22 to 2.10, with most of the values lie between 1.22 and 1.54. This is consistent to the previous suggestions except few samples at higher depth having pr/ph greater than 1.6. Hence most of the samples from well 35/4-1are charged from type II marine shale.

Generally the ratios of pr/ph of the samples from well 6610/3-1 are higher than 1.6 which typically represents type II shale and however, two ratios of pr/ph at depths of 1683.50 m and 2670.50 were found to be lower than 1.6 (See Table 4.5). The higher ratios of pr/ph samples are relatively deeper and their trend is little toward the oxic environment and indicating more terrestrial input.

The conclusion from the above discussion is that the depositional environment for the source rock that has generated the petroleum for these sample in this study is transitional, in other words it is marine environment with terrestrial input. The well 6610/3-1 showing more terrestrial input as the pristane to phytane ratios are higher than 1.6 as compare to the well 35/4-1 samples. In this study none of the samples show an evidence of being generated from a lacustrine depositional environment as none of the samples has pristane to phytane ratios (pr/ph) below 1.0 which typically represent the lacustrine environment.

5.5 Conclusion

The data set is comprised of 18 core samples from well 35/4-1 from the North Sea, 16 core samples from the well 6610/3-1 and 14 core samples from well 6610/2-1S both from the Norwegian Sea. The aim was to look for and investigate both core extracts and fluid inclusions within each well. The wells are on the NPD pages concluded to be dry without shows of migrated oil or gas. If evidences or proof of migrated petroleum is found in any of these wells, this represents data of major importance to exploration in these regions.

Gas from inclusions tells us about the overall gas signature of HC gas from water and petroleum inclusions. It is important to conclude on gas wetness, i.e. is the gas dry or condensate associated? Is in cases the gas even oil associated?

The observation of fluorescent petroleum inclusions is a unique set of information concerning GOR and API in the entrapped petroleum. While observed petroleum inclusions are singular data points compared to bulk crushing of sand grains to liberate gas from inclusions, the observation of petroleum inclusions, the fluorescent colors and the relative size of the gas bubble is of great importance to the understanding of what type of oil existed at one time in the paleo-reservoir.

In this section, the conclusions from this study are presented:

- There are strong evidences of the existence of migrated oil and gas in these wells on the basis of core samples used for gas analysis and bitumen core extracts from the selected core samples from these wells. All three wells are classified as having contained migrated petroleum in the past, i.e. these wells have mistakenly been classified by the industry and workers as dry. The implication of this fact is of major significance to future exploration in the 35/4 and the 6610 regions.
- In short, clear evidence is found for paleo-migration of oil into well 35/4-1, with oil and later condensate migration into well 6610/3-1 and 6610/2-1S. Below are more details presented on the wells and the HC signatures.
- In terms of gas (C_1-C_5) from inclusions, it was possible in all samples to extract gas. While dry gas, as found in well 6610/3-1 is likely to mainly represent gas from water inclusions, wet gas (C_{2+} content larger than 5%) was found in well 35/4-1and 6610/2-1S. Thus, it was also possible to determine the gas wetness parameters (C_2+ and C_1/C_2+C_3) and on the basis of that parameter it was clear that more than 80% gas in these wells was wet gas. Furthermore on the basis of vol. % of methane (vol. % C_1), vol. % of ethane (vol. % C_2) and vol. % of propane (vol. % C_3) it was possible to calculate the thermal maturity (% Ro) of the source rocks that generated the gas. In short, well 35/4-1 contains more wet gas as compare to well 6610/3-1 and 6610/2-1S.
- There were detectable n-C_{17}, n-C_{18}, pristane and phytane from the chromatograms in well 35/4-1 and 6610/2-1s, and the ratios of pristane to phytane (pr/ph), the ratios of pristane to n-C_{17} (pr/n-C_{17}) and ratios of phytane to n-C_{18} (ph/n-C_{18}) were calculated from the well 35/4-1 and 6610/3-1. It was not possible to detect any n-C_{17}, n-C_{18}, nor pristane and phytane from the well 6610/2-1S as the core samples were contaminated by polyethylene glycol and chromatograms produced typical signature for that chemical fluid that was used to preserve the core samples.
- The n-alkane profile of the studied samples is very different to that of North Sea Standard oil (NSO-1). The huge UCM which is observed in well 35/4-1 suggest that the palaeo-oil was biodegraded.

- On the basis of maturity and facies parameters, differences were observed from these wells. The samples from well 35/4-1 represent more mature petroleum which was derived from marine facies sources. The bitumen extracted from well 6610/3-1 were also derived from marine organic facies but with significant input from terrestrial environment compared to that of well 35/4-1.
- There were observable petroleum inclusions (observed under microscope) in selected samples from these wells but the intensity of these inclusions in well 35/4-1 was less as compare to the well 6610/3-1 and 6610/2-1S. In well 35/4-1 minute aqueous inclusion and potential petroleum inclusion were observed whilst in well 6610/3-1 gas/oil inclusions were observed under microscope as UV-fluorescent inclusions with large gas bubbles. Oil inclusions were documented when samples from the well 6610/2-1s were exposed to UV light under the microscope.
- Previous works show that these wells are dry with no commercial hydrocarbon content. However the results from this study show that there are clear indication for the paleo-presence of both gas and oil in all three wells. The GC-FID results of core bitumen show that well 35/4-1 contains n-alkane profiles comparable to some oil fields on the NOCS. With known oil potential in the NCS. While well 6610/3-1 clearly did in the past contain gas, well 6610/2-1S is suggested to have contained light oil and later a condensate.
- These findings should be incorporated into future exploration models on structures in the regions of these three wells.

References

Abay, T. B., 2010. Vertical variation in reservoir core geochemistry. Thesis in Geochemistry, Department of Geology, University of Oslo, Norway, 284 pp.

Alexander, R., Kagi, R. I., and Woodhouse, G. W., 1981: Geochemical correlation of Windalia oil and extracts of Winning Group (Cretaceous) potential source rocks, Barrow Sub-basin, Western Australia, AAPG Buletin, 65, 235-250

Bernard, B. B., Brooks, J. M. & Sackett, W. M. 1978. Light Hydrocarbons in Recent Texas Continental Shelf and Slope Sediments. J. Geophys. Res., 83, 4053-4061.

Berner, U., 1989, Entwicklung und Anwendung empirischer Modelle für dieKohlenstoffisotopenvariationen in Mischungen thermogener Erdgase: Ph. D. dissertation, T.U. Clausthal, FRG, 160 p.

Bering, D. 1992. The orientation of minor faultplane striae and the associated deviatoric stress tensor as a key to the fault geometry in part of the Møre-Trøndelag Fault Zone, onshore central Norway. In: Larsen, R. M., Brekke, H., Larsen, B. T. & Talleraas, E. (eds) Structural and Tectonic Modelling and its application to Petroleum Geology. Norwegian Petroleum Society Special Publication, 1, 83-90.

Blystad, P., Brekke, H., Færseth, R.B., Skogseid, J. & Tørudbakken, B., 1995. Structural elements of the Norwegian continental shelf. Part II: The Norwegian Sea Region. NPD-Bulletin No. 8, The Norwegian Petroleum Directorate, 45 pp.

Bodnar, R.J., 1990. Petroleum migration in the Miocene Monterey Formation, California, USA. Constraints from fluid inclusion studies. Min. Mag. 54, 259-304.

Bodnar RJ (2003) Introduction to fluid inclusions. In I. Samson, A. Anderson, & D. Marshall, eds. Fluid Inclusions: Analysis and Interpretation. Mineral. Assoc. Canada, Short Course 32, 1-8.

Brekke, H., 2000. The tectonic evolution of the Norwegian Sea Continental Margin with emphasis on the Vøring and Møre Basins. In A. Nøttvedt et al. (eds) Dynamics of the Norwegian Margin. Geological Society, London, Special Publications, 167, 327-378.

Brekke, H., Sjulstad, H.I., Magnus, C. & Williams, R.W. (2001). Sedimentary environments offshore Norway. In O.J. Martinsen and T. Dreyer (eds). Sedimentary Environments Offshore Norway – Palaeozoic to Recent. Proceedings of the Norwegian Petroleum Society Conference, 3-5 May 1999, Bergen, Norway. NPF Special publication, no. 10, Amsterdam, Elsevier, 7-37.

Bugge, T., Eidvin, T., Smelror, M., Ayers, S., Ottesen, D., Rise, L., Andersen, E.S., Dahlgren, T., Evans, D., Henriksen, S., 2004. The Middle and Upper Cenozoic depositional systems on the Mid-Norwegian continental margin. NGFAbstr. Proc.Geol. Soc.Norway, vol. 3, pp. 14–15.

Butt, F.A., Drange, H., Elverhøi, A., Otterå, O.H., Solheim, A., 2002. Modelling late Cenozoic isostatic elevation changes in the Barents Sea and their implications for oceanic and climatic regimes; preliminary results. Quat. Sci. Rev. 21, 1643–1660.

Bukovics, C., Cartier, E.G., Shaw, N.D. and Ziegler, P.A., 1984. Structure and development of the mid-Norway Continental Margin. In: A.M. Spencer (Editor), North European Margin Symposium. Petroleum Geology of the North European Margin. Graham & Trotman Ltd., Norwegian Institute of Technology (NTH) in Trondheim, Norway, pp. 407-425.

Bukovics, C. and Ziegler, P.A., 1985. Tectonic development of the Mid-Norway continental margin. Marine and Petroleum Geology, 2: 2-22.

Burruss, R. C., Cercone, K. R. & Harris, P. M. 1983. Fluid inclusion petrography and tectonic-burial history of the Al Ali No. 2 well: Evidence for the timing of diagenesis and oil migration, northern Oman Foredeep. Geology, 11, 567-570.

Dalland, A., Worsley, D., Ofstad, K., 1988. A lithostratigraphic scheme for the Mesozoic and Cenozoic succession offshore midand northern Norway. NPD-Bull. 4, 1–65.

Didyk, B. M., Simoneit, B. R. T., Brassell, S. C., and Eglinton, 1978: Organic geochemical indicators of paleoenvironmental conditions of sedimentation: Nature, v. 272, p. 216-222

Doré, A.G., Lundin, E.R., 1996. Cenozoic compressional structures on the NE Atlantic margin: nature, origin and potential significance for hydrocarbon exploration. Pet. Geosci. 2, 299–311.

Doré, A.G., Lundin, E.R., Jensen, L.N., Birkeland, Ø., Eliassen, P.E., Fichler, C., 1999. Principal tectonic events in the evolution of the northwest European Atlantic margin. In: Fleet, A.J., Boldy, S.A.R. (Eds.), Petroleum Geology of Northwest Europe: Proceedings of the 5th Conference. Geol. Soc., London, pp. 41–61.

Ehrenberg, S.N., Gjerstad, H. M., & Hadler-Jacobsen, E, 1992, Smcrbukk Field - a gas condensate fault trap in the Haltenbanken Province, offshore Mid-Norway. In: M. Z. Halbouty, (ed.) Giant Oil and Gas Fields of the Decade 1978-1988. American Association of Petroleum Geologists, Memoir, v. 54, p. 323-348.

Ellenor, D.W., & Mozetic, A, 1986, The Draugen oil discovery. In A. M. Spencer, et al., (eds.) Habitat of Hydrocarbons on the Norwegian Continental Shelf. Norwegian Petroleum Society, Graham & Trotman, London, p. 313-316.

Elisasbeth B. Sletten, 2003. A comparison of petroleum from reservoirs and petroleum inclusions in authigenic minerals cements- Haltenbanken. Thesis in Geochemistry, Department of Geology, University of Oslo, Norway, 107 pp.

Elvsborg, A., Hagevang, T. and Throndsen, T., 1985: Origin of the gas condensate of the Midgard field at Haltenbanken. Petroleum geochemistry in exploration of the Norwegian Shelf., Larsen Rolf, M., Ed., Graham and Trotman, 213-219.

Evans, C.R. and F. L. Staplin, 1971, Regional facies of organic metamorphism in geochemical exploration, in Third International Geochemical Exploration Symposium: Proceedings of Canadian Institute of Mining and Metallurgy, Special Volume 11, p. 517-520.

Evans, D., McGiverson, S., Harrison, Z., Bryn, P., Berg, K., 2002. Along slope variation in the late Neogene evolution of the Mid Norwegian margin in response to uplift and tectonism. Petroleum Exploration Society of London Special Publication, Vol. 196.

Floodgate, G. D. & Judd, A. G. 1992. The origins of shallow gas. Continental Shelf Research, 12, 1145-1156.

Forbes, P.L., Ungerer, P. M., Kuhfuss, g. B., Riis, F., & Eggen, S., 1991, Compositional modelling of petroleum generation and expulsion: trial application to local mass balance in the Smørbukk Sør Field, Haltenbanken Area, Norway: American Association of Petroleum Geologists, Bulletin, 75, p. 873-893.

Gabrielsen, R.H., Kyrkjebø, R., Faleide, J.I., Fjeldskaar, W., Kjennerud, T., 2001. The Cretaceous post-rift basin configuration of the northern North Sea. Pet. Geosci. 7, 137–154.

Gabrielsen, R. H., Faleide, J. I., Pascal, C., Braathen., A., Nystuen, J. P., Etzelmuller, B., & O'Donnell, S. 2005. Latest Caledonian to present tectomorphological development of southern Norway. Marine and Petroleum Geology 27 (2010) pp. 709-723.

Ganjavar Khavari, K. 1987. Novel development in fluorescence microscopy of complex organic mixtures: Application in petroleum geochemistry. Organic Geochemistry, 11, 157-168.

Gee, D., 1975. A tectonic model for the central part of the Scandinavian Caleodonides. Am. J. Sci. 275-A, 468-515.

Gradstein, F. M., Ogg, J. G., Smith, A. G., Bleeker, W. & Lourens, L. J., 2004. A new geologic time scale with special reference to Precambrian and Neogene. Episodes, Vol. 27, no.2 pp. 83-100.

Grønlie, A., Naseer, C. W., Naseer, N. D., Mitchell, J.G., Sturt, B. A., & Ineson, P. R., 1994. Fission track dating and K-Ar dating of tectonic activity in a transect across the Møre-Trøndelag Fault Zone central Norway. Norsk Geologisk Tidsskkrift, 74, 24-34.

Guilhaumou, N., Szdlowskii, N. and Pradier, B., 1990. Characterization of hydrocarbon fluid inclusions by infra-red and fluorescence microspectrometry. Min. Mag., 54: 311-324.

Hagemann, H. W. & Hollerbach, A. 1986. The fluorescence behaviour of crude oils with respect to their thermal maturation and degradation. Organic Geochemistry, 10, 473-480.

Henriksen, S., Fichler, C., Grønlie, A., Henningsen, T., Laursen, I., Løseth, H., Ottesen, D. & Prince, I., 2005. The Norwegian Sea during the Cenozoic. In: Wandås et al. (eds) Onshore-Offshore Relationships on the North Atlantic Margin. NPF Special Publication, 12, 111-133, Elsevier.

Heum, O.R., Dalland, A., & Meisingset, K. K., 1986, Habitat of hydrocarbons at Haltenbanken (PVTmodelling as predictive tool in hydrocarbon exploration). In: A. M.Spencer, et al., (eds.) Habitat of Hydrocarbons in the Norwegian Continental Shelf. Norwegian Petroleum Society, Graham & Trotman, London, p. 259-274.

Hjelstuen. B. O., Eldholm, O., Skogseid, J., 1999.Cenozoic evolution of the northern Vøring Margin. Geological Society of America Bulletin 111, 1792-1807.

Hjelstuen. B. O., Sejrup, H. P., Haflidason, H., Nygård, A., Ceramicola, S., Brynn, P., 2004. late Cenozoic glacial history and evolution of the Storegga slide area and adjacent slide flank regions, Norwegian Continental margin Marine and Petroleum Geology 22 (2005) 57-69.

Hollander, N.B., 1984, Geohistory and hydrocarbon evolution of the Haltenbanken Area: A. M. Spencer, (ed.) Petroleum Geology of the North European Margin. Norwegian Petroleum Society, Graham & Trotman, London, p. 383-388.

Hunt, J. M., 1979, Petroleum Geochemistry and Geology: San Francisco, W.H. Freeman, 617 p.

Hunt, J.M., 1996. Petroleum geochemistry and geology. W. H. Freeman and company, 743 pp.

Ingrid Anne, M. 2001. Petroleum inclusions in sedimentary basins: systematics, analytical methods and applications. Lithos, 55, 195-212.

Jensenius, J. & Burruss, R. C. 1990. Hydrocarbon-water interactions during brine migration: Evidence from hydrocarbon inclusions in calcite cements from Danish North Sea oil fields. Geochimica et Cosmochimica Acta, 54, 705-713.

Karlsen, D. A., Nedkvitne, T., Larter, S. R. & Bjørlykke, K. 1993. Hydrocarbon composition of authigenic inclusions: Application to elucidation of petroleum reservoir filling history. Geochemical et Cosmochimica Act, 57, 3641-3659.

Karlsen, D. A., Nedkvitne, T., Larter, S., and Bjorlykke, K., 1995, the best paper award in organic geochemistry-hydrocarbon composition of authigenic inclusions-application to

elucidation of petroleum reservoir filling history: Geochemical et Cosmochimica Acta, v. 59, p. 1439-1439.

Karlsen, D. A., Skeie, J. E., Backer-Owe, K., Bjørlykke, K., Olstad, R., Berge, K., Cecchi, M., Vik, E. and Schaefer, R. G., 2004: Petroleum migration, faults and overpressure. Part II. Case history: The Haltenbanken Petroleum Province, offshore Norway Geological Society, London, Special Publications , 237: 305-372.

Karlsen, D. and Skeie, J. E. (2006), Petroleum migration, faults and overpressure, part I: calibration basin modelling using petroleum in traps — a review. Journal of Petroleum Geology, 29: 227–256.

Karlson, W., 1984, Sedimentology and diagenesis of Jurassic sediments offshore Mid-Norway. In: A. M. Spencer, (ed.) Petroleum Geology of the North European Margin. Norwegian Petroleum Directorate Society, Graham & Trotman, London, p. 389-396.

Koch, J. O., Heum, O.R., 1995. Exploration trends of the Halten Terrace. In: Hanslien, S. (Eds.), Petroleum exploration in Norway. Norw. Petr. Soc. Spec. Publ., vol. 4, pp. 235–251.

Kyrkjebø, R., Gabrielsen, R.H., Faleide, J.I., 2004. Unconformities related to Jurassic–Cretaceous syn/post-rift transition of the Northern North Sea. J. Geol. Soc. (Lond.) 161, 1–17.

Lumb. D. M., 1978. Organic Luminescence. In: D. M. Lumb (Editor), Luminescence Spectroscopy. Academic Press, New York, N. Y., pp. 93-148.

Lundin, E., Doré, A.G., 1997. A tectonic model for the Norwegian passive margin with implications for the NE Atlantic: early Cretaceous to break-up. J. Geol. Soc. (Lond.) 154, 545–550.

Lundin, E.R., Doré, A.G., 2002. Mid-Cenozoic post-breakup deformation in the “passive” margins bordering the Norwegian–Greenland Sea. Mar. Pet. Geol. 19, 79–93.

Martin, S. 1980. The hydrogen and carbon isotopic composition of methane from natural gases of various origins. Geochimica et Cosmochimica Acta, 44, 649-661.

Michael J. Whitaker (1994); Correlation of Natural Gases with Their Sources: Centre for Earth and Ocean Studies University of Victoria, Victoria, British Columbia, Canada.

Muller, R., Nystuen., J. P., Eide, F., & Lie, H., 2005. Late Permian to Triassic basin infill history and basin paleogeography of the Mid-Norwegian shelf-East Greenland region. Norwegian Petroleum Society (NPF) Special Publication 12, pp. 165-189.

Munz, I. A., Iden, K., Johansen, H. & Vagle, K. 1998. The fluid regime during fracturing of the Embla field, Central Trough, North Sea. Marine and Petroleum Geology, 15, 751-768.

Munz, I. A., Johansen, H., Holm, K. & Lacharpagne, J. C. 1999. The petroleum characteristics and filling history of the Frøy field and the Rind discovery, Norwegian North Sea. Marine and Petroleum Geology, 16, 633-651.

Munz, I.A., Johansen, H., Johansen, I., 1999b. Characterisation of composition and PVT properties of petroleum inclusions: Implication of reservoir filling and compartmentalisation. Paper SPE 56519 presented at the 1999 SPE Annual Technical Conference and Exhibition in Houston, 3-6 Octobor 1999.

Nedkvitne, T., Karlsen, D. A., Bjørlykke, K. & Larter, S. R. 1993. Relationship between reservoir diagenetic evolution and petroleum emplacement in the Ula Field, North Sea. Marine and Petroleum Geology, 10, 255-270.

Ottesen, D., Dowdeswell, J.A., Rise, L., 2005. Submarine landforms and reconstruction of fast-flowing ice streams within a large Quaternary ice sheet: The 2500-km-long Norwegian–Svalbard Margin (57°–80° N). GSA Bull. 117, 1033–1050.

Oxtoby, N. H., Mitchell, A. W. & Gluyas, J. G. 1995. The filling and emptying of the Ula Oilfield: fluid inclusion constraints. Geological Society, London, Special Publications, 86, 141-157.

Pedersen, J. H., 2002. Atypical oils, unusual condensates and bitumen of the Norwegian Continental Shelf: an organic geochemical study, Cand. Scient. Thesis in Geology, Department of Geosciences, University of Oslo.

Pedersen, J.H., Karlsen, D.A., Backer-Owe, K., Lie, J.E., and Brunstad, H., 2006. The geochemistry of two unusual oils from the Norwegian North Sea: Implications for new source rock and play scenario: Petroleum Geosciences, v. 12, p. 85-96.

Peters, K. E. and Moldowan, J. M., 1993: The biomarker guide. Interpreting molecular fossils in petroleum and ancient sediments. Prentice Hall Englewood Cliffs, N. J., 363 pp.

Peters, K.E., Moldowan, J.M., and Walters, C.C., 2005. The biomarker guide: Cambridge, Cambridge University press, 2 b.p.

Provan, D.M.J., 1992, Draugen Oil Field, Haltenbanken Province, Offshore Norway. In: M. T. HALBOUTY, (ed.) Giant Oil and Gas Fields of the Decade 1978-1988. American Association of Petroleum Geologists, Memoir, 54, p. 371-382.

Rise, L., Ottesen, D., Berg, K., Lundin, E., 2005. Large-scale development of the mid-Norwegian shelf and margin during the last 3 million years. Mar. Pet. Geol. 22, 33–44.

Roedder, E. (1984): Fluid Inclusions, Min. Soc. Am. Rev. in Min. 12, 644 pp.

Roger K, M. 1987. The application of fluid inclusions to migration of oil and diagenesis in petroleum reservoirs. Applied Geochemistry, 2, 585-603.

Sellwood, B. W., Wilkes, M. & James, B. 1993. Hydrocarbon inclusions in late calcite cements: migration indicators in the Great Oolite Group, Weald Basin, S. England. Sedimentary Geology, 84, 51-55.

Skogseid, J., Pedersen, T. and Larsen, V.B., 1992. Vøring basin: subsidence and tectonic evolution. Structural and Tectonic Modelling and its Application to Petroleum Geology. NPF Special Publication, 1. Norsk Petroleumsforening (NPF) 55-82 pp.

Skogseid, J., Planke, S., Faleide, J.I., Pedersen, T., Eldholm, O., Neverdal, F., 2000. NE Atlantic continental rifting and volcanic margin formation. In: Nøttvedt, A., et al. (Eds.), Dynamics of the Norwegian Margin. Geol. Soc., London, Spec. Publ., vol. 167, pp. 327–378.

Smelror, M., Dehls, J., Ebbing, J., Larsen, E., Lundin, E.R., Nordgulen, Ø. Osmundsen, P.T., Olesen, O., Ottesen, D., Pascal, C., Redfield, T.F. & Rise, L., 2007. Towards a 4D topographic view of the Norwegian Sea margin. Global and Planetary Change, 58, 382–410.

Smelror, M., Mørk, A., Mørk, M.B.E., Weiss, H.M., Løseth, H., 2001. Middle Jurassic–Lower Cretaceous transgressive–regressive sequences and facies distribution off northern Nordland and Troms, Norway. In: Martinsen, O.J., Dreyer, T. (Eds.), Sedimentary Environments Offshore Norway. Norw. Petr. Soc. Spec. Publ., vol. 10, pp. 211–232.

Sterner, S. M. & Bodnar, R. J. 1984. Synthetic fluid inclusions in natural quartz I. Compositional types synthesized and applications to experimental geochemistry. Geochimica et Cosmochimica Acta, 48, 2659-2668.

Ten Haven, H. L., De Leeuw, J. W., Rullkoetter, J. and Sinninghe Damste, J. S., 1987: Restricted utility of the pristane/phytane ratio as a paleoenvironment indicator. Nature (London), 330, 641-643.

Tissot, B., Califet, D.Y., Deroo, and Oudin, J. L., 1971. Origin and Evolution of Hydrocarbons in Early Toarcian Shales, Paris Basin, France. The American Association of Petroleum Geologists Bulletin, 55, 2177-2193.

Tissot, B.P. and Welte, D.H., 1978. Petroleum formation and occurrence: a new approach to oil and gas exploration. Springer-Verlag, 538pp.

Tissot, B.P. and Welte, D.H., 1984. Petroleum formation and occurrence, (2nd edition) Springer-Verlag, p. 380-381.

Underhill, J.R., 1998. Jurassic, In: Glennie, K.W. (Eds.), Petroleum Geology of the North Sea. Basic Concepts and Recent Advances, 4th ed. Blackwell Science Ltd., London, pp. 245–293.

Walderhaug, O. 1994. Precipitation rates for quartz cement in sandstones determined by fluid-inclusion microthermometry and temperature-history modeling. Journal of sedimentary research, 64, 324-333.

Watanabe, K. 1987. Inclusions in flux-grown crystals of corundum. Crystal Research and Technology, 22, 345-355.

Whitley, P.K., 1992, The geology of the Heidrun, a giant oil and gas field on the Mid-Norwegian Shelf. In: M. T. Halbouty, (ed.) Giant Oil and Gas Fields of the Decade 1978-1988. American Association of Petroleum Geologists, Memoir, 54, p. 383-406.

Appendix - A

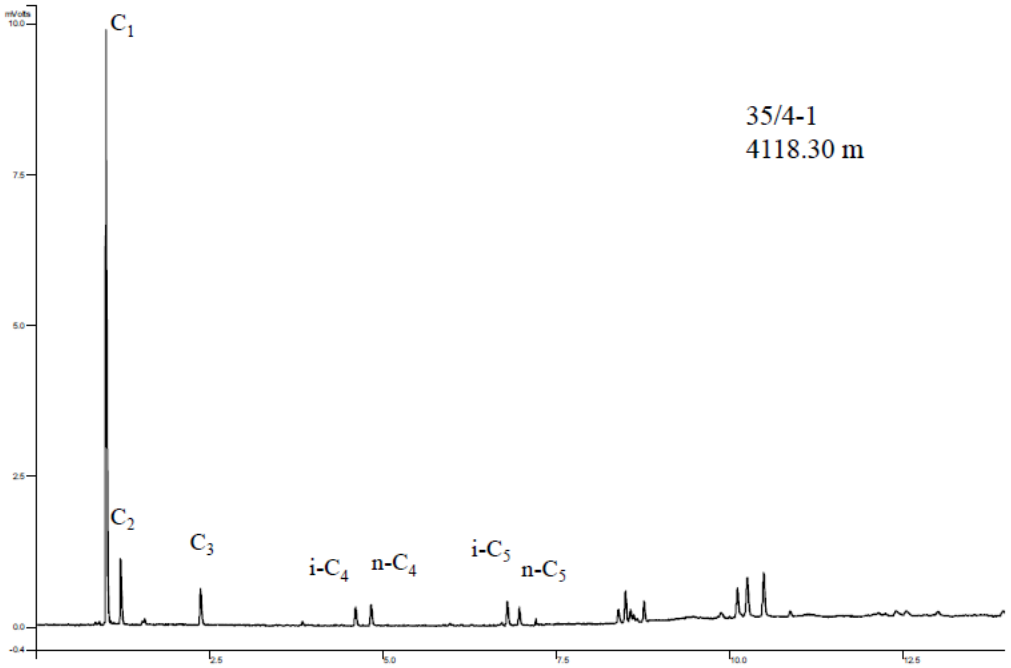
C1
C2
C3
i-C4
n-C4
i-C5
n-C5
35/4-1
4118.30 m

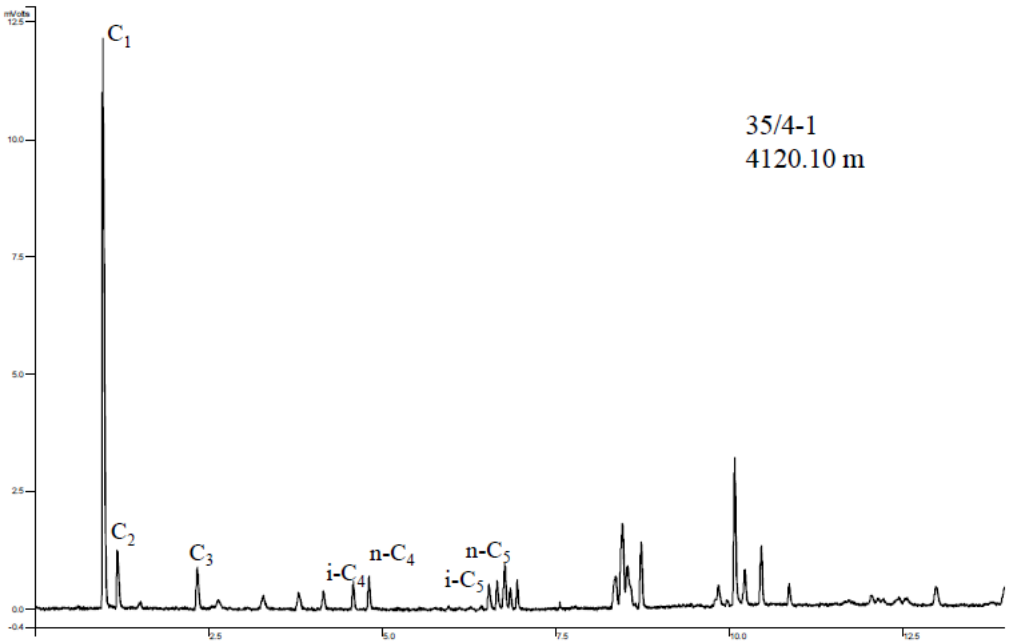
C1
C2
C3
i-C4
n-C4
i-C5
n-C5
35/4-1
4120.10 m

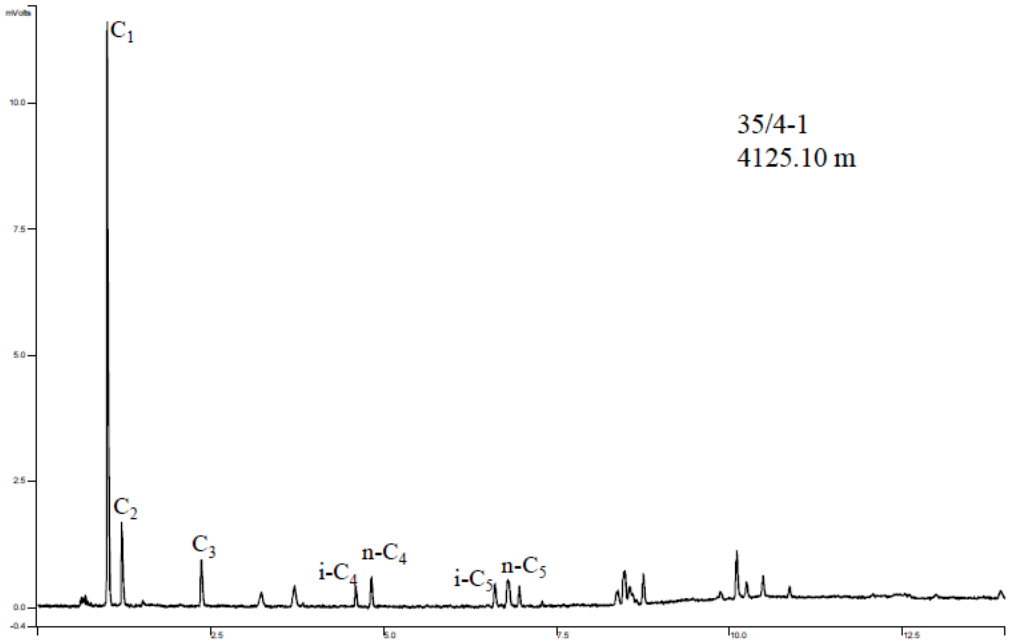
mVolts
C1
C2
C3
i-C4
n-C4
i-C5
n-C5
35/4-1
4125.10 m

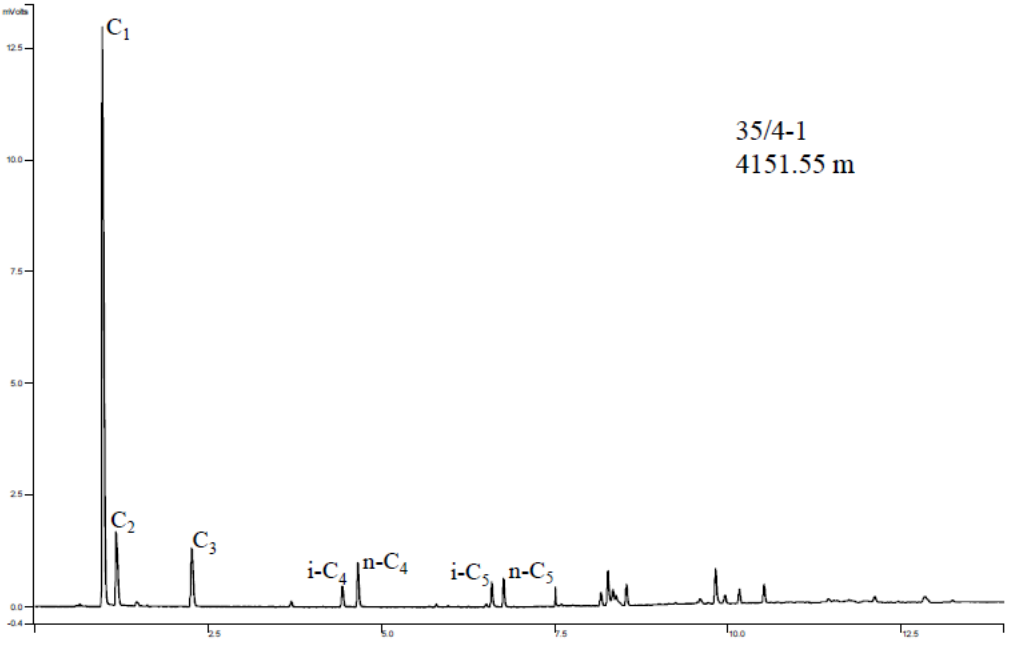
mVolts
C1
C2
C3
i-C4
n-C4
i-C5
n-C5
35/4-1
4151.55 m

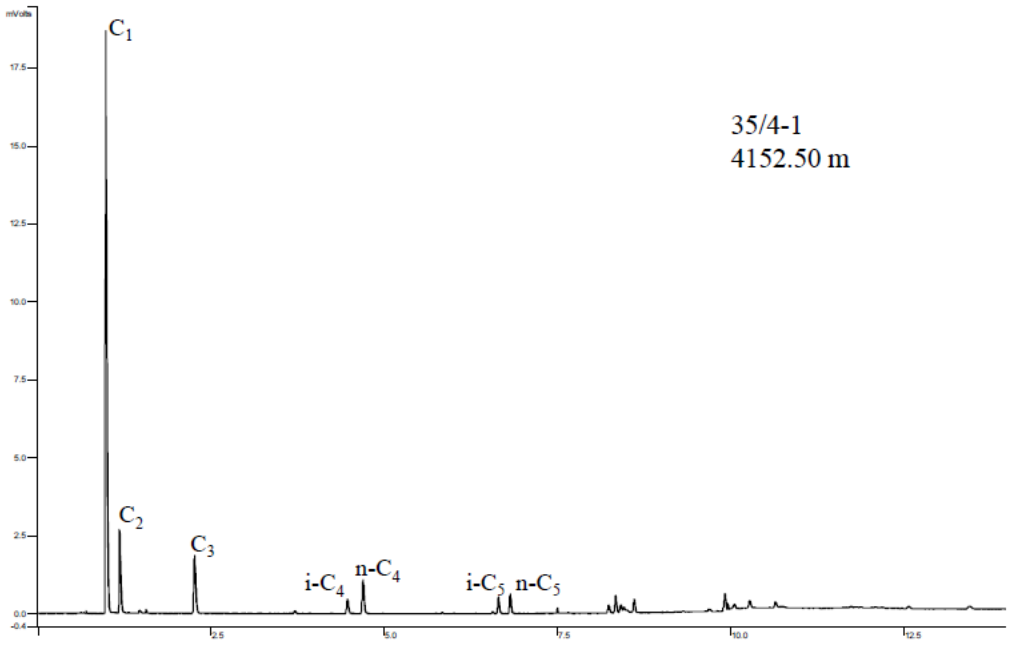
mVolts
17.5
15.0
12.5
10.0
7.5
5.0
2.5
0.0
-0.4
C1
C2
C3
i-C4
n-C4
i-C5
n-C5
2.5
5.0
7.5
10.0
12.5
35/4-1
4152.50 m

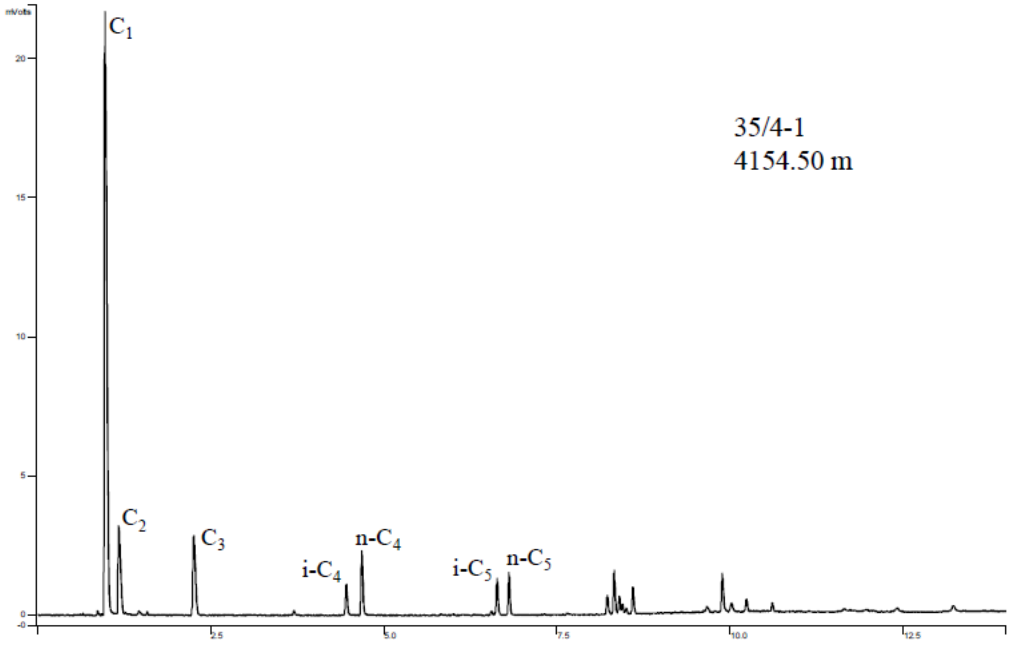
mVolts
20
15
10
5
0
-0
C1
C2
C3
i-C4
n-C4
i-C5
n-C5
2.5
5.0
7.5
10.0
12.5
35/4-1
4154.50 m

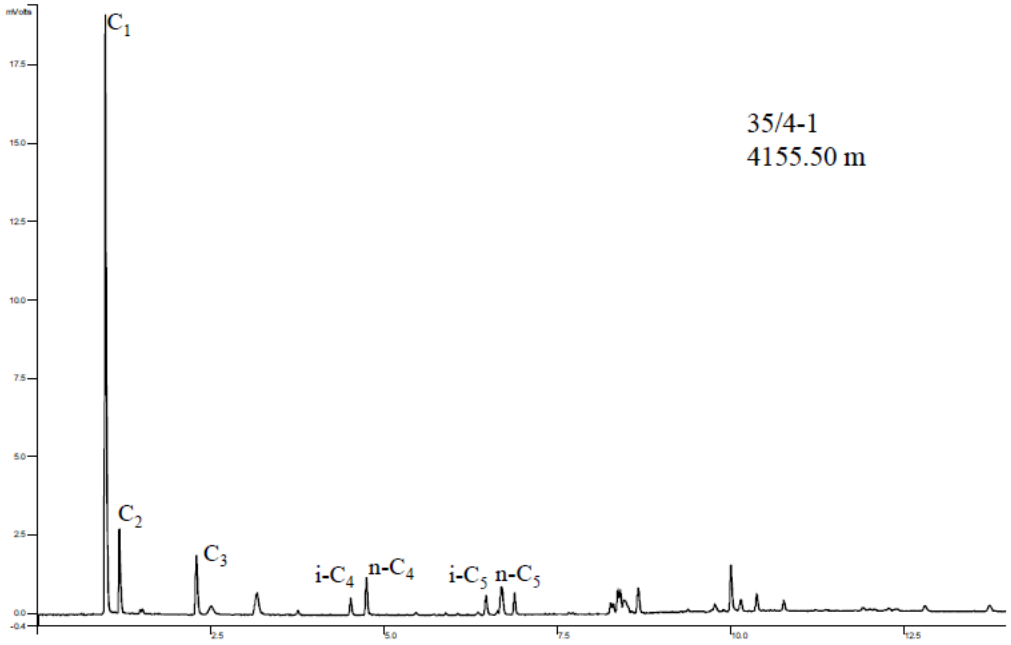
mVolts
17.5
15.0
12.5
10.0
7.5
5.0
2.5
0.0
-0.4
C1
C2
C3
i-C4
n-C4
i-C5
n-C5
2.5
5.0
7.5
10.0
12.5
35/4-1
4155.50 m

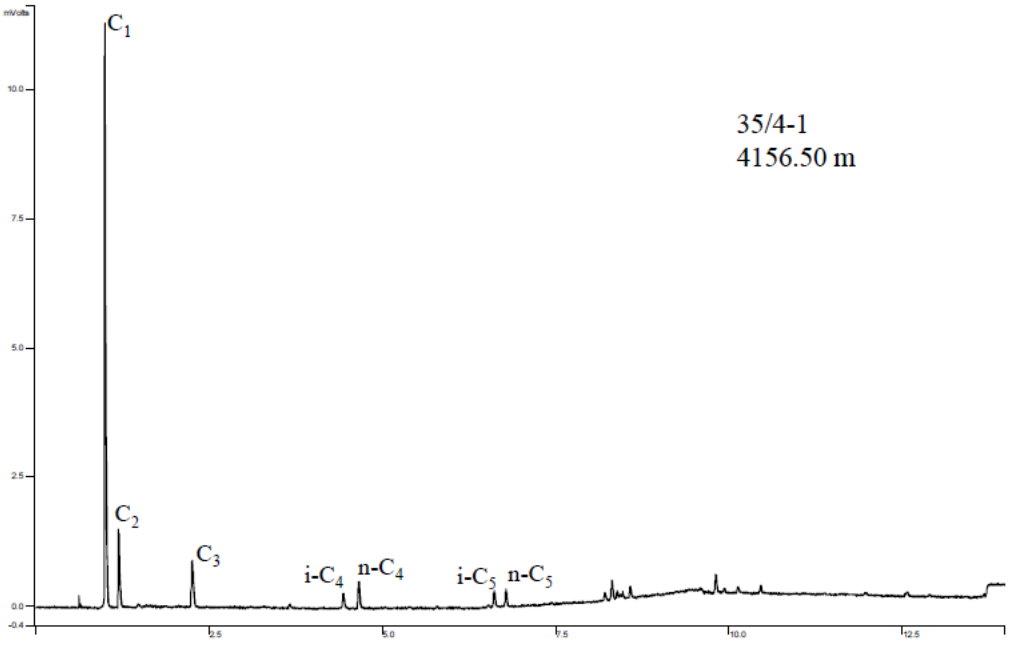
mVolts
10.0
7.5
5.0
2.5
0.0
-0.4
C1
C2
C3
i-C4
n-C4
i-C5
n-C5
2.5
5.0
7.5
10.0
12.5
35/4-1
4156.50 m

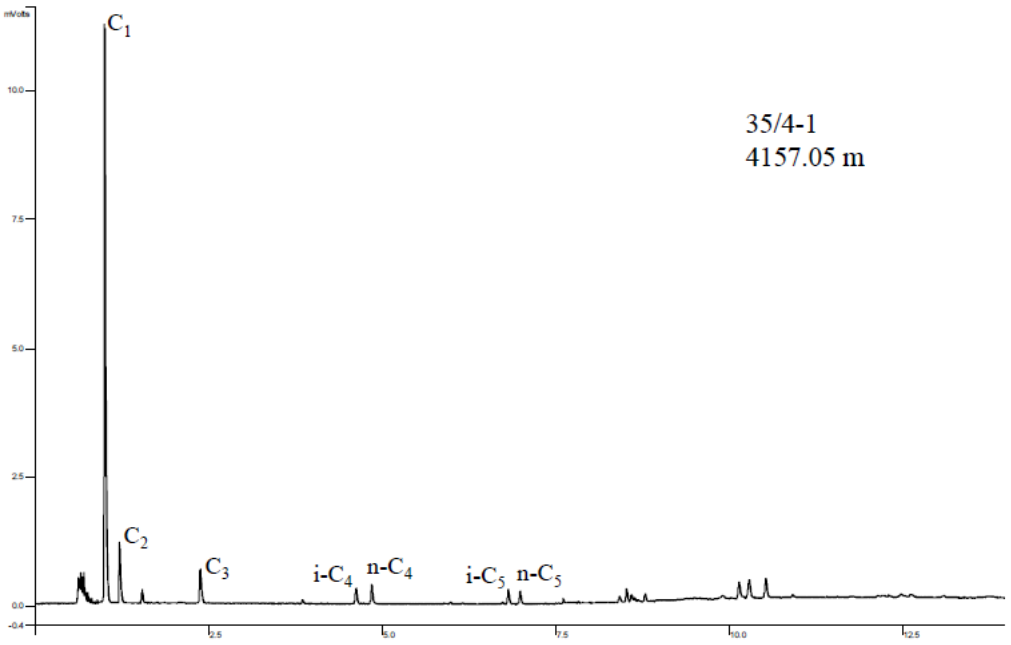
mVolts
10.0
7.5
5.0
2.5
0.0
-0.4
C1
C2
C3
i-C4
n-C4
i-C5
n-C5
2.5
5.0
7.5
10.0
12.5
35/4-1
4157.05 m

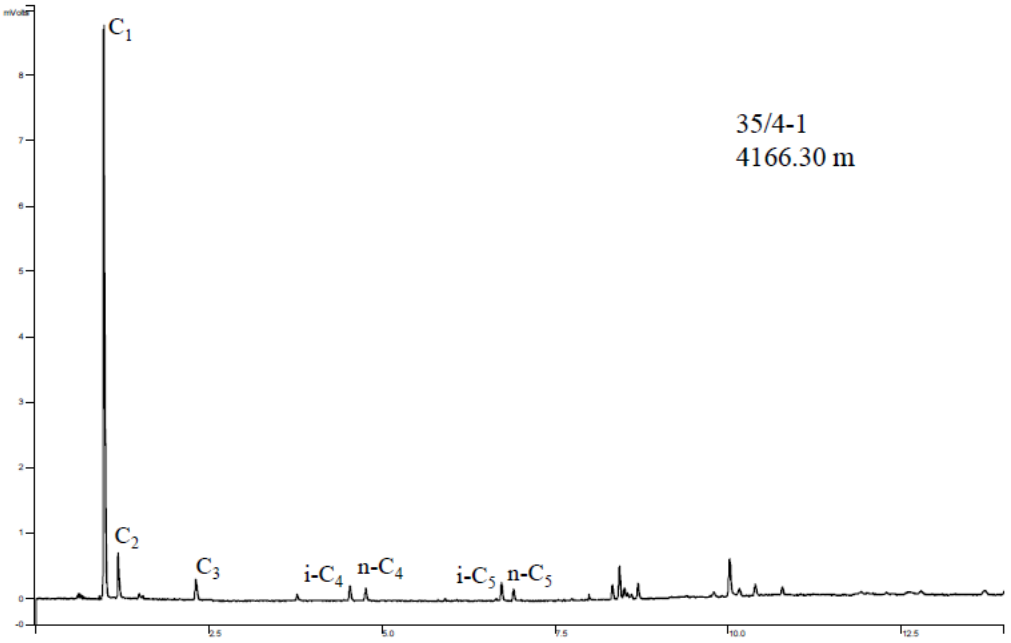
mVolts
8
7
6
5
4
3
2
1
0
-0
C1
C2
C3
i-C4
n-C4
i-C5
n-C5
2.5
5.0
7.5
10.0
12.5
35/4-1
4166.30 m

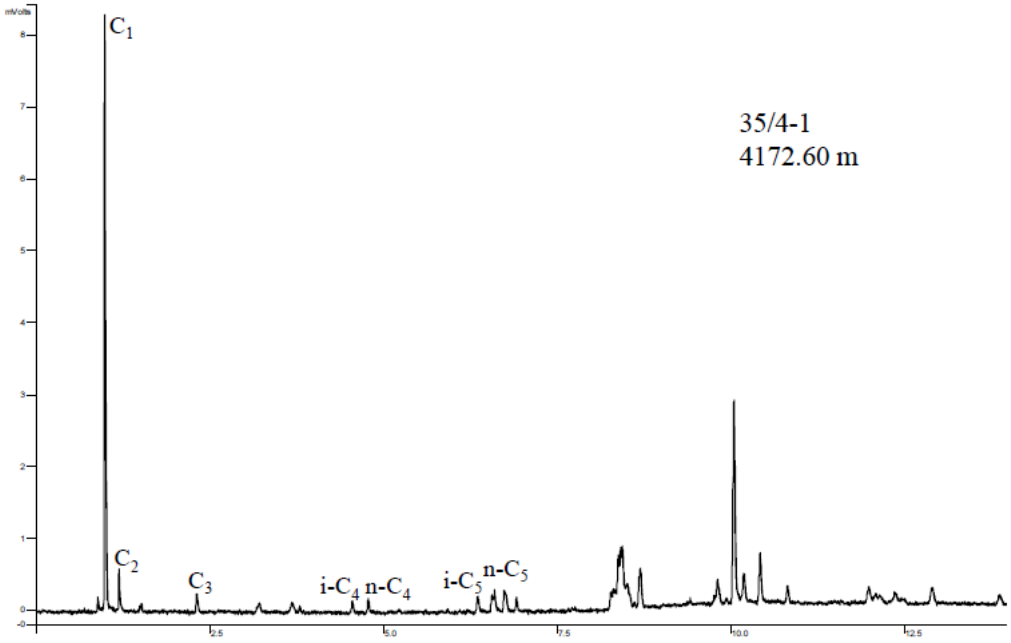
mV/olts
C1
C2
C3
i-C4
n-C4
i-C5
n-C5
35/4-1
4172.60 m

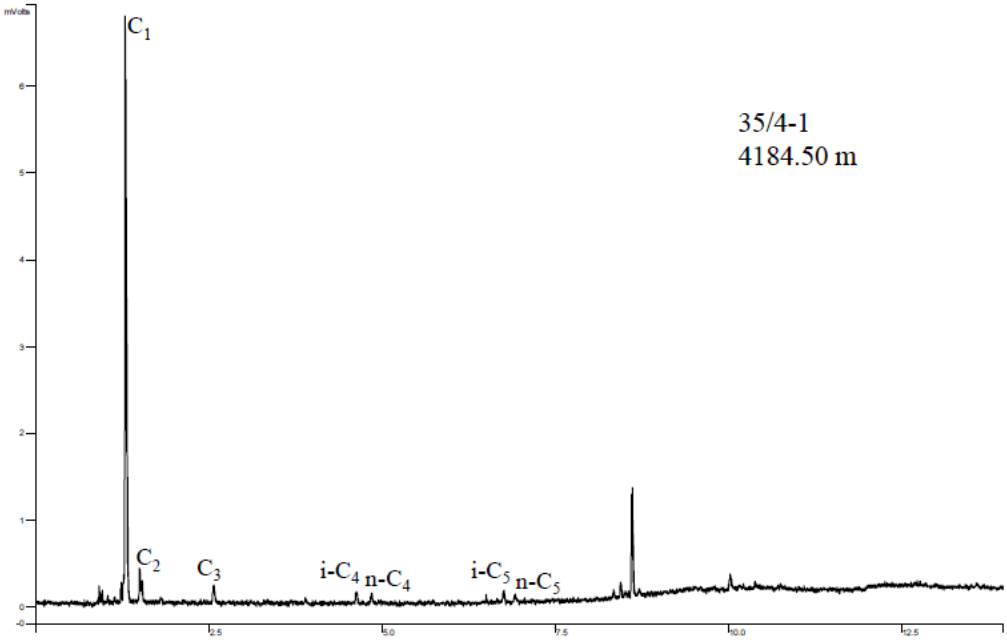
mV/olts
C1
C2
C3
i-C4
n-C4
i-C5
n-C5
35/4-1
4184.50 m

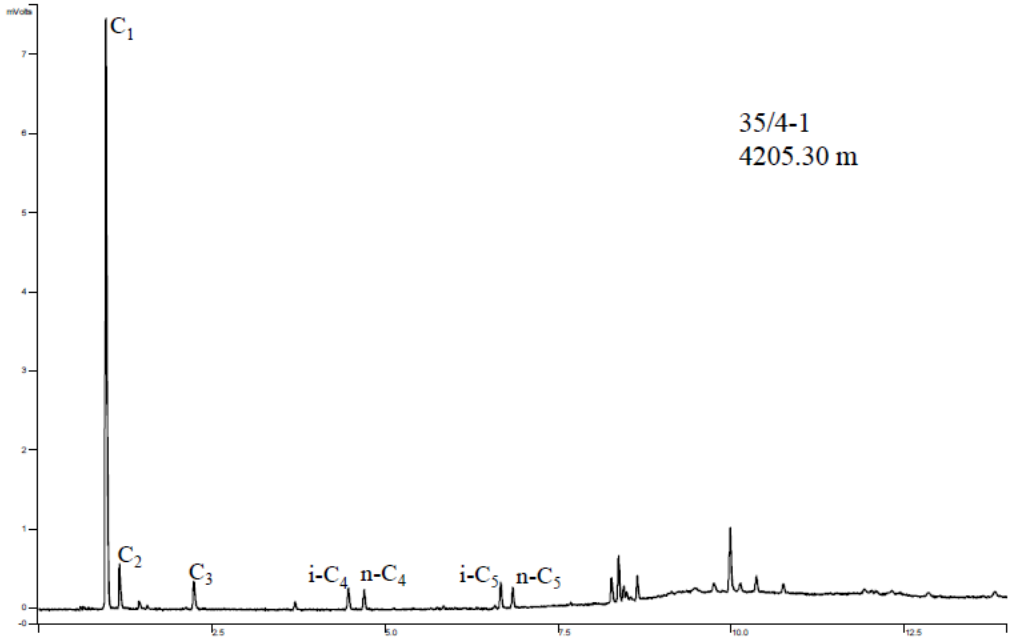
mVolts
C1
C2
C3
i-C4
n-C4
i-C5
n-C5
35/4-1
4205.30 m

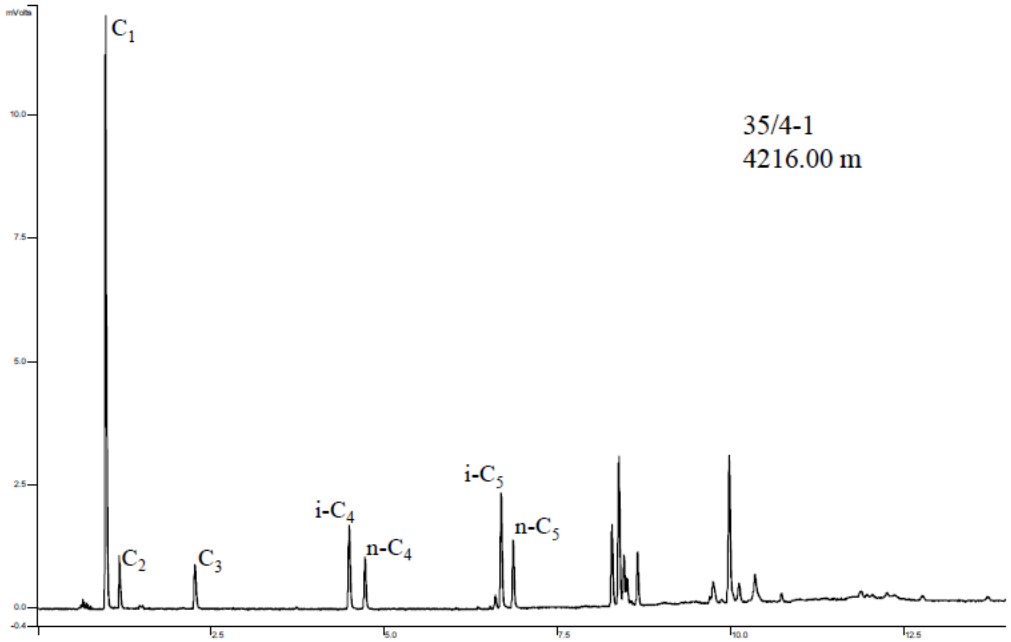
mVolts
C1
C2
C3
i-C4
n-C4
i-C5
n-C5
35/4-1
4216.00 m

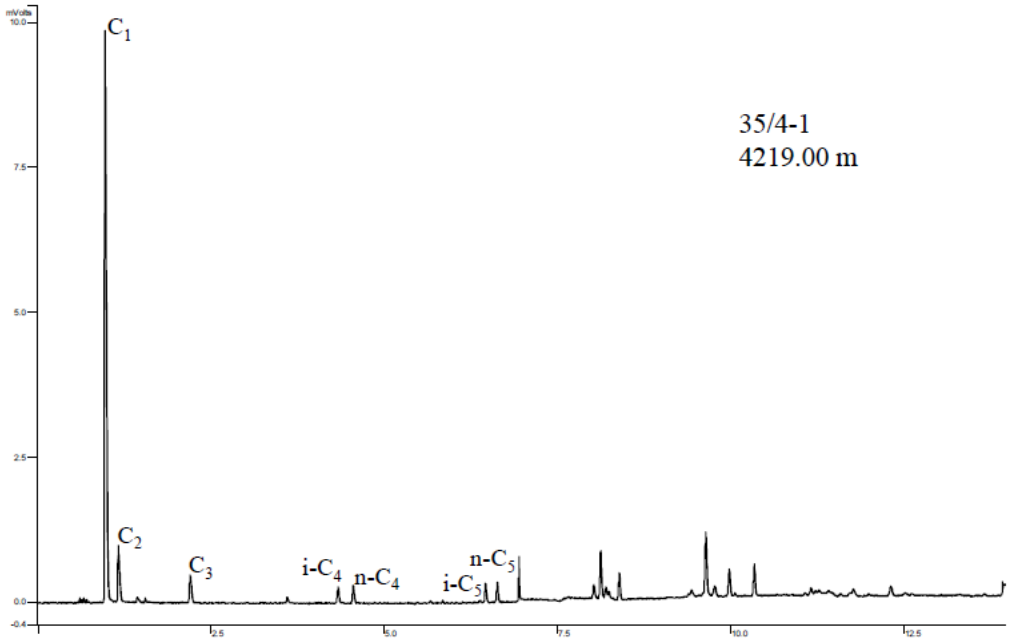
C1
C2
C3
i-C4
n-C4
i-C5
n-C5
35/4-1
4219.00 m

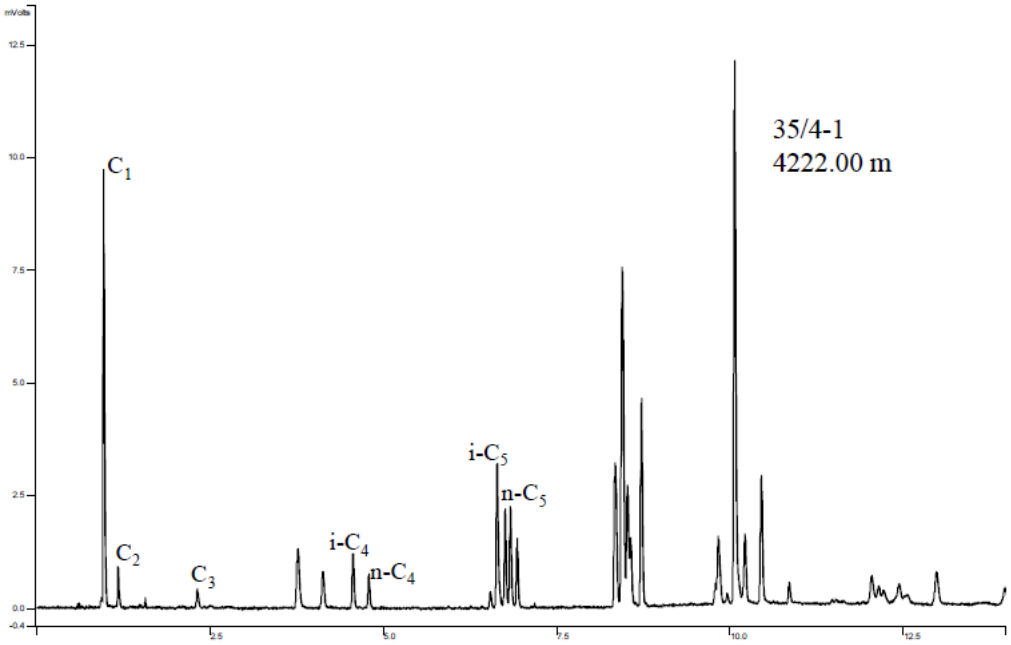
C1
C2
C3
i-C4
n-C4
i-C5
n-C5
35/4-1
4222.00 m

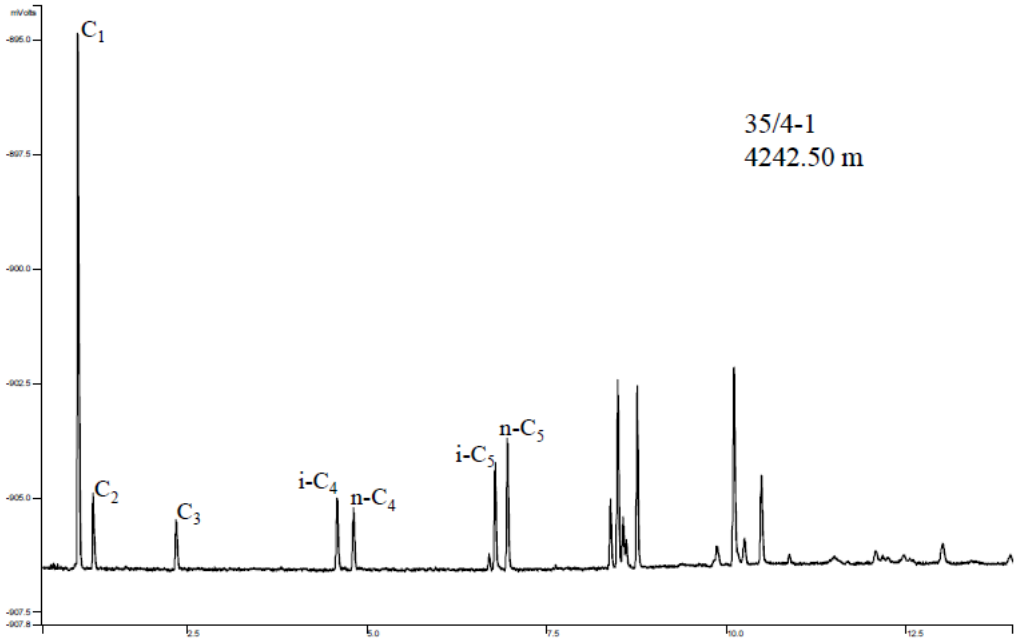
C1
C2
C3
i-C4
n-C4
i-C5
n-C5
35/4-1
4242.50 m

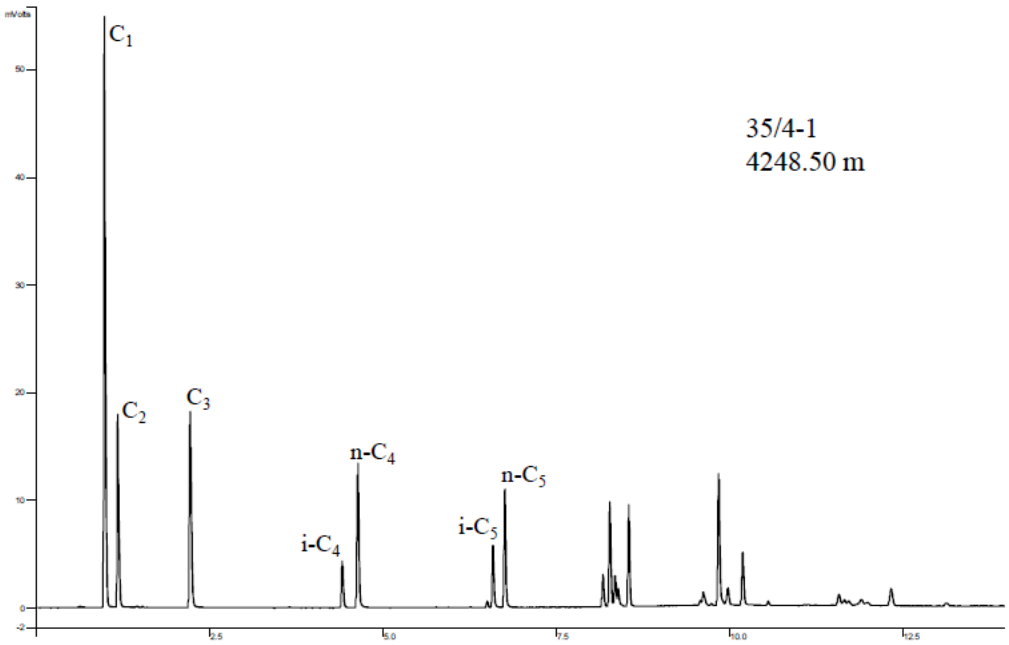
C1
C2
C3
i-C4
n-C4
i-C5
n-C5
35/4-1
4248.50 m

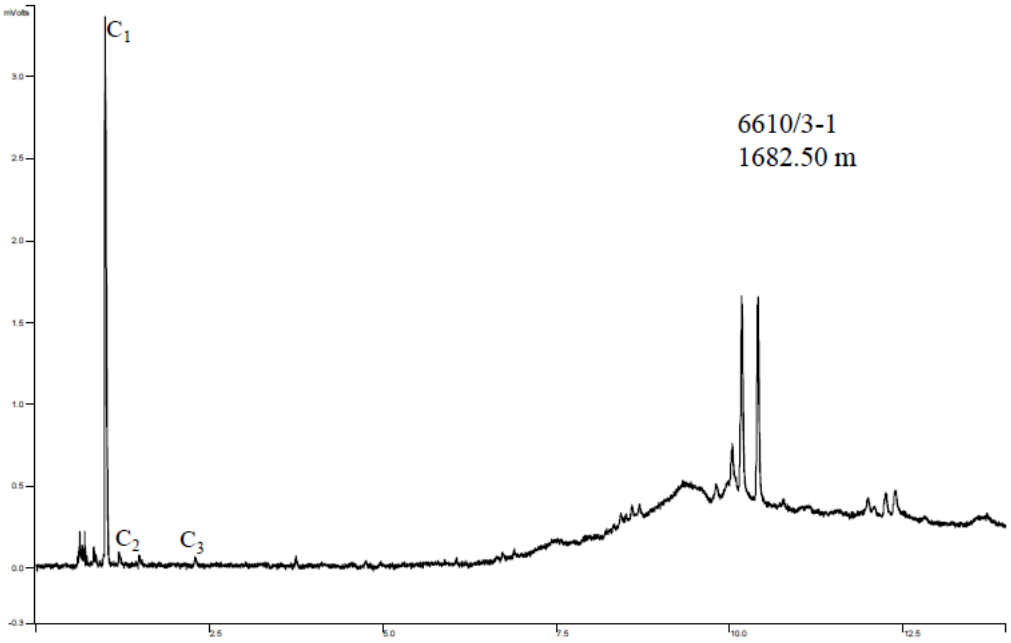
mVolts
3.0
2.5
2.0
1.5
1.0
0.5
0.0
-0.3
C1
C2
C3
6610/3-1
1682.50 m
2.5
5.0
7.5
10.0
12.5

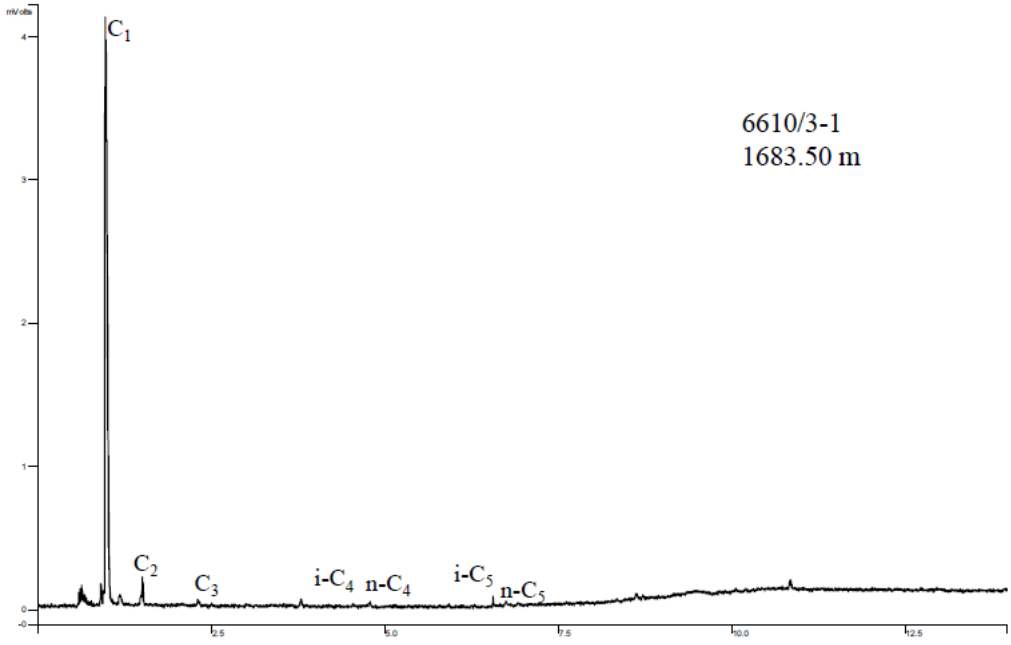
mVolts
4
3
2
1
0
-0
C1
C2
C3
i-C4
n-C4
i-C5
n-C5
6610/3-1
1683.50 m
2.5
5.0
7.5
10.0
12.5

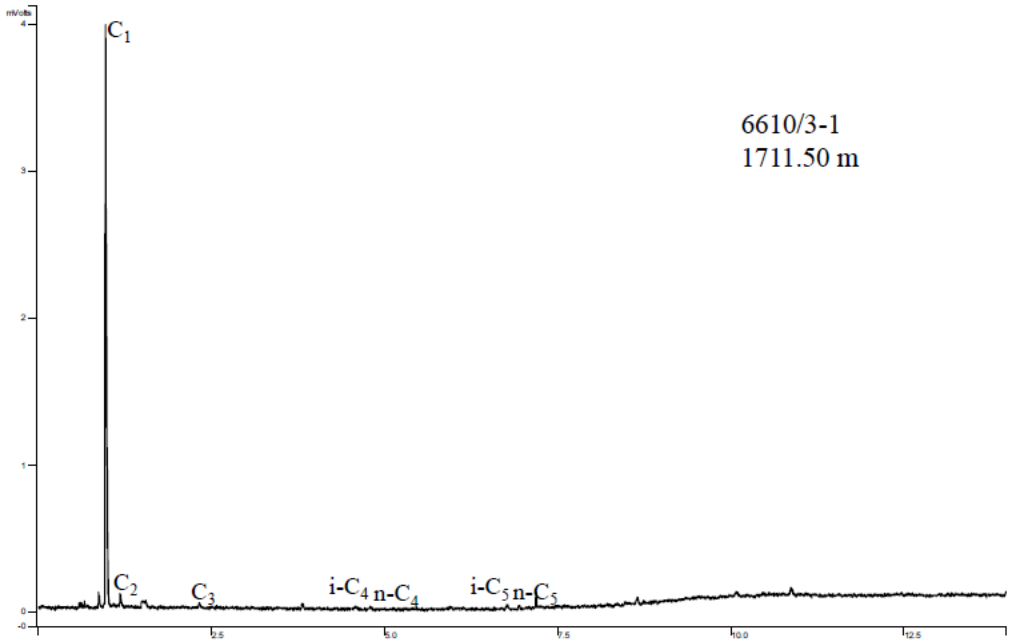
mV/olts
C1
C2
C3
i-C4 n-C4
i-C5 n-C5
6610/3-1
1711.50 m

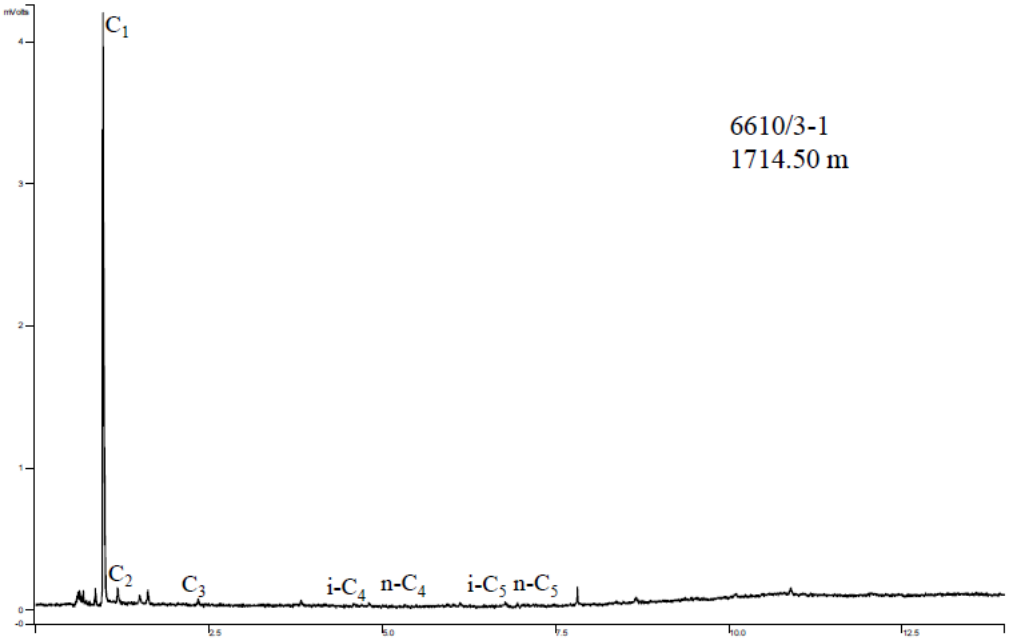
mV/olts
C1
C2
C3
i-C4
n-C4
i-C5 n-C5
6610/3-1
1714.50 m

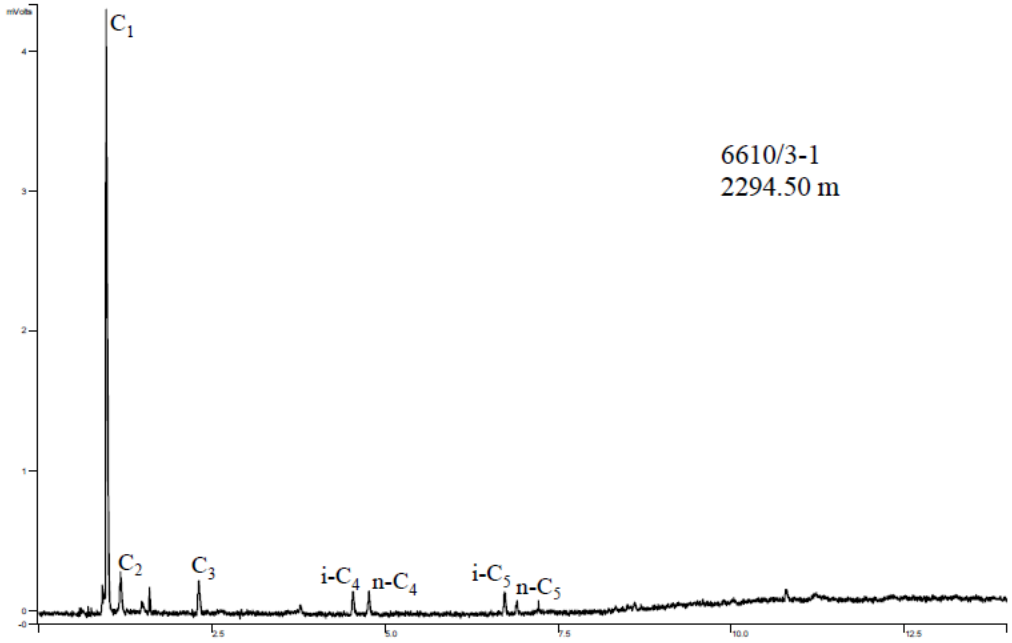
C1
C2
C3
i-C4
n-C4
i-C5
n-C5
6610/3-1
2294.50 m

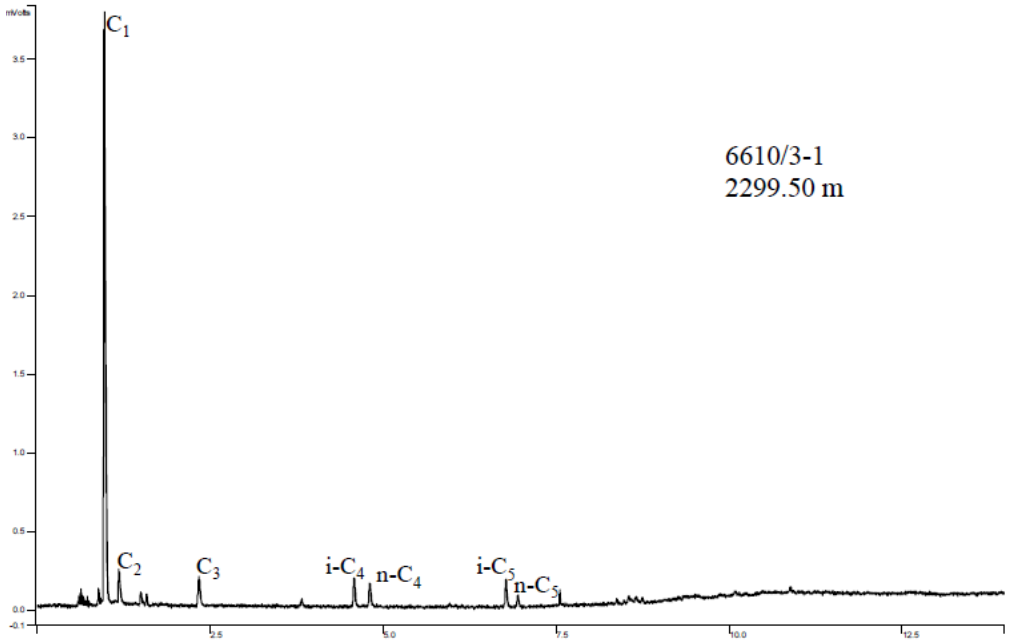
C1
C2
C3
i-C4
n-C4
i-C5
n-C5
6610/3-1
2299.50 m

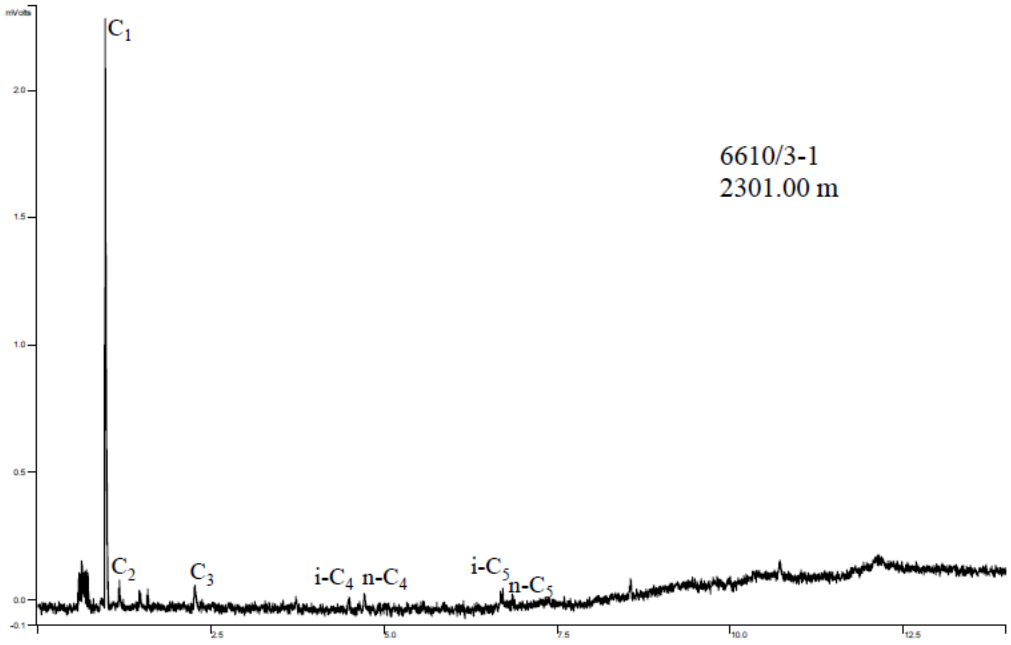
mVolts
C1
C2
C3
i-C4
n-C4
i-C5
n-C5
6610/3-1
2301.00 m

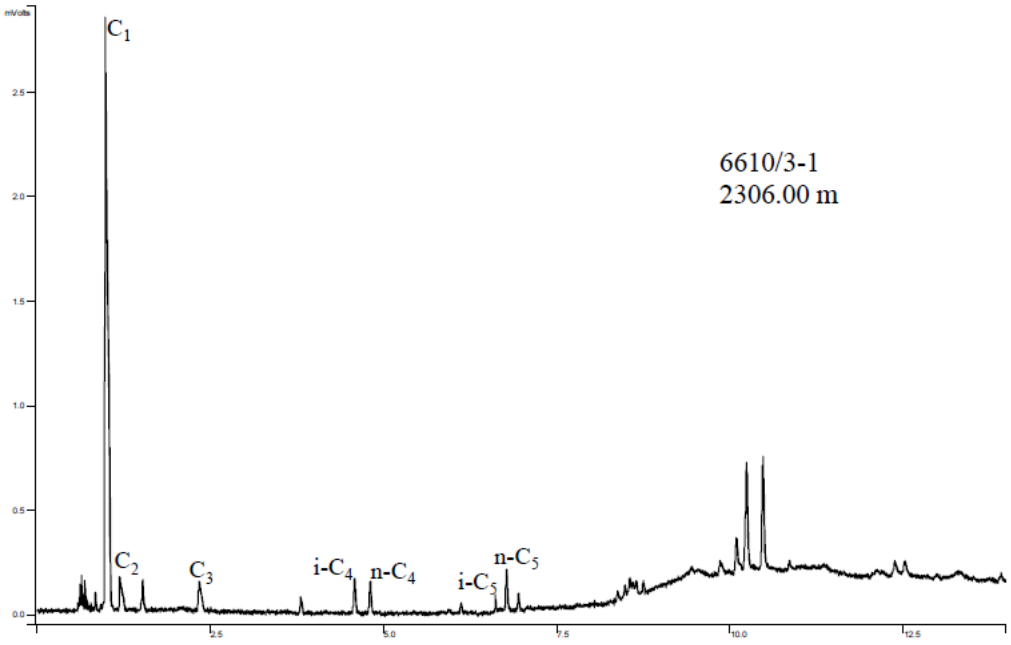
mVolts
C1
C2
C3
i-C4
n-C4
i-C5
n-C5
6610/3-1
2306.00 m

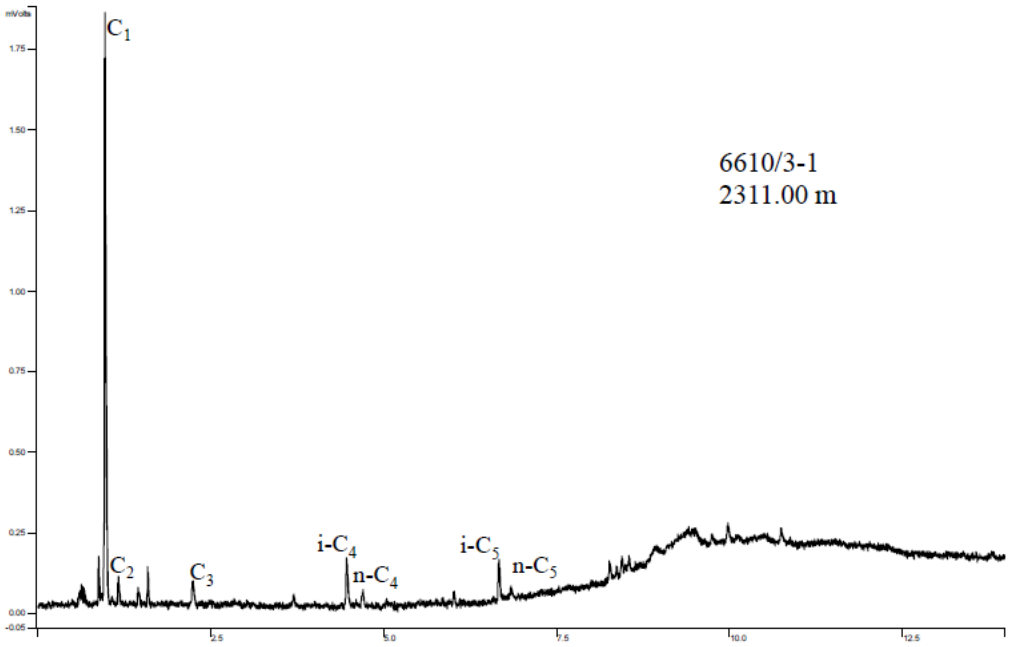
mVolts
1.75
1.50
1.25
1.00
0.75
0.50
0.25
0.00
-0.05
C1
C2
C3
i-C4
n-C4
i-C5
n-C5
2.5
5.0
7.5
10.0
12.5
6610/3-1
2311.00 m

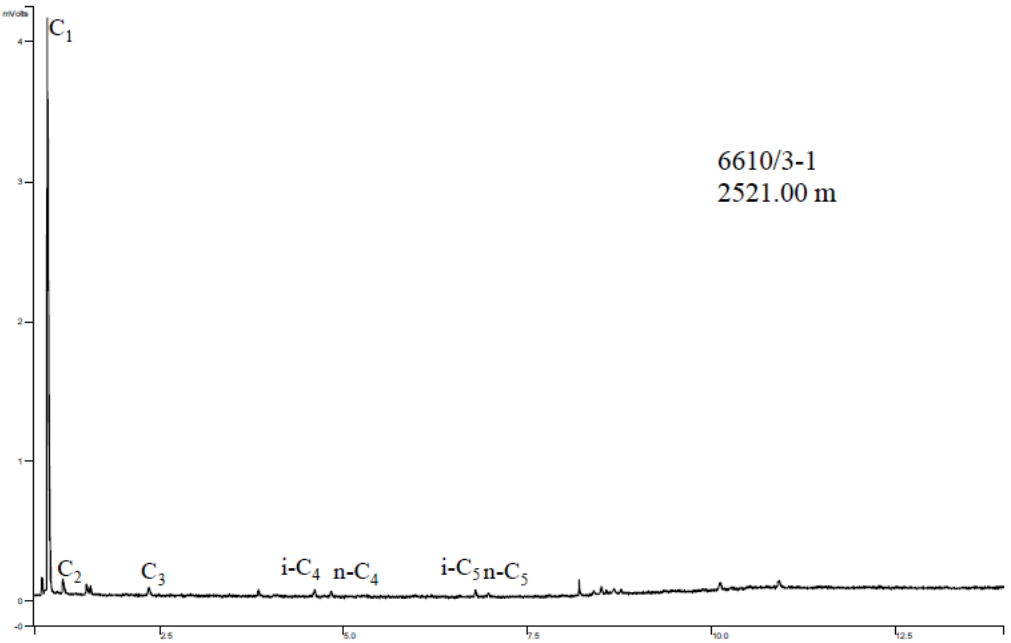
mVolts
4
3
2
1
0
-0
C1
C2
C3
i-C4
n-C4
i-C5
n-C5
2.5
5.0
7.5
10.0
12.5
6610/3-1
2521.00 m

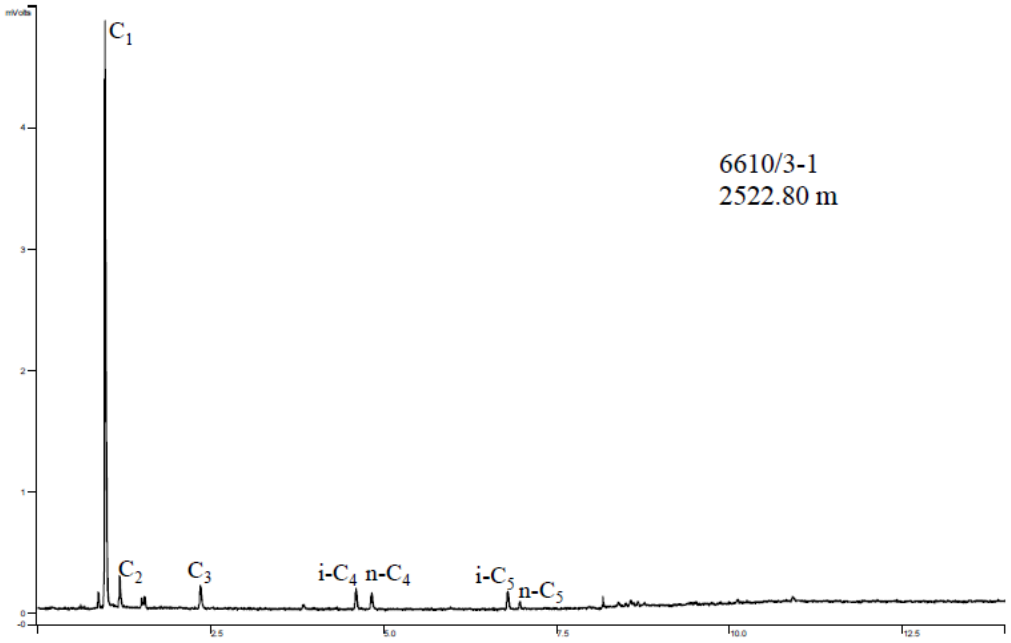
mVolts
C1
C2
C3
i-C4
n-C4
i-C5
n-C5
6610/3-1
2522.80 m

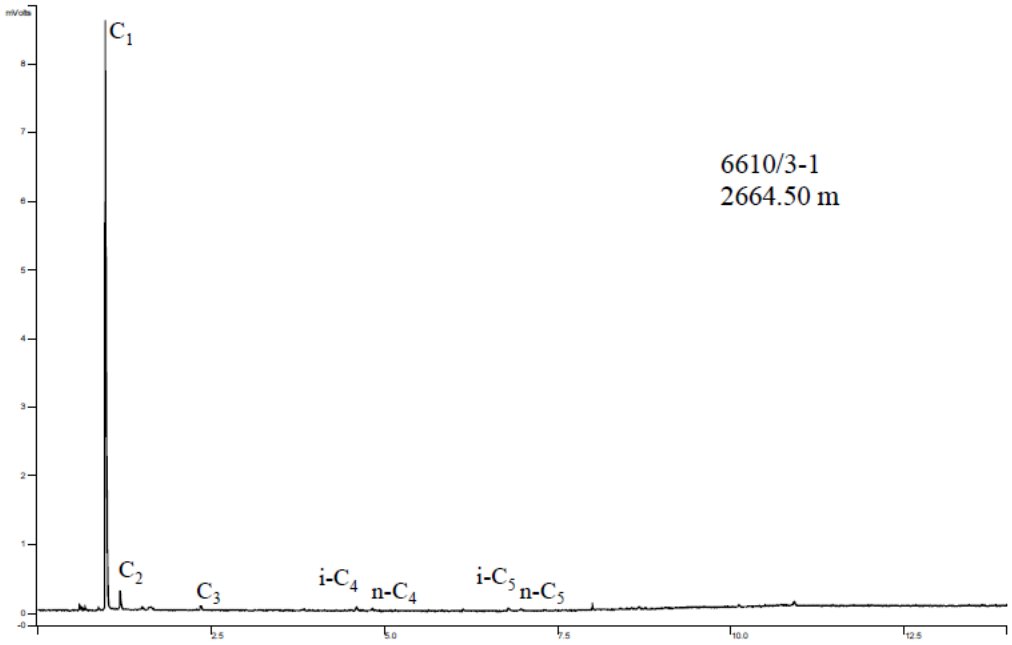
mVolts
C1
C2
C3
i-C4
n-C4
i-C5
n-C5
6610/3-1
2664.50 m

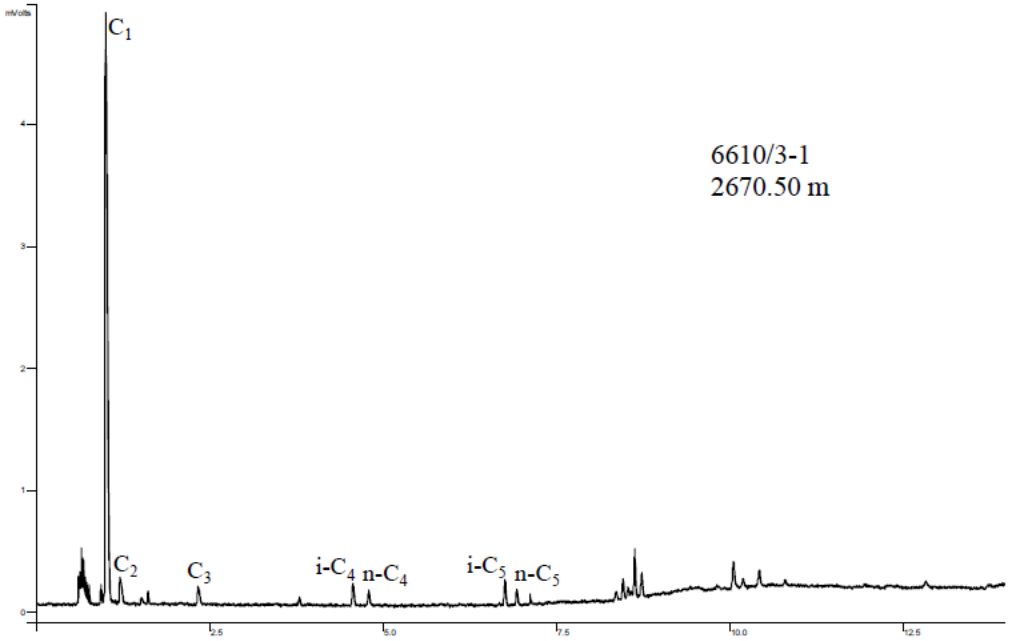
mVolts
C1
C2
C3
i-C4
n-C4
i-C5
n-C5
6610/3-1
2670.50 m

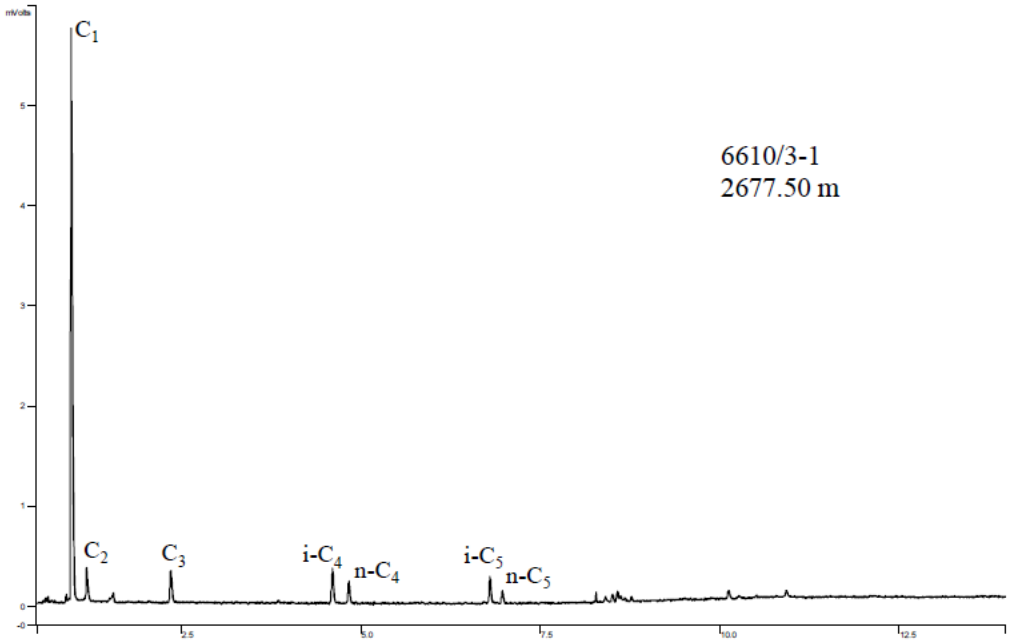
mVolts
C1
C2
C3
i-C4
n-C4
i-C5
n-C5
6610/3-1
2677.50 m

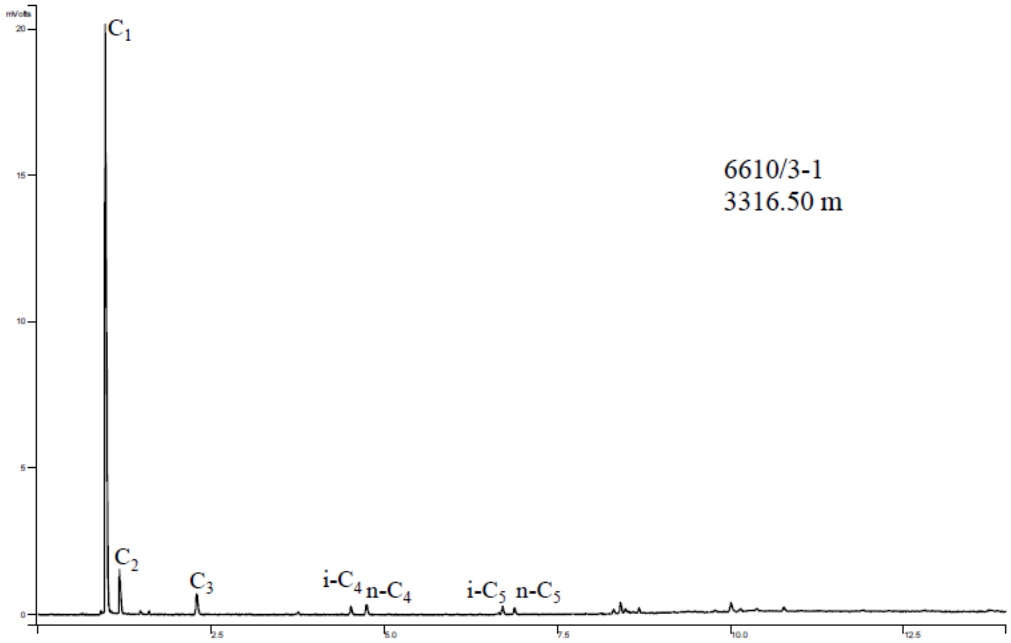
mV/dls
20
15
10
5
0
C1
C2
C3
i-C4
n-C4
i-C5
n-C5
2.5
5.0
7.5
10.0
12.5
6610/3-1
3316.50 m

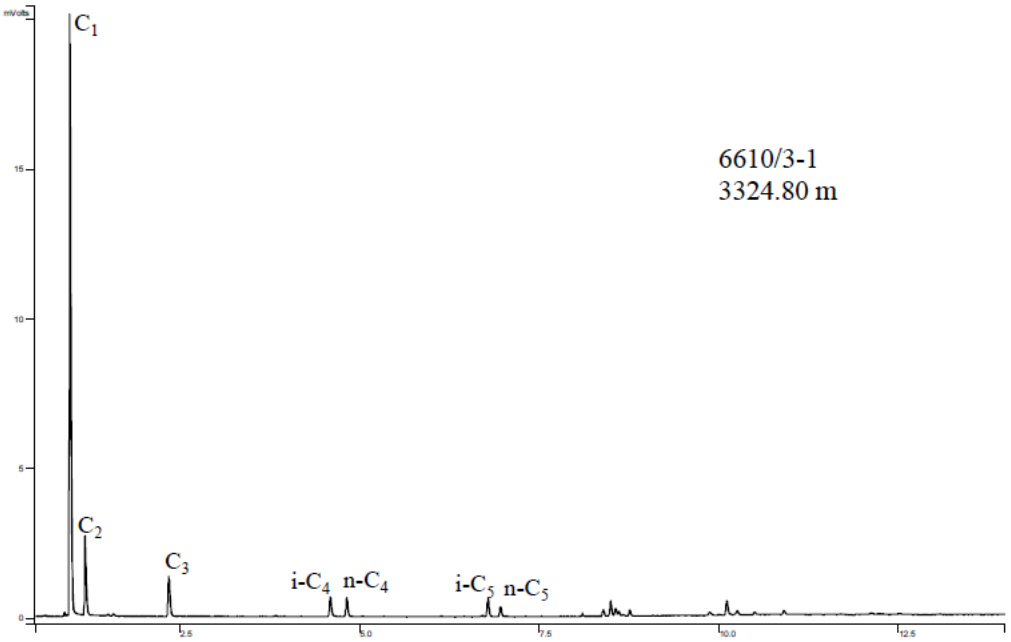
mV/dls
15
10
5
0
C1
C2
C3
i-C4
n-C4
i-C5
n-C5
2.5
5.0
7.5
10.0
12.5
6610/3-1
3324.80 m

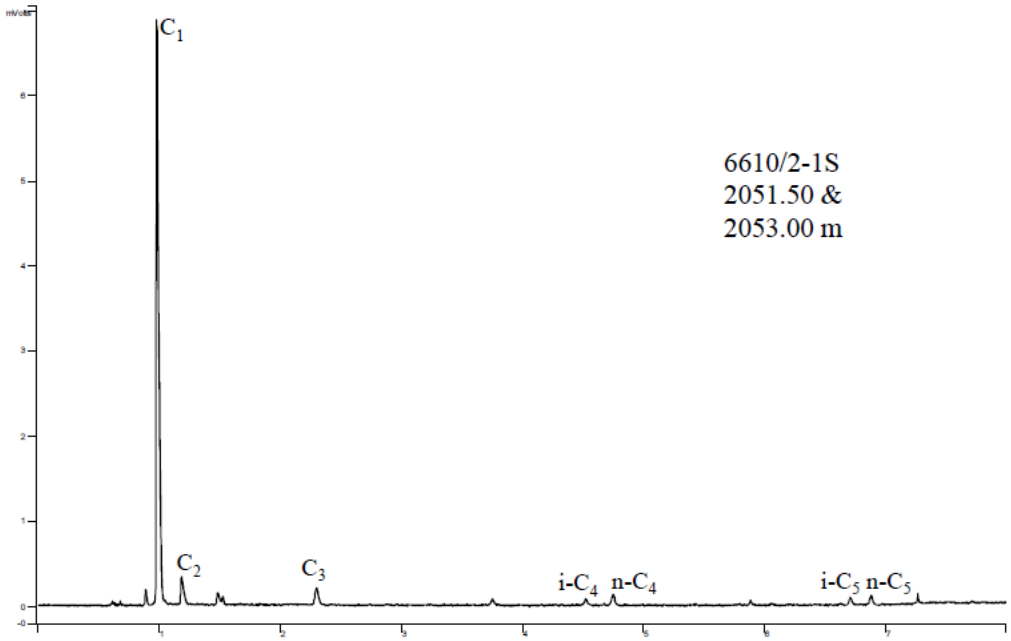
C1
C2
C3
i-C4
n-C4
i-C5
n-C5
6610/2-1S
2051.50 &
2053.00 m

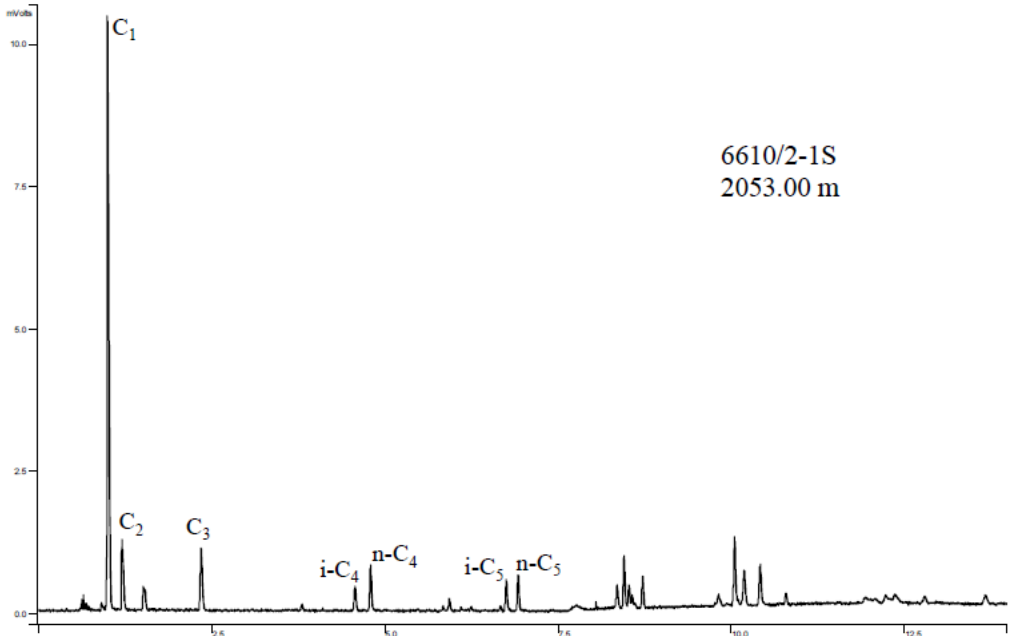
C1
C2
C3
i-C4
n-C4
i-C5
n-C5
6610/2-1S
2053.00 m

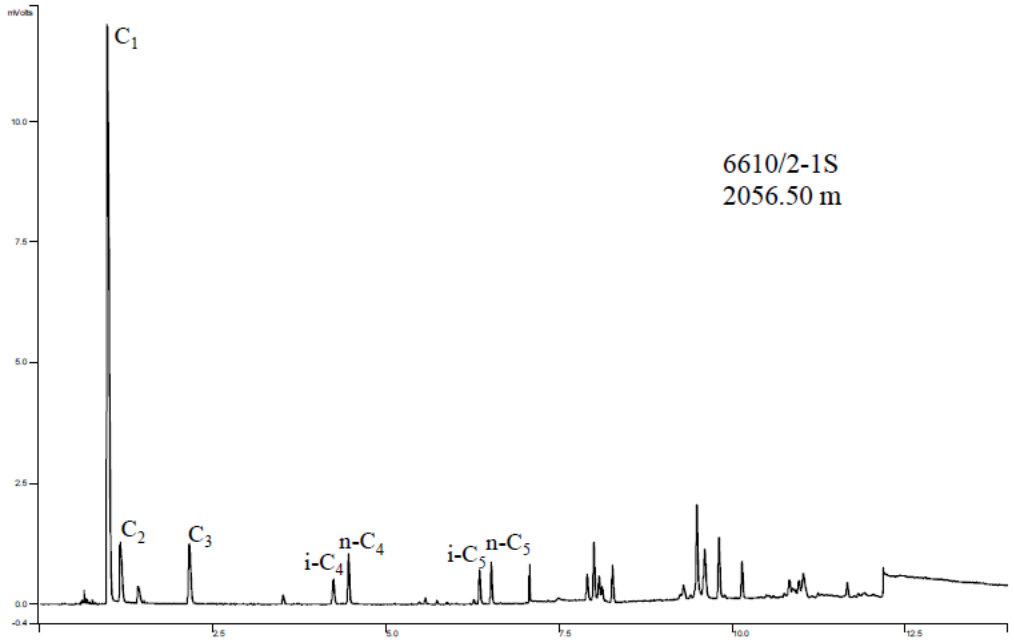
mVolts
10.0
7.5
5.0
2.5
0.0
-0.4
2.5
5.0
7.5
10.0
12.5
C1
C2
C3
i-C4
n-C4
i-C5
n-C5
6610/2-1S
2056.50 m

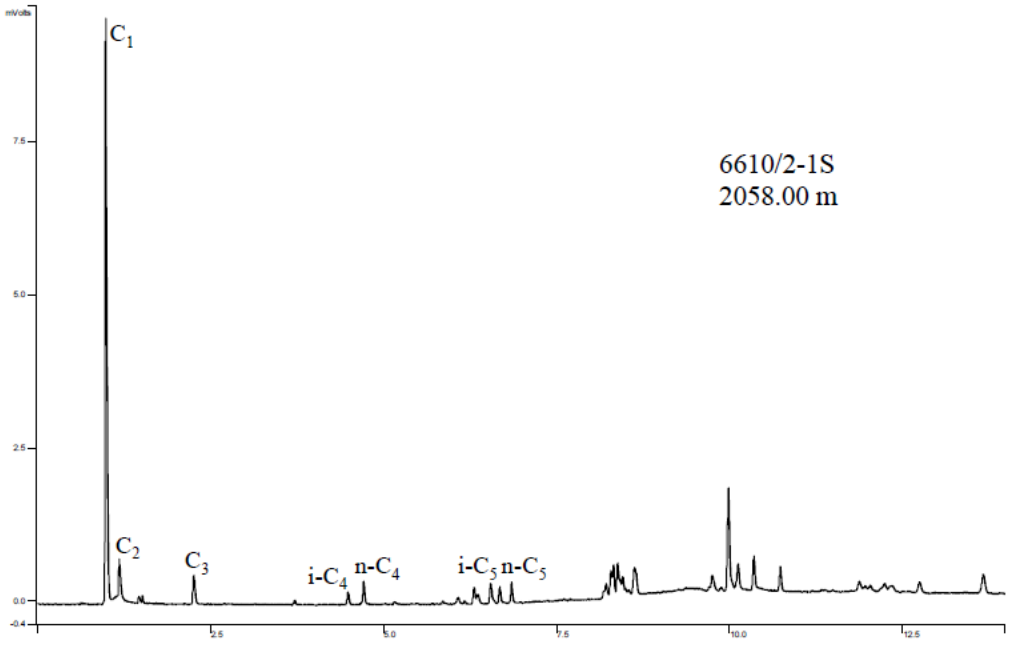
mVolts
7.5
5.0
2.5
0.0
-0.4
2.5
5.0
7.5
10.0
12.5
C1
C2
C3
i-C4
n-C4
i-C5
n-C5
6610/2-1S
2058.00 m

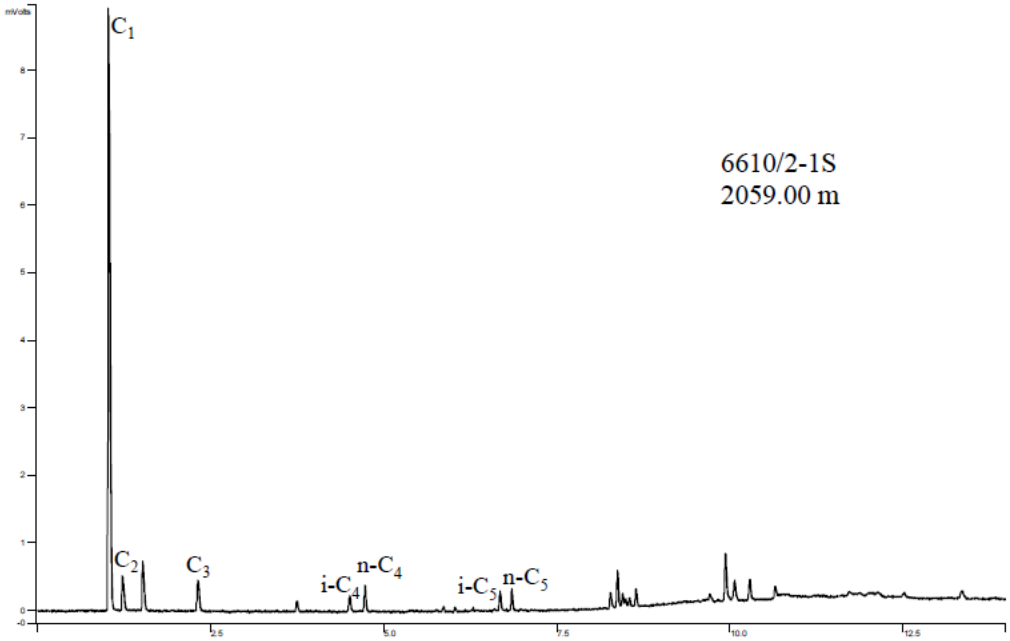
mVolts
C1
C2
C3
i-C4
n-C4
i-C5
n-C5
6610/2-1S
2059.00 m

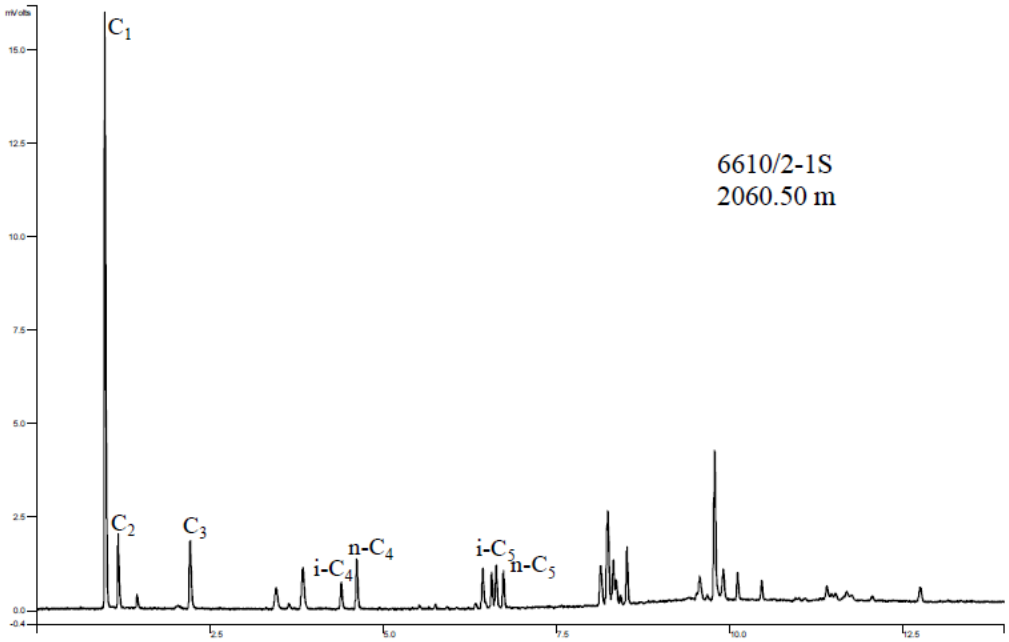
mVolts
C1
C2
C3
i-C4
n-C4
i-C5
n-C5
6610/2-1S
2060.50 m

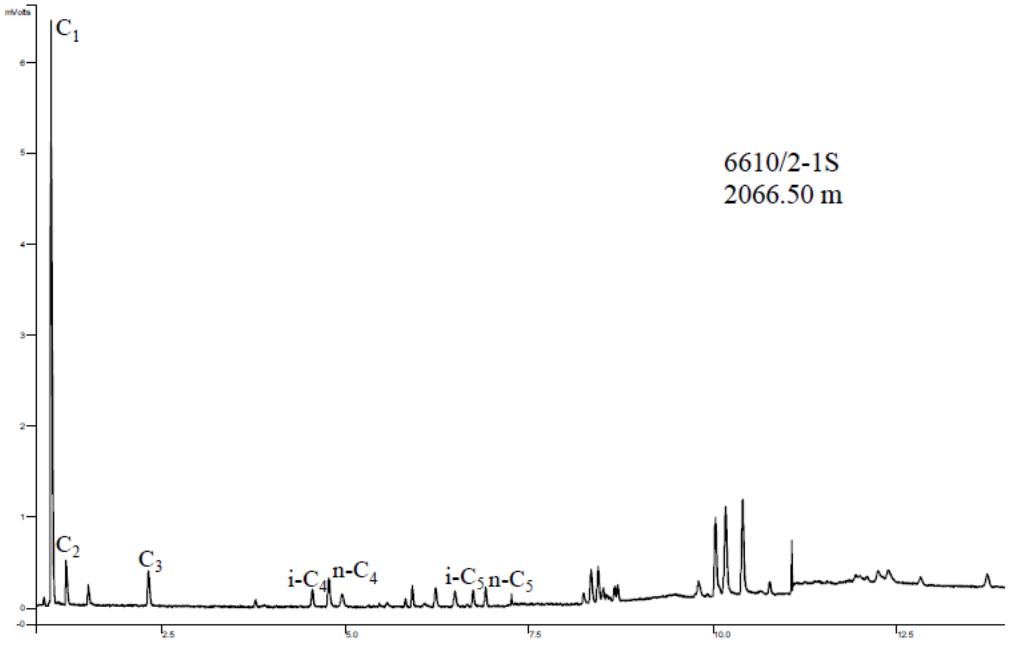
mVolts
C1
C2
C3
i-C4
n-C4
i-C5
n-C5
6610/2-1S
2066.50 m

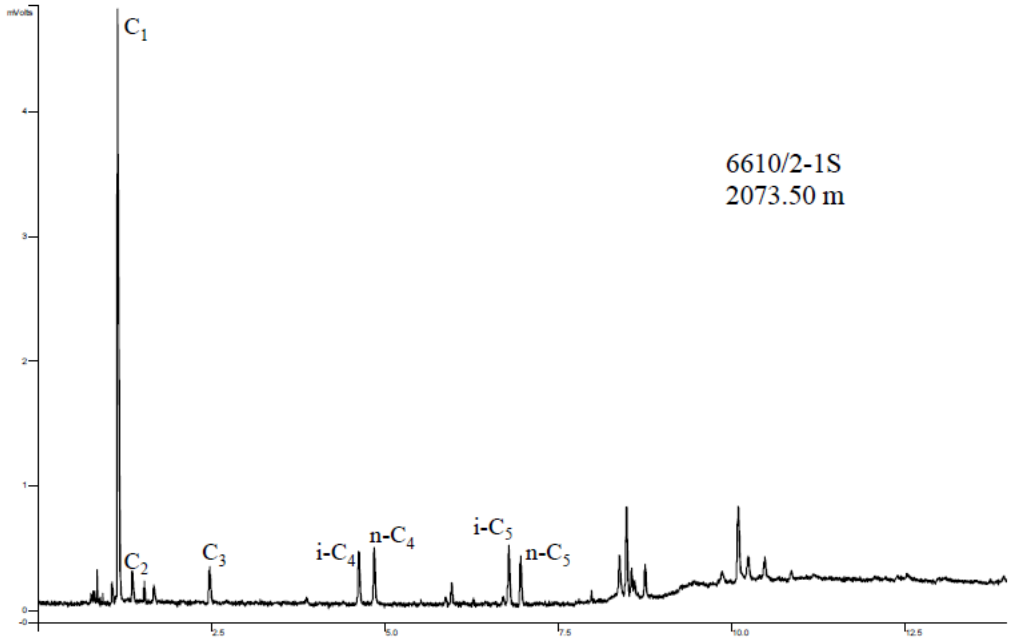
mVolts
C1
C2
C3
i-C4
n-C4
i-C5
n-C5
6610/2-1S
2073.50 m

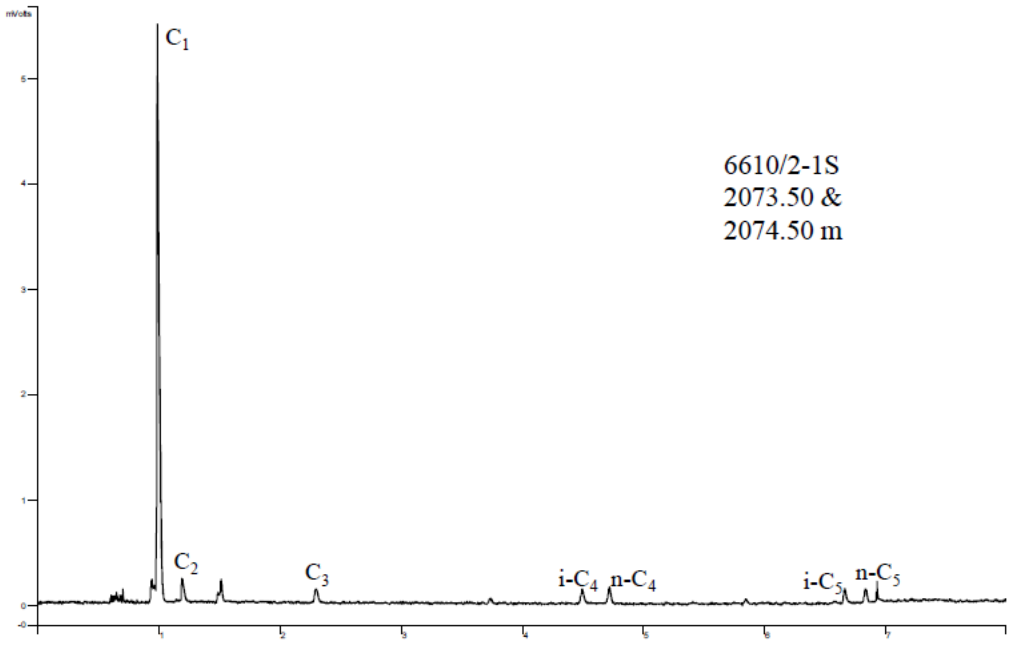
mVolts
C1
C2
C3
i-C4
n-C4
i-C5
n-C5
6610/2-1S
2073.50 &
2074.50 m

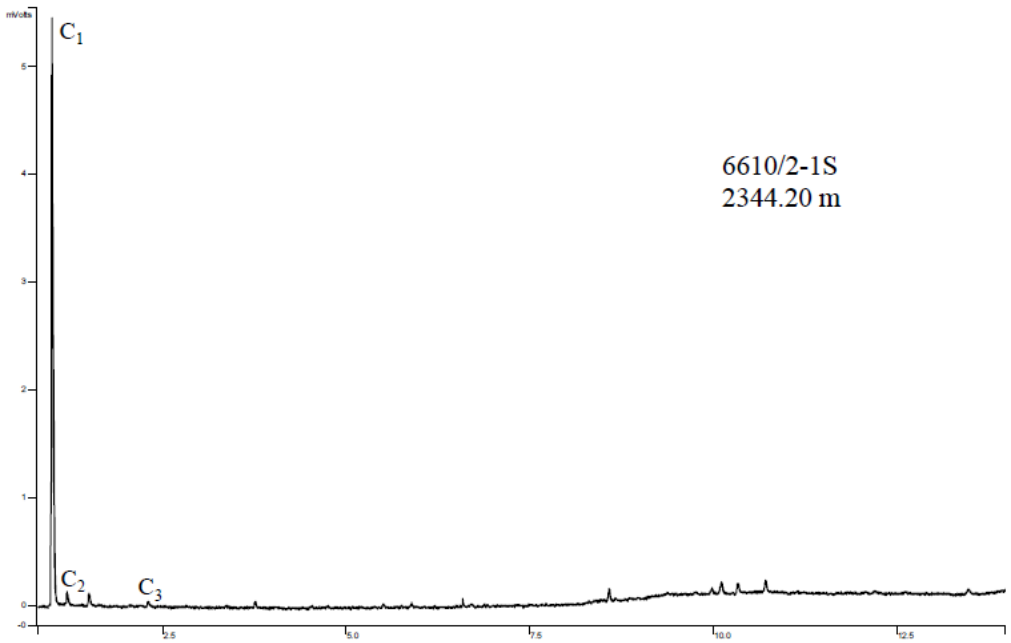
mVolts
C1
C2
C3
6610/2-1S
2344.20 m

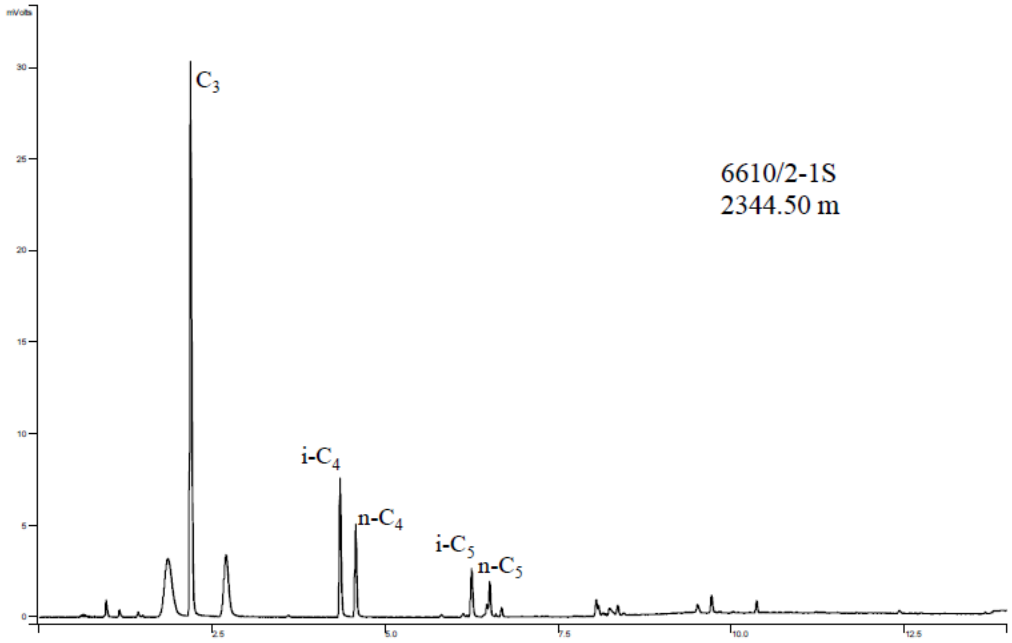
mVolts
30
25
20
15
10
5
0
C3
i-C4
n-C4
i-C5
n-C5
2.5
5.0
7.5
10.0
12.5
6610/2-1S
2344.50 m

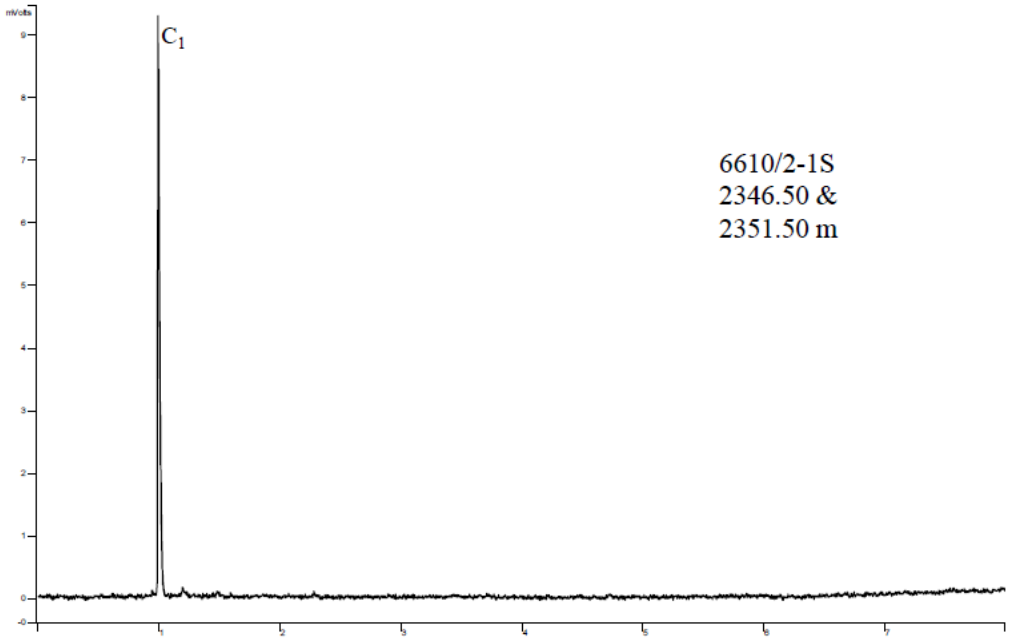
mVolts
9
8
7
6
5
4
3
2
1
0
-0
C1
1
2
3
4
5
6
7
6610/2-1S
2346.50 &
2351.50 m

Appendix – B

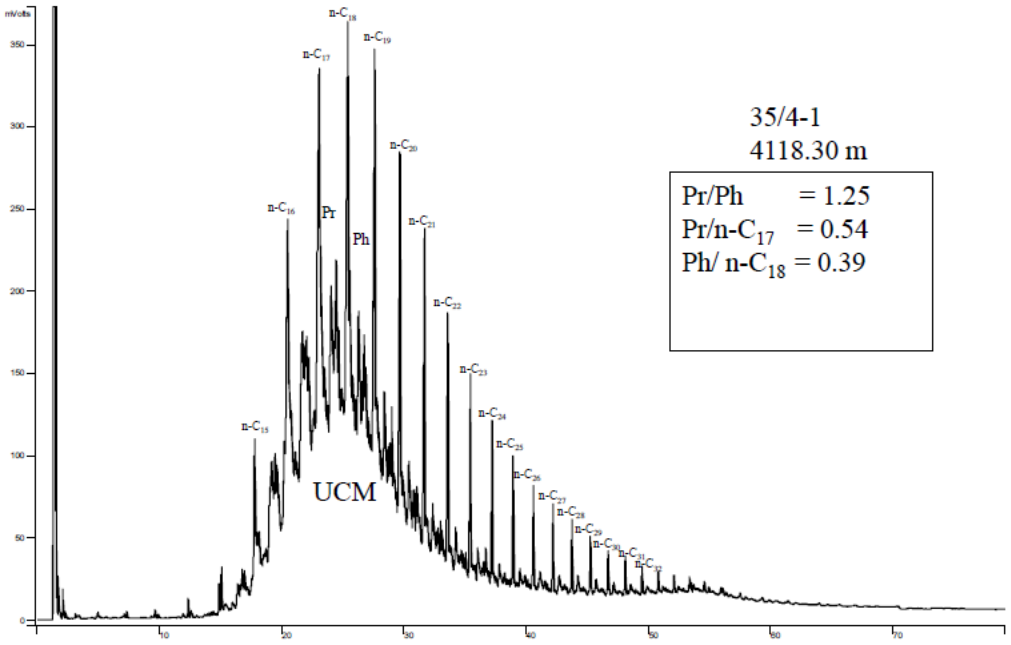
n-C15
n-C16
n-C17
Pr
n-C18
Ph
n-C19
n-C20
n-C21
n-C22
n-C23
n-C24
n-C25
n-C26
n-C27
n-C28
n-C29
UCM
35/4-1
4118.30 m
Pr/Ph = 1.25
Pr/n-C17 = 0.54
Ph/ n-C18 = 0.39

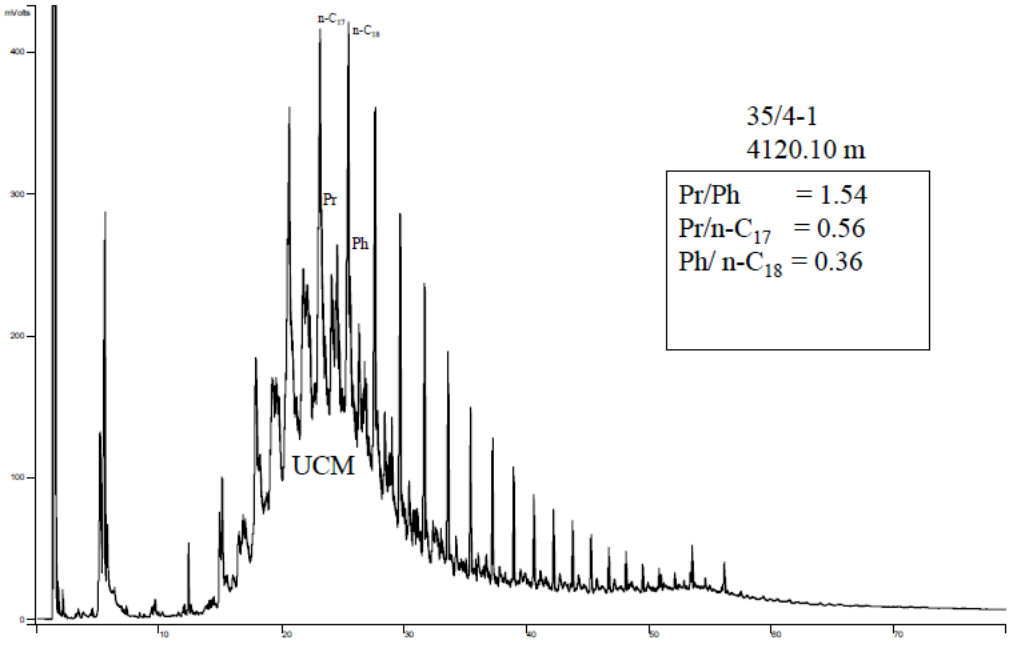
n-C17
n-C18
Pr
Ph
UCM
35/4-1
4120.10 m
Pr/Ph = 1.54
Pr/n-C17 = 0.56
Ph/ n-C18 = 0.36

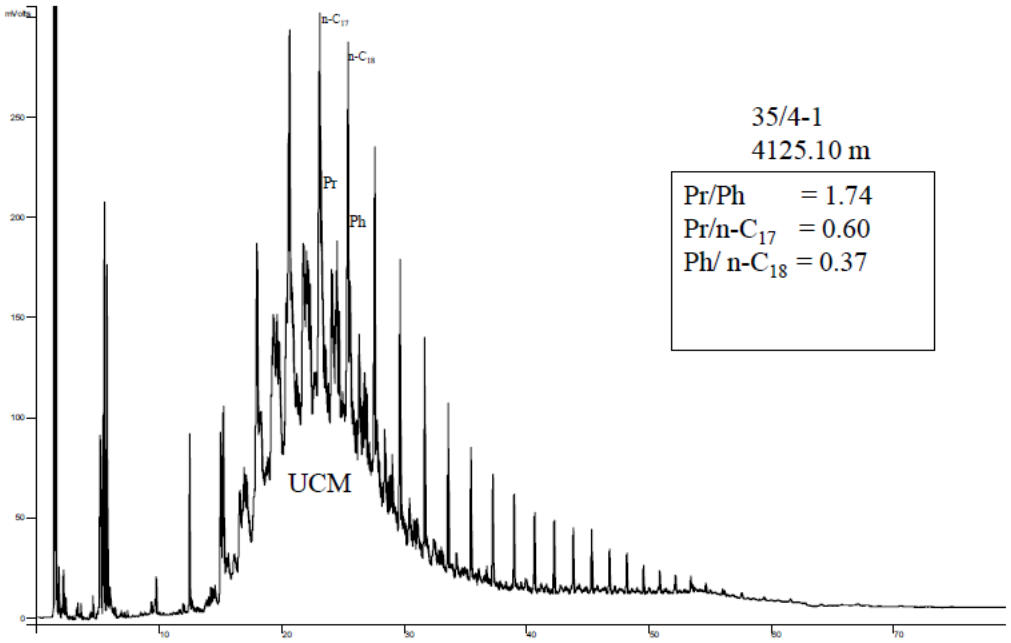
n-C17
n-C18
Pr
Ph
UCM
35/4-1
4125.10 m
Pr/Ph = 1.74
Pr/n-C17 = 0.60
Ph/ n-C18 = 0.37

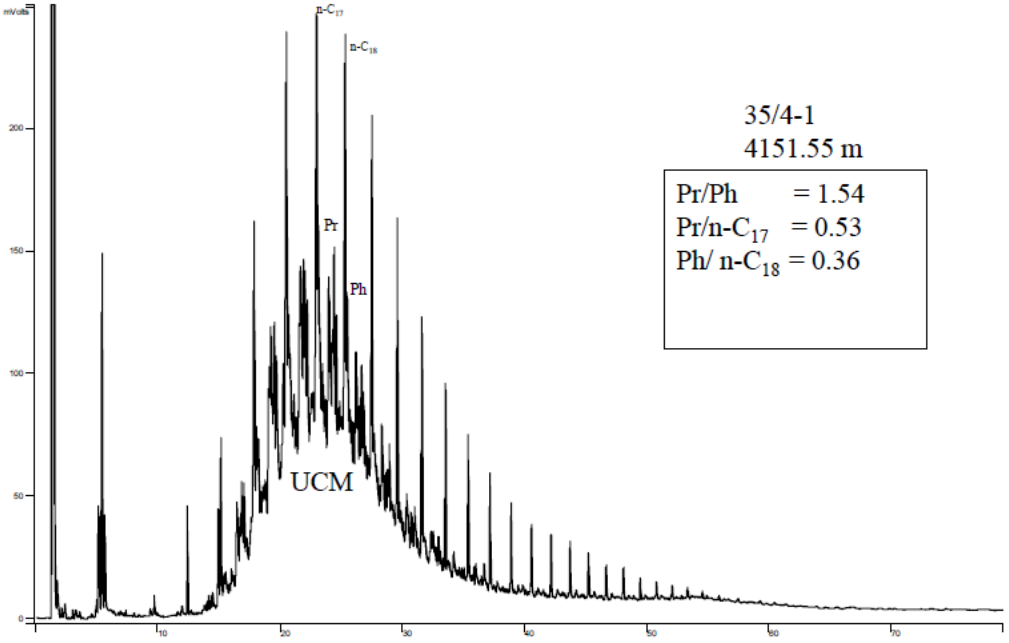
n-C17
n-C18
Pr
Ph
UCM
35/4-1
4151.55 m
Pr/Ph = 1.54
Pr/n-C17 = 0.53
Ph/ n-C18 = 0.36

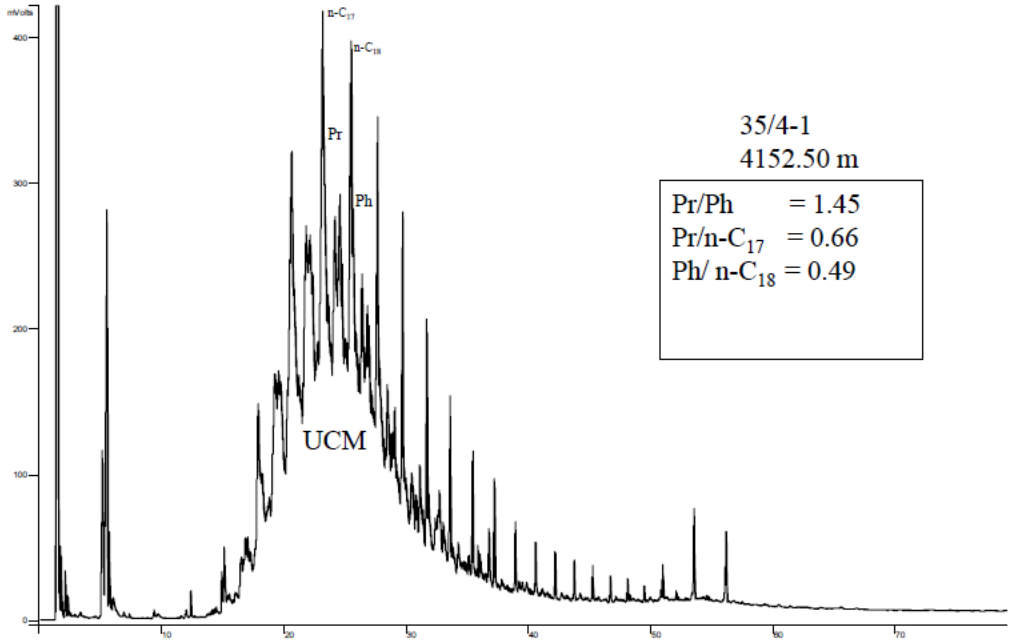
n-C17
n-C18
Pr
Ph
UCM
35/4-1
4152.50 m
Pr/Ph = 1.45
Pr/n-C17 = 0.66
Ph/ n-C18 = 0.49

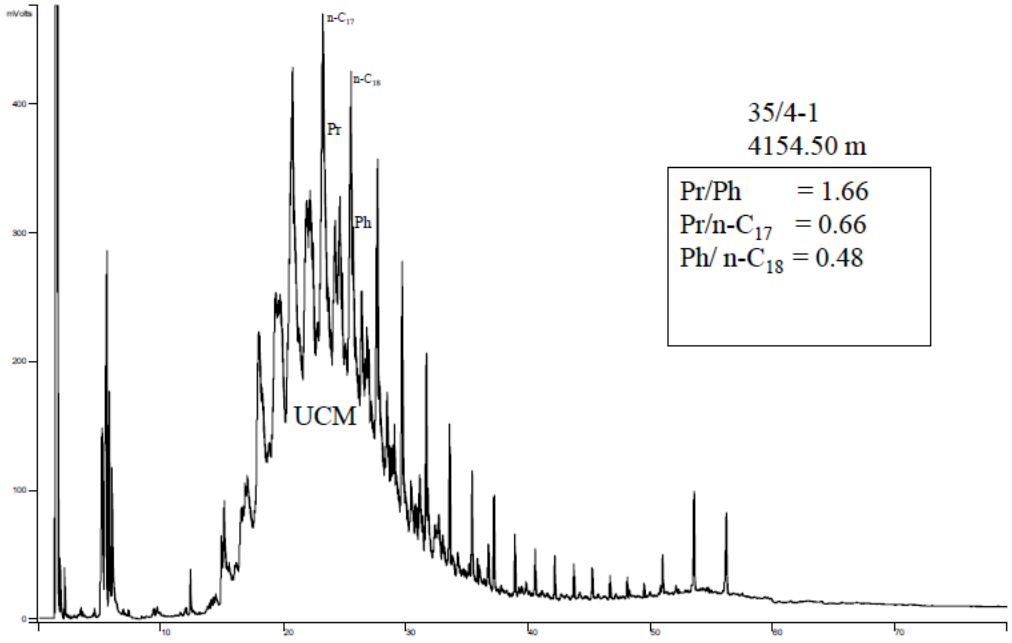
n-C17
n-C18
Pr
Ph
UCM
35/4-1
4154.50 m
Pr/Ph = 1.66
Pr/n-C17 = 0.66
Ph/ n-C18 = 0.48

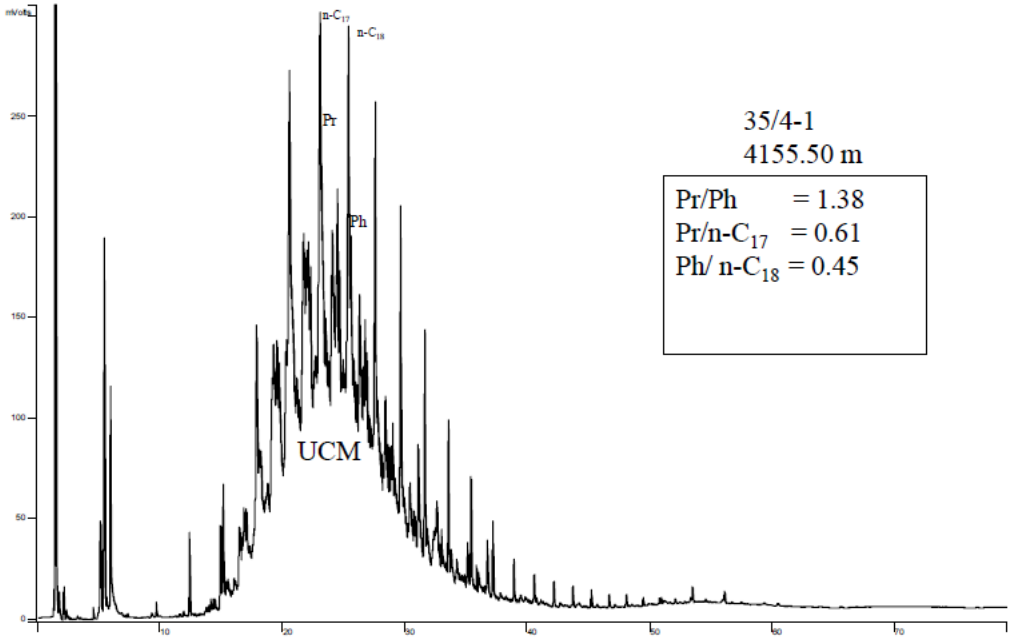
n-C17
n-C18
Pr
Ph
UCM
35/4-1
4155.50 m
Pr/Ph = 1.38
Pr/n-C17 = 0.61
Ph/ n-C18 = 0.45

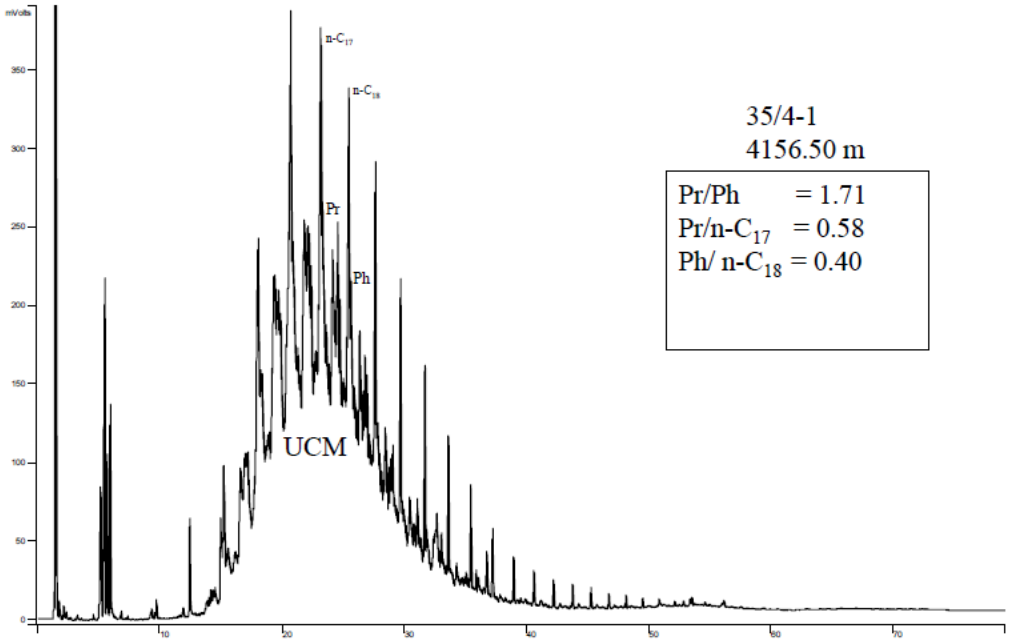
n-C17
n-C18
Pr
Ph
UCM
35/4-1
4156.50 m
Pr/Ph = 1.71
Pr/n-C17 = 0.58
Ph/ n-C18 = 0.40

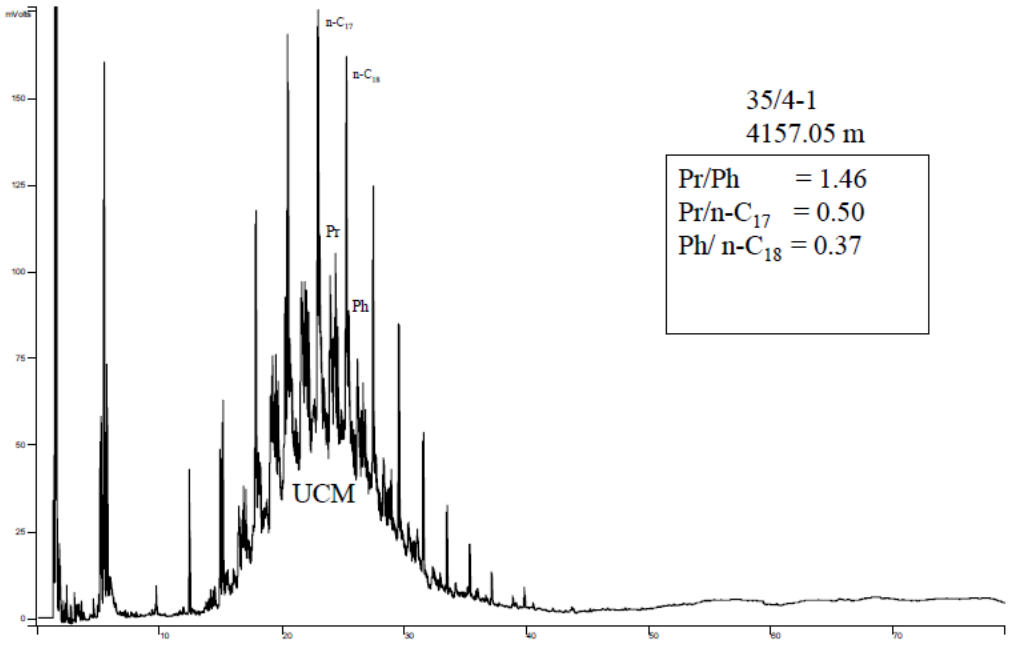
n-C17
n-C18
Pr
Ph
UCM
35/4-1
4157.05 m
Pr/Ph = 1.46
Pr/n-C17 = 0.50
Ph/ n-C18 = 0.37

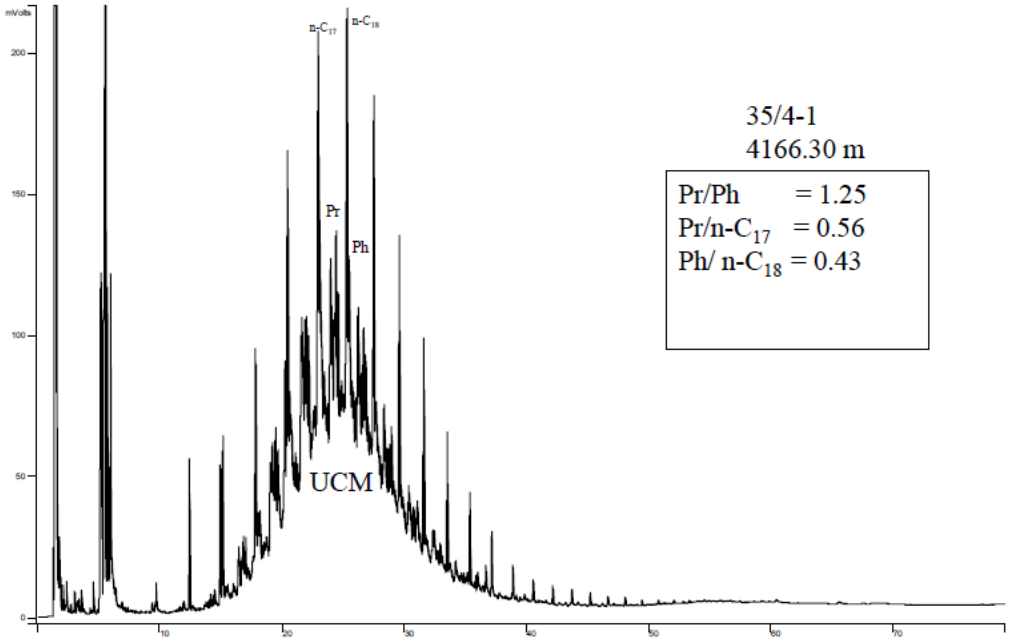
n-C17
n-C18
Pr
Ph
UCM
35/4-1
4166.30 m
Pr/Ph = 1.25
Pr/n-C17 = 0.56
Ph/ n-C18 = 0.43

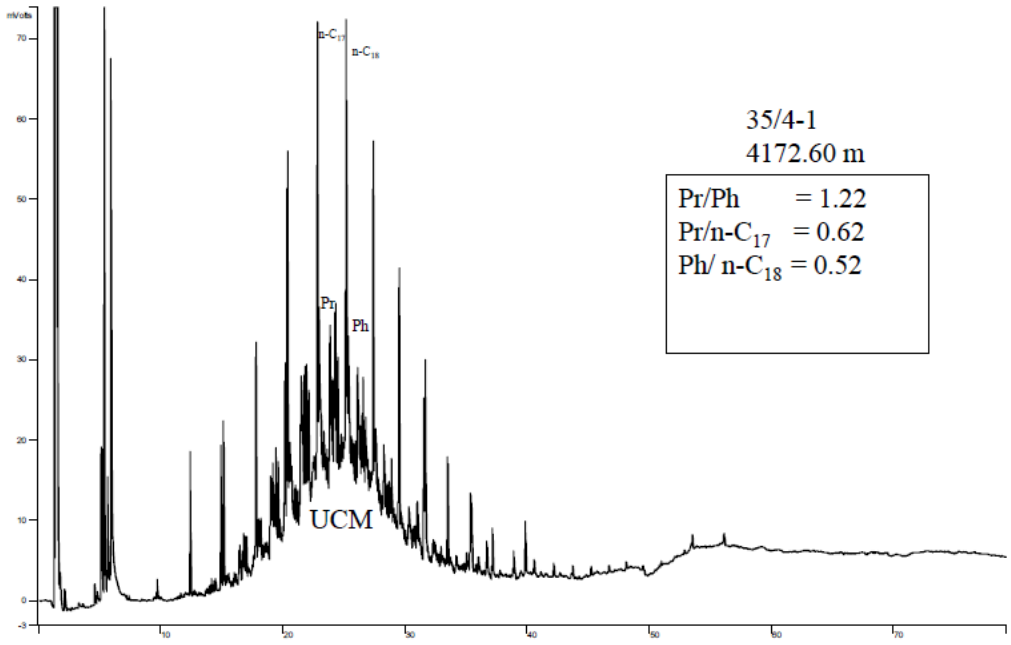
mV/olts
n-C17
n-C18
Pr
Ph
UCM
35/4-1
4172.60 m
Pr/Ph = 1.22
Pr/n-C17 = 0.62
Ph/ n-C18 = 0.52

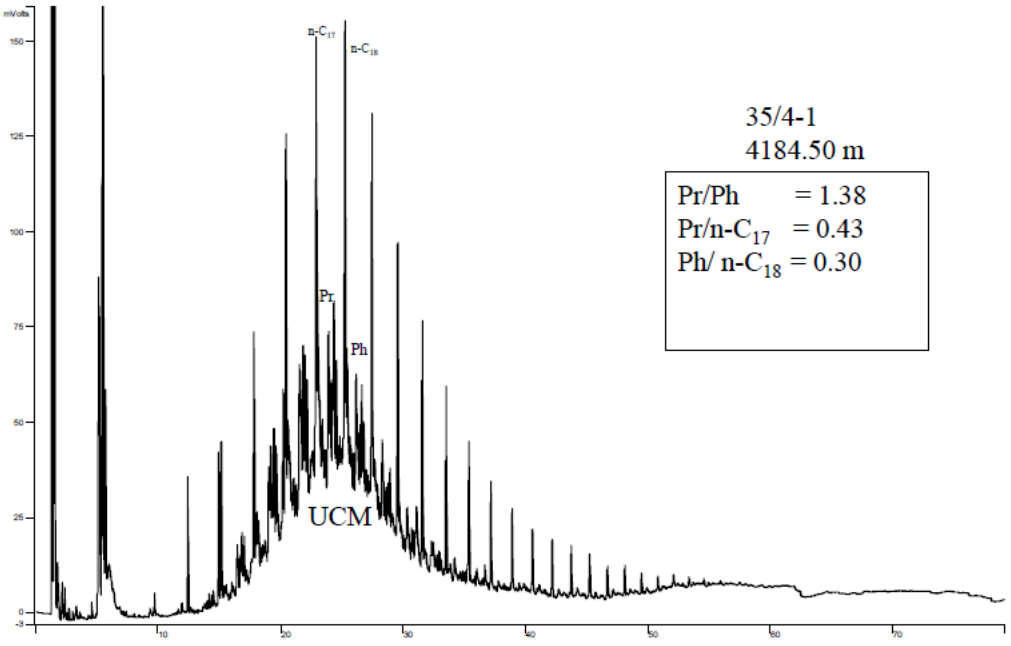
mV/olts
n-C17
n-C18
Pr
Ph
UCM
35/4-1
4184.50 m
Pr/Ph = 1.38
Pr/n-C17 = 0.43
Ph/ n-C18 = 0.30

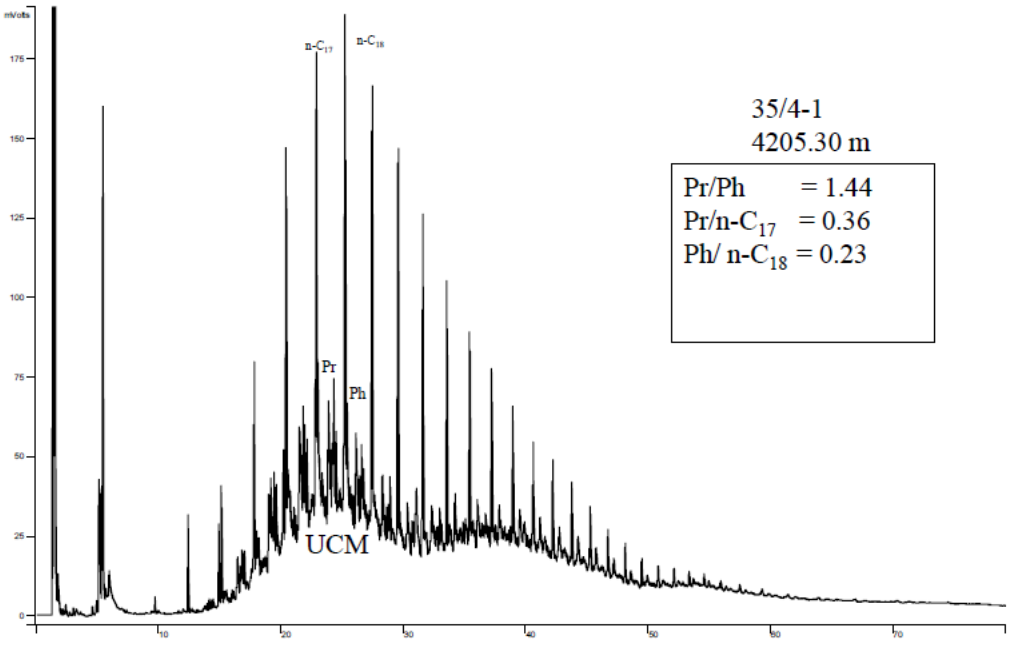

35/4-1
4205.30 m

Pr/Ph = 1.44
Pr/n-C_{17} = 0.36
Ph/ n-C_{18} = 0.23

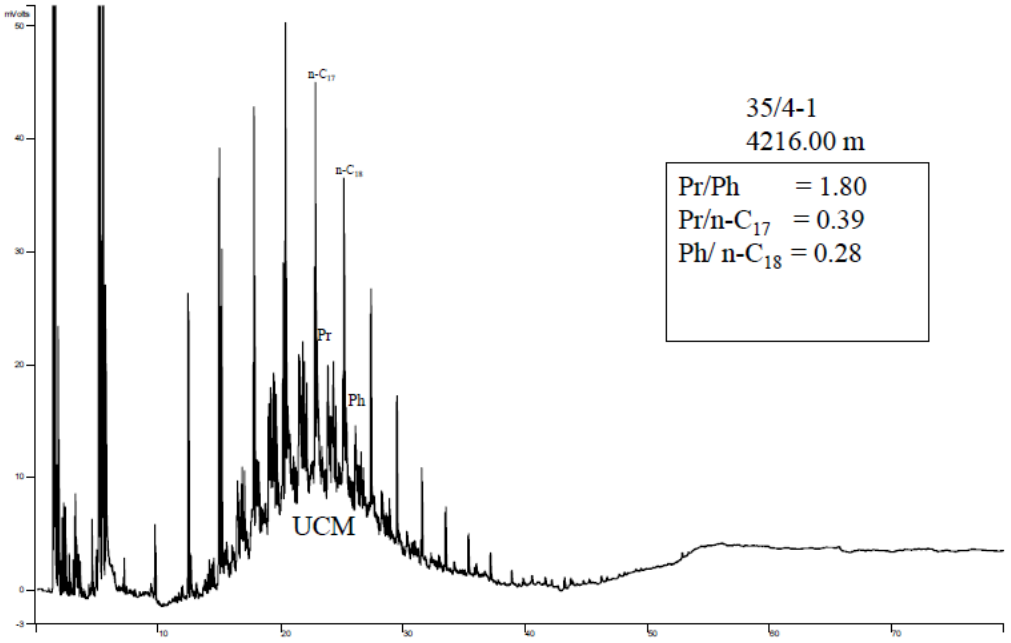

35/4-1
4216.00 m

Pr/Ph = 1.80
Pr/n-C_{17} = 0.39
Ph/ n-C_{18} = 0.28

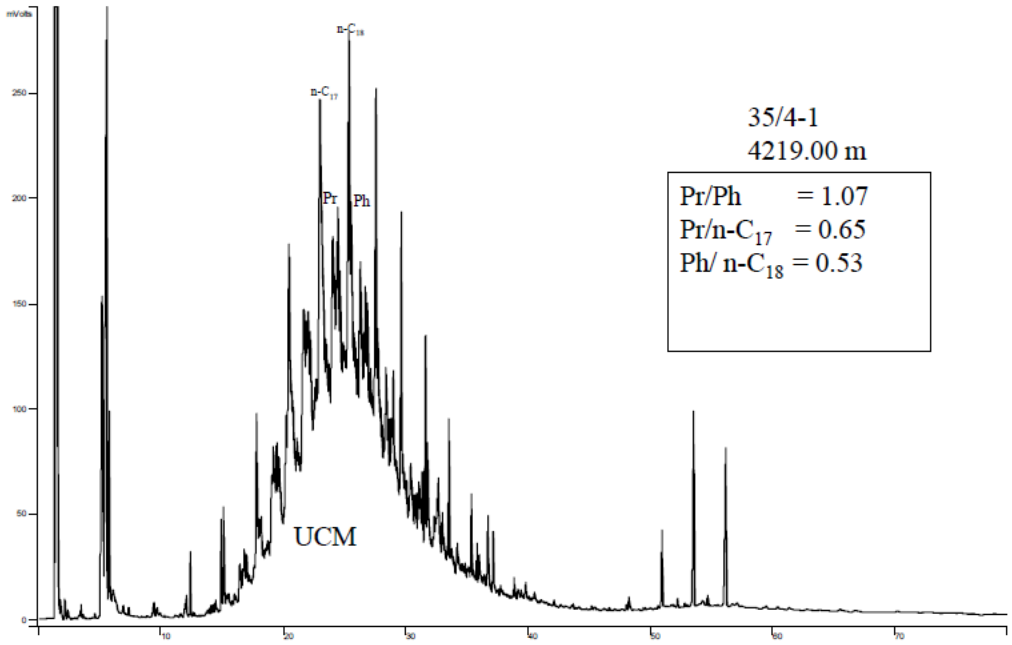
mVolts
n-C18
n-C17
Pr
Ph
UCM
35/4-1
4219.00 m
Pr/Ph = 1.07
Pr/n-C17 = 0.65
Ph/ n-C18 = 0.53

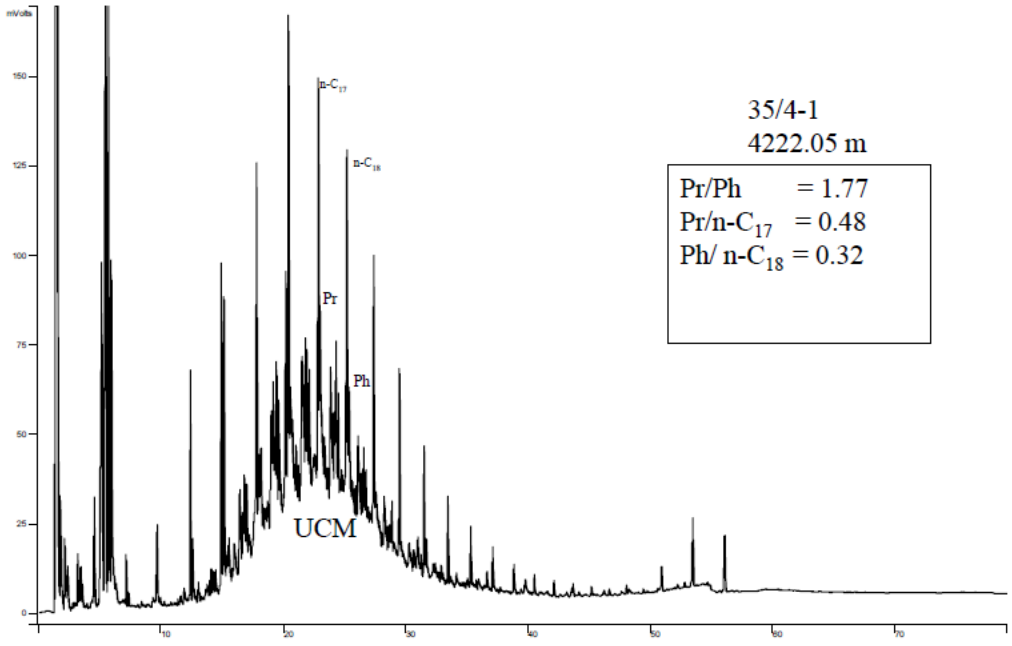
mVolts
n-C17
n-C18
Pr
Ph
UCM
35/4-1
4222.05 m
Pr/Ph = 1.77
Pr/n-C17 = 0.48
Ph/ n-C18 = 0.32

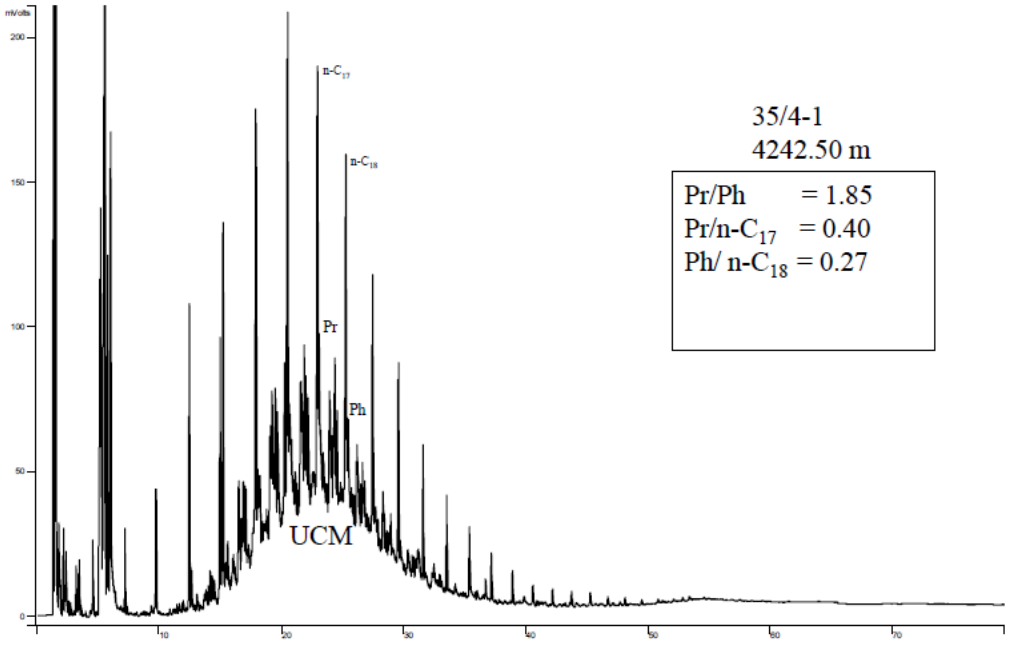

35/4-1
4242.50 m

Pr/Ph = 1.85
Pr/n-C_{17} = 0.40
Ph/ n-C_{18} = 0.27

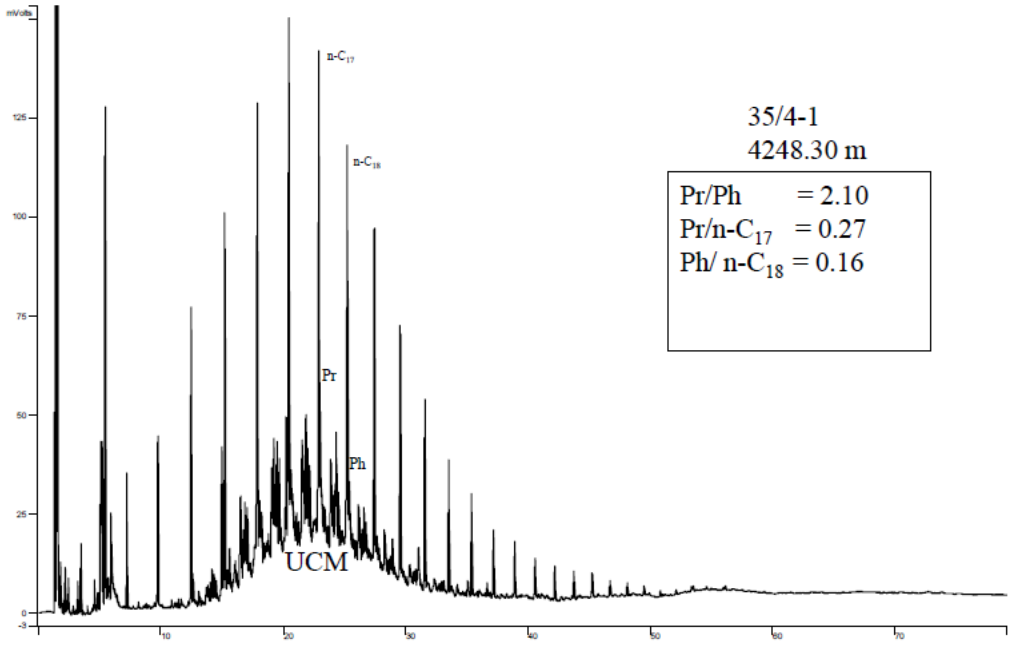

35/4-1
4248.30 m

Pr/Ph = 2.10
Pr/n-C_{17} = 0.27
Ph/ n-C_{18} = 0.16

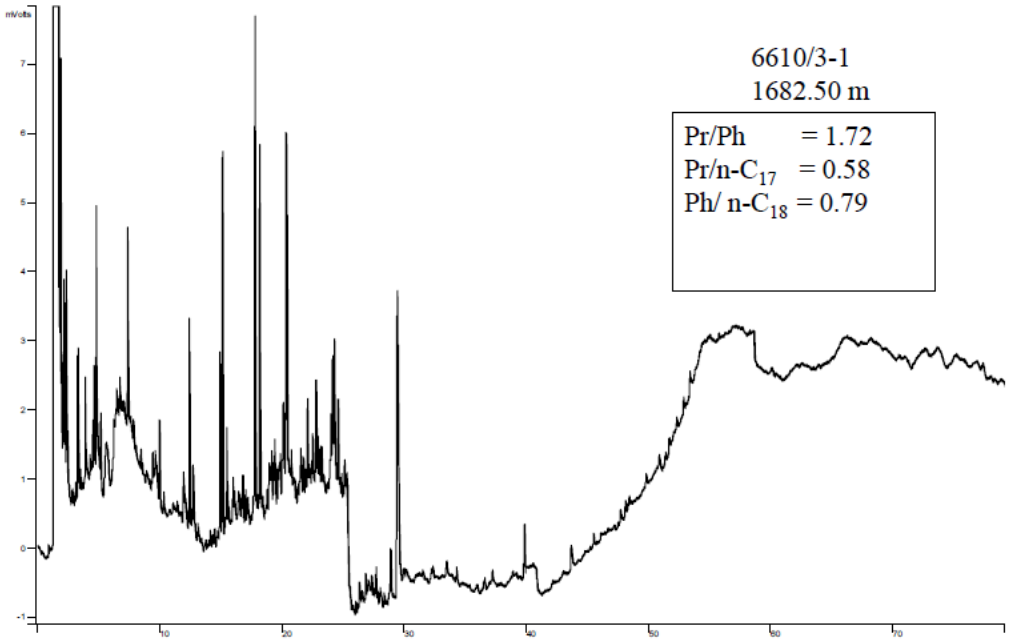
6610/3-1
1682.50 m
Pr/Ph = 1.72
Pr/n-C17 = 0.58
Ph/ n-C18 = 0.79

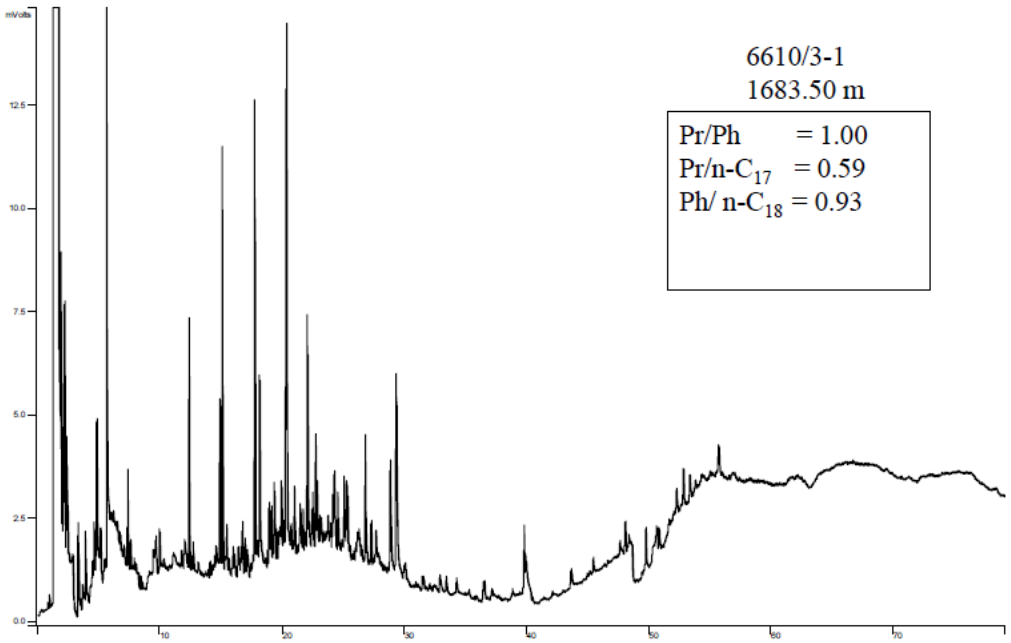
6610/3-1
1683.50 m
Pr/Ph = 1.00
Pr/n-C17 = 0.59
Ph/ n-C18 = 0.93

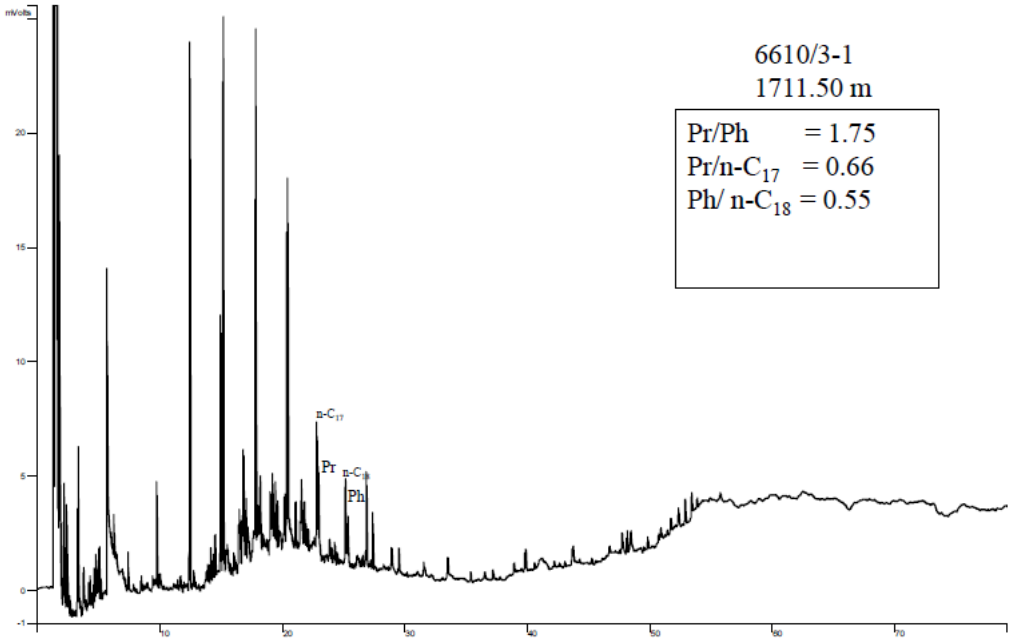

6610/3-1
1711.50 m

Pr/Ph = 1.75
Pr/n-C_{17} = 0.66
Ph/ n-C_{18} = 0.55

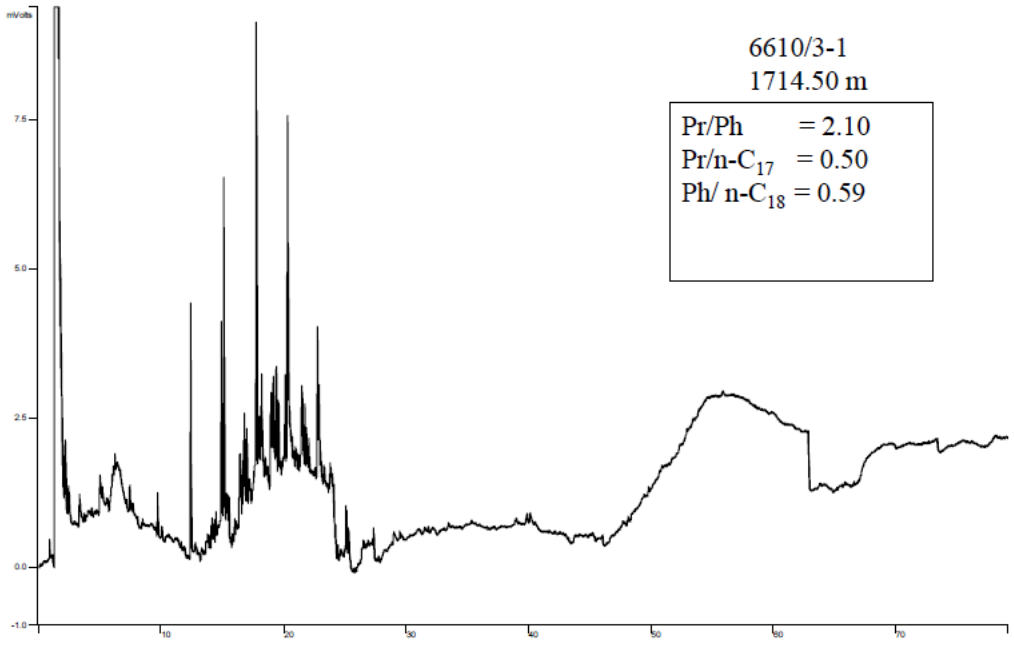

6610/3-1
1714.50 m

Pr/Ph = 2.10
Pr/n-C_{17} = 0.50
Ph/ n-C_{18} = 0.59

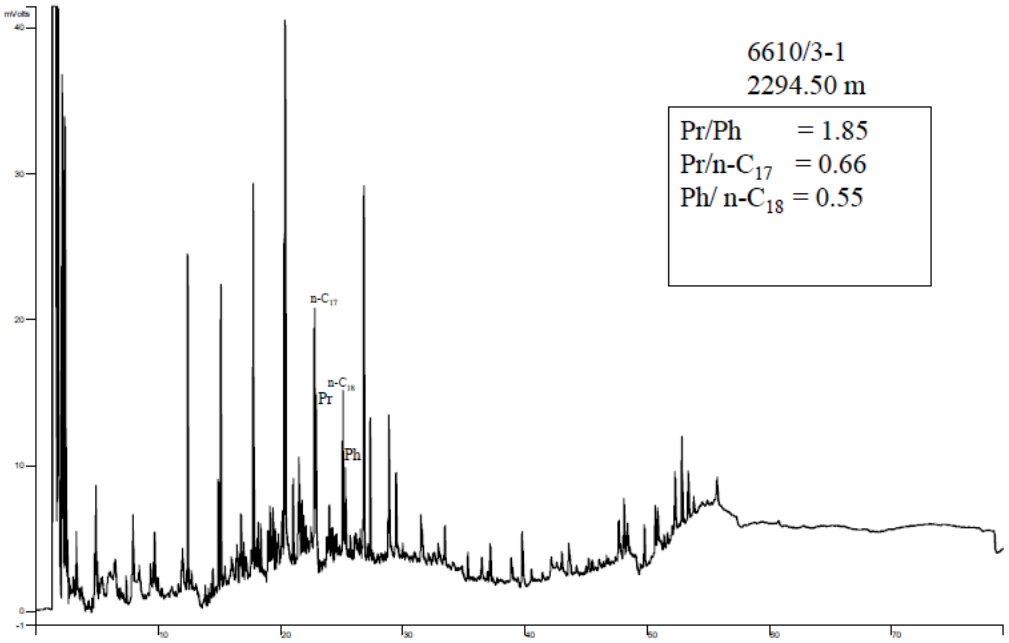
6610/3-1
2294.50 m
Pr/Ph = 1.85
Pr/n-C17 = 0.66
Ph/ n-C18 = 0.55
n-C17
Pr
n-C18
Ph

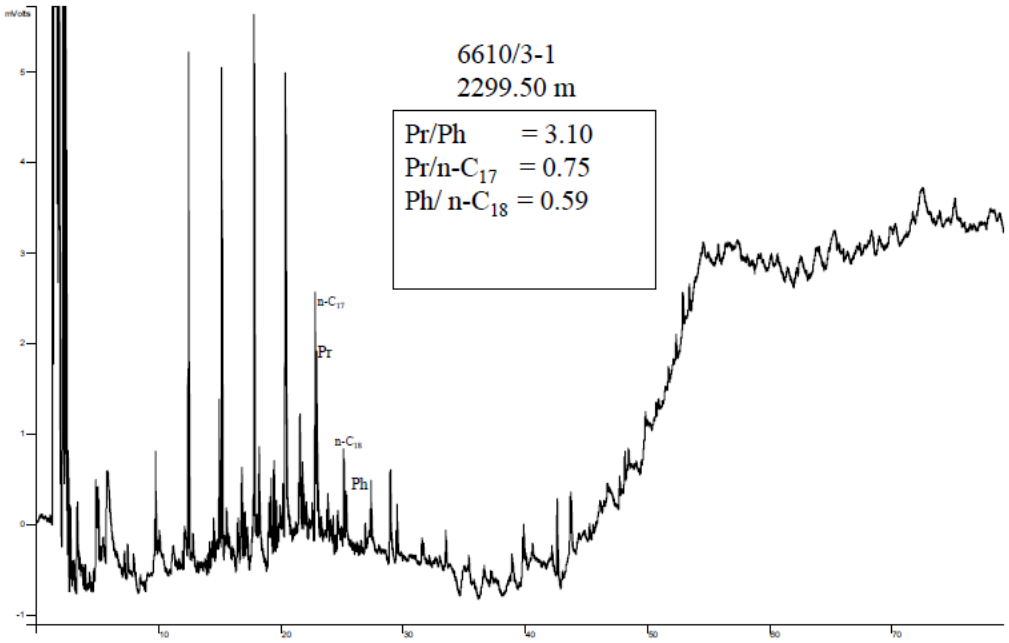
6610/3-1
2299.50 m
Pr/Ph = 3.10
Pr/n-C17 = 0.75
Ph/ n-C18 = 0.59
n-C17
Pr
n-C18
Ph

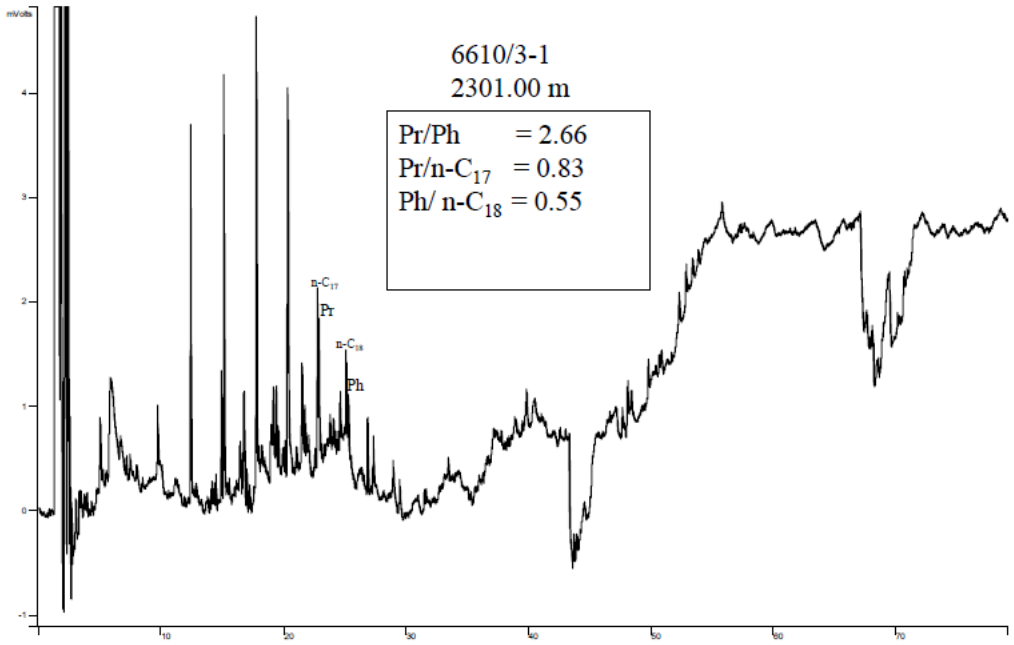
6610/3-1
2301.00 m
Pr/Ph = 2.66
Pr/n-C17 = 0.83
Ph/ n-C18 = 0.55
n-C17
Pr
n-C18
Ph

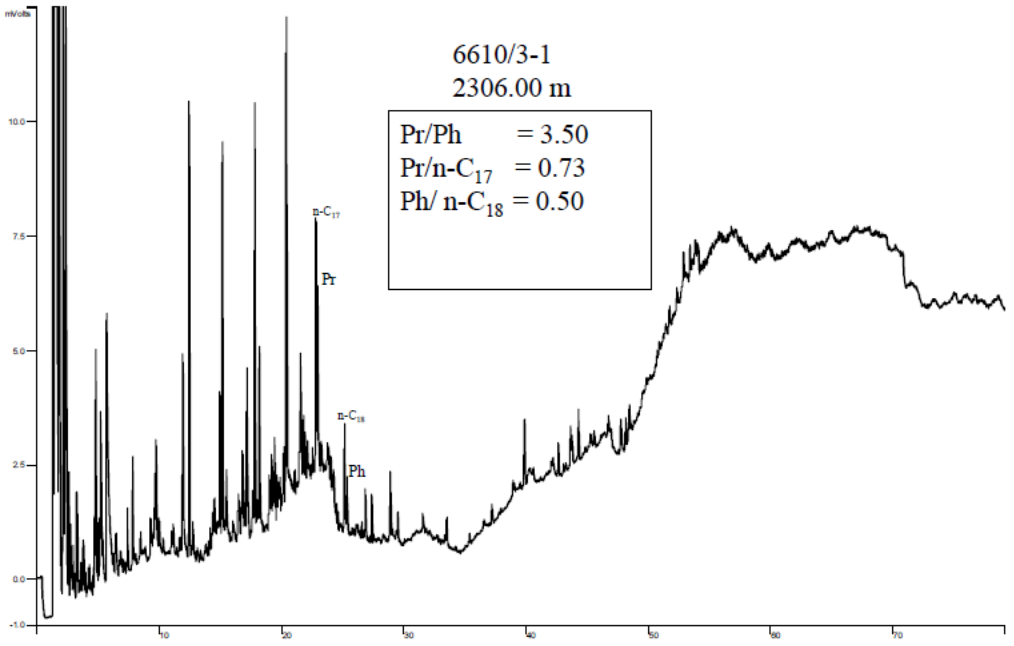
6610/3-1
2306.00 m
Pr/Ph = 3.50
Pr/n-C17 = 0.73
Ph/ n-C18 = 0.50
n-C17
Pr
n-C18
Ph

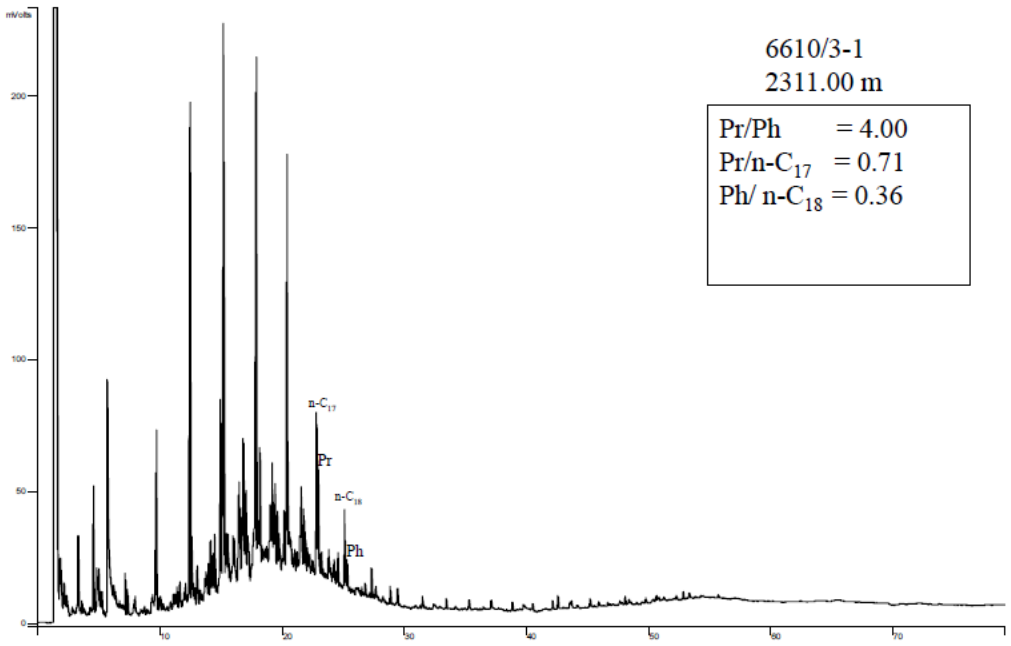
6610/3-1
2311.00 m
Pr/Ph = 4.00
Pr/n-C17 = 0.71
Ph/ n-C18 = 0.36
n-C17
Pr
n-C18
Ph

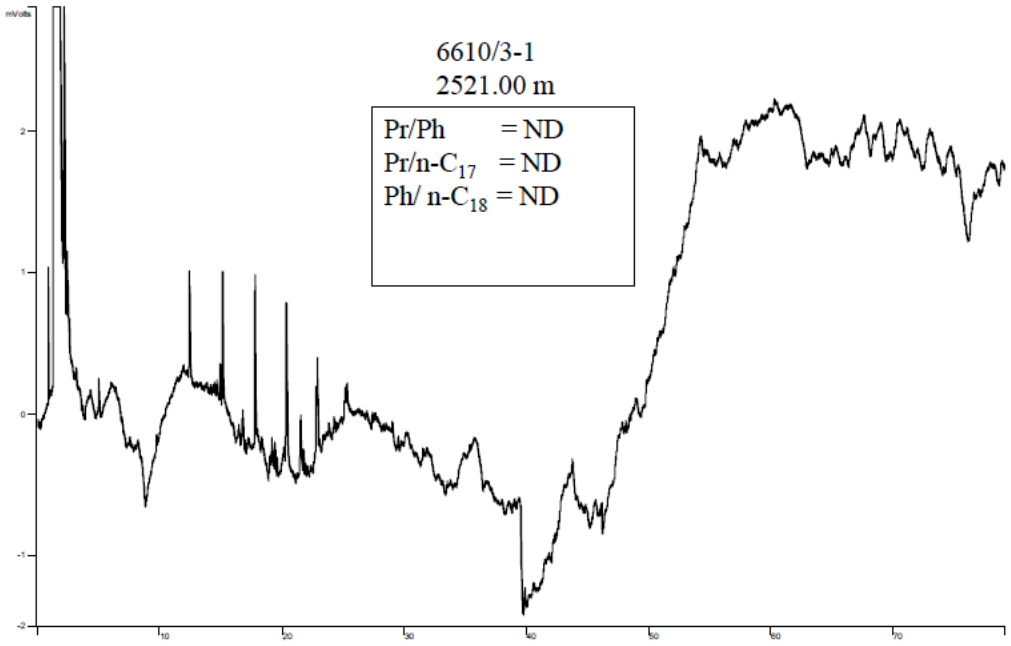
6610/3-1
2521.00 m
Pr/Ph = ND
Pr/n-C17 = ND
Ph/ n-C18 = ND

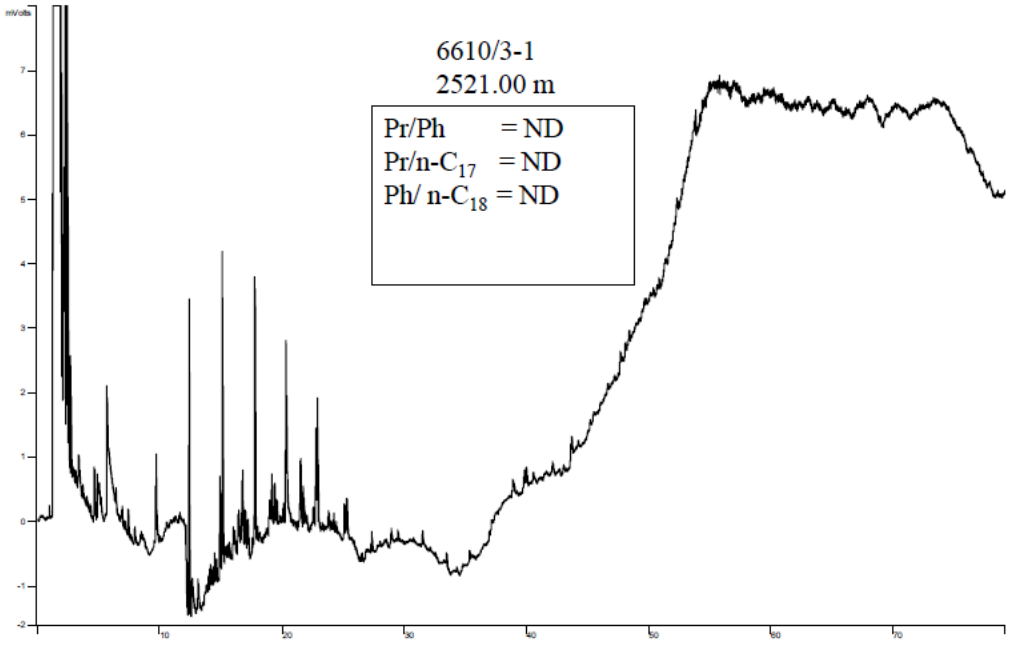
6610/3-1
2521.00 m
Pr/Ph = ND
Pr/n-C17 = ND
Ph/ n-C18 = ND

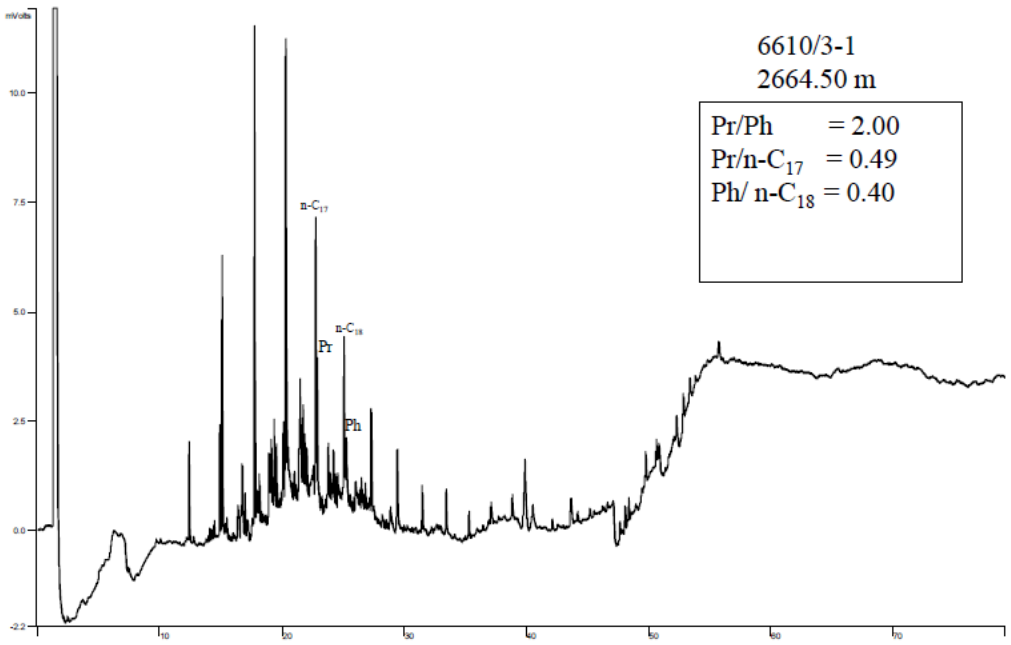
6610/3-1
2664.50 m
Pr/Ph = 2.00
Pr/n-C17 = 0.49
Ph/ n-C18 = 0.40
n-C17
Pr
n-C18
Ph

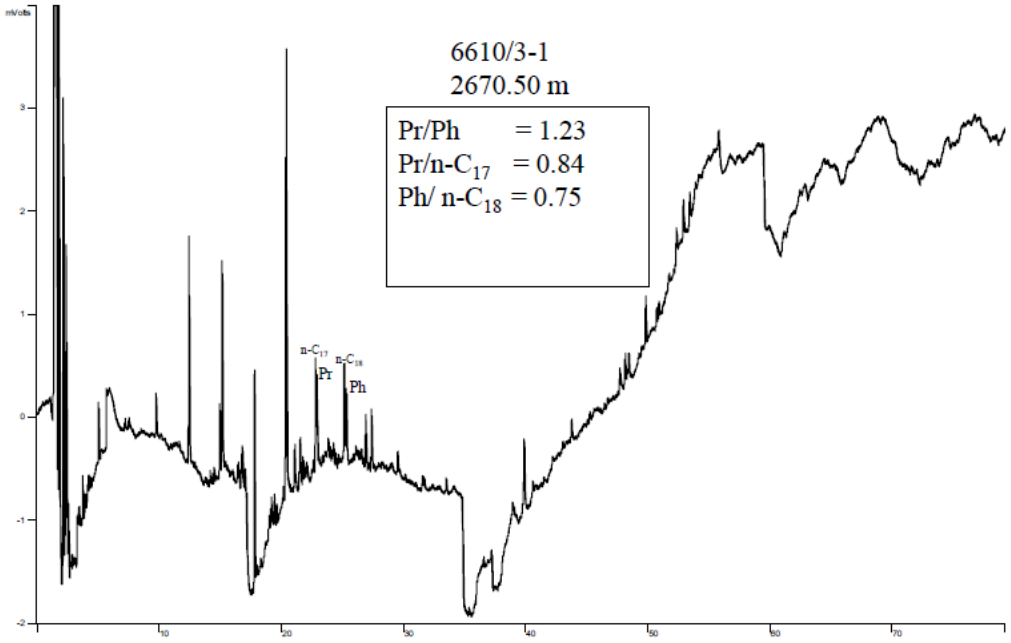
6610/3-1
2670.50 m
Pr/Ph = 1.23
Pr/n-C17 = 0.84
Ph/ n-C18 = 0.75
n-C17
Pr
n-C18
Ph

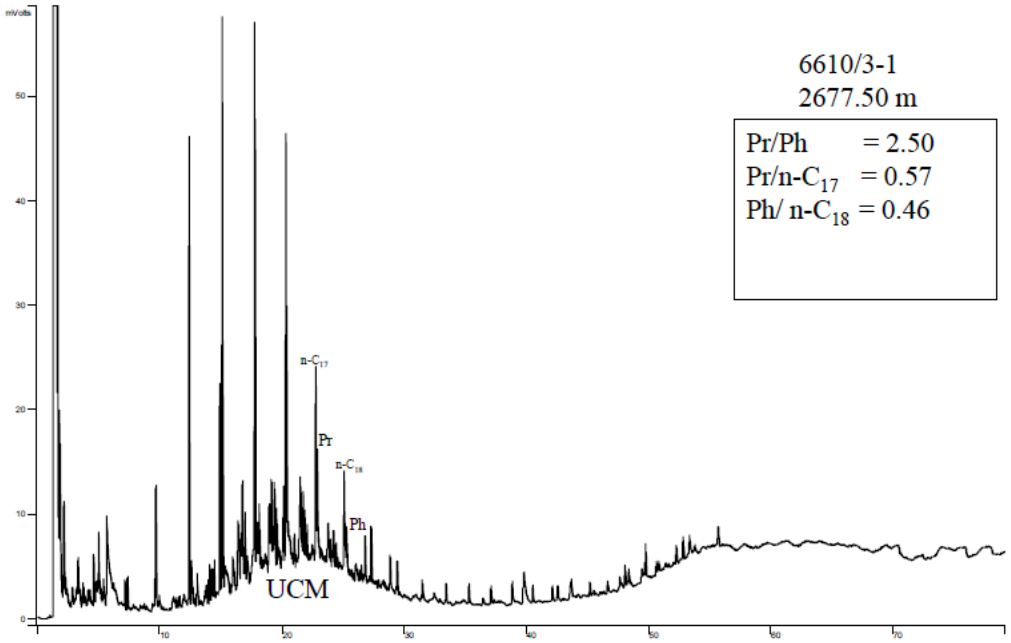
6610/3-1
2677.50 m
Pr/Ph = 2.50
Pr/n-C17 = 0.57
Ph/ n-C18 = 0.46
n-C17
Pr
n-C18
Ph
UCM

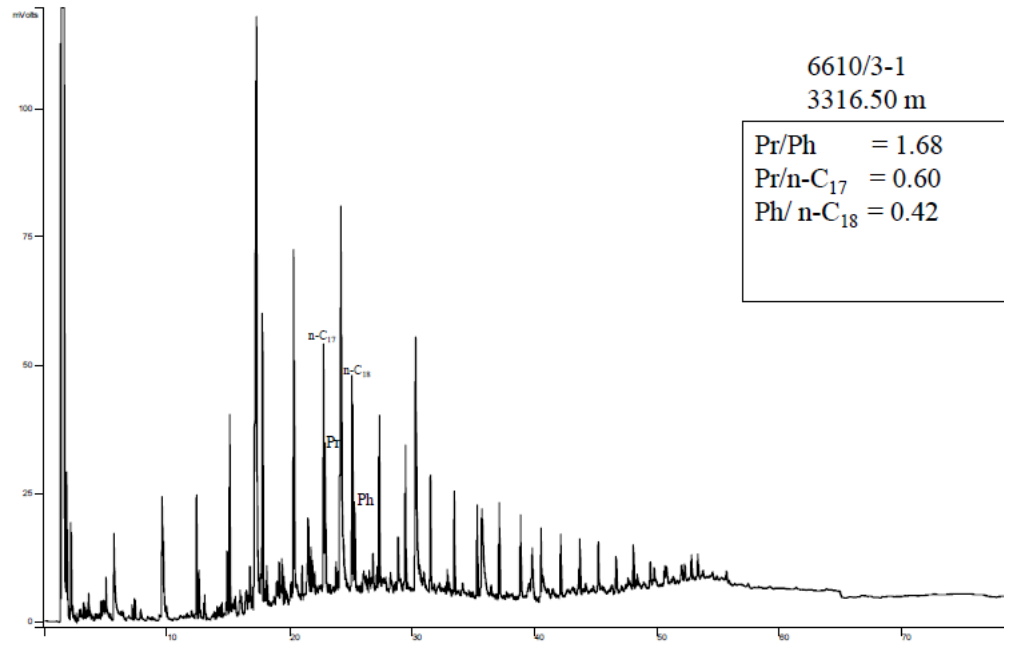
6610/3-1
3316.50 m
Pr/Ph = 1.68
Pr/n-C17 = 0.60
Ph/ n-C18 = 0.42
n-C17
n-C18
Pr
Ph

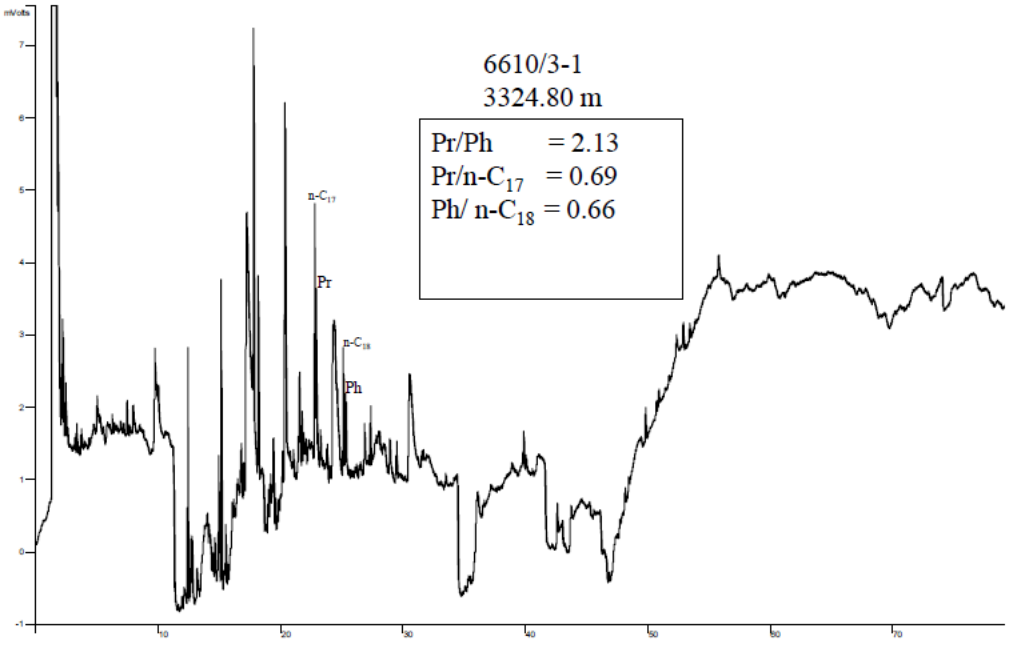
6610/3-1
3324.80 m
Pr/Ph = 2.13
Pr/n-C17 = 0.69
Ph/ n-C18 = 0.66
n-C17
Pr
n-C18
Ph

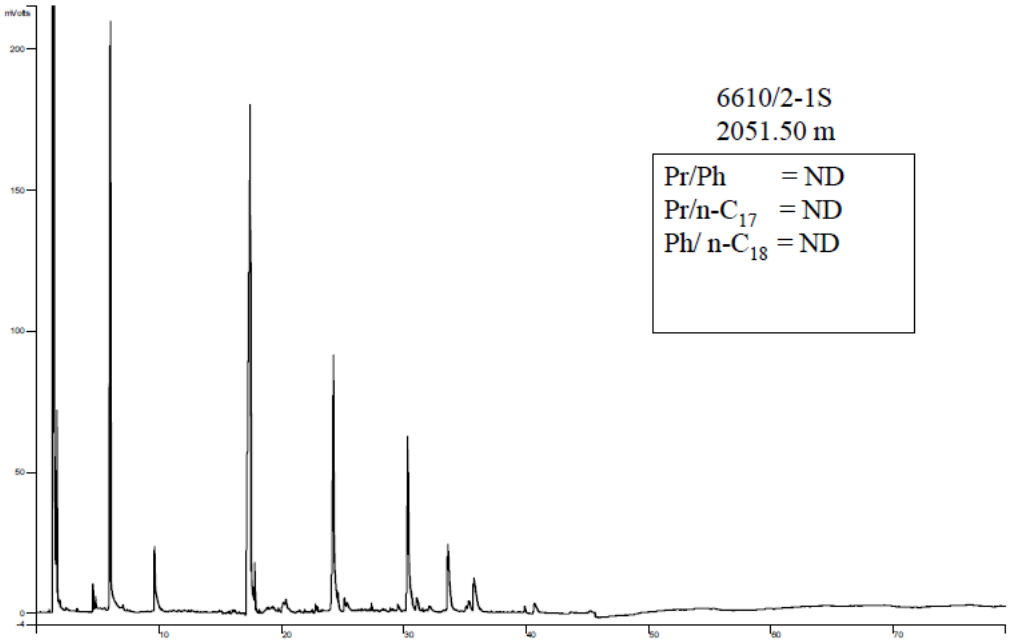

6610/2-1S
2051.50 m

Pr/Ph = ND
Pr/n-C_{17} = ND
Ph/ n-C_{18} = ND

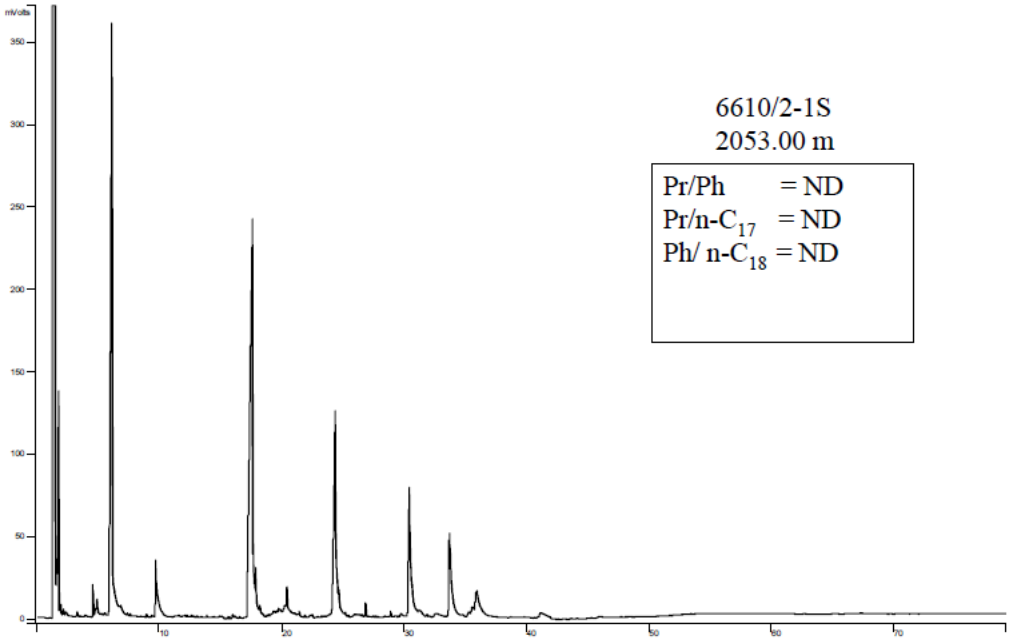

6610/2-1S
2053.00 m

Pr/Ph = ND
Pr/n-C_{17} = ND
Ph/ n-C_{18} = ND

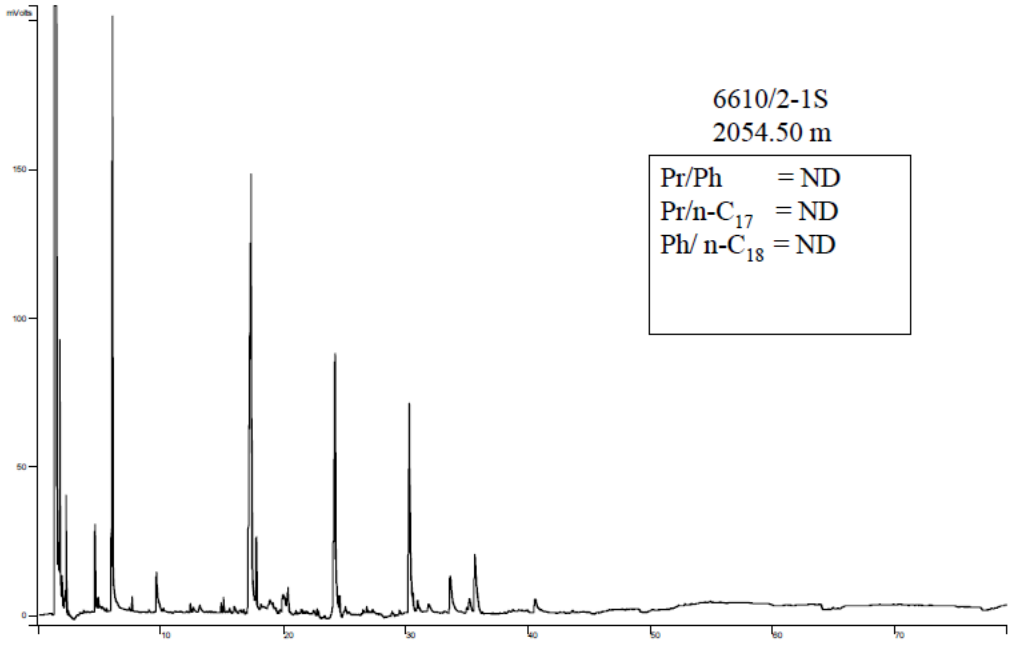

6610/2-1S
2054.50 m

Pr/Ph = ND
Pr/n-C_{17} = ND
Ph/ n-C_{18} = ND

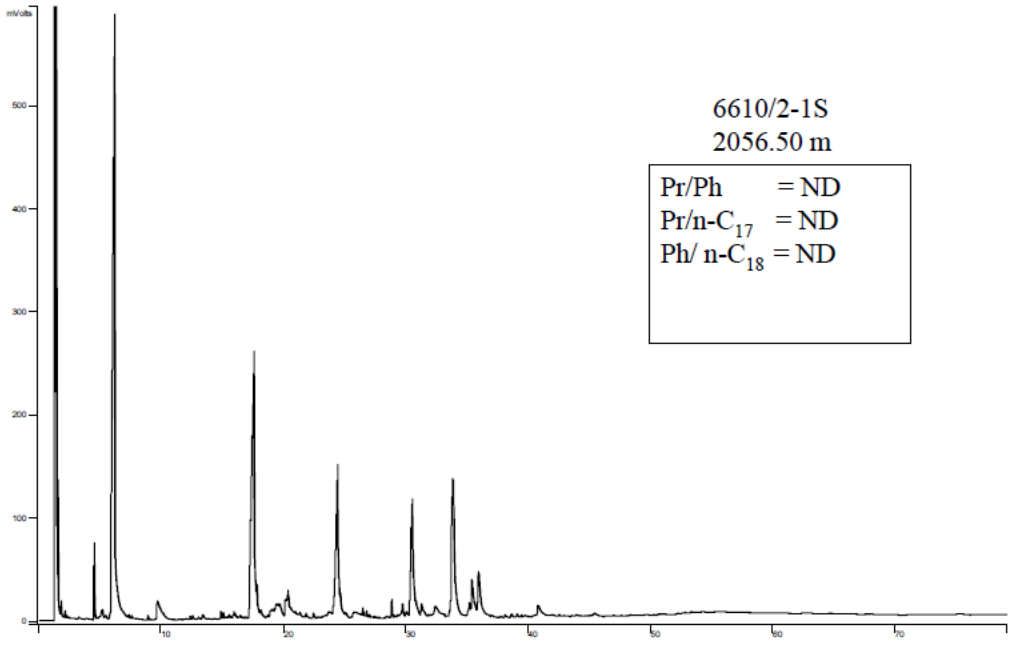

6610/2-1S
2056.50 m

Pr/Ph = ND
Pr/n-C_{17} = ND
Ph/ n-C_{18} = ND

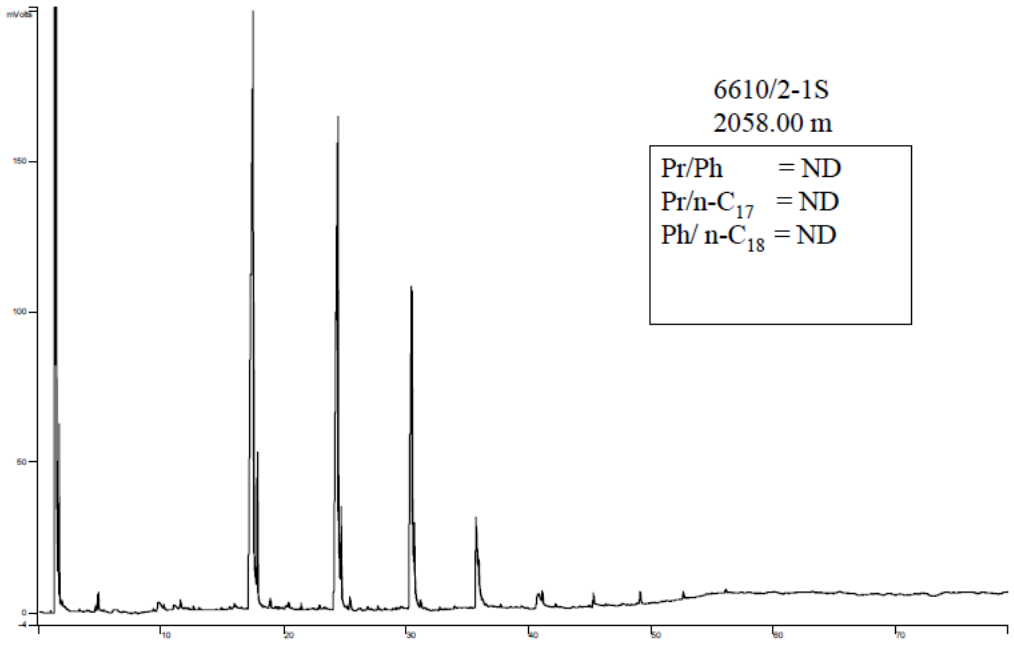

6610/2-1S
2058.00 m

Pr/Ph = ND
Pr/n-C_{17} = ND
Ph/ n-C_{18} = ND

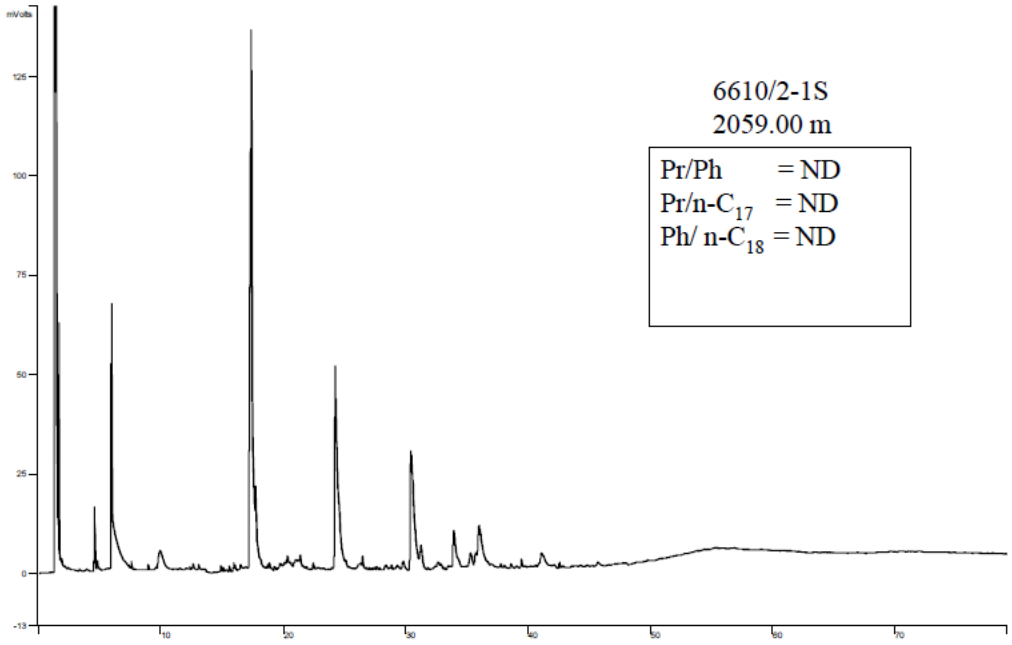

6610/2-1S
2059.00 m

Pr/Ph = ND
Pr/n-C_{17} = ND
Ph/ n-C_{18} = ND

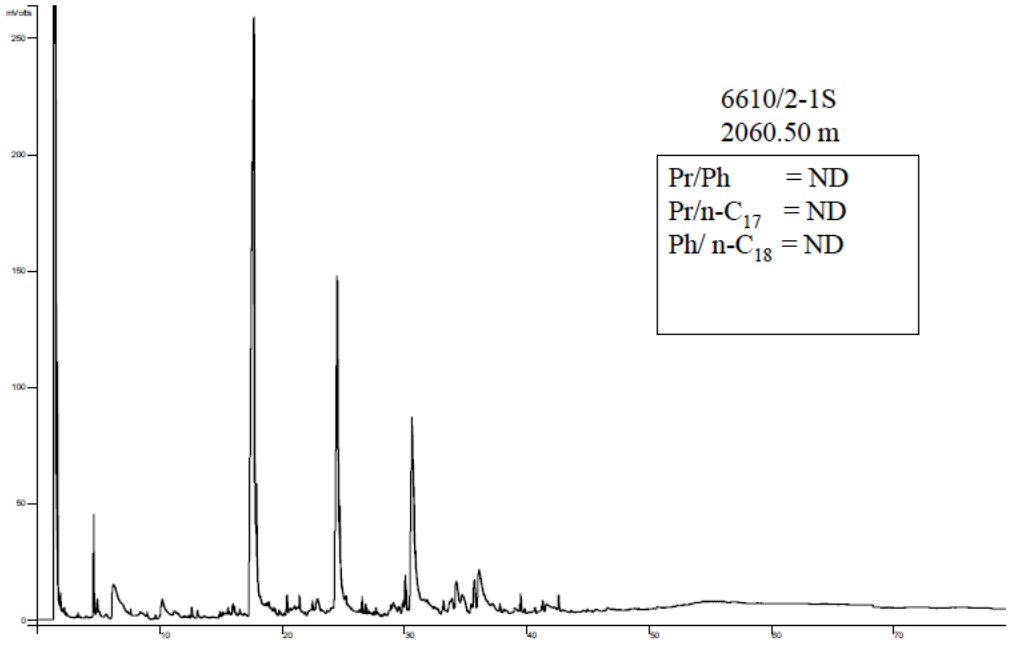

6610/2-1S
2060.50 m

Pr/Ph = ND
Pr/n-C_{17} = ND
Ph/ n-C_{18} = ND

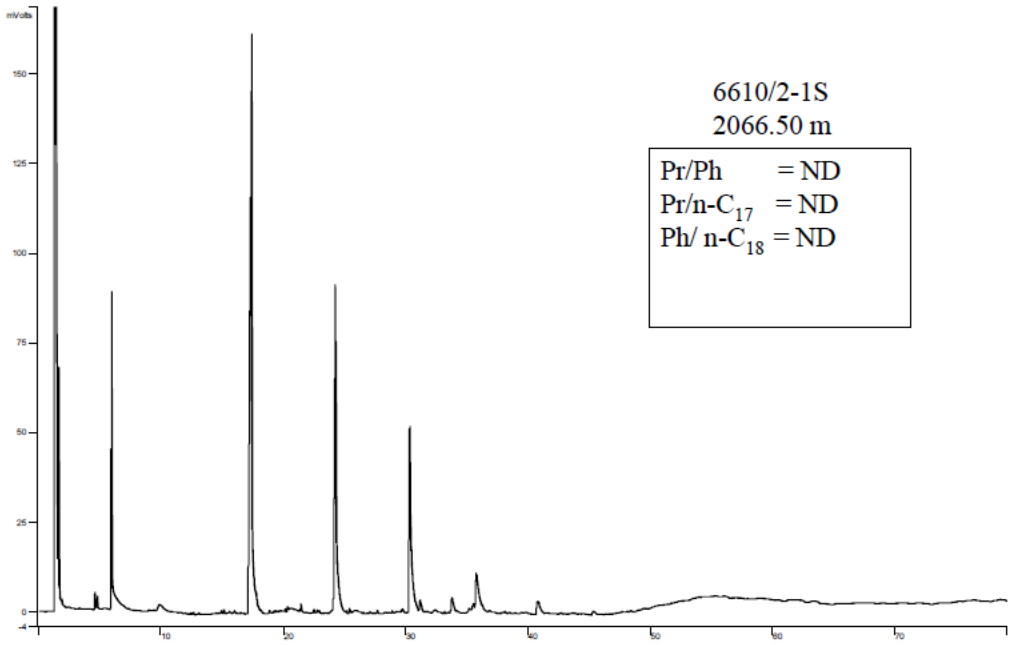

6610/2-1S
2066.50 m

Pr/Ph = ND
Pr/n-C_{17} = ND
Ph/ n-C_{18} = ND

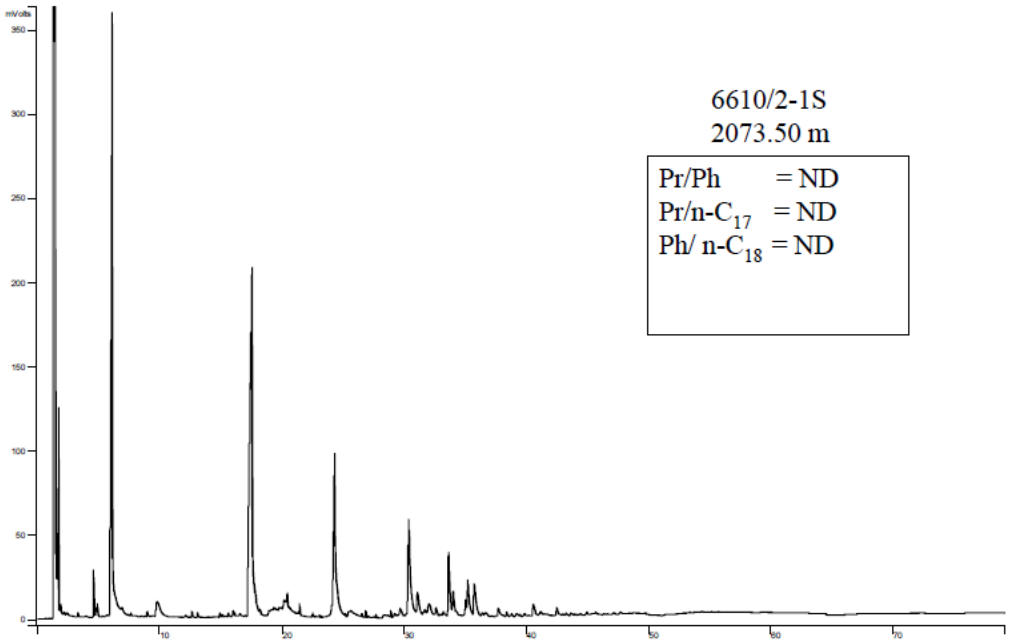

6610/2-1S
2073.50 m

Pr/Ph = ND
Pr/n-C_{17} = ND
Ph/ n-C_{18} = ND

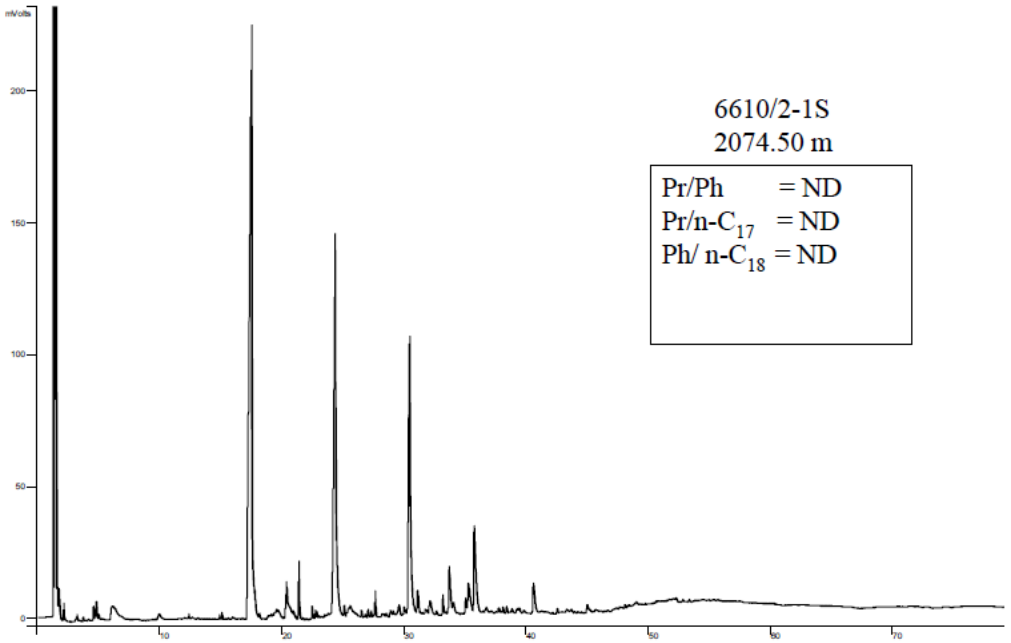

6610/2-1S
2074.50 m

Pr/Ph = ND
Pr/n-C_{17} = ND
Ph/ n-C_{18} = ND

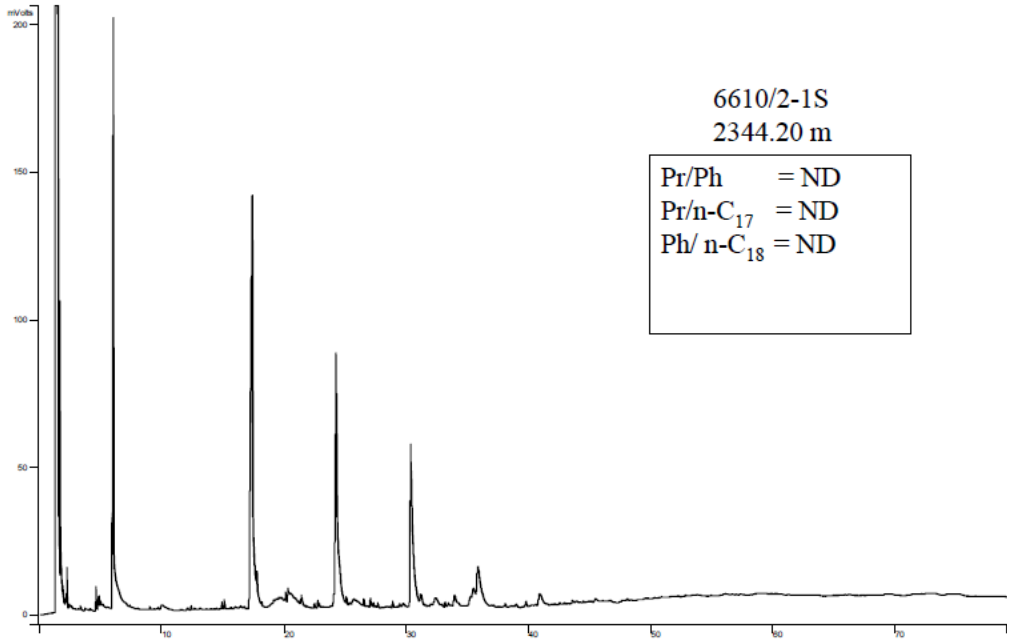

6610/2-1S
2344.20 m

Pr/Ph = ND
Pr/n-C_{17} = ND
Ph/ n-C_{18} = ND

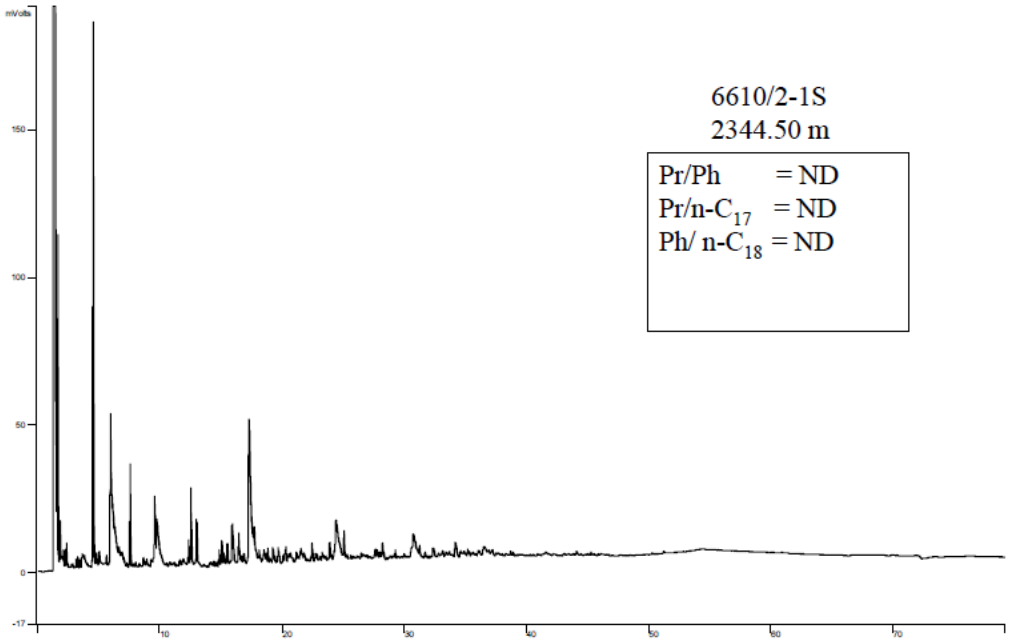

6610/2-1S
2344.50 m

Pr/Ph = ND
Pr/n-C_{17} = ND
Ph/ n-C_{18} = ND

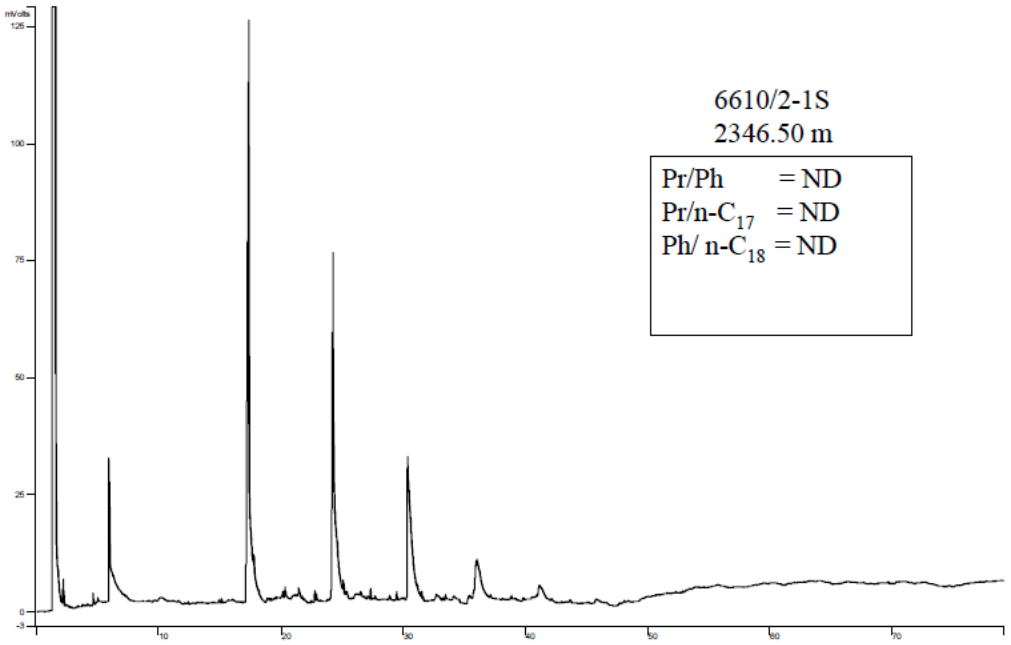

6610/2-1S
2346.50 m

Pr/Ph = ND
Pr/n-C_{17} = ND
Ph/ n-C_{18} = ND

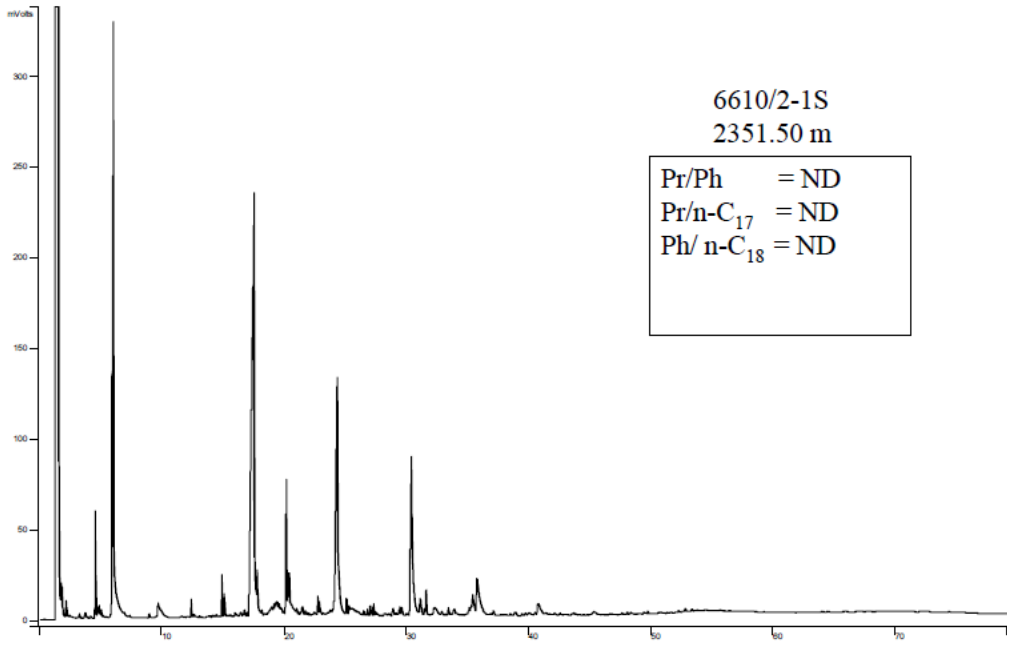

6610/2-1S
2351.50 m

Pr/Ph = ND
Pr/n-C_{17} = ND
Ph/ n-C_{18} = ND